Composites Science and Technology

Hemalata Jena
Jitendra Kumar Katiyar
Amar Patnaik *Editors*

Tribology of Polymer and Polymer Composites for Industry 4.0

Springer

Composites Science and Technology

Series Editor

Mohammad Jawaid, Lab of Biocomposite Technology, Universiti Putra Malaysia, INTROP, Serdang, Malaysia

Composites Science and Technology (CST) book series publishes the latest developments in the field of composite science and technology. It aims to publish cutting edge research monographs (both edited and authored volumes) comprehensively covering topics shown below:

- Composites from agricultural biomass/natural fibres include conventional composites-Plywood/MDF/Fiberboard
- Fabrication of Composites/conventional composites from biomass and natural fibers
- Utilization of biomass in polymer composites
- Wood, and Wood based materials
- Chemistry and biology of Composites and Biocomposites
- Modelling of damage of Composites and Biocomposites
- Failure Analysis of Composites and Biocomposites
- Structural Health Monitoring of Composites and Biocomposites
- Durability of Composites and Biocomposites
- Biodegradability of Composites and Biocomposites
- Thermal properties of Composites and Biocomposites
- Flammability of Composites and Biocomposites
- Tribology of Composites and Biocomposites
- Bionanocomposites and Nanocomposites
- Applications of Composites, and Biocomposites

To submit a proposal for a research monograph or have further inquries, please contact springer editor, Ramesh Premnath (ramesh.premnath@springer.com).

More information about this series at http://www.springer.com/series/16333

Hemalata Jena · Jitendra Kumar Katiyar ·
Amar Patnaik
Editors

Tribology of Polymer and Polymer Composites for Industry 4.0

Springer

Editors
Hemalata Jena
School of Mechanical Engineering
Kalinga Institute of Industrial Technology
Bhubaneswar, India

Jitendra Kumar Katiyar
Department of Mechanical Engineering
SRM Institute of Science and Technology
Chennai, Tamil Nadu, India

Amar Patnaik
Department of Mechanical Engineering
Malaviya National Institute of Technology
Jaipur
Jaipur, India

ISSN 2662-1819 ISSN 2662-1827 (electronic)
Composites Science and Technology
ISBN 978-981-16-3902-9 ISBN 978-981-16-3903-6 (eBook)
https://doi.org/10.1007/978-981-16-3903-6

© The Editor(s) (if applicable) and The Author(s), under exclusive license to Springer Nature Singapore Pte Ltd. 2021
This work is subject to copyright. All rights are solely and exclusively licensed by the Publisher, whether the whole or part of the material is concerned, specifically the rights of translation, reprinting, reuse of illustrations, recitation, broadcasting, reproduction on microfilms or in any other physical way, and transmission or information storage and retrieval, electronic adaptation, computer software, or by similar or dissimilar methodology now known or hereafter developed.
The use of general descriptive names, registered names, trademarks, service marks, etc. in this publication does not imply, even in the absence of a specific statement, that such names are exempt from the relevant protective laws and regulations and therefore free for general use.
The publisher, the authors and the editors are safe to assume that the advice and information in this book are believed to be true and accurate at the date of publication. Neither the publisher nor the authors or the editors give a warranty, expressed or implied, with respect to the material contained herein or for any errors or omissions that may have been made. The publisher remains neutral with regard to jurisdictional claims in published maps and institutional affiliations.

This Springer imprint is published by the registered company Springer Nature Singapore Pte Ltd.
The registered company address is: 152 Beach Road, #21-01/04 Gateway East, Singapore 189721, Singapore

Contents

Tribology in Polymers and Polymers Composites

Frictional and Wear Behavior of Epoxy Resin Based Nano-Composite in Dry Sliding Contact

Avinash V. Borgaonkar and Shital B. Potdar

Abstract Recently, there has been a growing interest in polymers as well as polymer composites and their industrial demands as an efficient alternative for pure metals and hybrid materials. In the present work, tribological investigation of MoS_2 and ZrO_2 reinforced polymer nano-composites have been carried out. The effects of different wt. % of MoS_2 and ZrO_2 on the tribological properties of MoS_2 and ZrO_2 reinforced polymer nano-composites have been studied. A tribological study of the fabricated polymer nano-composites were performed using the pin-on-disc friction and wear test rig at different operating conditions (such as contact pressure and sliding speed). It was observed that MoS_2 reinforced polymer nano-composite exhibits low frictional coefficient compared to ZrO_2 reinforced polymer nano-composite. However, ZrO_2 reinforced polymer nano-composite possesses higher wear resistance compared to MoS_2 reinforced polymer nano-composite. In addition, the particle size of reinforcement material may also affect the tribological properties of the fabricated polymer nano-composites. Among all samples of MoS_2 and ZrO_2 reinforced polymer nano-composites, the samples with 15% wt. depicts the lowest friction coefficient and wear rate.

Keywords Friction · Molybdenum disulphide (MoS_2) · Polymer nano-composites · Tribological properties · Wear · Zirconium dioxide (ZrO_2)

A. V. Borgaonkar (✉)
Department of Mechanical Engineering, National Institute of Technology Warangal, Telangana Warangal-506004, India

S. B. Potdar
Department of Chemical Engineering, National Institute of Technology Warangal, Telangana Warangal-506004, India

H. Jena et al. (eds.), *Tribology of Polymer and Polymer Composites for Industry 4.0*, Composites Science and Technology, https://doi.org/10.1007/978-981-16-3903-6_1

1 Introduction

Polymers and polymer based composites have been extensively used in dry sliding applications, where external aid of lubricant is not recommended or impossible. In the recent years, the self-lubricating materials have been popularly used in tribological applications. From the past few decades, polymers and polymer composites have substituted many conventional metals for sliding components. This provides reduction in weight and enhanced corrosion resistance; at the same time improved excellent tribological properties. Based on the molecular structure the polymers are classified into three groups: thermoplastics, thermosets and elastomers. Figure 1 depicts the polymer classifications and the possible reinforcements.

Thermoplastic materials have gained importance since they possess self-lubricating properties. The polytetrafluoroethylene (PTFE) is the most widely used thermoplastic material. PTFE in combination with metals exhibits lower friction coefficient (COF) operating at high load and low sliding speed. Also PTFE has low yield strength. These advantages make PTFE as an excellent material for sliding bearings (Khedkar et al. 2002). The anti-frictional PTFE composed materials with different fillers (such as coke, soot, fibres, metal powders, graphite, molybdenum disulphide) helps to enhance the strength of the matrix polymer (Aldousiri et al. 2013). In addition, PTFE is also used as filler material to reduce COF for thermoplastic as well as thermosetting polymers. The bearing liners made of a steel substrate having top porous bronze layer impregnated with PTFE composites. These bearings are highly efficient in dry sliding conditions under high contact pressure and at lower sliding speed. Polyamides are mostly preferred for sliding bearings reinforced with fillers as well as dry lubricants. These are also used for fabricating gears as well as thin film polymer coatings. Polyformaldehyde, polyarylates and polycarbonate are also used

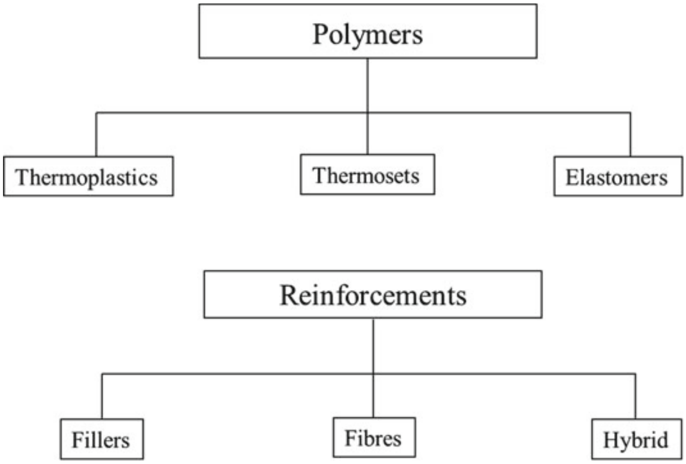

Fig. 1 Classification and reinforcement used for polymers

for manufacturing gears, bushings, and sliding bearings. Among these thermosetting polymers, polyimides sustain at a higher operating temperature (up to 260 °C). Epoxy and phenolic resin composites dispersed employing solid lubricants such as graphite or MoS_2 are often used as matrices for antifriction linings of machine guides (Ching et al. 2017). Thermosetting polymers are majorly used as base matrix materials for clutches, brakes and other frictional components. Elastomers like polyurethanes and rubbers are mainly being used as anti-abrasion linings for metallic surfaces as well as seals. The most popular application of elastomers is automotive tires (Peters 2014). The various aspects affecting the tribological properties of polymers are structure and position of macromolecules on the surface, multi-phase nature, degree of crystallinity; kind of polymers, such as homo-polymers, block copolymers, etc., composition for blends, chain orientation acquired in processing such as extrusion, molecular structure such as linear, branched or cross-linked and molecular mass distribution (Brostow et al. 2003). Samyn et al. (2007) were reviewed the tribological behavior of sintered and thermoplastic polyamides under adhesive sliding. They were reported that polyimides functions well at higher temperature. The tribological performance mainly influenced due to applied load, sliding velocity and humidity. Based on the referred literature they have developed theoretical models sintered and thermoplastic polyimides. They have observed that the tribo-chemical and tribo-physical reactions plays very important role in frictional and wear analysis of the polymers.

The different polymers and its composites have been used so far in order to study their tribological properties have been reported in this section. Sınmazcelik and Yilmaz (2007) were studied the thermal aging effects on the tribological behavior of pure poly-ether-ether-ketone (PEEK) and PEEK reinforced with random oriented short fibres. They observed that due to isothermal aging process, the degree of crystallinity is decreased considerably but at the same time well-organized crystalline structure has been achieved. The resulting trans-crystalline layer formation helps to improve its flexural modulus. Thermal aging process also influences the impact testing properties of pure PEEK and its composites dramatically. Thermal aging makes the material becomes highly brittle and also decreases the toughness remarkably. They observed that percentage (%) crystallinity is not the unique parameter which affects the polymers performance; the crystal orientation is also an important parameter which plays an outstanding role in enhancing mechanical as well as tribological properties of PEEK and its composites. The study reveals that there is a strong co-relation exists between thermal aging and micro-structure. At the same instance nonlinear relationship has been observed between its micro-structure and tribological properties. Micro-structural changes took place after thermal aging helps to improve the mechanical properties which eventually results in improved tribological properties. Burris and Sawyer (2006) were developed a PEEK filled PTFE composite with different wt. % addition of PEEK from 0 to 70%. The tribological tests were performed using a linear reciprocating tribometer against lapped steel counter-disc surface. The tests for all the samples performed at same operating conditions. The composite material exhibits a low COF and wear rate than pure PEEK and PTFE samples. The microscopic analysis shows that the interfacial connection between PTFE and PEEK significantly improves the tribological properties. The composites were prepared PEEK with wt. % of 50 and wt. % of 32 exhibiting lowest COF and wear rate respectively.

Unal (2004) and Unal et al. (2006) have performed the tribological study for the bronze filled with PTFE (25 wt. %) polymer against stainless steel counter-disc in dry sliding conditions using a pin-on-disc test rig. The tribological tests were performed under various load and speed conditions. The test results reveal that, at all sliding speeds, the COF of composite filled with PTFE decreases suddenly with rise in load, whereas the wear rate decreases linearly with the rise in the load. In addition, the wear rate was less sensitive to the speed and highly sensitive to the load, especially at higher loads. In another study Unal et al. (2010) analysed the tribological performance of pure PTFE, and PTFE +17 wt. % glass fibers reinforced (GFR). The study has shown that, the COF reduces as applied load increases. The PTFE +17 wt. % GFR exhibits higher wear resistance in comparison with pure PTFE and PTFE +35 wt. % C. The microscopic analysis showed that the wear took place by both adhesive and abrasive mechanism.

Sumer et al. (2008) analysed tribological behavior of pure PEEK and PEEK reinforced with 30 wt. % GFR under dry sliding and water lubricated conditions. The tribological tests were performed against AISI steel disc under different operating conditions (such as load and speed). For dry sliding condition, slight increase in COF and specific wear rates have been observed with increase in load for both unfilled PEEK and PEEK filled with GFR composite. Whereas, with increase in sliding speed the decrease in COF while increase in specific wear rate have been observed. In addition, under same operating parameters in case of water lubricated conditions lower values of both COF and specific wear rate have been observed compared to dry condition. The addition of glass fibres significantly improves the tribological performance of the composite under dry sliding condition. Greco et al. (2011) have evaluated the tribological properties of unfilled PEEK and PEEK reinforced using short and long woven fibres with random orientations. These polymer materials used to fabricate the disc and operated at higher sliding speed against steel balls using a 3 ball-on-flat test rig. The test results have demonstrated that composite comprised of long woven fibres exhibit the lower COF and wear rate. Yamamoto and Takashima (2002), Yamamoto and Hashimoto (2004) were investigated the tribological properties of PEEK and polyphenylenesulfide (PPS) under water lubricated condition employing a face-contact sliding tester. They have observed formation of ferrous sulphide (FeS) layer in case of PPS, on the counter steel surface due to reaction of sulphur with the steel surface. The formation of FeS layer assists for transfer/adhesion of PPS onto the counter steel surface which results into reduction in wear. However, only immersion of PEEK in water not reduces its hardness but it leads to reduce the hardness of sliding surface which promotes high wear rate.

Unal and Findik (2008) performed tribological tests of industrial polyamides (PA) against the counterbody made of different polymers in dry sliding conditions. The PA 66 polymer and PA 46 filled with 30 wt. % of GFR composite have been used in this study. The test results reveal that for these polymers the COF is decreasing with increase in load up to 40 N and above this COF is increasing. Whereas, the low wear rate was observed, for GFR reinforced PA 46 polymer composite against the same counterbody material. Author demonstrated that GFR reinforced PA 46 polymer composite was a favourable thermoplastic material for electrical contact breaker applications. Further Unal and Mimaroglu (2003), Unal et al. (2004, 2005) have extended the study for PA 66, polyoxymethylene (POM), ultrahigh molecular weight polyethylene (UHMWPE), GFR reinforced PPS and aliphatic polyketone (APK) polymers. Their study shown that, for all the considered polymers, the COF reduces in linear manner along with the increase in load, whereas the sliding velocity has significant effect on the specific wear rate of the polymers. The PA 66 exhibits lowest specific wear rate while POM exhibits highest one. Li et al. (2017) were fabricated polymer composites using nylon-6 (MC PA6) and graphene (GN) nano-composites by doping polyethylene glycol (PEG) as a compatibilizer as well as solid lubricant. The microscopic analysis showed that addition of PEG tends to superior grafting of PA6 molecules on graphene surface, while graphene was uniformly dispersed in the matrix. The experimental test results shown that in comparison with pure MC PA6, addition of 0.5 wt. % of GN enhances tensile strength by 12% while impact strength by 20.6%. The tribological test results shown that in comparison with pure MC PA6, 0.7 wt. % addition of GN reduces the COF by 13% and specific wear rate by 75%. From the microscopic analysis of worn surface it has been observed that the surface exhibits flat and smooth features with uniform distribution of graphene, and get annealed due to lower frictional heat generated at the contacting surfaces. The synergistic effect of reinforcing and lubrication of GN-PEG, helps to improve their mechanical as well as tribological properties significantly.

In order avoid the loosening of nano-particle agglomerates in polymer composites; Zhang et al. (2002) introduced an irradiation grafting method. They have fabricated composite employing covalent bonding of polyacrylamide (PAAM) onto the nano-silica. They experienced that due to grafting PAAM supports for the curing of epoxy which enhances the chemical bonding between fillers and matrix. The study showed that nano-silica/epoxy composites exhibits excellent tribological performance in comparison with pure epoxy. Further Rong et al. (2003) extended the study by introducing a chemical grafting method. They fabricated PAAM composite with doping silicon carbide, alumina and silicon nitride nano-particles. The tribological analysis reveals that the COF and specific wear rate of the developed PAAM composite are lower than that of pure epoxy. This is because of improved bond strength caused due to the enhanced interfacial interaction between filler and epoxy matrix. The COF is reduced due to production of lubricity by fine wear debris. Whereas, the improvement in the wear resistance due to increase in micro-hardness and enhanced thermal conducting capability. Yoon et al. (2006) developed patterns with different aspect ratios of polymethylmethacrylate (PMMA) on silicon wafer employing lithographic method. They investigated the tribological response of these fabricated nano-patterns with flat PMMA thin films. The test results reveal that the patterned samples demonstrated excellent tribological performance. The nano-patterned structures were exhibited superior bond strength and tribological behaviour because of their hydrophobic nature and decreased contact area. Polybenzimidazole (PBI) polymer having higher thermal stability, but due to problems related with its processing, it has not been used popularly. In order to resolve this problem, a composite of PBI and Polyetherketone

(PEK) was fabricated by Bijwe et al. (2015) and their mechanical as well as tribological properties were analysed. In addition a number of composites comprised with solid lubricants, glass fibres and carbon were fabricated. The mechanical, physical, thermal as well as tribological properties of these composites were evaluated. There is no any significant improvement has been observed in the tribological performance of composites blended with only solid lubricants or fibres. Whereas the composites containing polymers, solid lubricants, glass as well as carbon fibres, produces a remarkable improvement in the tribological properties. The developed composite demonstrated excellent tribological properties as compared with the commercially available PBI–PEEK blend composite.

Pihtili (2009) have investigated the frictional and wear properties of GFR reinforced epoxy resin and GFR reinforced polyester resin composite at different load and speed conditions by employing a block-on-shaft test rig in dry sliding condition. For all test conditions GFR reinforced epoxy resin composites demonstrated high strength and wear resistance in comparison with GFR reinforced polyester resin composites. Rong et al. (2001) developed TiO_2 nano-particles dispersed epoxy polymer composite. The tribological tests of the fabricated composites were performed against a smooth steel counterpart in dry sliding condition. The microscopic analysis showed that the homogeneous dispersion of the nano-particles enhances wear resistance. For homogeneous phase dispersion of epoxy and the nano-particles chloroform has been used and at the mixture was continuously stirred and heated unless the composite was fully cured. They concluded that the developed polymer composite exhibits excellent tribological performance compared with pure epoxy composites.

Up till now, very few studies have been reported the tribological properties of epoxy resin based nano-composites. The study in this direction is very much essential, since currently significant development is happening in the area of epoxy resin based nano-composites for current industrial applications. Hence, the objective of the present study is to investigate the tribological behavior of epoxy based nano-composites reinforced using MoS_2 and ZrO_2 nano-particles.

2 Materials and Methods

2.1 Materials

In order to fabricate polymer based nano-composites the base matrix epoxy resin and curing agent procured from Sisco Research Laboratories Pvt. Ltd., Mumbai, India. The different reinforcements materials such as MoS_2 (with average particle size 70–90 nm), ZrO_2 (with average particle size 170–200 nm) and ZrO_2 (with average particle size 90–120 nm) powders were purchased from Sisco Research Laboratories Pvt. Ltd., Mumbai, India.

2.2 *Characterization and Methods*

2.2.1 Surface Topography

The surface topography of the pin and the counter face disc surface was measured using the Surtronic S-100 (Taylor Hobson) Series Surface Roughness Tester. The required surface roughness was achieved by polishing with different grades of silicon carbide papers.

2.2.2 Pin on Disc Friction and Wear Test Rig

The tribological study of the fabricated epoxy resin based nano-composites were performed at different contact pressure and sliding speed conditions using the pin on disc test rig provided by Magnum, India. The pin is having flat end (12 mm diameter and 25 mm length), whereas the disk is made up of EN-31 steel material (165 mm diameter and thickness of 8 mm).

2.2.3 Sample Preparation

In order to prepare the epoxy based nano-composites the MoS_2 nano-particles were directly mixed with epoxy resin and the mixture was heated and kept in an oven with constant pre-set 80 °C temperature. After 30 min, the mixture was taken out of oven and stirred with magnetic stirrer for another 30 min. For uniform dispersion of nano-particles, the mixture was sonicated for 10 min. Eventually, the curing agent was poured, and the composites were cured by keeping the mixture in the oven at 80 °C temperature for 3 h. The same procedure was adopted to prepare nano-ZrO_2/epoxy composites. In order to investigate the optimum wt. % of MoS_2 and ZrO_2 into the epoxy base matrix which exhibits better tribological properties the wt. % of MoS_2 and ZrO_2 varied from 5 to 25%.

3 Experimental Testing

The experimental tests were performed at room temperature in air. The pin on disc friction-wear test rig is used in this study as depicted in Fig. 2. The stationary pin is pressed against rotating disk under the given load. The pin is cylindrical with flat end. During the test, the friction force and wear are continuously monitored. A typical friction curve measurement recorded using data acquisition system.

For obtaining reliable results each experiment was repeated three times. The test parameters employed in the experimental tests are indicated in Table 1.

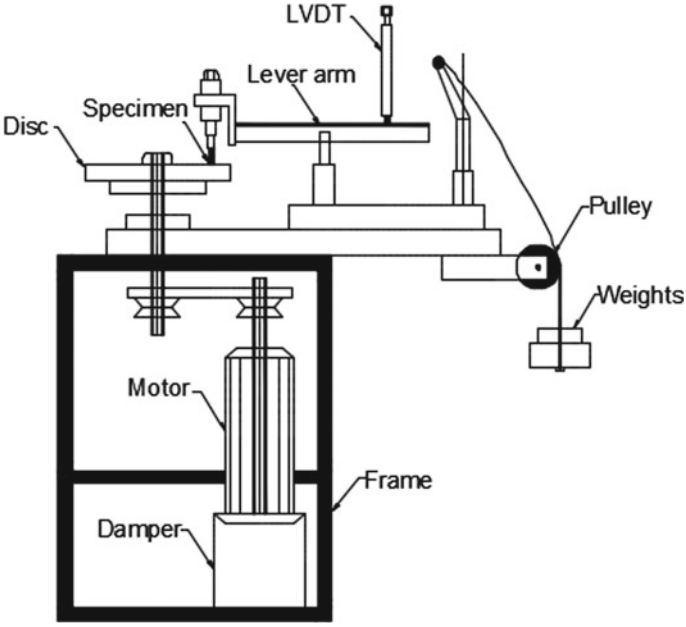

Fig. 2 Schematic set up of pin-on-disc friction and wear test rig

Table 1 Operating parameters and its ranges

Sr. No	Parameters	Operating conditions
1	Contact pressure	88, 176, 264 kPa
2	Sliding speed	1, 2, 3 m/sec
3	Track radius	40 mm
4	Sliding distance	3000 m

The composite specimens were tested using pin-on-disc test rig which consists of a pin holder sliding against a counter-disc. For minimising the running-in period time, the pin samples were pre-worn by grinding using silicon carbide (SiC) paper against the counter-disc. After polishing the surface roughness was measured at different locations using surface roughness tester. The average surface roughness value (Ra) was observed to be 0.4 µm. This helps to keep the same roughness of the samples before test as well as the parallel alignment of the two mating surfaces could be guaranteed. The counter disc steel discs surface was cleaned with acetone before service.

4 Results and Discussion

4.1 *Effect of Different Reinforcement Material (MoS_2/ZrO_2) Addition on COF*

The effect of reinforcement material i.e. MoS_2 addition on COF at different contact pressures and sliding speeds is shown in Fig. 3. It can be observed that the wt. % addition MoS_2, contact pressure and sliding speed shows a significant effect on the magnitude of COF.

The COF was observed to be higher for pure epoxy specimen (indicated by 0 wt. % MoS_2 addition). As the MoS_2 added into epoxy matrix the reduction in COF has been observed. MoS_2 offers low friction due to their anisotropic layered structure, i.e. covalent bonding and weak Vander Waals forces between the adjacent lamellae. With the increase in contact pressure and sliding speed the COF found to be reduced due to transfer of polymer composite film on to the counter surface. The addition of MoS_2 into the epoxy base matrix helps to reduce COF. However, the higher concentration of MoS_2 material leads to improper mixing between the reinforcement material and base matrix which results into poor bonding (Greco et al. (2011) and Rong et al. (2001)). Due to which after 15 wt. % addition the COF found to be increasing. The similar trend has been observed in case of ZrO_2 added polymer nano-composite.

The effect of reinforcement material i.e. MoS_2 and ZrO_2 addition on COF at 264 kPa contact pressure and 3 m/sec sliding speed is shown in Fig. 4. The magnitude of COF in case of ZrO_2 added polymer nano-composite found to be higher than MoS_2 added polymer nano-composite due to its particle size and hardness. The pure epoxy specimen exhibited Vickers microhardness value 123.8 ± 0.7 (MPa).

The hardness values of prepared nano-composite samples are mentioned in Table 2.

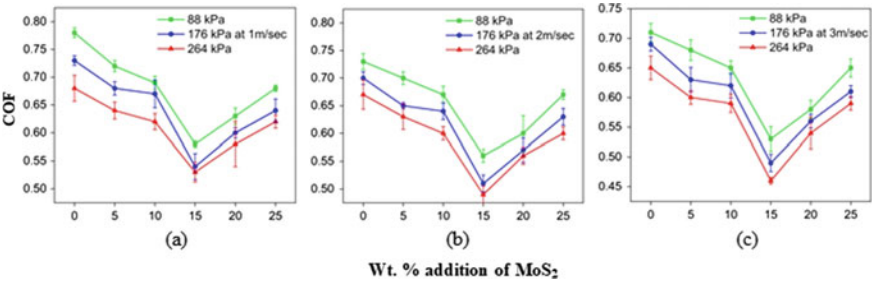

Fig. 3 COF for epoxy-MoS_2 polymer composite with different wt. % addition of MoS_2 at 88 kPa, 176 kPa, 264 kPa contact pressure **a** 1 m/sec **b** 2 m/sec **c** 3 m/sec sliding speed

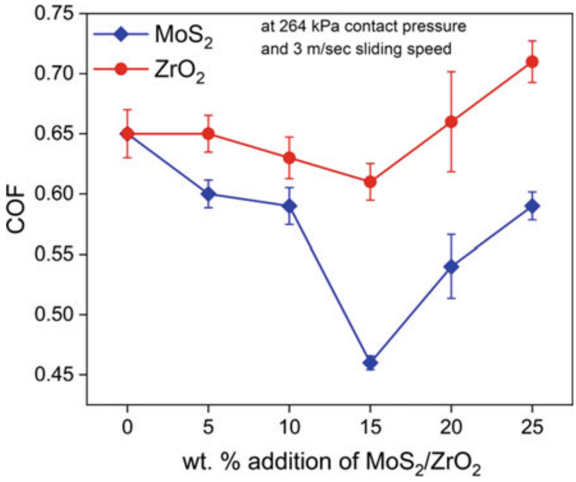

Fig. 4 COF for epoxy-MoS_2 and epoxy-ZrO_2 polymer composite at different wt. % addition of MoS_2/ZrO_2 at 264 kPa contact pressure and 3 m/sec sliding speed

Table 2 Micro-hardness values of epoxy based nano-composite specimens

Reinforcement material	HV (MPa)				
	5%	10%	15%	20%	25%
MoS_2	154.6 ± 13.2	163.2 ± 8.7	171.3 ± 11.9	166.7 ± 19.4	159.4 ± 13.5
ZrO_2	259.3 ± 5.8	273.1 ± 9.4	286.7 ± 6.9	262.6 ± 16.7	254.8 ± 3.9

4.2 Effect of Different Reinforcement Material Addition on Wear Rate

The effect of reinforcement material i.e. MoS_2 addition on wear rate at different contact pressures and sliding speeds is shown in Fig. 5. It can be observed that the wt. % addition MoS_2, contact pressure and sliding speed shows a remarkable effect on the magnitude of wear rate.

The wear rate was observed to be higher for pure epoxy specimen (indicated by 0 wt. % MoS_2 addition). As the MoS_2 offers low friction due to weak Vander Waals forces between the adjacent lamellae; the worn out MoS_2 particles get entrapped into asperities between the contacting surfaces. This resulted into decrease in wear rate with the addition of MoS_2 into the epoxy base matrix. However, as the concentration of MoS_2 increases; it leads to improper mixing between the reinforcement material and base matrix which results into poor bonding (Greco et al. (2011) and Zhang et al. (2002)). Due to which after 15 wt. % addition the wear found to be increasing. The similar trend has been observed in case of ZrO_2 added polymer nano-composite.

The effect of reinforcement material i.e. MoS_2 and ZrO_2 addition on wear rate at 264 kPa contact pressure and 3 m/sec sliding speed is shown in Fig. 6. The ZrO_2

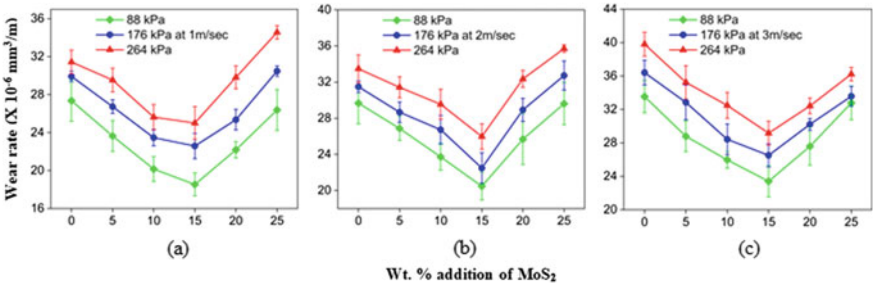

Fig. 5 Wear rate (mm^3/m) for epoxy-MoS$_2$ polymer composite with different wt. % addition of MoS$_2$ at 88 kPa, 176 kPa, 264 kPa contact pressure **a** 1 m/sec **b** 2 m/sec **c** 3 m/sec sliding speed

Fig. 6 Wear rate (mm^3/m) for epoxy-MoS$_2$ and epoxy-ZrO$_2$ polymer composite at different wt. % addition of MoS$_2$/ZrO$_2$ at 264 kPa contact pressure and 3 m/sec sliding speed

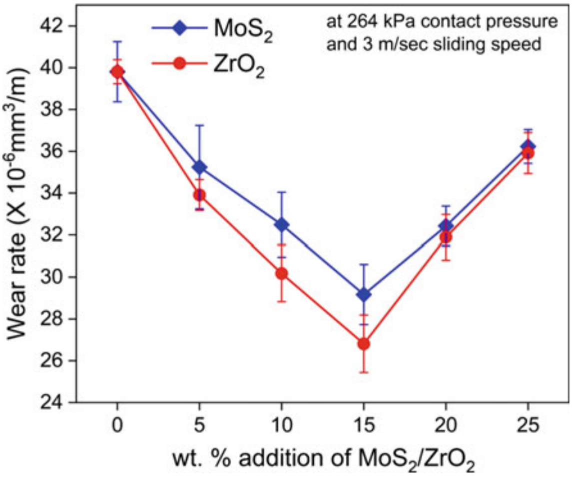

added polymer nano-composite exhibits higher wear resistance due to its higher hardness (Rong et al. (2001)).

5 Conclusion

Within the scope of this study, MoS$_2$ and ZrO$_2$ reinforced polymer nano-composites have been fabricated with different wt. % addition of reinforcing material. The frictional and wear behavior of the developed polymer nano-composites at different contact pressure and sliding speed have been investigated. The test results demonstrated that, the reinforced polymer nano-composites exhibit excellent tribological performance compared to pure epoxy composite in all considered operating conditions. The MoS$_2$ reinforced polymer nano-composites exhibits lower frictional coefficient due to weak Vander Waals forces between the adjacent lamellae and its easy shearing ability as reported by (Rong et al. (2001)). Whereas the ZrO_2 reinforced polymer nano-composites exhibits high wear resistance due to its higher hardness. The hardness of the ZrO2 reinforced polymer nano-composites enhanced by 54% compared to pure epoxy and 43% compared to TiO2 reinforced polymer nano-composites as reported by (Rong et al. (2001). In case of both the reinforced polymer nano-composites the sample with 15% wt. addition depicts the lowest frictional coefficient and wear rate.

6 Future Scope

Further research for the improvement of the performance of the MoS_2 and ZrO_2 reinforced polymer nano-composites is needed to explore the followings:

- Computational study of the developed reinforced polymer nano-composites can be performed for validating the experimental results.
- The tribological performance of polymers in combination with surface texturing can also be studied.

References

Aldousiri B, Shalwan A, Chin CW (2013) A review on tribological behaviour of polymeric composites and future reinforcements. Adv Mater Sci Eng 2013(1):1–8

Bijwe J, Gupta MK, Parida T, Trivedi P (2015) Design and development of advanced polymer composites as high performance tribo-materials based on blends of PEK and ABPBI. Wear 342:65–76

Brostow W, Deborde JL, Jaclewicz M, Olszynski P (2003) Tribology with emphasis on polymers: friction, scratch resistance and wear. J Mater Educ 25(4–6):119–132

Burris DL, Sawyer WG (2006) A low friction and ultra-low wear rate PEEK/PTFE composite. Wear 261(3–4):410–418

Ching YC, Chuah CH, Ching KY, Abdullah LC, Rahman A (2017) Applications of thermoplastic-based blends. In: Recent developments in polymer macro, micro and nano blends. Woodhead Publishing, pp 111–129

Greco AC, Erck R, Ajayi O, Fenske G (2011) Effect of reinforcement morphology on high-speed sliding friction and wear of PEEK polymers. Wear 271(9–10):2222–2229

Khedkar J, Negulescu I, Meletis EI (2002) Sliding wear behavior of PTFE composites. Wear 252(5–6):361–369

Li C, Xiang M, Ye L (2017) Intercalation structure and highly enhancing tribological performance of monomer casting nylon-6/graphene nano-composites. Compos A Appl Sci Manuf 95:274–285

Peters EN (2014) Thermoplastics, thermosets and elastomers-descriptions and properties. Mechanical Engineers Handbook, pp 1–48

Pihtili H (2009) An experimental investigation of wear of glass fibre–epoxy resin and glass fibre–polyester resin composite materials. Eur Polymer J 45(1):149–154

Rong MZ, Zhang MQ, Liu H, Zeng H, Wetzel B, Friedrich K (2001) Microstructure and tribological behavior of polymeric nanocomposites. Ind Lubr Tribol 53(2):72–77

Rong MZ, Zhang MQ, Shi G, Ji QL, Wetzel B, Friedrich K (2003) Graft polymerization onto inorganic nanoparticles and its effect on tribological performance improvement of polymer composites. Tribol Int 36(9):697–707

Samyn P, Schoukens G, Verpoort F, Van Craenenbroeck J, De Baets P (2007) Friction and wear mechanisms of sintered and thermoplastic polyimides under adhesive sliding. Macromol Mater Eng 292(5):523–556

Sınmazcelik T, Yilmaz T (2007) Thermal aging effects on mechanical and tribological performance of PEEK and short fiber reinforced PEEK composites. Mater Des 28(2):641–648

Sumer M, Unal H, Mimaroglu A (2008) Evaluation of tribological behavior of PEEK and glass fiber reinforced PEEK composite under dry sliding and water lubricated conditions. Wear 265:1061–1065

Unal H, Findik F (2008) Friction and wear behaviors of some industrial polyamides against different polymer counterparts under dry conditions. Industrial Lubrication and Tribology 60(4):195–200

Unal H, Mimaroglu A (2003) Friction and wear behavior of unfilled engineering thermoplastics. Mater Des 24:183–187

Unal H, Sen U, Mimaroglu A (2005) Abrasive wear behavior of polymeric materials. Mater Des 26:705–710

Unal H, Sen U, Mimaroglu A (2006) An approach to friction and wear properties of polytetrafluoroethylene composite. Mater Des 27:694–699

Unal H, Yetgin SH, Mimaroglu A, Sumer M (2010) The effect of test parameters on friction and wear performance of PTFE and PTFE composites. J Reinf Plast Comp 29(13):1978–1986

Unal H (2004) Tribological studies of bronze filled PTFE polymer. Sci Eng Comp Mater 11(1):27–34

Unal H, Sen U, Mimaroglu A (2004) Dry sliding wear characteristics of some industrial polymers against steel counterface. Tribol Int 37(9):727–732

Yamamoto Y, Hashimoto M (2004) Friction and wear of water lubricated PEEK and PPS sliding contacts: Part 2. Composites with carbon or glass fibre. Wear 257(1–2):181–189

Yamamoto Y, Takashima T (2002) Friction and wear of water lubricated PEEK and PPS sliding contacts. Wear 253(7–8):820–826

Yoon ES, Singh RA, Kong H, Kim B, Kim DH, Jeong HE, Suh KY (2006) Tribological properties of bio-mimetic nano-patterned polymeric surfaces on silicon wafer. Tribol Lett 21(1):31–37

Zhang MQ, Rong MZ, Yu SL, Wetzel B, Friedrich K (2002) Effect of particle surface treatment on the tribological performance of epoxy based nanocomposites. Wear 253(9–10):1086–1093

Tribology in Polymers and Polymers Composites

Scientific Insights on Tribological Aspects of Polymer Based Composites

Dheeraj Kumar Gara, G. Raghavendra, Shakuntala Ojha, Sri Bandyopadhyay, Syed Ismail, and R. Narasimha Rao

Abstract Polymer composites are those materials that form a synergistic mechanical advantage when reinforcement fillers are integrated into polymer. This advantage of the multiphase material possesses excellent wear and friction properties, hence found to be amenable with aerospace, automobile, and biomedical applications. The current article emphasizes the Tribological properties of various polymer composites concisely. However, alongside the Tribological advantage, there is a compromise in mechanical properties due to exposure of polymer composites to hazardous environments resulting in degradation and plasticization. With the advent of new manufacturing and processing techniques, by retaining the mechanical properties, the Tribological properties can be enhanced. In the current article, detailed attention to the microscopic and macroscopic Tribological aspects of polymer composites will be emphasized.

Keywords Tribology · Polymer composites · Characterization · Crystallography · Wear · Friction

1 Introduction

Realizing the friction (Gnecco and Meyer 2015; Mo et al. 2009) and wear (Bhushan et al. 1995; Gotsmann and Lantz 2008) at nanoscale provides interesting insights into the physical behavior of the material. Materials possess good wear resistance at a macro scale such as diamond can be used as a coating, but the same diamond-like

---

D. K. Gara · G. Raghavendra (✉) · S. Ismail · R. N. Rao
Department of Mechanical Engineering, National Institute of Technology Warangal, Warangal, Telangana 506004, India
e-mail: raghavendra.gujjala@nitw.ac.in

S. Ojha
Department of Mechanical Engineering, Kakatiya Institute of Technology and Science, Warangal, Telangana, India

S. Bandyopadhyay
School of Materials Science & Engineering, UNSW. Sydney, Kensington, NSW 2052, Australia

H. Jena et al. (eds.), *Tribology of Polymer and Polymer Composites for Industry 4.0*, Composites Science and Technology, https://doi.org/10.1007/978-981-16-3903-6_2

carbon structure is difficult to manufacture at nanoscale fidelity. Hence it can be inferred that it is more important to realize the design of materials at the nanoscale is more prominent than the macro level. The realization of understanding the wear mechanism atom by atom (Bennewitz and Dickinson 2008) per micrometer of sliding the surface and the critical length scale that controls the mechanism of wear (Bhushan and Kwak 2007) have provided substantial insight on the formation of wear debris between contacting asperities. However, It is evident from the literature that there are no adequate physical models available to predict the material loss due to wear (Aghababaei et al. 2016). It is intuitive to realize that friction and wear are the same but with different manifestations indicating they are not physical properties of the material but are responses to a system subjected to various loading environments. In this context, a distinction between the friction and wear must be revisited, wherein the friction is the resistant force developed between the two contact surfaces to initiate the micro-displacement of the sliding body and wear is the phenomenon of physical or chemical damage that influences the quality of material in contact.

2 Types of Wear

Thanks to the technology that most of the mechanical systems in the current industries such as aerospace, automotive, and biomedical have enabled the scientific community to understand wear at greater extinction due to their demand for new materials. Wear mechanism is classified depending on the type of loading environment and the type of response. For instance, consider there are two surfaces sliding over each other in the presence of strong adhesive forces, the asperities of one surface may fracture that results in debris and upon sliding will transfer this debris between the surfaces of the materials. This type of wear is referred to as adhesive wear whereas, if there is a loss of material due to relative motion resulting in damage of the actual surface is referred to as abrasive wear. In terms of area contact of polymer composites, the viscoelastic, viscoplastic, and relaxation phenomena are taken into account, whereas in the adhesion component of polymer composites, long-range Vander Waals forces play a crucial role. It is thus indicative that interfacial adhesion determines the bulk strength of a material within a solid. Theories such as Bowder and Tabor model, surface energy theory, and fracture mechanic model can determine adhesion components of friction such as interfacial shear strength and yield pressure of asperities.

In context to wear of polymer composites, an important observation is made by Wang (1999) suggesting that wear is cyclic in nature and begins with polymer matrix material (resin) at the initial stage. This phenomenon exposes the fiber to failure in either buckling or fracture where fibers are still supported by resin and if the fibers do not fail completely, they are observed as hairline burrs on materials and justified in Scanning Electron Microscopy (SEM). In order to discuss the wear at a wider perspective, the key events responsible for the material loss and generation of wear

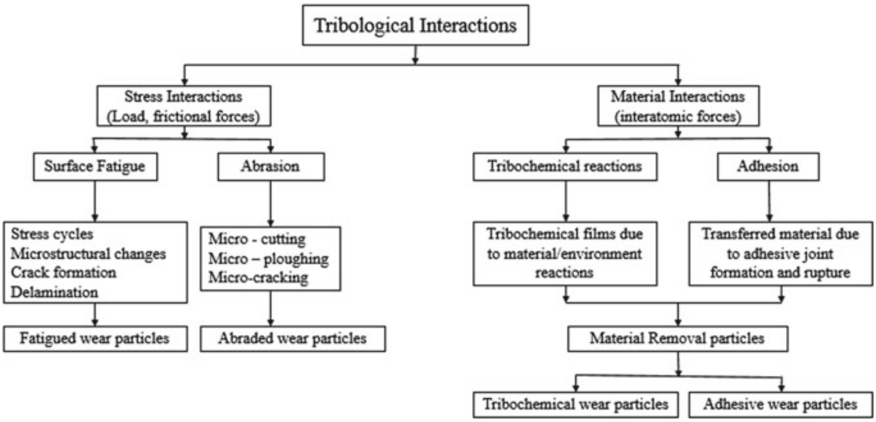

Fig. 1 Tribological interactions and wear mechanisms

particles from a given Tribological system are categorized into two broad classes as shown in Fig. 1.

The interactions and wear mechanisms displayed in the above Fig. 1 needs the attention of choosing a proper material that can alter the role of wear mechanism on the Tribological system. In lieu of this, to enhance the material Tribological properties, few polymer composites namely polymer/polymer and polymer/metal composites are predominantly elastic, as a result, the polymer tribology doesn't obey because the coefficient of friction varies according to normal load, sliding speed, temperature and glass transition temperature (Friedrich 2018; Omrani et al. 2016). To decide the reliability of the developed polymer composite, we calibrate the normal pressure- sliding velocity envelope as shown in Fig. 2.

It is implicative from various researches in the literature in pretext to above Fig. 2 that all material combinations exhibit a similar curve depicting coefficient of friction decreases linearly with the increase in applied pressure (Cirino et al. 1987). From the above discussion, it is intuitive to discuss the empirical relations between wear and

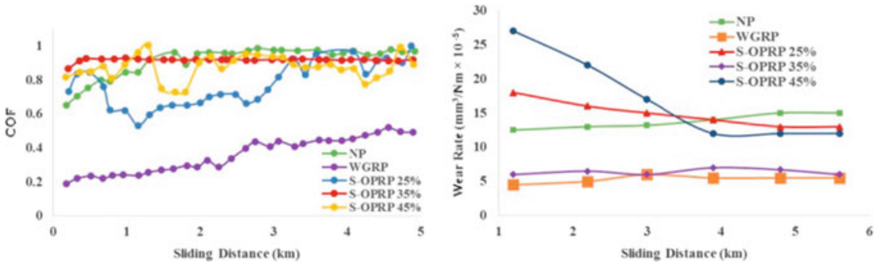

Fig. 2 Variation of friction coefficient and specific wear rate with sliding distance (Omrani et al. 2016)

other mechanical properties of polymer composites which will give a deeper insight into realizing structure–property correlation.

3 Mechanical Properties of the Polymer Composites

It is instinctive to discuss the mechanical properties of the polymer composites as they are sensitive to the microstructural variations that material undergoes. As it can be inferred that material wear which is purely a micro-phenomenon is implicative that the material mechanical properties get disturbed. Prior, it is important to emphasize the mechanical properties desired by the various industries such as biomedical, aerospace and automotive. In context to this, (Erenkov et al. 2010) emphasized the properties of polymer composites depend on electro-physical treatments, dipolymerization, cross-linking between the between matrix and filler. Key advantages of composites over conventional metals and alloys include high strength to weight ratio, excellent corrosion resistance and low thermal expansion. The major disadvantages include poor fire resistance and when exposed to high temperatures (typically higher than 400 °C), organic matrix will decompose and produce volatile and toxic gases. Composites most often creep, distort and soften which results in buckling and failure of load carrying capabilities. Properties of the polymer composites can be enhanced by the type of reinforcements, addition of nano-fillers. Few mechanical properties of natural fiber composites are discoursed in Ammar et al. (2018) as shown in Table 1 below.

These natural fiber reinforced composites depend on various parameters such as aspect ratio, volume fraction of fibers and fiber-matrix adhesion, orientation and stress transfer at the interface. Tensile strength is more sensitive to matrix properties and modulus is sensitive to fiber properties which can be inferred in Table 1. On the other hand, length of fiber, if exceeded than the critical length, upon the application of load increases the stress and results in higher strength of the composite. These properties are sensitive to microstructure and an emphasize between structure and property are correlated and will be discussed below.

Table 1 Mechanical properties of few natural fibers (Ammar et al. 2018)

S.NO	Fiber	Specific gravity	Tensile strength (MPa)	Modulus (GPa)	Specific modulus
1	Jute	1.3	393	55	38
2	Sisal	1.3	510	28	22
3	Flax	1.5	344	27	50
4	Sunhemp	1.07	389	35	32
5	Pineapple	1.56	170	62	40
6	Glass Fibre-E	2.5	3400	72	28

4 Structure–Property Correlations

An imperative work by Lancaster (1968) in this framework established an empirical relationship between wear and other mechanical properties such as young's modulus, hardness, fracture strength, and strain to break. To derive the above parametric relations works from (Myshkin et al. 2005; Halliday 1955) have closely worked on a polymer/metal Tribological system and observed that the temperature of the metal at which wear rates increase rigorously is nearly equal to the softening points of the materials. This implies that there is sufficient time for the speeds of sliding to reach thermal equilibrium throughout the polymer to be affected by wear. This observation is motivated by the previous works from (Halliday 1955; Greenwood and Williamson 1966) suggested Hardness to Elastic modulus *(H/E)* ratio played a crucial role in determining the rate of wear. They have also measured the plasticity criteria for the asperity contacts involved *(H/E)* ratio. (Smithies 1952), in support of the above evidence, has evaluated the relation between instantaneous temperature and temperature constantly flowing from metal to polymer as Eq. 1.

$$T = T_0\left(1 - erf\,\frac{x}{2\sqrt{\alpha t}}\right) \tag{1}$$

where, T is instantaneous temperature in Kelvin, Metal surface at constant temperature T_0, $erf\,\frac{x}{2\sqrt{\alpha t}}$ is error function.

The difference between these temperatures decides the wear and surface roughness of the polymer. From the linear relation, it is conclusive that as the temperature difference arises, the surface roughness and wear increases. It is important that heating/cooling rates are often more important than the determination of temperature itself and hence Newton's law of cooling cannot be applied. This process is mostly referred to as wear scar measurements. We shall discuss the loss of mass of the material during the expansion of load which also increases the wear rate. Works pertaining to this statement can be justified in (Nuruzzaman et al. 2012; Ang and Ahmed 2013). The complexities involved in predicting the weight loss during the wear are that, at elevated temperatures, the wear scars show elastic recovery, and hence there is misleading in the measurement of wear rate. To surmount this complexity, the surface roughness of the metal can be increased so that wear per traversal can be increased. It may be noted that the temperature at which the rapid weight loss measured keenly signifying occurs at the softening point. The material loss is determined by the following relation

$$w_s = \frac{\Delta m}{\rho F_n L} \tag{2}$$

where, F_n is normal force (N), Δm is mass loss(Kg), ρ is density (Kg/m^3) and L is sliding length (m). Another important factor, surface roughness plays a significant

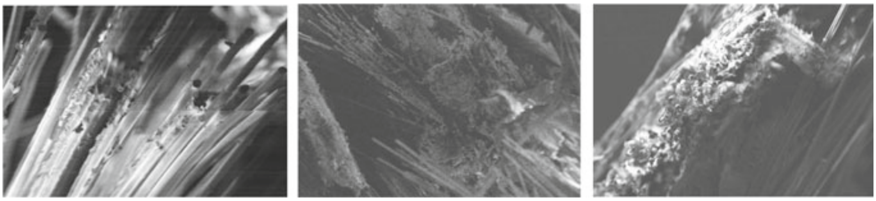

a. Fiber pull out b. Fiber breakage c. Smearing and Delamination

Fig. 3 Various surface failures of polymer composites

role in determining the magnitude of the wear rate. Impressive work by Kundalwal et al. (2014) analytically investigated the dependence of surface hardness of the polymer on the mechanical properties for the same. The paper demonstrated a shear lag model which concluded that when the surface roughness becomes larger, the tensile load transfer in the fiber/matrix interfaces also increases, this enhancing effect will gradually improve young's modulus of polymer composites. Interestingly, frictional shear transfer exists in thermoplastic composites and the interface is considered to be smooth if the ratio of amplitude to the wavelength of the matrix must be nearly zero, with few surface failures for reader understanding have been presented in the Fig. 3. The Fig. 3 discourses various surface failures and respective fiber failures at microstructure scale. Fiber pullout is one of the failure mechanisms that occurs due to weak bonding as it can be seen in the SEM image (first left). Fiber breakage is accompanied by interface debonding, this is because of the higher stress placed on fiber resulting in early fatigue. This is observed in the SEM image in the Fig. 3 (second left). Whereas influence of layup configuration and feed rate plays a crucial role resulting in matrix smearing and this can be reduced with a proper adhesive bonding, a SEM image shown in complete right of the Fig. 3 followed by delamination failure which is a most common failure observed in the polymer composites, this is generally developed because of the excessive out-of-plane and interlaminar stresses, the SEM image clearly shows the delamination concisely as shown in complete right image in Fig. 4. Similarly for the elastic transfer for thermosetting polymers. In the preprocessing discussion of surface roughness, processing techniques define the surface properties of any polymer. In lieu of machining context, (Jaśkiewicz 2019) indicated the surface roughness enhanced with an increase in cutting speed whereas decreased with increasing feed rate. An extension of Lanz et al. (2001), the authors have also conferred that the machining direction of milling has also played a significant role.

Due to the advent of technologies, various materials have been developed by the researchers in the scientific community that can be cited in the literature. Polymer composites received ample attention from the aviation industry due to their intriguing properties such as high strength to weight ratio, good thermal and corrosion resistance. Hence the development of polymer composites from various materials such as in combinations of natural fibers and metals has foreseen tremendous effort by researchers. As a result, erosive wear has received ample attention, in lieu of this,

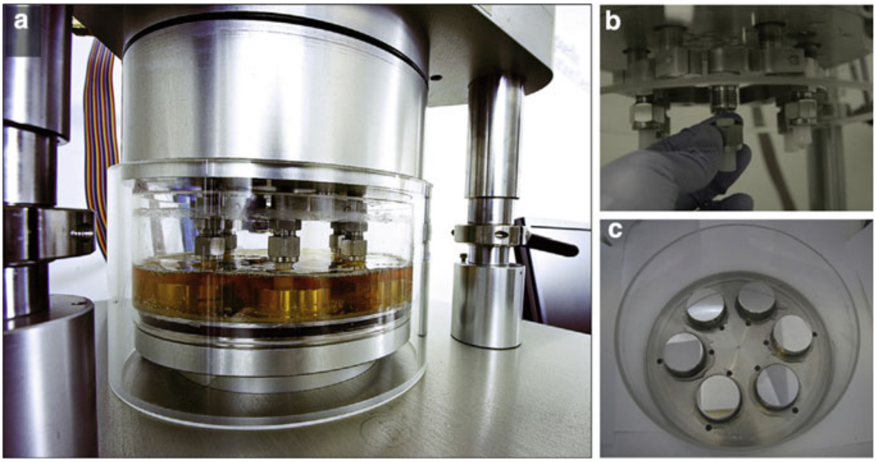

Fig. 4 Typical POD wear tester. **a** Assembled POD wear tester, **b** UHMWPE pins secured in the holder, **c** CoCr disks secured in the test chamber (Zdero et al. 2017)

(Tewari et al. 2003) has earmarked with erosive studies of polypropylene composites reinforced with glass fibers at different sand impact angle (30, 60 and 90) and concluded that erosion wear of the polymer composites depends on the orientation angle mostly between the range of 45–60. An idea on how wear behaves and its effect on material properties have discoursed sufficiently. An intuition to understand the behavior of wear from testing is always challenging as they are not tested under a similar environment and hence there might be a scatter in the data due to environmental exposures. Therefore we shall discuss the standard testing procedures followed for the wear test in the following session.

5 Wear Test and Characterization

The difficulty of replacement, repair, and maintenance of industrial tools and equipment has become so tedious and hence there is a decline in production due to wear. In more detail, erosion wear is one of the categories of wear mostly observed in industrial applications. As a result, standard wear testing procedures have developed. However, there is inadequate work pertaining to the erosive wear behavior of the polymer composites. This is due to the composite characteristics such as particle size, fiber content, impingement angle, impact velocity, and temperature. Works from (Harsha et al. 2003; Tewari et al. 2002) have experimentally confirmed that natural fiber polymer composites semi-brittle behaviors when tested for an erosion wear behavior. This is because of the non-uniform distribution of the filler in the polymer matrix which induces large voids yielding severe premature cracks. This measurement is very crucial in determining the strength of the composite material that enables scientists to establish a proper structure–property correlation. Next to that, the experimental conditions such as impact angle, erodent shape, and angle and erodent flux rate, etc. have a crucial role in altering the wear behavior of the composites. Since the matrix is removed first, the erosion characteristics of resin materials are the prime factor for the resistance of composites.

Pin on the Disk wear test is the standard test procedure followed by the scientific community to evaluate the wear behavior of polymer composites. Setup pertaining to PoD can be seen in Fig. 4 as shown below which is retrieved from Zdero et al. (2017). More detailed information can be retrieved from the citation. The procedure followed by the PoD wear test is categorized in stages as.

1. Methodology
2. Materials and tool list
3. Specimen preparation
4. Specimen testing
5. Raw data collection
6. Raw data analysis
7. Results.

The results contain weight loss and average surface roughness, gravimetric wear rate (steady-state wear rate) followed by illustrative wear patterns.

The most interactive and powerful experimental techniques such as scanning electron microscopy (SEM) and atomic force microscopy (AFM) which provide deeper insights into the microstructure on which physical properties of the polymer composites depend. The important observations that are needed to be observed during the microstructural evolution of polymer composite behavior include changes to individual macromolecular segments (on a nanometer scale), localized plastic yielding in the form of crazing or shear bands (at the micrometer scale), up to crack propagation and macroscopic fracture (at the millimeter scale) as shown in Fig. 5.

The easiest way is to study composite materials is to produce a brittle-fracture surface as it can give a clear picture by eliminating the plastic deformation that

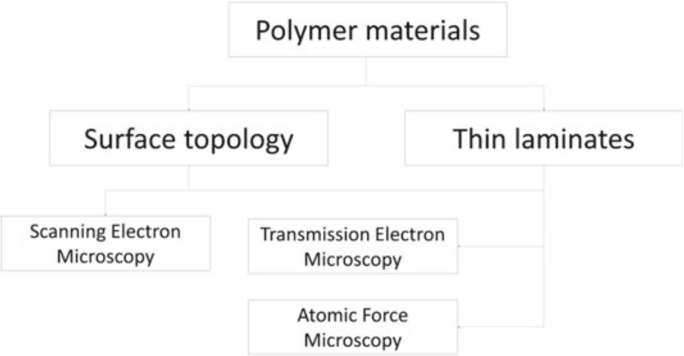

Fig. 5 Microscopy process of polymer composites

hides surface morphology. This is achieved at low temperatures (equivalent to liquid nitrogen). But still, there are complexities to locate the hard filler particles in a matrix visible, to overcome this complexity, soft matrix fracture, a fracture phenomenon at elevated temperatures enables hard filler particles visible. Evidence to this context, (Srivastava et al. 2020) calibrated the visibility of inorganic filler particles in a PP matrix on fracture surface using SEM for Acrylonitrile butadiene styrene (ABS) thermoplastic polymer composite which can be visualized in Fig. 6.

To enhance the contrast of the structure, there are various techniques but the simultaneous evaporation of platinum/carbon film has proven to be the best. SEM investigations have the advantage of revealing morphology and micromechanical properties that enable researchers to establish structure–property relations at ease. A figure to overview this understanding is given in below Fig. 7 that emphasizes the micromechanical processes in polymers (Greenhalgh 2009).

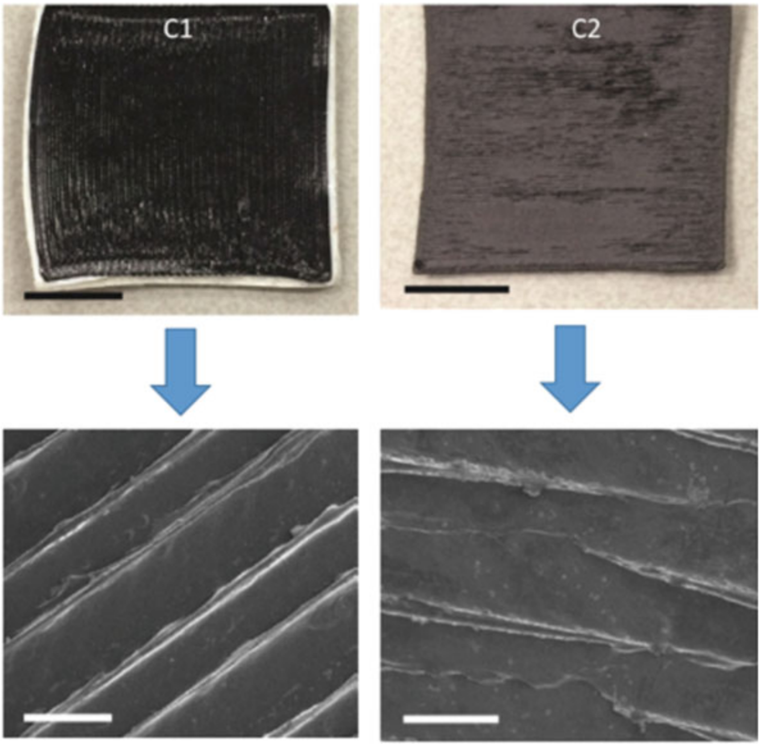

Fig. 6 SEM 3D-printed monolayer of polybutylene terephthalate (PBT)/CNT composite (C1) and PBT/graphene composite (C2) with their SEM images (Srivastava et al. 2020)

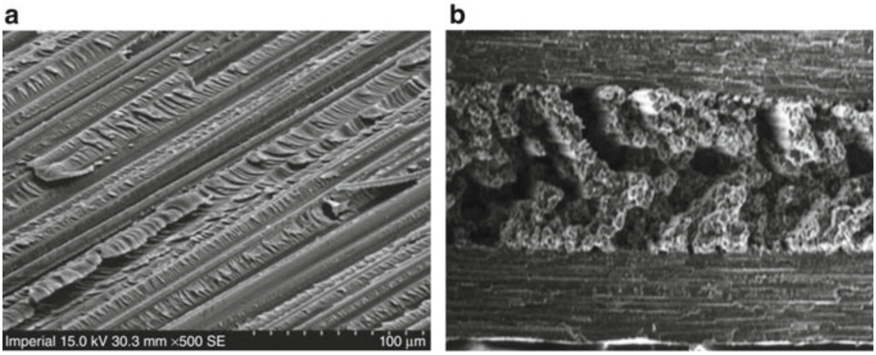

Fig. 7 Micromechanical processes in polymers **a** Fracture surface for high tilt (55°) **b** cross ply laminate failed in tension (Greenhalgh 2009)

6 Structural Hierarchy and Enhancement of Wear Resistance of Polymers

Classification of polymeric materials shows a wide variety of molecular hierarchy such as structures ranging from 0.1 nm to 1 mm orders of magnitude. It includes molecular level 0.1 nm, microscopic 10 nm, mesoscopic level 1000 nm, and macroscopic level > 0.1 mm scale. In realizing the relationship between the micro and macroscopic mechanical properties, the constitution influences polymerization, configuration, and conformation influences processing temperatures and free volume influences yield stresses of the polymers. With an increase in the molecular weight, the strength of the polymer increases with a sharp increase at critical molecular weight, this is because of the rest molecules that help to form entanglements in the amorphous interlamellar regions and the defects therein (Michler 2008). In conjunction with this statement, the following Fig. 8 refers to the defects and entanglements of the polymer.

For the polymer composites, the presence of fewer weak entanglements of polymer chains suggests that the polymer has better strength. Whereas the toughening of the polymer composites depends on interfacial strength, void formation, and deformability of interparticle matrix strands which in detail is discussed in Lednicky and Michler (1990).

Enhancement of wear resistance of the polymer composites has received ample attention in the materials community due to their intriguing properties such as high strength to weight ratio, corrosion resistance, and thermal resistance, as a result, a compromise in the wear of the composites have been constrained the limitations for the applications. To surmount this hierarchy, nanocomposites have been introduced extensively to the material group which enhanced the Tribological properties of polymer composites to a greater extent. We shall in the current context discuss few works from the literature and work carried out by the composites group from the authors' experience. The synergism required to add Nano fillers into polymers has

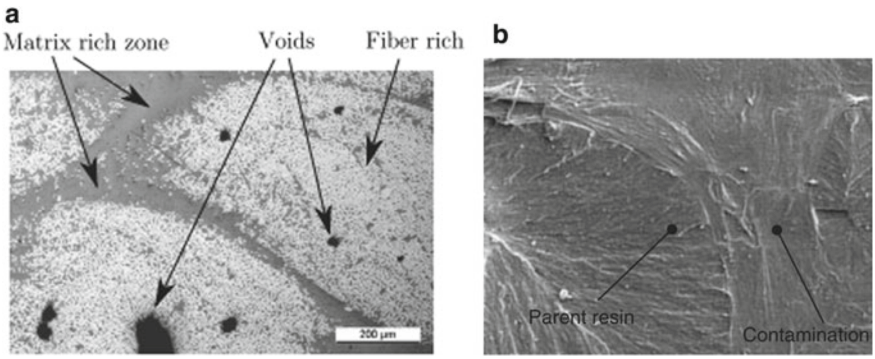

Fig. 8 **a** Defects (Vajari et al. 2014) and **b** entanglements of the polymer composite (Greenhalgh 2009)

to satisfy the size of the nanoparticle filler, the number of filler particles, and the interfacial area. These three natures can be visualized in the following Fig. 9 as follows (Michler 1999; Robertson 1976; Fukushima and Inagaki 1987; Giannelis 1996).

Based on the filler particle dimensions, nanocomposites are classified as Zero dimensional fillers, one-dimensional fillers, two-dimensional fillers, and three-dimensional fillers. An excellent review of the intrusion of filler particles into polymers has been cited in Friedrich et al. (2005) is listed below in Table 2 along with the respective micrograph as shown in Fig. 10

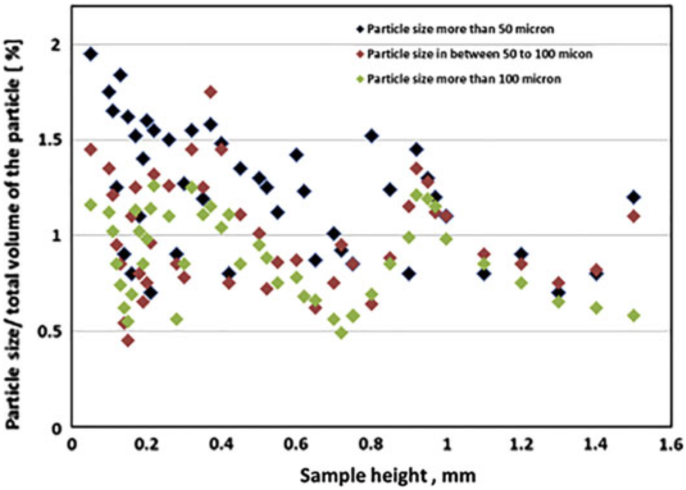

Fig. 9 Nature of filler particles and their percentage of intrusion as a function of shape and size/volume (Samal 2020)

Table 2 Various fillers for polymer composites and their wear behavior (Friedrich et al. 2005)

Material composition (Vol%) Specific wear rate (10^{-6} mm/Nm)							
PTFE	PPS	PEEK	Graphite	CF	Bronze	Al_2O_3	
51.6	31.8	–	4.8	11.8	–	–	1.53
51	31.6	–	3.9	13.5	–	–	1.40
51.9	32.4	–	2.6	13.1	–	–	1.20
12.4	–	61.8	11.7	14.1	–	–	4.31
9.7	–	49.7	12.5	28.1	–	–	6.33
76.8	–	–	19.8	–	–	3.4	22.40
84.1	–	–	–	12.6	–	3.3	1.25
52.5	28	–	–	19.5	–	–	1.69
78.6	–	–	–	21.4	–	–	1.75
80	–	–	–	10	10	–	0.565

Block-on-Test-ring tests. Testing conditions $p = 2$ Mpa; $\vartheta = 1$ m/s; $T = Rt$; $t = 8$ h; counterpart: steel

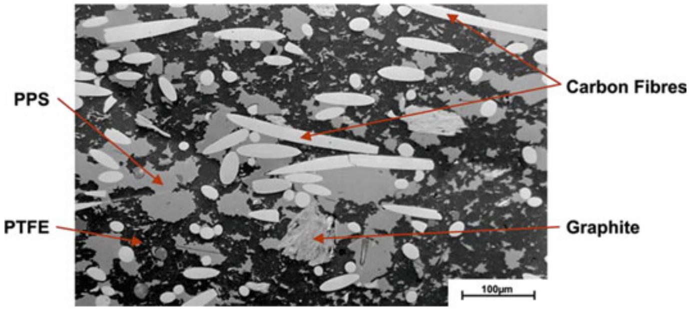

Fig. 10 Micrographs of various filler particles (Friedrich et al. 2005)

7 Case Study

An extensive Work from Prakash et al. (2020) on investigation of Tribological properties of porous nano activated carbon has been discoursed. The paper credits the enhancement of wear resistance of composites by 106% by inclusion of 1% of nanocarbon and more importantly irrespective of percentage of carbon content (1–3%), composites exhibited semi ductile erosion wear behavior. These composites were tested for solid particle wear on the sand erosion test rig as per ASTM G76 standards with 200 μm size of silica as erodent. After finishing the test, the samples were cleaned with acetone and are weighed to near accuracy of 0.001 mg. The author concluded with previous investigations that due to proper arrangement of filler particles, the wear resistance has shown substantial improvement which can be attributed to impressive mechanical properties as shown in Fig. 11.

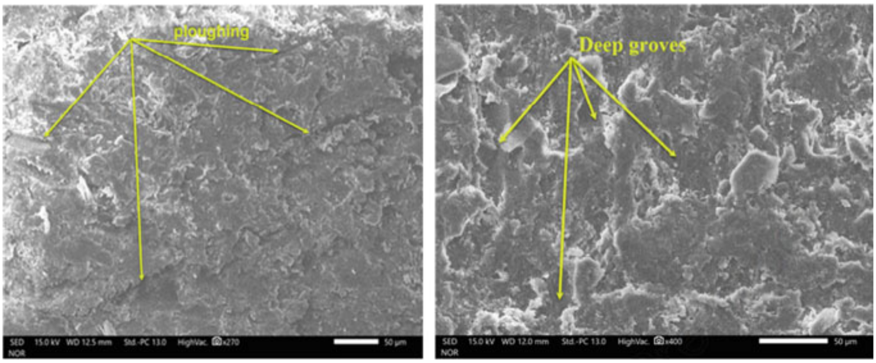

Fig. 11 SEM Micrographs of ploughing and deep groves for 2 wt% porous activated nano carbon (Prakash et al. 2020)

From the SEM observations, further increase in the carbon content will decrease the wear resistance and this is attributed to poor interfacial bonding and wettability. Thus as discussed earlier, it is important to realize proper content of filler that a polymer can accommodate to enhance the properties of the composite. The paper also credits the impact of load on the wear rate, after a suitable load (for an instance in the current work 20 N) led to increase in wear rate, and upon increasing the abrasive particles deeply penetrate in the material causing removal of material. These worn surfaces have deep groves just as shown in Fig. 12 above and respective detached filler particles in Fig. 12 below.

Another work from Ojha et al. (2014) have investigated wear behavior of carbon filled polymer composites and found that carbon black particulates showed excellent wear as compared to raw particulate composite and semi-ductile failure as discussed earlier in the beginning of the chapter have been reported indicting the enhancement

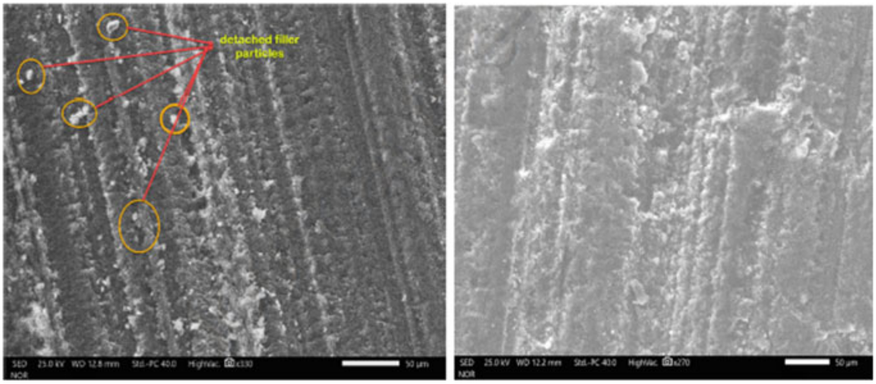

Fig. 12 SEM Micrographs for 2% carbon reinforced composite (particle detachment-left), ploughing (right) (Prakash et al. 2020)

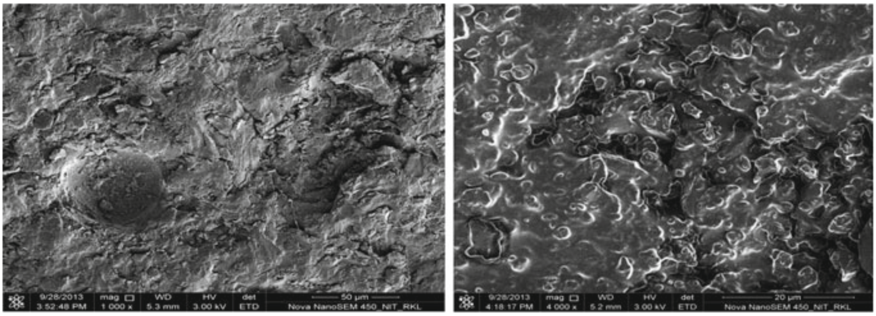

Fig. 13 SEM Micrograph for carbon black filer polymer composite (right) and raw composite (left) (Ojha et al. 2014)

of mechanical properties. It is conferred that with 10 wt% filler composite has shown good interfacial bonding between fibre and composite material whereas after adding 20 wt% of carbon black particulates the surface has become hard compared to raw composite due to increase of carbon composites as shown in Fig. 13.

8 Conclusions and Future Scope

Polymer composites show excellent mechanical properties when compared to the Tribological wear properties. But their provision to enhancement of these properties has processing advantage. Hence a wide range of opportunities in terms of filler materials can be added at a suitable percentage to the polymer chain that can accommodate the third party filler particles into the matrix that can exhibit excellent wear resistance alongside improving the other mechanical properties. These materials poses excellent wear materials has huge potential for the aviation, automobile and biomedical industries. A foresee to improve more advanced materials where wear is expected to have inherently the best that can simply be altered by just processing parameters. These materials sometimes referred to be as Functionally Graded Materials (FGMs) and smart materials.

References

Aghababaei R, Warner DH, Molinari JF (2016) Critical length scale controls adhesive wear mechanisms. Nat Commun 7(1):1–8

Ammar IM, Huzaifah MRM, Sapuan SM, Ishak MR, Leman ZB (2018) Development of sugar palm fiber reinforced vinyl ester composites. In: Natural Fibre Reinforced Vinyl Ester and Vinyl Polymer Composites (pp 211–224). Woodhead Publishing

Ang KK, Ahmed KS (2013) An improved shear-lag model for carbon nanotube reinforced polymer composites. Compos B Eng 50:7–14

Bennewitz R, Dickinson JT (2008) Fundamental studies of nanometer-scale wear mechanisms. MRS Bull 33(12):1174–1180

Bhushan B, Israelachvili JN, Landman U (1995) Nanotribology: friction, wear and lubrication at the atomic scale. Nature 374(6523):607–616

Bhushan B, Kwak KJ (2007) Velocity dependence of nanoscale wear in atomic force microscopy. Appl Phys Lett 91(16):163113

Cirino M, Pipes RB, Friedrich K (1987) The abrasive wear behaviour of continuous fibre polymer composites. J Mater Sci 22(7):2481–2492

Erenkov OY, Igumnov PV, Nikishechkin VL (2010) Mechanical properties of polymer composites. Russ Eng Res 30(4):373–375

Friedrich K (2018) Polymer composites for tribological applications. Adv Ind Eng Polym Res 1(1):3–39

Friedrich K, Zhang Z, Schlarb AK (2005) Effects of various fillers on the sliding wear of polymer composites. Compos Sci Technol 65(15–16):2329–2343

Fukushima Y, Inagaki S (1987) J IncluPhen 5: 473–482. In: Fukushima Y, Okada A, Kawasumi M, Kurauchi T, Kamigaito O (eds) (1988) Clay Miner 23, pp 27–34

Giannelis EP (1996) Polymer layered silicate nanocomposites. Adv Mater 8(1):29–35

Gnecco E, Meyer E (eds) (2015) Fundamentals of friction and wear on the nanoscale. Springer, New York

Gotsmann B, Lantz MA (2008) Atomistic wear in a single asperity sliding contact. Phys Rev Lett 101(12):125501

Greenhalgh E (2009) Failure analysis and fractography of polymer composites. Elsevier

Greenwood JA, Williamson JP (1966) Contact of nominally flat surfaces. In: Proceedings of the royal society of London. Series A. Mathematical and physical sciences 295(1442):300–319

Halliday JS (1955) Surface examination by reflection electron microscopy. In: Proceedings of the Institution of mechanical engineers 169(1):777–787

Harsha AP, Tewari US, Venkatraman B (2003) Solid particle erosion behaviour of various polyaryletherketone composites. Wear 254(7–8):693–712

Jaśkiewicz R (2019) Comparison of composite laminates machining methods and its influence on process temperature and edge quality. Trans Aerosp Res 2019(4):46–54

Kundalwal SI, Ray MC, Meguid SA (2014) Shear lag model for regularly staggered short fuzzy fiber reinforced composite. J Appl Mech 81(9)

Lancaster JK (1968) Relationships between the wear of polymers and their mechanical properties. In: Proceedings of the Institution of Mechanical Engineers, Conference Proceedings (vol 183, No. 16, pp 98–106). Sage UK: London, England: SAGE Publications

Lanz RW, Melkote SN, Kotnis M (2001) Effect of process parameters and tool shape on the machinability of a particulate filled-polymer composite material for rapid tooling

Lednicky F, Michler GH (1990) Soft matrix fracture surface as a means to reveal the morphology of multi-phase polymer systems. J Mater Sci 25(10):4549–4554

Michler GH (2008) Electron microscopy of polymers. Springer Science & Business Media

Michler GH (1999) Micromechanics of polymers. J Macromol Sci Phys 38(5–6):787–802

Mo Y, Turner KT, Szlufarska I (2009) Friction laws at the nanoscale. Nature 457(7233):1116–1119

Myshkin NK, Petrokovets MI, Kovalev AV (2005) Tribology of polymers: adhesion, friction, wear, and mass-transfer. Tribol Int 38(11–12):910–921

Nuruzzaman DM, Rahaman ML, Chowdhury MA (2012) Friction coefficient and wear rate of polymer and composite materials at different sliding speeds. Int J Surf Sci Eng 6(3):231–245

Ojha S, Acharya SK, Gujjala R (2014) Characterization and wear behavior of carbon black filled polymer composites. Procedia Mater Sci 6:468–475

Omrani E, Menezes PL, Rohatgi PK (2016) State of the art on tribological behavior of polymer matrix composites reinforced with natural fibers in the green materials world. Eng Sci Technol Int J 19(2):717–736

Prakash MO, Raghavendra G, Ojha S, Kumar D (2020) Investigation of tribological properties of biomass developed porous nano activated carbon composites. Wear 203523

Robertson RE (1976) Toughness and brittleness of plastics. Adv Chem Ser 154

Samal S (2020) Effect of shape and size of filler particle on the aggregation and sedimentation behavior of the polymer composite. Powder Technol

Smithies F (1952) Conduction of heat in solids. By HS Carslaw and JC Jaeger Pp. viii 386. 30s. 1947.(Oxford, at the Clarendon Press). The Mathematical Gazette 36(316):142–143

Srivastava VK, Jain PK, Kumar P, Pegoretti A, Bowen CR (2020) Smart manufacturing process of carbon-based low-dimensional structures and fiber-reinforced polymer composites for engineering applications. J Mater Eng Perform 29(7):4162–4186

Tewari US, Harsha AP, Häger AM, Friedrich K (2002) Solid particle erosion of unidirectional carbon fibre reinforced polyetheretherketone composites. Wear 252(11–12):992–1000

Tewari US, Harsha AP, Häger AM, Friedrich K (2003) Solid particle erosion of carbon fibre–and glass fibre–epoxy composites. Compos Sci Technol 63(3–4):549–557

Vajari DA, González C, Llorca J, Legarth BN (2014) A numerical study of the influence of microvoids in the transverse mechanical response of unidirectional composites. Compos Sci Technol 97:46–54

Wang J (1999) Abrasive waterjet machining of polymer matrix composites–cutting performance, erosive process and predictive models. Int J Adv Manufact Technol 15(10):757–768

Zdero R, Guenther LE, Gascoyne TC (2017) Pin-on-disk wear testing of biomaterials used for total joint replacements. In: Experimental methods in orthopaedic biomechanics (pp 299–311). Academic Press

Friction and Wear of Polymer and Polymer Composites

Ahmed Abdelbary

Abstract Friction and wear of polymers and their composites introduce further difficulty that polymers are simply affected by working conditions and sliding media. The disagreement between friction in polymers and metallic friction is resulting from the alterations in the elastic and plastic behavior of metallic materials and the viscoelastic performance of polymeric materials. It is expected that, compared to metals, polymers are easily to meet elastic distortion when in contact. The wear mechanisms are described through extensive categories: abrasive, adhesive, surface fatigue, and others. The influences controlling friction and wear of polymers are broadly argued. There are various mechanisms governing the tribological behavior of the polymer moving on metal tribosystems including transfer film, wear regimes, and *pv*-limit. The basics of polymeric composites and how numerous compositions and structures can affect their tribological behavior are explained.

Keywords Friction · Wear · Polymer · Polymer composites

1 Introduction

Polymer and polymer composites are being used progressively in numerous tribological applications. This is essentially resulting from the fact that they have significantly low resistance for friction and wear. For many reasons, tribology of polymeric materials and their composites is dissimilar from tribology of metallic materials. Polymer materials are viscoelastic and consequently, their properties are time dependent. Lubrication by external fluid, which typically applied in other types of materials, are simply absorbed by polymers. However, it is an attractive area since polymers can be altered by numerous physical and chemical processes to suit specific requests. Therefore, they developed excellent applicants and very hopeful materials for engineering with a capability to adjust their tribological behaviour. This results in several tribosystems containing polymers, metals (or non-metals) in either sliding or rolling interactions.

A. Abdelbary (✉)
Egyptian Government, Alexandria, Egypt

H. Jena et al. (eds.), *Tribology of Polymer and Polymer Composites for Industry 4.0*,
Composites Science and Technology, https://doi.org/10.1007/978-981-16-3903-6_3

2 Friction of Polymer

The difference between friction of polymers and metals is according to the alterations in the elasticity properties of metallic materials and, on the other hand, the viso-elastic properties of polymeric materials. The main mechanisms that would be regarded in reviewing friction for materials, including polymeric materials, are *Adhesion* and *Deformation.* The formation and failure of interfacial junctions during sliding action are affected by the state of areas of contact, chemistry of surface, and stress at the layers of the surface. Given that, at contact, the real area at the asperity is $A_{r1.}$ According to friction law (Tabor 1982), the force of shear F_a that oppose movement can be calculated from:

$$F_a = \tau_s \cdot A_{r1} \tag{1}$$

where τ_s represents the required shear stress to make sliding for the matting counterparts, which matches with the adhesion bonds at the interface of asperities and the shear strength of the polymer. For nearly all of the thermoplastic, the strength behaviour are of the same value. It also alters with temperature, specifically close to *Tg* "glass transition temperature".

Deformation, on the other hand, is formed by stiff peaks on the counterface digging (plastically) into the softer polymer surface producing grooves. The foremost feature contributes the deformation is the mechanical energy dissipation. Usually, this deformation be contingent to sliding conditions, mechanical properties, sliding media and other factors. The deformation characterized by ploughing action is related to the other friction constituent, F_d, given by:

$$F_d = \sigma_y \cdot A_{r2} \tag{2}$$

where σ_y is the yield pressure of polymer and A_{r2} is the groove area.

In the situation of polymer-metallic sliding system, the material is ploughing from the rubbing surface of polymer to metal counterface. After appropriate distance of sliding, the friction becomes as that of polymer–polymer sliding. Accordingly, the transfer film which generates on the counterpart results in the adhesion component of friction for polymer significantly exceeds the component of deformation (Briscoe and Sinha 2013). Nevertheless, it is not an easy to separately explore the influences of both friction components. Also, many experimental investigations supposed that it is frequently adequate to reflect that friction is the summation of the estimates of asperity deformation and, F_d, adhesion, F_a, terms; henceforward, the overall force of friction F becomes:

$$F = F_a + F_d \tag{3}$$

Equation (3) shows that the first term is the further significant with metals. However, in the case of polymers sliding against rough hard surface, or in the existence of a fluid lubrication. The deformation component may, also, become rather important. The role of the influence of both of each component to the overall force of frictional correlates to the form of motion (sliding or rolling), the topography of surface and mechanical characteristics of the polymer.

Involving the friction coefficient to the mechanical characteristics of a polymer moving against metal is not an easy issue. A hypothesis that should be considered is that all the deformation terms are insignificant and that each of the matting surfaces are smooth. The force of friction, therefore, is:

$$F = \tau_s \cdot A_r \tag{4}$$

where

A_r real contact area.

If the asperities are under a stress that is enough to make plastic distortion, the area will be $A_r = \frac{L}{p}$ where L is the normal load and p is the polymer flow pressure.

Thus, plastic deformation occurs when:

$$\mu = \frac{\tau_s}{p} \tag{5}$$

In case of elastic deformation, the estimation of real contact area becomes problematic and some expectations should be done about the shape, size, and asperities dispersal. Therefore, for elastic deformation:

$$\mu = K \frac{\tau_s}{E^x} \cdot L^{x-1} \tag{6}$$

where

E	Young's modulus.
K and x	and parameters characterize the surface.

Subsequently, it is significant to describe the deformation type which elaborate with polymers. Haliiday (1955) introduced Eq. (7) to conclude an expression involving the mechanical characteristics of a material to the asperity extreme slope angle of an, θ.

$$\tan\theta_{\text{lim}} = K \frac{H}{E} \left(1 - \nu^2\right) \tag{7}$$

where

H Indentation hardness
ν Poisson's ratio
K Constant

The considered values of θ demonstrated that the angle values for polymers are significantly higher than in metals.

3 Wear of Polymer

3.1 Abrasive Wear

Usually, abrasion wear in polymer is produced by hard asperities (peaks) on the counterpart. These asperities penetrate the polymer of soft matting surface and eradicate material. This action results in surface grooves, micro-machining, tearing, ploughing, scratching, and surface cracks, as shown in Fig. 1a. In abrasive wear, the generated debris usually take the form of fine chips or flacks, like those generated in machining, as seen in Fig. 1b.

Usually, the abrasion wear in polymers is related inversely to the product of the elongation-to-break ε_u and the nominal tensile breaking stress σ_u, as shown in Fig. 2. Additionally, the abrasion may relate with its yield strain, cohesive energy, energy-to-rupture, or modulus of flexure (Giltrow 1970). It is established that the abrasive wear action includes shear and plastic deformation while the dominate material property for abrasion is the fracture energy of the polymer (Lancaster 1969).

Various formulas were introduced to calculate the abrasive wear based on the three steps elaborate in the generation of wear debris (Ratner et al. 1964):

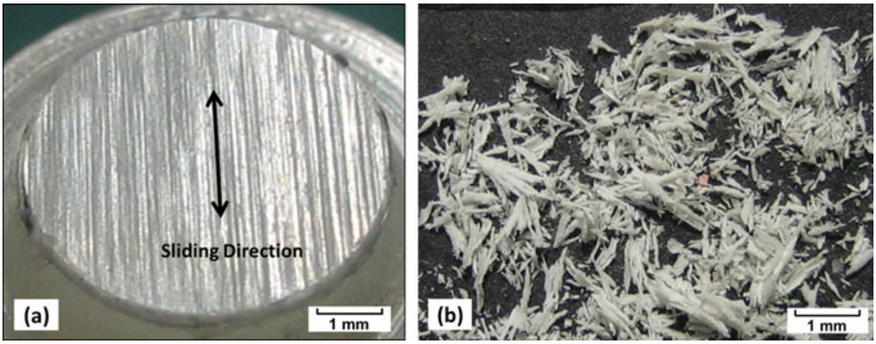

Fig. 1 **a** Worn surface of polymer (PA 66) 66 sliding on dry steel showing surface grooves on the polymer parallel to the path of sliding, **b** Wear debris. Adapted from Abdelbary (2011)

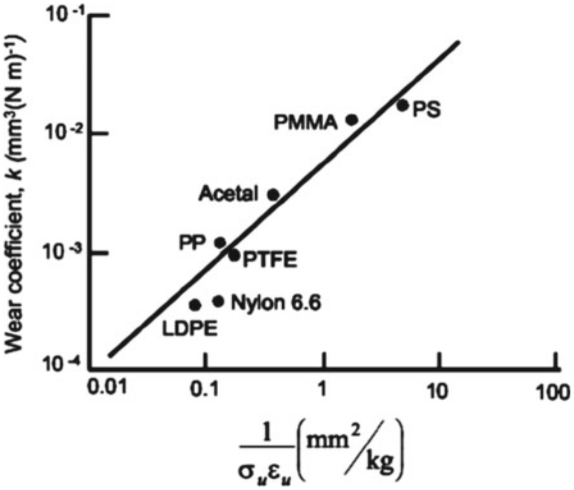

Fig. 2 Ratner–Lancaster correlation for abrasion. Adapted from Lancaster (1969) with permission from Elsevier

(1) Deformation of the polymer surfaces can be introduced by the hardness, H.
(2) Material disruption of at the asperity's interaction.
(3) Motion countered by the friction force (f), $f = \mu L$.

where

L normal load,
μ sliding friction coefficient.

An estimated quantity of the friction force is the multiplication of the failure stress to the elongation to failure. Since the aforementioned processes arise consecutively, the overall wear become related to the possibility of accomplishment of each stage. Consequently, at distance of sliding X, the removed volume, V, can be written as (Lancaster 1969):

$$V = \frac{\mu L X}{H(\sigma_u \varepsilon_u)} \tag{8}$$

The product ($\sigma_u \varepsilon_u$) is correlated to the area under the stress–strain plot, therefore the material impact strength or toughness. So, relationships were pursued between impact strength and abrasive wear. The specific significant of the parameter $\frac{1}{\sigma_u \varepsilon_u}$ has been established. A linear relation between $\frac{1}{\sigma_u \varepsilon_u}$ and the consequential wear through single traversals of diverse polymers was also presented. It is postulated that both breaking strength and elongation are delicate to rate of strain and differences of temperature. Nevertheless, other investigations performed to relate the wear behaviour of a number of polymers to notched impact strength, but the relationship obtained was not considerable.

3.2 Adhesive Wear

This type of wear is occurred when polymer repeatedly slides on a smooth metallic counterface over the same wear track. Subsequent sliding results in a high pressure which experienced between the surface of polymer and the counterpart. Consequently, causes permanent distortion which leads to the establishment of an adhesive bonds. Additional sliding leads to continuous generation and failure of adhesive bonds. As a result, thin film of the soft polymer is adhered on the metallic surface. Since the polymer film builds up, the surface topography of the metallic counterface enhanced and balance situation can be reached.

Additional significance of polymer transfer is an alteration in roughness of both contact surfaces. The polymer surface roughness experiences large differences during the running-in stage until the steady state stage of wear is obtained. On the other hand, metallic counterpart roughness is improved due to polymer transfer. In several situations, adhesive wear is not related to the roughness and may occur in rough surfaces as well as smoothers.

Investigations were performed to examine the wear of polymer (PA 66) moving on dry steel and stainless steel (Abdelbary 2011). Through the running-in phase, the polymer film thickness increases with sliding distance until a limiting value. It is concluded that the maximum thickness of the polymer transfer film is possibly a characteristic feature of each of the rubbing surface and operating variables, as shown in Fig. 3.

Fatigue wear

It has been known as a significant wear type that occurs when the polymeric material experiences frequent stressing during reciprocating sliding or rolling motion. Individual asperity of polymer rubbing surface undergoes repeated loading/unloading cyclic from asperities on the hard counterpart. The cyclic loading phase led to a generation of subsurface crack at the polymer surface. Further deformation led to propagation of the formed cracks in a direction parallel to the polymer face. Subsequently, by continued motion, wear debris can be spalled off the polymer. Correspondingly,

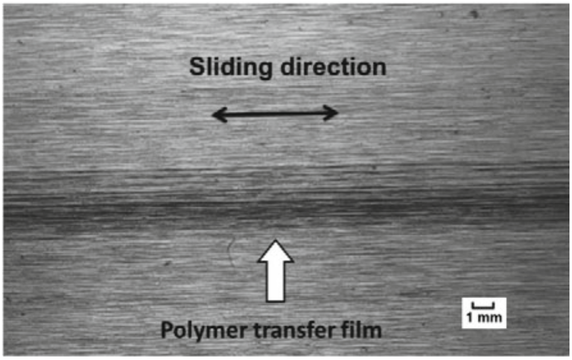

Fig. 3 Polymer transfer film formed on steel counterface showing after 20 km of sliding. Adapted from Abdelbary (2011)

the polymer fresh surface experiences the same repeated stressing which, in turn, leads to advanced action and quick flaking off of debris.

For several decades, researchers focused their work to understanding the fatigue wear mechanisms in polymers and to discover a direct association between the fatigue parameters and the wear rate. These parameters of fatigue include normal applied load, stress cycles number to failure, asperity roundness, friction factor, and modulus of elasticity of both mating surfaces. Equation (9) was introduced (Hollander and Lancaster 1973) to calculate wear factor (*WF*) of polymer based on measurement of the parameters of fracture mechanics which characterizing fatigue crack growth. The fracture toughness k_{IC} is found to be a utmost significant property of material which governs abrasive wear. Consequently, the wear rate should be correlated to $1/k_{IC}^2$. They proposed equation for adhesion-fatigue wear was conducted based on the applying of the linear elastic fracture mechanics concepts to the crack propagation stage of the wear. Given that *WF* is inversely relative to the number of cycles N_f that essential to propagate a crack of a_o length to some critical length. Critical length of crack is defined as "the length at which the peak fluctuating load can detach a wear particle". Consequently, the following relation can be obtained:

$$W F \alpha\, b \cdot a_o^{(n/2)-1} (\Delta\sigma_F)^n \pi^{n/2} [(n/2) - 1] \tag{9}$$

where

σ_F peak stress,
b and n empirical constants.

3.3 Other Types of Wear

Fretting Wear: arises in machinery, due to fretting process, where loaded or unloaded polymer suffer continuous vibration. Due to fretting, produced and accumulated wear debris are difficult to escape from the contact and play a vital role in rushing the wear progression by three body abrasion. Finally, this primes the loss of clearance and substantial damage in the mechanical parts. Researches conducted (Guo and Luo 2001; Tan et al. 2011) in order to study the polymers fretting wear in reciprocating sliding on numerous metallic counterfaces established that frequency, amplitude, stress at contact, temperature, and the structure of the material have serious effect on the rate of ferreting wear.

Delamination wear: arises in a way which is rather similar to fatigue wear. However, the mechanisms of delamination wear can be pointed as:

(a) Plastic deformation of polymer surface.
(b) Plastic deformation initiates sub-surface cracks.
(c) Cracks propagate in a direction parallel to the polymer surface.
(d) At a critical crack length, it breaks through to the surface forming detached long thin wear sheets.

Fig. 4 Delaminated polymer (PA 66) at 50 km sliding distance on steel, dry condition. Adapted from Abdelbary (2011)

Microscopic examination of wear sheets shows a flake shape, as shown in Fig. 4. The operation on aggressive environment motives the delamination process by increasing propagation of crack.

Corrosive Wear: this type arises during sliding in a chemical media when both chemical corrosion and classical wear are elaborated. This definite condition can generate overall volume loss that is considerably more than the additive effects of each process taken alone. Usually occurs in two phases;

(I) Chemical corrosion which occurs on the surface of polymer due to chemical environment.
(II) Abrasion due to sliding action take away the corroded outer layer. Subsequently, the new face will expose to progressive chemical reaction, and the wear progress is augmented by abrasive process.

4 Factors Contributing to Friction and Wear

4.1 Applied Load

Generally, mechanisms of wear and friction in polymeric materials differ according to the load. Under high loads, the crucial part in considering the actual area of contact of the polymer is the permanent deformation arises at the interaction of the asperity and thermal softening. For numerous polymers, it is demonstrated that at high loads (10–100 N), the coefficient of friction is constant (Bowers et al. 1953; Shooter and Tabor 1952). On the other hand, at lower loads (0.02–1 N), the surface deformed elastically and asperities administer the sliding action with a consequent increase of the friction (Rees 1957). It can be concluded that the impact of load on the sliding friction coefficient of polymer matches to change from the elastic to plastic contact.

Likewise, we should consider that the rise in polymer sliding temperature due to applied load can has a further influence on the visco-elastic transitions in polymers and hence the friction mechanism.

The force of friction F and applied load L can be correlated as:

$$F = \mu L^n \tag{10}$$

where μ expresses the friction coefficient and n is a constant (exponential) of a value related to the polymer type (ex.: Polyamide $n = 0.8$ and Cellulose acetate $n = 0.96$).

Several efforts were conducted in order to introduce a formula for the wear-load relationship. As one of these equations, Eq. (11) was presented by Archard (1959) to find a relation between the worn volume (V) and both load (L), hardness (H), and sliding distance (x).

$$V = k\frac{Lx}{H} \tag{11}$$

The expression is generally believed for metals and a number of polymers. Nevertheless, in some specific situations, the wear factor *WF* exponentially rises with load. Therefore, the correlation between wear parameter and applied load could be contingent on the parameter *n*, consequently the direct straight correlation will occur at *n* $\cong$ 3 (Bijwe, Sen, & Ghosh, 2005).*

$$WF \propto L^{\frac{n}{3}} \tag{12}$$

The linear relationship of wear in metals suggests that *WF* is independent of contact pressure and, in polymers, it may only be an estimated relationship. This can be attributed to the viscoelastic properties of the bulk polymer. When thermoplastic polymers become contacted to a metallic counterpart, actual contact is only limited near rough surface peaks. Under such high pressure, the number of localized spots grows and also increases spot sizes. At enormously high contact pressures, it would be considered that the area of real contact approaches the area of apparent contact, consequently the impact of micro-asperity is minor.

Reviewing the consequence of contact pressure on is an fascinating research topic for many researchers. Kar and Bahadur (1978) reported that the contact applied pressure in polymers is the main cause for rising temperature in various viscoelastic transitions. At relatively low pressures, consequently small frictional heating, the polymer wear rate becomes comparative to the normal pressure. Whereas, the rate of wear abruptly rises at higher applied pressure. This can be due to the prospect of thermal influences at the asperity contact. The thermal heating is sufficient to make softening or melting of the polymer rubbing surface (Barbour et al. 1995).

4.2 Sliding Speed

In tribosystems of polymer-metal combination, the consequence of speed is to raise the rate of wear due to an increase in interfacial temperature of the rubbing surface. Though, in thermoplastics there is a speed limits over which the localized (flash) temperature can be reached. Accordingly, the rate of wear decreases somewhat due to thermal softening and surface melting. The instantaneous flash temperature at the asperity tip is usually produced by adhesive friction. Nonetheless, it is problematic to measure the instantaneous temperature during sliding (or rolling) with acceptable precision. This would give an explanation for the complicated dependence of the coefficient of friction μ on the polymer sliding speed compared to metals. The high dependency of the coefficient of friction on the sliding speed is detected when the polymer temperature approaches the glass-transition temperature (Ainbinder and Tyunina, 1974). Yet, at lower temperatures, there is no significant dependence on the sliding speed. Stability and thickness of transfer film is also influenced by the speed of sliding. Excremental results performed to investigate the connection between sliding speed and wear represent in Figs. 5 and 6 (Byett and Allen 1992; Unal et al. 2004).

Fig. 5 Wear of Derlin slids (dry) on steel counterface, $v = 0.1$–0.7 m/s. Adapted from Unal et al. (2004) with permission from Elsevier

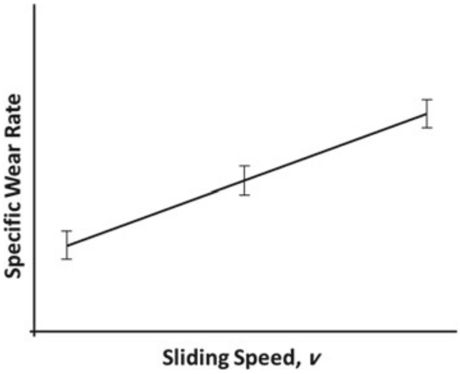

Fig. 6 Friction coefficient (μ) against sliding speed for selected polymers. Adapted from Unal et al. (2004) with permission from Elsevier

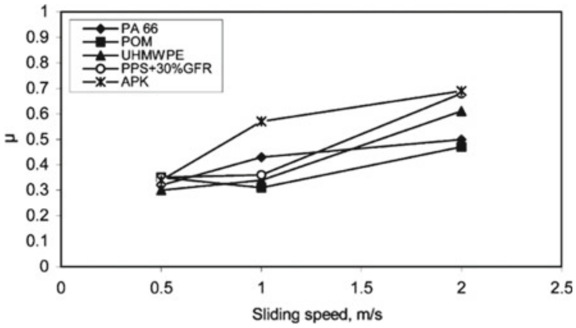

4.3 Counterface Roughness

Surface topography investigations have demonstrated an evidence of a strong relationship between the roughness of the metallic counterface and tribology of polymers. It is extensively recognized that the friction resistance and the wear mechanism of polymers are administered by the surface roughness. In polymer/metal tribosystem, as the counterface roughness reduced the coefficients of friction decrease. Nonetheless, at a limiting value of R_Z (the mean peak-to-valley) further decrease in the roughness may cause a high friction. In such cases, the force of adhesion become the leading contributor, while abrasive wear prevails in higher surface roughness.

Generally, it was assumed that smooth counterpart resulted in a minor wear rate in polymers. Nevertheless, earlier work (Dowson et al. 1985) showed that there is an optimum degree of surface roughness which leads to a lowest wear for a polymer (polyethylene) sliding on dry stainless steel, as shown in Fig. 7. The roughness has an effect on the type of accumulated polymer film and it is probably that high rates of wear detected in very fine surfaces are caused by polymer adhesion "lumps". This finding is possibly very significant specially in biomedicals. For example, in artificial hip joint, as the distinctive roughness (R_a) of the femoral head is (0.02–0.05 μm), which obviously rises the charge of such bonds as they have to be exposed to prolonged refining processes.

The wear behaviour of a number of polymers were considered in pin-on-disc tribometer (Bellow and Viswanath 1993). The polymer specimens are slide on steel (AISI 1018) counterface with a roughness, R_a, ranging from 0.05 to 0.4 μm. It is found that wear rate of Teflon and high-density polyethylene increases with the increase of counterface roughness. Though, the experimental findings did not show any indistinct connection between wear and surface roughness. In contrast, as the counterface roughness increased, the friction coefficient decreases with an increase

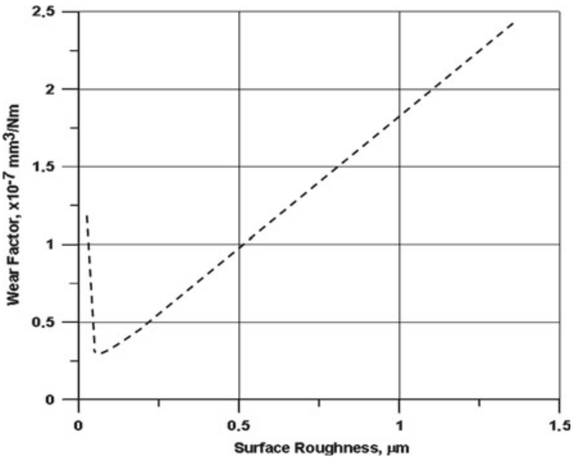

Fig. 7 Relation between surface roughness, R_a, in (μm) and wear factor, WF, in (mm^3/Nm). Dry sliding of polyethylene on stainless steel

in wear volume. It was also indicated that, in some special cases, the polymer layer transferred to the metallic surface contributes to alteration in the surface topography.

Furthermore, it is established that a single imposed imperfection, either transverse or longitudinal scratches, upon the metallic counterface has a perceptible consequence on the wear rate of ultra-high molecular weight polyethylene UHMWPE (Dowson et al. 1987). It is postulated that a single scratch on the metallic countersurface, transverse to the sliding direction, can increase the polymer wear rate to one order of magnitude, at least. This is due to the piled-up metallic material flanking each transverse scratch after the ploughing action. Such scratches, on a femoral head of artificial hip joint, that may be resulted from bone fragments and act as "third body" particles.

5 Polymer Sliding Mechanisms

5.1 Transfer Film Formation of Polymer

When a polymeric material slide against a dry metallic countersurface, adhesion bonds formed between the rubbing surfaces. If these bonds become tougher than the cohesive strength of the polymer, some fragments of the polymer material will transfer onto the metallic counterface as a transfer film. On the Other hand, other parts of the worn polymer, are removed generating wear debris. Progressive transfer of polymer occurs and bands formation by the accumulation of wear fragments. As sliding progresses, the transfer film grows in length and bands widen. The film may be in the form of a continuous uniform layer or can be as irregular lumps adhered to the metallic counterface.

During the running-in wear, the polymer surface roughness experiences great variation until reaching the steady state wear. Moreover, the counterface roughness is improved due to the polymer film. After sliding period, an equilibrium state is achieved.

On the other hand, in lubricated sliding, the washing action of lubricant fluid inhibit the formation of polymer film. The polymer wear rate in such cases is six-times higher compared to those in dry condition (Abdelbary 2014).

5.2 Wear Regimes

In almost of polymer/metal tribosystems, when a polymer worn volume V is plotted versus the distance of sliding X, the resulted wear curve is usually containing two distinct regimes. The first phase is termed "*Running-in*" or "*Unsteady State*" wear. This regime is associated to the removal of the initial highly residual strain layer of surface of the polymer. The second regime, "*Steady-state*" wear where the polymer

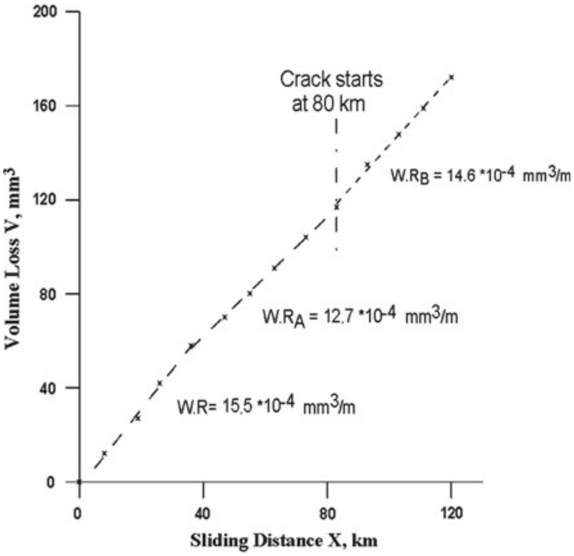

Fig. 8 Section-B wear of polyamide (PA 66) sliding on steel. Adapted from Abdelbary (2011)

is worn in a uniform and steady mode in a relatively lower and linear wear rate. This regime is also distinguished by formation of a stable transfer film layer of polymer. However, Dowson et al. (Atkinson et al. 1985; Brown et al. 1974) reported another (third) wear regime termed "*Section B*" arises after prolonged (120–150 km) of sliding distance characterized by a remarkable increase (about 10:30%) in the wear rate. Section B wear is assumed to be a surface fatigue which occurs after a certain sliding distance.

Abdelbary et al. (2011) found that the existence of a single transverse crack upon the rubbing surface of the polymer also resulted in the generation of Section B wear, as shown in Fig. 8. These finding establishes the significant of detection of surface fatigue cracks in polymer/metal bearings which play a role in increasing the wear of sliding components.

According to abovementioned argument, three distinct regimes are now recognized for representing a typical wear stages in polymers: running-in, steady-state and accelerated wear. Where in the accelerated wear stage the wear rate increases exponentially resulting in fatigue failure, as presented in Fig. 9.

5.3 *Surface and Subsurface Cracks*

In sliding (or rolling) of thermoplastic polymers on hard counterfaces, individual surface peaks practises experience a repeated stress from counterface peaks. As a result, plastic strain and stress cycling accumulate and ultimately initiate many subsurface and surface cracks. These cracks deeply propagate into the substrate and

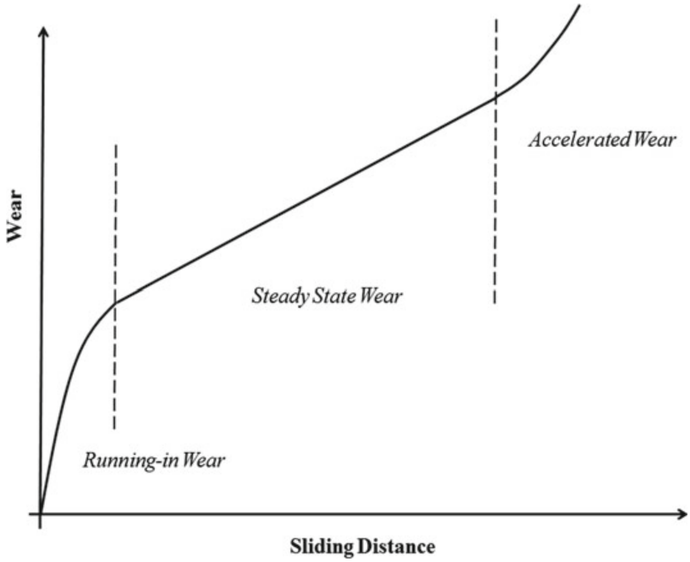

Fig. 9 Wear regimes in polymer tribological systems

join the adjacent cracks. This action generates a large crack that can break from the bulk producing spalling and pitting. The process endures, leading to an advanced loss of polymer. The locations of crack initiation are related to the form of loading exerted on the surface as well as the sliding conditions that exist in the tribosystem during this exertion (Terheci 2000).

5.4 pv-*Limit*

The upper perimeter of operation is a significant parameters of the rubbing limitation beyond which a catastrophic or severe wear of polymer may arise. Lancaster ("Lancaster JK (1971) Estimation of the limiting PV relationships for thermoplastic bearing materials. Tribology, 4(2):82–86; 6 figs., 8 refs," 1972) defined the *pv* limit as "the value above which the wear rate increases rapidly". This perimeter is frequently standing on the extreme acceptable *pv* value.

where

P Contact pressure
V Sliding Speed.

Under regular operating condition, *pv* parameter is usually introduced as a limiting criterion for polymer bearings and characterizes an upper permissible value for the contact pressure against the speed.

Fig. 10. *pv* curve

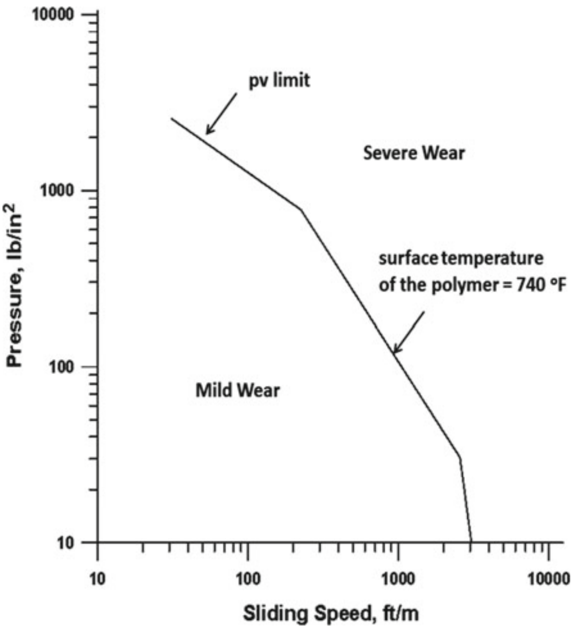

Individually, any polymer has a sole *pv* limit which can be determined by "washer" test. The limiting value is defined when the polymer specimen cannot dissipate the accumulated heat. Consequently, the polymer reaches the point of failure, i.e. surface temperature of the polymer T^* reaches the melting point (Evans and Lancaster 1979). Figure 10 represents a representative *pv* curve of a polymer (PA66) slides on a steel surface. Also, the maximum suggested *pv* values of selected polymers are presented in Tables 1 and 2.

6 Friction and Wear and of Polymer Composites

The positive implementations of polymers in machinery led to the application of polymeric materials as composites where alteration to their characteristics could be realised by addition of one or more reinforcements. The reinforcement filling materials may take the form of particles and provide a superior mechanical performance. On the other hand, the polymer matrix increases self-lubrication.

Yet, there have been extensive studies investigating the impact of reinforcements on the friction and wear performance of polymeric composites. A general conclusion is that the tribology of polymer composites cannot be an intrinsic property. In fact, it strongly relates to the constituent variables such as the material of fiber, fiber orientation, matrix polymer,… etc. Also, it depends on process variables such as counterface material, normal load, sliding velocity, etc. (Vishwanath et al. 1992).

Table 1 Wear rate for selected polymers at given *pv* values. Adapted from Lancaster (1971), with permission from Elsevier

Sliding conditions			Wear rate of polymer × 10^{-6} mm/N.m			
Speed m.s. $^{-1}$	Pressure MPA	*pv* value MPa m.s^{-1}	PTFE	Acetal	UHMWPE	Nylon 66
0.25	0.28	0.07	20			4
0.10	1	0.10	800			
0.01	1.4	0.014	107	2.8		5.8
0.10	5	0.50		1.5	0.50	20
0.24	2.5	0.606			0.25	
0.25	5	1.25		2.1		16
0.24	10	2.4			0.20	
0.24	10	2.4			0.27	
0.25	10	2.5		12	0.51	
12.4	0.15	1.86			2.9	

Table 2 Some suggested *pv* limits for selected polymers. Adapted from Franklin (2001), with permission from Elsevier

Name	Polymer	Maximum *pv* (N/m.s)
POM	Polyoxymethylene	130,000
POM + 30%GF	POM + 30% glass-fibres	350,000
POM + 20%PTFE	POM + 20% polytetrafluorethylene	400,000
PA6.6	Polyamide 6.6	90,000
PA6.6 + 30%GF	PA6.6 + 30% glass-fibres	400,000
UHMWPE	Ultra-high molecular weight polyethelene	70,000

6.1 Friction and Wear of Fiber Reinforced Polymer Composites

One of the famous typical concepts applied to enhance tribological performance of polymers, is to eliminate their adhesion. Also, to augment their stiffness, compressive strength, and hardness. This could be efficiently realized by introducing several types of fibers. The choice of appropriate fibers is regularly a comptonization among the polymer properties and its tribological behaviour. For instant, polytetrafluoroethylene (PTFE) polymer matrix combines with and fibers made from graphite as internal lubricants to minimize the adhesion. Also, carbon, glass and aramide fibers are applied to improve creep performance and polymer compressive strength (Zhang et al. 2002). Carbon fibers and glass fibers suggestively decrease (up to 50%) the friction coefficient of polyamide composites compared to unreinforced polymer. Also, polymers reinforced with such type of fibers are usually stiffer (1to 4) times than bulk unfilled polymers (Suresha et al. 2010). In addition, the wear rate increases with load by about a factor of 10 over those for unreinforced polymers.

In particular, continuous fiber reinforced polymer composites are presented for a diversity of applications (mechanical, biomedical, and others) due to their excessive wear resistance either parallel or normal to the direction of sliding. When polymer reinforced with continuous fiber slide on a rough surface, the force of friction persuade tensile or combined tensile and shear stresses in the fibers surface, according to the fiber orientation (Ovaert, 1997). Nevertheless, the fiber orientation consequence on the wear rate is depending on the type of composite and the tribological system characteristics (Cirino et al. 1988).

In short fibres reinforced polymer composites with short fiber, the fiber's length is considered as one of the foremost influences contributing the tribological performance. Comparatively longer fibers appeared to be much more operative in enhancing the abrasive wear behaviour of thermosetting polymer composites (Zhang et al. 2002). During wear process, the longer fibers usually become locally damaged by abrasive particles, and the remaining fibers contributed to the wear resistance. Studying the dry sliding of epoxy composites (SCF/EP) reinforced with short carbon fiber, demonstrated that the response of friction and wear is associated to the length of the fibers (Zhang et al. 2007). Friction and wear experiments were conducted using (90 μm and 400 μm) fiber lengths while the polymer matrix was a bisphenol-A type epoxy resin. Fillers were in the form of 20 μm Graphite flakes and particles from TiO_2 with a (300 nm) average diameter of have been applied as additional fillers. Length of the fiber demonstrates different consequence on the wear rate. As the average length of fibers were increased from 67 μm up to 236 μm, a reductio by three times in the wear rate is obtained, as illustrated in Fig. 11.

Fiber orientation is also a vital factor manipulates the tribological conduct of short fiber composites. Typically, a fiber orientation in short fiber composites is achieved often via injection molding technique. Consequently, an isotropic property of the composites along the different fiber directions are obtained.

Fig. 11 Influence of length of fibre on wear of epoxy composites. Adapted from Zhang et al. (2007) with permission from Elsevier

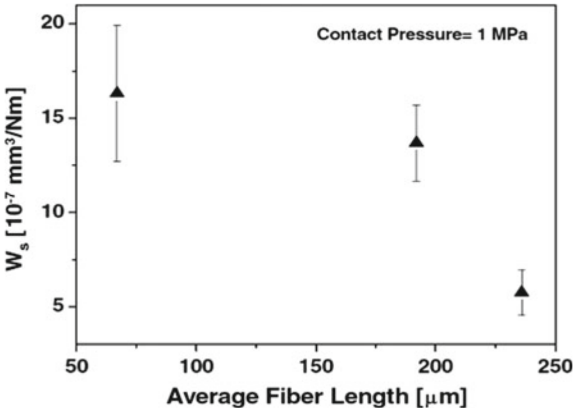

Rasheva et al. (2010) investigated correlation of the tribological behaviour of short carbon fibers/PTFE/graphite filled PEEK composites considering various fiber orientations. The sliding wear tests were performed using block-on-ring tribometer where the tested polymer is loaded in two directions, parallel and perpendicular, with respect to the direction of fiber axis, as illustrated in Fig. 12. Table 3 summarizes the results of wear tests.

The lowest wear rate was detected in the case of composite MB with parallel fiber displays as a consequence of no fiber removal and fiber breakage within the friction zone, as shown in Fig. 13b. On the other hand, in compositions MA and MC there is

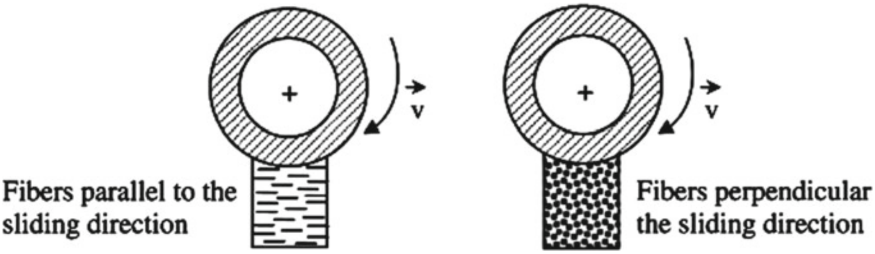

Fig. 12 Fiber orientation in the wear tests. Adopted from Rasheva et al. (2010), with permission

Table 3 Data of wear rates according to the fiber direction. Adopted from. Rasheva et al. (2010), with permission

Material code PEEK/PTFE/Graphite/SCF	Apparent Pressure (MPa	Spec. wear rate parallel (10^{-6} mm^3/Nm)	Relative error (%)	Spec. wear rate perpendicular (10^{-6} mm^3/Nm)	Relative error (%)
MA 70/10/10/10	1	0.554	8.66	0.410	5.85
	4	0.494	6.88	0.367	2.39
MB 65/10/10/15	1	0.413	15.74	0.424	17.68
	4	0.420	5.00	0.468	8.33
MC 75/05/05/15	1	0.501	13.77	0.397	10.30
	4	0.454	11.23	0.525	15.12

Fig. 13 Fibers parallel to the direction of sliding at high pressure **a** MA composite; **b** MB composite; and **c** MC composite. Adopted from Rasheva et al. (2010), with permission

indication of an increased quantity of fiber breakdown, which possess its maximum in case of composite MA, as shown in Fig. 13a. It is assumed that, along the direction of sliding, fibers are pulled out resulting in high wear rate.

Regarding to the Fig. 13c, it can be expected that a combination of less solid lubricant content MC and more fibers content in the direction of fiber with parallel orientation results in high wear. Consequently, if a short carbon fiber with parallel orientation exists (MB composite), the fibers content and the solid lubricant content seem to be almost the same significant. The MB composite, Fig. 13b, shows a smooth abraded surface.

6.2 Friction and Wear of Particulate-Filled Polymer Composites

It is widely agreed that all macroscopic characteristics of polymeric materials rely on the micro- and nano- structure and molecular interactions. Consequently, several inorganic materials (ex. metal powders, oxides, minerals, carbon black, and solid lubricants) were introduced in micro and nanometer sizes as filler materials.

Commonly, such fillers shown a success in minimizing the friction coefficient and also improve the wear resistance. However, in some cases, the introduction of particulate fillers leads to degradation in the wear performance of polymers.

The influences of inorganic particles, for example SiC, Si_3N_4, SiO_2, ZnO, ZrO_2, $CaCO_3$, Al_2O_3, CuO, and TiO_2, on tribology of polymer matrix (PEEK, PTFE, PMMA, and epoxy) have been extensively inspected in numerous publications. A number of fillers demonstrate promising tribological results. For instance, introducing 20 wt% TiO and 40 wt% ZrO_2 fillers distinctly improve the wear of PTFE polymer matrix (Tanaka and Kawakami, 1982). While the frictional coefficient is increased, both fillers can improve the wear resistance of polymer matrix (Sawyer et al. 2003). Also, the addition of 20 wt% Al_2O_3 nanoparticles to PTFE improve the wear rate of the polymer down to about $1.2 * 10^{-6}$ mm^3/Nm.

The filler size has a vital role to enhance friction and wear simultaneously. Smaller fillers have a better contribution to the enhancement of tribological characteristics compared to larger particles. It is demonstrated that a few inorganic fillers at micro size, results in benefits in almost of their usages in tribological applications. Likewise, submicron particles displayed significant effects on the wear performance of polymer composites (Chauhan and Thakur, 2013).

Conclusions

Although polymers and their composites are promising materials for many tribological applications, there are great challenges considering their sensitivity to operating conditions. adhesion and deformation are the main components that should be regarded in reviewing friction for polymers. Abrasive, adhesive, and surface fatigue wear are the principal mechanisms of wear, however other mechanism may also could be expected. There are several factors contributing friction and wear of polymers. Tribological behavior of the polymer/metal tribosystems are governed by a number of mechanisms. Structure and composition of polymeric composites have a substantial impact on the wear and friction behavior.

References

Abdelbary A (2014) 2 - Sliding mechanics of polymers. In: Abdelbary A (ed) Wear of polymers and composites. Woodhead Publishing, Oxford, pp 37–66

Abdelbary A (2011) Effect of vertical cracks at the surface of polyamide 66 on the wear characteristics during sliding under variable loading conditions. PhD, Alexandria University, Alexandria

Abdelbary A, Abouelwafa MN, Fahham IME, Hamdy AH (2011) The influence of surface crack on the wear behavior of polyamide 66 under dry sliding condition. Wear 271(9):2234–2241. https://doi.org/10.1016/j.wear.2010.11.042

Ainbinder SB, Tyunina EL (1974) Friction of polymeric materials. 4. effect of temperature and relative sliding velocity on the coefficient of friction of elastomers. Polym Mech 10(6):905–910.https://doi.org/10.1007/BF00856240

Archard JF (1959) The temperature of rubbing surfaces. Wear 2(6):438–455. https://doi.org/10.1016/0043-1648(59)90159-0

Atkinson JR, Dowson D, Isaac JH, Wroblewski BM (1985) Laboratory wear tests and clinical observations of the penetration of femoral heads into acetabular cups in total replacement hip joints: III: the measurement of internal volume changes in explanted Charnley sockets after 2–16 years in vivo and the determination of wear factors. Wear 104(3):225–244. https://doi.org/10.1016/0043-1648(85)90050-X

Barbour PSM, Barton DC, Fisher J (1995) The influence of contact stress on the wear of UHMWPE for total replacement hip prostheses. Wear 181–183:250–257. https://doi.org/10.1016/0043-1648(95)90031-4

Bellow DG, Viswanath NS (1993) An analysis of the wear of polymers. Wear 162–164:1048–1053. https://doi.org/10.1016/0043-1648(93)90121-2

Bijwe J, Sen S, Ghosh A (2005) Influence of PTFE content in PEEK–PTFE blends on mechanical properties and tribo-performance in various wear modes. Wear 258(10):1536–1542. https://doi.org/10.1016/j.wear.2004.10.008

Bowers RC, Clinton WC, Zisman WA, Naval Research L, Naval Postgraduate S (1953) Frictional behavior of polyethylene polytetrafluoroethylene and halogenated derivatives. Naval Research Laboratory, Washington, D.C. For sale by the Superintendent of Documents, U.S. G.P.O.

Briscoe BJ, Sinha SK (2013) Chapter 1 - Tribological applications of polymers and their composites – past, present and future prospects. In: Friedrich K, Schlarb AK (eds) Tribology of polymeric nanocomposites, 2nd edn. Butterworth-Heinemann, Oxford, pp 1–22

Brown KJ, Atkinson JR, Dowson D (1974) The wear of HMWPE with particular reference to its use in artificial human joints. Polym Sci Technol 5

Byett JH, Allen C (1992) Dry sliding wear behaviour of polyamide 66 and polycarbonate composites. Tribol Int 25(4):237–246. https://doi.org/10.1016/0301-679X(92)90061-Q

Chauhan SR, Thakur S (2013) Effects of particle size, particle loading and sliding distance on the friction and wear properties of cenosphere particulate filled vinylester composites. Mater Des 51:398–408. https://doi.org/10.1016/j.matdes.2013.03.071

Cirino M, Friedrich K, Pipes RB (1988) The effect of fiber orientation on the abrasive wear behavior of polymer composite materials. Wear 121(2):127–141. https://doi.org/10.1016/0043-1648(88)90038-5

Dowson D, Diab MMEH, Gillis BJ, Atkinson JR (1985) Influence of counterface topography on the wear of ultra high molecular weight polyethylene under wet or dry conditions. In Polymer wear and its control, vol 287, pp 171–187, American Chemical Society

Dowson D, Taheri S, Wallbridge NC (1987) The role of counterface imperfections in the wear of polyethylene. Wear 119(3):277–293. https://doi.org/10.1016/0043-1648(87)90036-6

Evans DC, Lancaster JK (1979) The wear of polymers. In Scott D (ed) Treatise on materials science & technology, vol 13, Elsevier, pp 85–139

Franklin SE (2001) Wear experiments with selected engineering polymers and polymer composites under dry reciprocating sliding conditions. Wear 251(1):1591–1598. https://doi.org/10.1016/S0043-1648(01)00795-5

Giltrow JP (1970) A relationship between abrasive wear and the cohesive energy of materials. Wear 15(1):71–78. https://doi.org/10.1016/0043-1648(70)90187-0

Guo Q, Luo W (2001) Mechanisms of fretting wear resistance in terms of material structures for unfilled engineering polymers. Wear 249(10):924–931. https://doi.org/10.1016/S0043-1648(01)00827-4

Haliiday JS (1955) Surface examination by reflection electron microscopy. In: Paper presented at the proceedings of the institution of mechanical engineers London

Hollander AE, Lancaster JK (1973) An application of topographical analysis to the wear of polymers. Wear 25(2):155–170. https://doi.org/10.1016/0043-1648(73)90068-9

Kar MK, Bahadur S (1978) Micromechanism of wear at polymer-metal sliding interface. Wear 46(1):189–202. https://doi.org/10.1016/0043-1648(78)90120-5

Lancaster JK (1969) Abrasive wear of polymers. Wear 14(4):223–239. https://doi.org/10.1016/0043-1648(69)90047-7

Lancaster JK (1971) Estimation of the limiting PV relationships for thermoplastic bearing materials. Tribology 4(2):82–86; 6 figs., 8 refs (1972). Wear, 19(3):364. https://doi.org/10.1016/0043-1648(72)90201-3

Ovaert TC (1997) Wear of unidirectional polymer matrix composites with fiber orientation in the plane of contact. Tribol Trans 40(2):227–234. https://doi.org/10.1080/10402009708983649

Rasheva Z, Zhang G, Burkhart T (2010) A correlation between the tribological and mechanical properties of short carbon fibers reinforced PEEK materials with different fiber orientations. Tribol Int 43(8):1430–1437. https://doi.org/10.1016/j.triboint.2010.01.020

Ratner SB, Farberova I, Radyukevich OV, Lure EG (1964) Connection between the wear resistance of plastics and other mechanical properties. Sov Plast 7

Rees BL (1957) Static friction of bulk polymers over a temperature range. Research 10

Sawyer WG, Freudenberg KD, Bhimaraj P, Schadler LS (2003) A study on the friction and wear behavior of PTFE filled with alumina nanoparticles. Wear 254(5):573–580. https://doi.org/10.1016/S0043-1648(03)00252-7

Shooter KV, Tabor D (1952) The frictional properties of plastics. Proc Phys Soc B 65(9):661

Suresha B, Shiva Kumar K, Seetharamu S, Sampath Kumaran P (2010) Friction and dry sliding wear behavior of carbon and glass fabric reinforced vinyl ester composites. Tribol Int 43(3):602–609. https://doi.org/10.1016/j.triboint.2009.09.009

Tabor D (1982) Friction and wear: calculation methods I.V. Kragelsky, M.N. Dobychin and V.S. Kombalov. Tribol Int 15(5): 283–284. https://doi.org/10.1016/0301-679X(82)90085-8

Tanaka K, Kawakami S (1982) Effect of various fillers on the friction and wear of polytetrafluoroethylene-based composites. Wear 79(2):221–234. https://doi.org/10.1016/0043-1648(82)90170-3

Tan ZH, Guo Q, Zhao ZP, Liu HB, Wang LX (2011) Characteristics of fretting wear resistance for unfilled engineering thermoplastics. Wear 271(9):2269–2273. https://doi.org/10.1016/j.wear.2011.02.029

Terheci M (2000) Microscopic investigation on the origin of wear by surface fatigue in dry sliding. Mater Charact 45(1):1–15. https://doi.org/10.1016/S1044-5803(00)00045-0

Unal H, Sen U, Mimaroglu A (2004) Dry sliding wear characteristics of some industrial polymers against steel counterface. Tribol Int 37(9):727–732. https://doi.org/10.1016/j.triboint.2004.03.002

Vishwanath B, Verma AP, Kameswara Rao CVS (1992) Effect of matrix content on strength and wear of woven roving glass polymeric composites. Compos Sci Technol 44(1):77–86. https://doi.org/10.1016/0266-3538(92)90027-Z

Zhang Z, Friedrich K, Velten K (2002) Prediction on tribological properties of short fibre composites using artificial neural networks. Wear 252(7):668–675. https://doi.org/10.1016/S0043-1648(02)00023-6

Zhang H, Zhang Z, Friedrich K (2007) Effect of fiber length on the wear resistance of short carbon fiber reinforced epoxy composites. Compos Sci Technol 67(2):222–230. https://doi.org/10.1016/j.compscitech.2006.08.001

Tribological Behaviour of Natural Fibre Based Polymer Composites

Rajiv Kumar, Mir Irfan Ul Haq, Ankush Raina, Sanjay Mohan Sharma, Ankush Anand, and Mohd Fadzli Bin Abdollah

Abstract Researchers are continuously working on materials with lower weight, higher strength and lesser in cost. Polymer composites are promising candidate in this category. Natural fibre based polymer composites are being considered for various applications due to environmental concerns and requirement of sustainable environment. Natural fibres are environment friendly, available in abundance, biodegradable, cheap and low in density in comparison to synthetic fibres. Reinforcement of natural fibres have improved mechanical and physical properties of these composites. Researchers are working on various industrial applications of these composites. Study of the tribological aspects of these composites is the new research area. Based on their attractive properties researchers are interested in knowing the feasibility of natural fibres for tribological applications. Developing green friction materials, bearings for automotive applications is the need of the hour. The present chapter highlights the significance of friction and wear behaviour of natural fibre based composites. The work focuses on effect of reinforcement of natural fibres on tribological properties of these composites and also exposes limitations of these fibres. A brief introduction of natural fibres, polymers and tribology is also provided to give the background for the readers. The work will help the enthusiast researchers interested in the tribological study of natural fibre reinforced composites.

Keywords Natural fibres · Bio-composites · Tribology · Wear · Friction · Green composites · Polymers · Green tribology

---

R. Kumar (✉) · M. I. U. Haq · A. Raina · S. M. Sharma · A. Anand
School of Mechanical Engineering, Shri Mata Vaishno Devi University, Katra, Jammu and Kashmir, India

M. F. B. Abdollah
Fakulti Kejuruteraan Mekanikal, Universiti Teknikal Malaysia Melaka, Hang Tuah Jaya, 76100 Durian Tunggal, Melaka, Malaysia

H. Jena et al. (eds.), *Tribology of Polymer and Polymer Composites for Industry 4.0*,
Composites Science and Technology, https://doi.org/10.1007/978-981-16-3903-6_4

1 Introduction

The quest for new materials with properties like light in weight, high strength to weight ratio, low cost, environment friendly, etc. will never end (Baba et al. 2019). Designing machine components with these materials involves different aspects like wear, friction and lubrication for the smooth functioning of the system. Therefore, tribology plays a vital role in designing various machine components. The term "tribology' coined by Dr. Peter Jost in England in 1966. He defines it as "The science and technology of interacting surfaces in relative motion, having its origin in the Greek word *tribos* meaning rubbing". He highlighted the huge losses in industry associated with tribological aspects. A saving of 515 million pounds per year can be achieved by the better designing of components from tribological perspective in the industries. Tribology is a multidisciplinary and a complex field involving material science, mechanical engineering, chemistry, fluid dynamics, heat transfer, thermodynamic, etc. (Jost 1990).

During the last decade, polymer composites have emerged as a potential candidate for conventional materials due to their excellent properties like lightweight, easy processing, high strength to weight ratio, low cost, etc. (Vohra et al. 2015; Rajak et al. 2019). These composites mainly involve fibre reinforcement (synthetic or natural) in a polymer matrix. Fibres have higher strength and stiffness, while the matrix material facilitates the transfer of stress to the fibre and also, protect the fibre from direct environmental contact. In the last few years researchers are shifting their focus from synthetic to natural fibres due to strict environmental guidelines and various other benefits of these fibres over synthetic fibres (Nirmal et al. 2015).

Natural fibres are available in abundance throughout the world. Natural fibres include fibres from natural sources (plants, animals, minerals) like jute, flax, hemp, ramie, sisal, banana, cotton, etc. India have abundance availability of natural fibres like jute, bamboo, banana, coir, ramie, sisal, pineapple, etc. composites based on these fibres are good alternatives to wood in housing and construction industries. The motive force behind development of these composites in India mainly is due to two reasons. Firstly, saving of forest resources, and secondly ensuring good economic results to farmers for cultivation of these natural fibres (Kumar et al. 2019).

Natural fibre reinforced polymer composites consist of a polymer matrix reinforced with natural fibre. Polymer composites having natural fibres as reinforcement are known as bio-composites (Faruk et al. 2012). Bio-composites based on different types of polymer and natural fibre are shown in Fig. 1. When two or more than two different fibres are mixed with the polymer then that composite is termed as hybrid composite. Hybrid composites have higher mechanical properties as compared to individual fibre based composite (Gupta et al. 2019). The present work highlights the work of various researchers in the field of tribological behaviour of bio-composites during last decade. There are different fabrication methods for these composites. The key features for different fabrication techniques are also tabulated in the current work to give a brief idea for these techniques. Environmental benefits, applications and

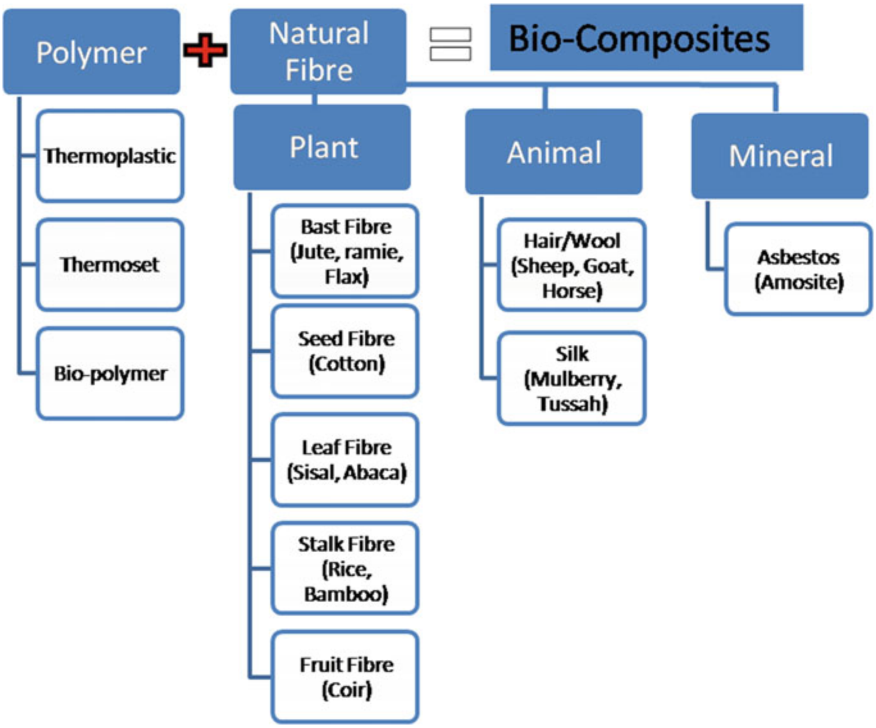

Fig. 1 Bio-composites based on various type of polymers and natural fibres

challenges associated with these composites are also discussed to give an overview to the researchers new to the field.

2 Fabrication Methods of Bio-Composites

All the fabrication methods used to produce synthetic fibre reinforced polymer composites can also be utilized to produce bio-composites with slight modifications. Researchers mainly utilize hand layup technique for fabrication of bio-composites due its easy processing and economical. Figure 2 shows open mold hand layup process. Different fabrication routes for bio-composites are summarized in Table 1.

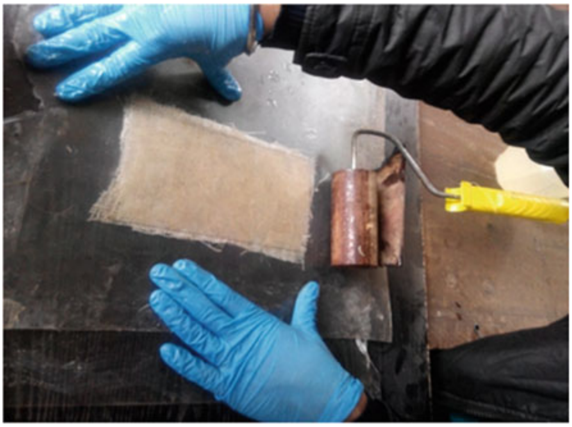

Fig. 2 Hand layup technique

Table 1 Processing methods for bio-composites

Fabrication method	Key features
Hand layup	• Manual procedure to put resin and reinforcement in an open mold • Hand roller removes the entrapped air during the fabrication • Economic, no bar on size of the part. Examples: storage tanks, tubs, boats, etc
Spray layup	• Spray gun is used to spray the mixture of chopped reinforcement and resin in an open mold • Faster than hand layup technique. Examples: storage tanks, tubs, boats, etc
Injection molding	• Reinforcement and resin mixture is pushed into a closed mold by screw extruders through a nozzle • High production. Examples: automobile body panels, bumpers, floor pans, etc
Compression molding	• Resin and reinforcement are placed in a closed mold. Temperature, pressure and time are controlled in the fabrication process • Lesser post processing requirements, better adhesion. Examples: structural components, Automobile components, etc
Resin transfer molding	• High pressurized resin is transferred in the closed mold cavity in which reinforcement is already placed • High fibre content, faster, products with complex geometry, high surface finish, etc
Vaccum bag molding	• Laminates are produced using vacuum bag covers over the mold • Improved mechanical strength, uniformity, no voids
Filament winding	• Continuous reinforcement wounds on to a revolving mandrel, automatic and controllable fibre orientation • High fibre content, hollow cylindrical products. Examples: pressure vessels, chemical storage tanks, etc
Pultrusion method	• Mixture of fibre and resin pulled through heated die • Uniform cross sectional shaped products, high fibre content. Examples: Long rods, beams, channels, etc

3 Tribological Properties of Bio-Composites

Researchers are working on to expedite new sectors of engineering applications for bio-composites. Tribology is one such emerging area. A wide scope is available on tribological behaviour of NFPC. Researchers have worked on the tribological behaviour of bio-composites like kenaf/epoxy (Chin and Yousif 2010), sugarcane/polyester (El-Tayeb 2008), sisal/PLA (Bajpai et al. 2014), cotton/polyester (Hashmi et al. 2007), bamboo/epoxy (Nirmal et al. 2012), betelnut/polyester (Nirmal et al. 2010; Gill and Yousif 2009), hemp/epoxy etc. (Chaudhary et al. 2018). It is also evident from Fig. 3 that during last five years focus of researchers is shifting from synthetic fibres to natural fibres in the area of tribology also. Research work based on tribological characterization of natural fibres reinforced composites has been increased during these years. The detailed review of the work related to tribological behaviour of bio-composites by various researchers is discussed as below.

Sundarakannan et al. (2020) investigated wear and erosion performance of pineapple fibre (40 wt. %) reinforced polyester polymer composites. Redmud an industrial waste was used as filler by wt. % of 10 and 20. The composites were developed by compression moulding machine. Erosive resistance was tested by solid particle erosion test on Ducom tester. It was observed by the authors that redmud fillers enhanced the erosive resistance of the developed composites. The developed composites with 10 wt. % redmud fillers exhibited low erosive wear rate.

Rajesh Kumar (2020) investigated tribological behaviour of Phoenix Sp./epoxy composites. Composites were fabricated by compression molding method based on

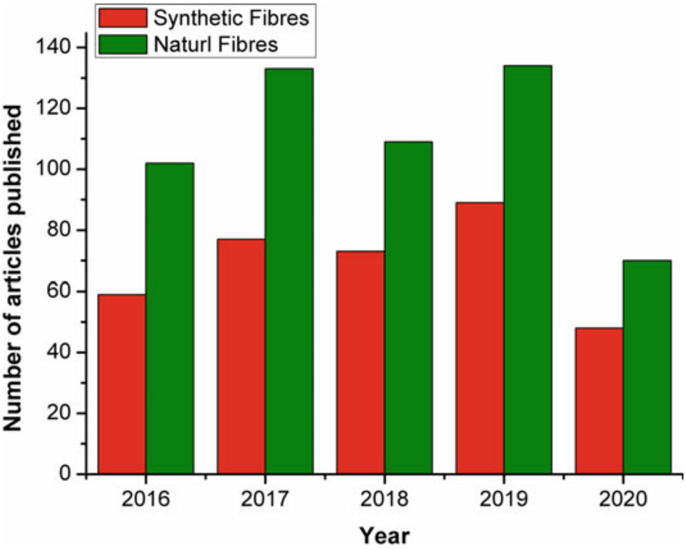

Fig. 3 Articles published on triblogy of synthetic as well as natural fibres in last 5 years (Using keywords—Tribology, synthetic fibres, natural fibres on https://www.sciencedirect.com)

different volume fraction of fibre including 10 to 50%. Fibre length was also varied to check its impact on tribological properties. Pin on disk tribo testing machine was used for three loads including 10, 20 and 30 N. Three Sliding speeds varied in the range of 1–3 m/s and sliding distances varied from 1 to 3 km. The authors observed that reinforcement of Phoenix Sp. Fibre improved the tribological properties of developed composites in comparison to neat polymer.

Suresh et al. (2020) analyzed wear behaviour of agricultural residues reinforced vinyl ester composites. Agricultural residues included bagasse, rice husk and coconut shell in different weight fractions from 5 to 25% for various type of composites. Composites were developed by compression molding technique. The tribo testing was carried out on pin on disc tribometer. The different experimental parameters included normal load from 20 to 40 N, sliding velocity of 2 and 4 m/s. The sliding distance considered for the experimentation purpose was 500 m. The authors revealed that hybrid composites having 20 wt. % of each natural fibre exhibited lower wear loss and low coefficient of friction.

Pari khand Gohil (2019) developed cotton fibre/polyester composites and analyzed the wear performance. Different weight fractions of fly ash as filler was also used to analyze its impact on wear behaviour. Cotton fibre was used by 18 wt. % and fly ash had two variations of 3 and 5 wt. %. Composites were developed by hand layup compression molding technique. Authors revealed that fly ash as filler had significant impact on wear performance. Authors concluded that composites with 3 wt. % of fly ash filler exhibited highest wear resistance and recommended use of these materials in high wear conditions.

Zhen et al. (2019) examined effect of banana fibre reinforced phenolic based polymer composites on tribological properties. Composites were fabricated using banana and barium sulphate as reinforcements using hot compression technique. Developed composites containing 10 wt. % banana fibre and 45 wt. % barium sulphate exhibited highest coefficient of friction, in comparison to other composites. Authors concluded that the lower banana fibre ($\leq$10 wt. %) loading, enhanced the friction and wear performance of the composites.

Shivamurthy et al. (2019) analyzed sliding wear behaviour of waste tyre rubber reinforced epoxy composites. Composites were developed by open moulding method based on the different weight fractions of reinforcement including 15, 30 and 45 wt. %. Effect of particle size (100, 200, and 300 μm) of the reinforcement was also investigated. It was observed that both the parameters i.e. weight fraction of filler and the particle size has significant impact on wear behaviour of developed composites. The authors concluded that by the reinforcement of waste tyre rubber enhanced the sliding wear behaviour.

Ranganathan et al. (2019) investigated wear and friction behaviour of sisal fibre reinforced composites with cashew nut shell liquid (CNSL) and epoxy resin. Composites were fabricated by hot press technique. Composites were examined for the tribo conditions of varying loads of 10–40 N and sliding distances of 1000 and 2000 m. Graphite and alumina fillers were also added in CNSL composites. Composites having CNSL resin exhibited good wear resistance and frictional properties in comparison to epoxy resin based composites. Lesser wear resistance and frictional coefficient were observed at the load of 40 N and sliding distance of 2000 m.

Kumar and Anand (2018) investigated friction and wear behaviour of Indian ramie reinforced epoxy composites. Composites were developed on the basis of different weight fractions of fibre varying from 0 to 40%. Hand layup technique was used for fabricating the composites. Pin on disc tribometer was used for tribo testing with five different normal loads ranging from 10 to 30 N, sliding speeds of 1, 1.5 and 2 m/s with a constant sliding distance of 1000 m. Composites with 30 wt. % fibre loading offered highest wear resistance and an increment of 75% in wear resistance at 10 N load in comparison to neat epoxy. Frictional coefficient enhanced with the enhancement in fibre content.

Shuhimi et al. (2016) analyzed frictional and wear performance of oil-palm/epoxy (OPF/E) and kenaf/epoxy (KF/E) composites under dry sliding conditions. Composites were developed by hot compaction technique. Tribological testing was performed using POD tribo machine. With the increase in fibre loading of the OPF/E composite observed severe wear. However, in case of the KF/E composite, the same change exhibited higher wear performance. The study revealed that for both the developed composites, wear loss enhanced and frictional coefficient reduced after the temperature increase.

Bajpai et al. (2013) analyzed the tribological behavior of nettle, grewia-optiva and sisal fibre reinforced polypropylene composites using pin-on disc (POD) machine. Significant increase in the specific wear rate of the reinforced composites was observed in comparison to neat polypropylene. Authors also observed that specific wear rate was more sensitive to applied load changes (10–33 N) than the sliding speeds changes (1–3 m/s). Authors observed that 30 wt. % of sisal fibre reinforcement substantially improved wear behaviour of the neat polypropylene.

Yousif et al. (2010) analyzed tribological characteristics of betelnut fibre/polyester composite. To analyze frictional and wear behaviour of developed composites by changing various parameters like sliding distance, sliding speed and load, experiments were carried out on block-on-disc (BOD) machine under dry/wet sliding contact conditions. The study revealed that developed composite exhibited improved wear and frictional behaviour under wet contact condition. Wear and frictional behaviour of developed composites improved by about 50% and 94% respectively.

Many researchers have worked on study of tribological behaviour of bio-composites. Researchers performed the experiments on different tribo testing machines with dry/wet sliding contact conditions using different parameters such as applied load, sliding velocity and, sliding distance. The counterface used was steel or other materials and concluded that bio-composites are a potential alternative for conventional materials. The properties can be improved by adding other filler materials and proper chemical treatment of the fibre.

Wear mechanism of these composites can be analyzed with the help of SEM micrographs of wear our specimen during triobological testing. SEM micrographs presented in Fig. 4 include ramie/epoxy bio-composites with 10% fibre loading (Fig. 4a) and 30% fibre loading (Fig. 4b) at 20 N normal load, 1 m/s sliding speed and 1000 m sliding distance. Fibre fracture, matrix breakage, debonding, ploughing

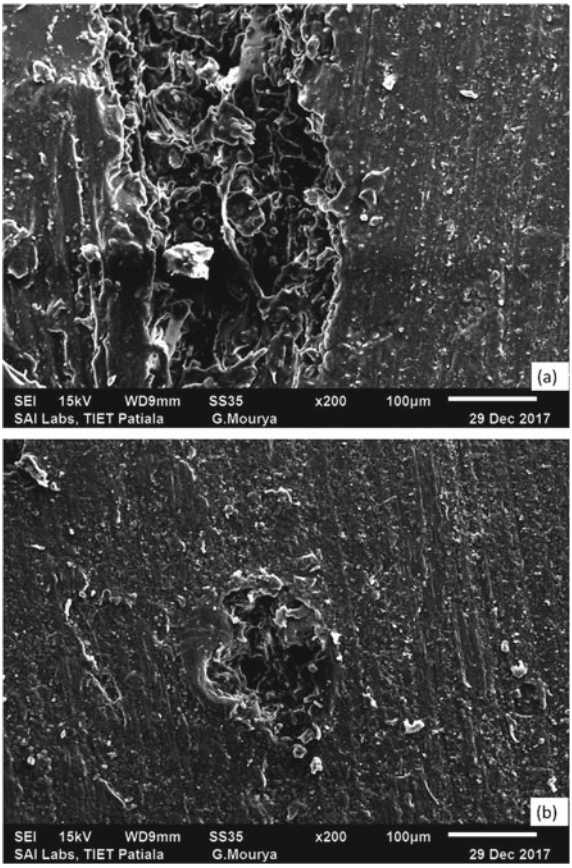

Fig. 4 Wear mechanism of Ramie/epoxy bio-composites with **a** 10% fibre loading and **b** 30% fibre loading at 20 N normal load, 1 m/s sliding speed and 1000 m sliding distance

can be observed in the micrographs. Ploughing and cutting marks indicate abrasive wear mechanism in these composites. Higher matrix breakage, debonding and fibre fracture can be seen in composites with 10% ramie fibre loading. This can be attributed to poor interfacial adhesion between fibre and matrix. As fibre loading increases interfacial adhesion improves and leading to lesser fibre fracture and matrix breakage. That's why composites with 30% ramie fibre loading exhibited better wear performance (Bajpai et al. 2013; Kumar and Anand 2018; Chaudhary et al. 2018).

4 Parameters

Based on the work by different researchers the various parameters in tribological investigation of bio-composites are listed below:

1. Type of fibre
2. Fibre Orientation
3. Fibre loading
4. Type of polymer
5. Applied normal load
6. Sliding speed
7. Sliding distance
8. Sliding direction.

These parameters will influence the frictional and wear behaviour of the bio-composites. Figure 5 represents all these parameters in a fish bone diagram that have a significant impact on the tribological behaviour of bio-composites. The effect of above mentioned parameters on tribological properties of bio-composites is discussed as below:

Type of Fibre: Fibre type has a significant impact on the tribological behaviour. It includes fibre length and chemical composition (governs physical and mechanical properties) of the fibre. Type of fibre also includes treated or untreated fibres. Fibre treatment involves surface treatment of fibres for better properties like reducing moisture absorption and enhancing adhesion at fibre-matrix interface. Most commonly

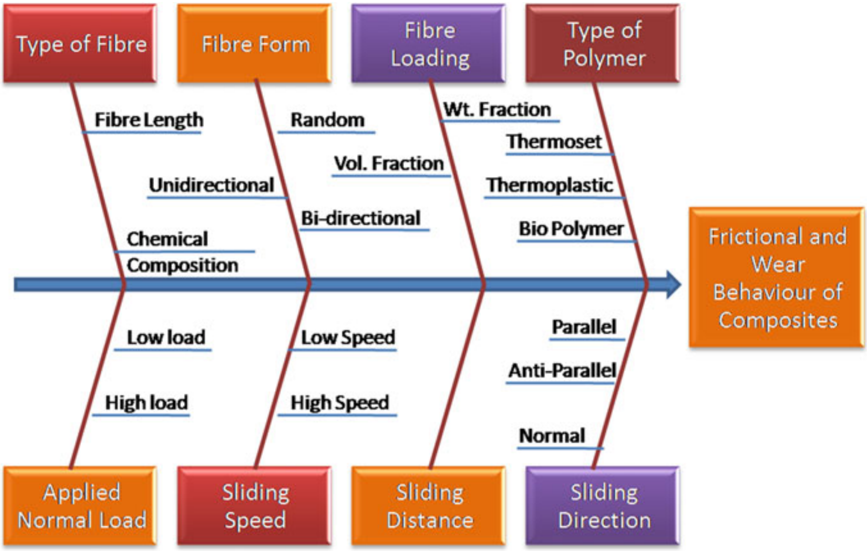

Fig. 5 Fish bone diagram of tribological behavior of polymer composites

used treatments are alkali treatment and acetylation (Omrani et al. 2016). By studying the effect of these components of a fibre one can select the fibre.

Fibre Orientation: Fibre orientation (with respect to applied load) involves random, unidirectional, bidirectional etc. As fibres act as carriers of load and stress under loading conditions, therefore, fibre orientation will have significant effects on tribological behaviour of the composite. Each fibre orientation produces different tribological behaviour as far as various properties are concerned for these composites. By analyzing the requirement, one can finalize the fibre form for reinforcement.

Fibre Loading: Fibre loading means percentage of fibre content in the composite. Researchers normally use fibre loading by weight % or by volume %. With the increase in fibre loading normally wear behaviour of these composites improves and over a specific value it starts decreasing. As the fibre loading increases the adhesion at fibre-matrix interface and proper wetting of fibres by the matrix varies. Therefore, for a particular fibre optimum fibre loading has to be found by experimentation. Coefficient of friction may increase or decrease with the increase in fibre loading depending on the type of fibre.

Type of Polymer: Polymer type includes thermoplastic, thermoset and biopolymers. Thermoset polymers have good mechanical properties than thermoplastics and have ability to work at higher temperatures. Bio-polymers are produced by biodegradable sources like animal proteins, plants etc. Mechanical properties of bio-polymers are not so good in comparison to other polymers. Composite of biopolymer and natural fibre is known as green composite. Therefore, by analyzing the application of the composite one can select the polymer type. Each type will exhibit different tribological behaviour.

Applied Normal Load: It is a critical parameter for tribological behaviour of composites. Minimum and maximum loads are finalized based on the load bearing capacity of these composites. As per Archard's wear law with the increase in applied normal load wear loss increases. The reason behind this is the penetration of hard asperities of steel counterface into the softer material of the bio-composite. Also, at higher loads, temperature increases and which softens the polymer, leading to higher material loss. Wear loss is comparatively low in case of reinforced composites in comparison to neat polymer (Kumar and Anand 2018).

Sliding Speed: Sliding speed also, influences the tribological properties of these composites. With the increase in sliding speed, friction and wear performance may increase or decrease depending upon different properties of fibre and polymer. As per literature, different fibre polymer combinations exhibited different behaviour with the change in sliding speed. Temperature also increases at higher speeds and has significant impact on friction and wear properties of the composite at those speeds (Bajpai et al. 2013).

Sliding Distance: Sliding distance is also an vital parameter and has significant impact on tribological properties of bio-composites. Generally, with the increase in sliding distance coefficient of friction attains a steady state. As far as wear loss is concerned with the increase in sliding distance generally, wear loss increased for bio-composites. Effect of sliding distance is generally predictable, therefore, many researchers use constant sliding distance in their work.

Sliding Direction: Sliding direction plays an important role in determining tribological performance of the composites. Based on the direction rotating disc with respect to fibres, there are three orientations. These include parallel, anti-parallel and normal orientation. Anti-parallel orientation exhibits better wear performance in comparison to other orientations since, more resistance is provided by fibres in this case (Chaudhary et al. 2018). These orientations are normally used for composites having unidirectional and bidirectional form normally.

5 Environmental Benefits

Natural fibres have emerged to be more environmental friendly as compared to synthetic fibres for the following reasons:

(1) Production of natural fibres consume less energy than synthetic fibre.
(2) Natural fibres have higher volume fraction than synthetic fibres for equivalent performance. That will reduce volume and weight of synthetic matrix, therefore, reduction in emissions and energy use for the production of polymers.
(3) Natural fibre composites when incinerated, lead to positive carbon credit and lesser air emissions due to lower mass in comparison to synthetic fibre composites.
(4) Natural fibre possess lower weight (around 20–30 by wt. %) and more volume in comparison to synthetic fibres. Therefore, higher fuel efficiency and lesser emission during the working stage in auto applications.
(5) Natural fibres have lower cost (200–1000 $/ton) and energy (4 GJ/ton) to produce in comparison to glass fibre (1200–1800 $/ton; 30 GJ/ton) and carbon fibre (12,500 $/ton; 130 GJ/ton) (Shalwan and Yousif 2013).

These advantages are the driving forces for the increased use of natural fibre composites in various applications. Environmental benefits of natural fibres are also summarized in Fig. 6.

6 Applications

The use of natural fibre composites has shown significant applications in the automotive industry throughout the world. Natural fibres are being preferred in this sector due to their low density and increasing environmental concerns. These composites are being utilized in various applications where, load carrying capacity and dimensional stability in moist environment are not significant. Flax/polyolefins composites are extensively used in automotive sector for non-structural interior panels (Holbery and Houston 2006). Various other automotive parts produced using natural fibres are dashboards, glove box, trunk panel, door panels, seat coverings, trunk floor, spare

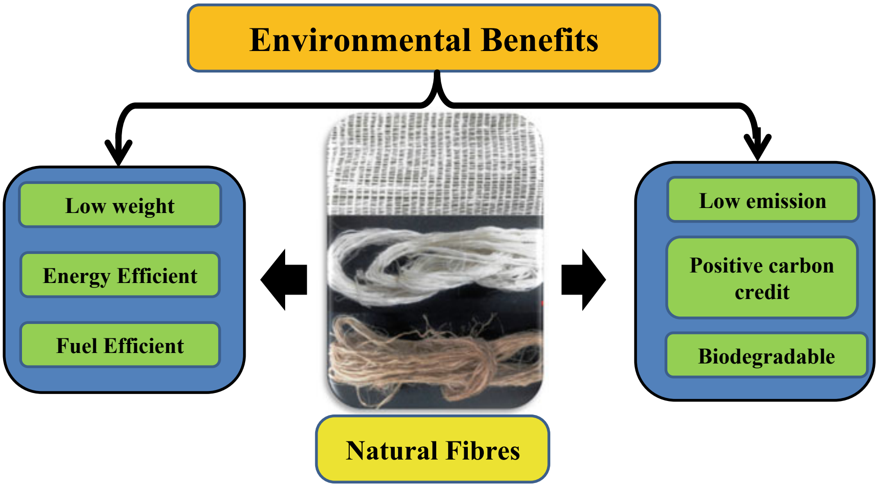

Fig. 6 Environmental benefits of natural fibres

tyre covers, floor panels, headliners etc. (Pandey et al. 2010; Das 2009; Nakamura et al. 2009).

Natural fibres being non-abrasive to the mixing and moulding equipments also, lower material cost make them an exciting prospect for household appliances and other applications. As these composites based on these fibres are low cost materials, they can play a vital role in application for various building and construction areas (e.g. partition, ceiling, walls, door and window frames, etc.). Bamboo-poplar/epoxy laminate, an attractive material developed for wind turbine rotor blades (Debnath et al. 2013). Some other application areas can be storage devices (e.g., bio-gas container, post boxes, etc.), electronic devices (outer casting of mobile phones), furniture (e.g., table, chair, tools, etc.), toys and other miscellaneous applications (e.g. suitcases, helmets, etc.). Jute/polyester composites are being used in buildings, elevators, panels and pipes (Oksman et al. 2003). Natural fibres and their composites have a great future in applications like fibre cement, foundations and interface elements (Smith and Walcott 2006). Figure 7 shows the various application areas of natural fibres and their composites.

7 Challenges

Usage of bio-composites is limited due to the challenges associated with these composites. Degradation of properties takes place, when exposed to external environment. The major challenges are mainly due to the presence of natural fibres, which include water absorption tendency, weak interfacial adhesion with the synthetic polymer, poor wettability and durability. Also, during the processing poor thermal

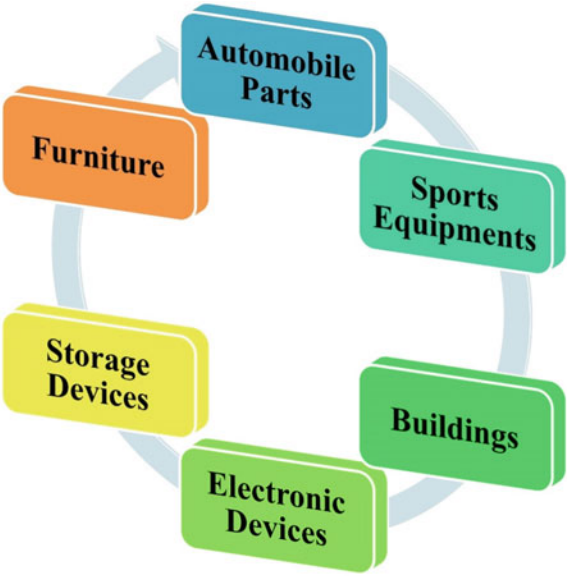

Fig. 7 Applications of natural fibre reinforced polymers

stability issue comes into picture with these composites (Gassan and Gutowski 2000; Debnath et al. 2013). Water absorption is the major challenge associated with these composites. Absorbed water bonds with fibre's hydroxyl group, weakens the bonding strength at the interface, eventually leading to reduced mechanical strength. As tribological properties are influenced by mechanical properties, therefore, decrement in wear performance is also observed. The moisture absorption behavior of natural fibres restricts the outdoor applications of bio-composites. There are various techniques like chemical treatment and coupling agents which are being used to avoid moisture absorption (Ahmad et al. 2015). Percentage moisture absorption by natural fibres lie in the range of 5 to 20% by wt. Moisture absorption by prominent fibres is as follows: Jute (10–13%), hemp (6–12%), flax (7–12%), ramie (7.5–17%), sisal (10–22), cotton (7.5–20%), abaca (5–10%), coir (0.2–10%), etc. (Kumar et al. 2019). Moisture content diminishes the physical and mechanical properties of the fibres and the composites.

8 Conclusions and Future Scope

Based on the work by various researchers, it can be concluded that bio-composites are potential candidates for tribological applications. Natural fibres like sisal, jute, ramie, flax, hemp, banana, pineapple etc. are being used by researchers as reinforcement for bio-composites in tribological investigations. Wear behaviour of bio-composites improved in comparison to neat polymer. This can be attributed to improved hardness and stiffness of bio-composites by reinforcing natural fibres. Coefficient of friction for these composites may increase or decrease depending on the type of fibre and other parameters. Therefore, these composites can act as friction and anti-friction materials depending upon the frictional behaviour of that particular bio-composite. Researchers are mainly working on general tribological behaviour of these composites. Now, there is a need to focus the research work on specific tribo based applications for those bio-composites, whose tribo-potential is known.

As far as future scope is concerned, there are still numerous natural fibres available which are still unexplored in this area. Work on hybrid bio-composites is still not explored much in tribological investigations. There are many fabrication techniques whose impact on tribological behaviour is not known. That can be an area where researchers have to focus. Researchers can also shift towards bio-polymers, making it a green composite. That will be a next step towards sustainable development.

References

Ahmad F, Choi HS, Park MK (2015) A review: natural fiber composites selection in view of mechanical, light weight, and economic properties. Macromol Mater Eng 300(1):10–24

Baba ZU, Shafi WK, Haq MIU, Raina A (2019) Towards sustainable automobiles-advancements and challenges. Prog Ind Ecol Int J 13(4):315–331

Bajpai PK, Singh I, Madaan J (2013) Frictional and adhesive wear performance of natural fibre reinforced polypropylene composites. Proc Inst Mech Eng Part J: J Eng Tribol 227(4):385–392

Bajpai PK, Singh I, Madaan J (2014) Development and characterization of PLA-based green composites: a review. J Thermoplast Compos Mater 27(1):52–81

Chaudhary V, Bajpai PK, Maheshwari S (2018) An investigation on wear and dynamic mechanical behavior of jute/hemp/flax reinforced composites and its hybrids for tribological applications. Fibers Polym 19(2):403–415

Chin CW, Yousif BF (2010) Tribological behaviour of KFRE composite. Int J Mod Phys B 24(28):5589–5599

Das S (2009) Jute composite and its applications. In: International workshop, IJSG, Indian Jute Industries Research Association, Kolkata, India. https://www.jute.org. Accessed July 2010

Debnath K, Singh I, Dvivedi A, Kumar P (2013) Natural fibre-reinforced polymer composites for wind turbine blades: Challenges and opportunities. In: Recent advances in composite materials for wind turbine blades. Hong Kong, WAP-AMSA, 25, 40

El-Tayeb NSM (2008) A study on the potential of sugarcane fibers/polyester composite for tribological applications. Wear, 265(1–2):223–235. DOI: https://doi.org/10.1016/j.wear.2007.10.006

Faruk O, Bledzki AK, Fink HP, Sain M (2012) Biocomposites reinforced with natural fibers: 2000–2010. Prog Polym Sci 37(11):1552–1596

Gassan J, Gutowski VS (2000) Effects of corona discharge and UV treatment on the properties of jute-fibre epoxy composites. Compos Sci Technol 60(15):2857–2863

Gill NS, Yousif BF (2009) Wear and frictional performance of betelnut fibre-reinforced polyester composite. Proc Inst Mech Eng 223(J2):183

Gupta S, Haq MIU, Mohan S, Anand A, Raina A, Dutta V, Vohra K, Kumar R (2019) Evaluation of mechanical properties of ramie/banana reinforced hybrid composites

Hashmi SAR, Dwivedi UK, Chand N (2007) Graphite modified cotton fibre reinforced polyester composites under sliding wear conditions. Wear 262(11–12):1426–1432

Holbery J, Houston D (2006) Natural-fiber-reinforced polymer composites in automotive applications. Jom 58(11):80–86

Jost HP (1990) Tribology—origin and future. Wear 136(1):1–17

Kumar R, Anand A (2018) Dry sliding friction and wear behavior of ramie fiber reinforced epoxy composites. Mater Res Express 6(1):015309

Kumar R, Ul Haq MI, Raina A, Anand A (2019) Industrial applications of natural fibre-reinforced polymer composites–challenges and opportunities. Int J Sustain Eng 12(3):212–220

Nakamura R, Goda K, Noda J, Ohgi J (2009) High temperature tensile properties and deep drawing of fully green composites. Express Polym Lett 3(1):19–24

Nirmal U, Hashim J, Ahmad MM (2015) A review on tribological performance of natural fibre polymeric composites. Tribol Int 83:77–104

Nirmal U, Hashim J, Low KO (2012) Adhesive wear and frictional performance of bamboo fibres reinforced epoxy composite. Tribol Int 47:122–133

Nirmal U, Yousif BF, Rilling D, Brevern PV (2010) Effect of betelnut fibres treatment and contact conditions on adhesive wear and frictional performance of polyester composites. Wear 268(11–12):1354–1370

Oksman K, Skrifvars M, Selin JF (2003) Natural fibres as reinforcement in polylactic acid (PLA) composites. Compos Sci Technol 63(9):1317–1324

Omrani E, Menezes PL, Rohatgi PK (2016) State of the art on tribological behavior of polymer matrix composites reinforced with natural fibers in the green materials world. Eng Sci Technol Int J 19(2):717–736

Pandey JK, Ahn SH, Lee CS, Mohanty AK, Misra M (2010) Recent advances in the application of natural fiber based composites. Macromol Mater Eng 295(11):975–989

Parikh HH, Gohil PP (2019) Experimental determination of tribo behavior of fiber-reinforced composites and its prediction with artificial neural networks. In: Durability and life prediction in biocomposites, fibre-reinforced composites and hybrid composites, pp 301–320. Woodhead Publishing

Rajak DK, Pagar DD, Kumar R, Pruncu CI (2019) Recent progress of reinforcement materials: a comprehensive overview of composite materials. J Market Res 8(6):6354–6374

Rajeshkumar G (2020) A new study on tribological performance of phoenix Sp. fiber-reinforced epoxy composites. J Nat Fibers 1–12

Ranganathan S, Gopal S, Magudeeswaran T, Rangasamy R (2019) Exploration of dry sliding wear behaviour of sisal fiber reinforced cashew nut shell liquid and epoxy polymer matrix composite as an alternative friction material in automobiles, no 2019-28-0173. SAE Technical Paper

Shalwan A, Yousif BF (2013) In state of art: mechanical and tribological behaviour of polymeric composites based on natural fibres. Mater Des 48:14–24

Shivamurthy B, Doreswamy D, Nishanth J, Shiva Prasad HC (2019) Physical and tribo-mechanical properties of waste rubber tyre/epoxy composites. Mater Res Express 6(9):095321

Shuhimi FF, Abdollah MFB, Kalam MA, Hassan M, Amiruddin H (2016) Tribological characteristics comparison for oil palm fibre/epoxy and kenaf fibre/epoxy composites under dry sliding conditions. Tribol Int 101:247–254

Smith PM, Wolcott MP (2006) Opportunities for wood/natural fiber-plastic composites in residential and industrial applications. For Prod J 56(3):4

Sundarakannan R, Arumugaprabu V, Manikandan V, Johnson RDJ (2020) Tribo performance studies on redmud filled pineapple fiber composite. Mater Today Proc 24:1225–1234

Suresh S, Sudhakara D, Vinod B (2020) Investigation on industrial waste eco-friendly natural fiber-reinforced polymer composites. J Bio Tribo-Corr 6(2):1–14

Vohra K, Anand A, Haq MIU (2015) Wear and friction behavior of self-lubricating polytetrafluoroethylene under dry conditions. Mater Focus 4(6):471–474

Yousif BF, Lau ST, McWilliam S (2010) Polyester composite based on betelnut fibre for tribological applications. Tribol Int 43(1–2):503–511

Zhen-Yu W, Jie W, Feng-Hong C, Yun-Hai M, Singh T, Fekete G (2019) Influence of banana fiber on physicomechanical and tribological properties of phenolic based friction composites. Mater Res Express 6(7):075103

Tribology of Polymers and Polymer-Modified Asphalt Binders Considering Linear Viscoelasticity

Hazratullah Paktin and Saqib Gulzar

Abstract In viscoelastic polymeric materials, the stress state depends not only on the strain history but also on deformation or strain rate. The mechanical response of such materials lies in between that of elastic solids and viscous fluids. It is essential to consider the linear viscoelasticity of polymers when studying their thin film mechanics. On the other hand, asphalt binders are heavily used in the construction of flexible pavements all over the word. When polymers are added to asphalt binders to improve their performance characteristics, there is a nexus of rheology and tribology at play as these form thin films around the aggregates. In this chapter, the nature of polymer viscoelasticity is discussed in detail and the fundamentals involved in understanding the linear viscoelastic behavior of polymers are presented. In order to establish the constitutive behavior of such materials, phenomenological as well as molecular models are reviewed. Further, the tribological behavior of polymer-based asphalt binders is discussed and its impact of overall binder rheology is articulated.

Keywords Thin film · Linear Viscoelasticity · Rheology · Tribology · Polymer · Asphalt · Pavement

1 Introduction

The classical approach which concerns with the study of mechanical properties of elastic solids is based on classical elastic theory of solids, defined by Hooke's law, where in, stress is always directly proportional to strain for small deformation, however, stress is independent of strain rate. On the other hand, another classical approach which concerns with the study of properties of viscous fluids mainly liquid is based on classical theory of hydrodynamics, defined by Newton's. law, where in, stress is always directly proportional to strain rate, however, stress is independent

---

H. Paktin
Department of Civil Engineering, Paktia University, Paktia, Afghanistan

S. Gulzar (✉)
Formerly, Department of Civil Engineering, Indian Institute of Technology Delhi, New Delhi, India

H. Jena et al. (eds.), *Tribology of Polymer and Polymer Composites for Industry 4.0*,
Composites Science and Technology, https://doi.org/10.1007/978-981-16-3903-6_5

of strain. These two extremely different theories are actually based on idealizations of the behavior of solids under Hooke's law valid for infinitesimal strain and that of liquids under Newton's law for infinitesimal strain rate, however for conditions other than these two, certain deviations from *elastic solid* and *viscous liquid* behaviors have been observed. These deviations can be categorized into two types. First, when solids are subjected to finite strains beyond the infinitesimal ranges, mostly in soft solids which undergo substantial deformation without breaking, the relationship of stress and strain cannot be explained by Hooke's law, means the direct proportionality between stress and strain ceases to exist, the materials are known to exhibit Non-Hookean behavior.

Similarly, when liquids are subjected to finite strain rates in steady flow beyond the infinitesimal ranges, mostly in solutions of polymeric nature as well as polymers with uncross-linked molecular chains in non-diluted state, the proportionality between stress and strain rates ceases to exist and strong deviations from Newton's law are observed, known as Non-Newtonian flow. Both Non-Hookean deformation and Non-Newtonian flow constitute first type of deviation. Second type of deviation from the behavior based on classical approaches occurs when both strain as well as strain rate are simultaneously infinitesimal, in that case the material shows a mixed behavior which is a combination of solid-like and liquid-like features. For instance, the body, which is not perfectly solid, when subjected to constant stress does not maintain a constant deformation, rather slowly deforms with time indicating time dependency of deformation under constant stress, known as creep. If the same body is subjected to constant deformation, the stress decreases gradually with time, known as relaxation. Similarly, a body which is not perfectly liquid, flows when being subjected to constant stress but may not dissipate all energy applied into heat rather store a part of the energy applied and subsequently show recovery of some deformation when the stress is removed, known as elastic recoil. When such a body is subjected to sinusoidally oscillating stress, the strain response does not exactly follow stress input like a perfectly elastic solid nor does it completely phase out by 90° like a perfectly viscous liquid, rather shows an interim response as shown in Fig. 1 where in some part of the applied energy is stored, some part is recovered while remaining part is dissipated as heat in each load cycle.

The materials which exhibit such interim characteristics between elastic solids and viscous liquids are called viscoelastic materials. In linear viscoelasticity, when both strain and strain rate are within the infinitesimal ranges, the relationship between stress and strain are time-dependent which are usually expressed by linear differential equations with constant coefficient, the ratio of stress to strain or otherwise is a function of time (or in terms of frequency), known as creep compliance or relaxation modulus depending upon the input loading or test. In general, the relations between stress, strain and their time dependencies are known as constitutive relations. In modeling viscoelastic behavior of materials, the objective function is mainly to develop the constitutive relation which explains the related viscoelastic behavior most accurately. From past four to five decades, almost all the advancements in understanding and modeling viscoelasticity has been in relation to polymeric materials. Polymers may be crystalline or amorphous in nature. The mechanical response of

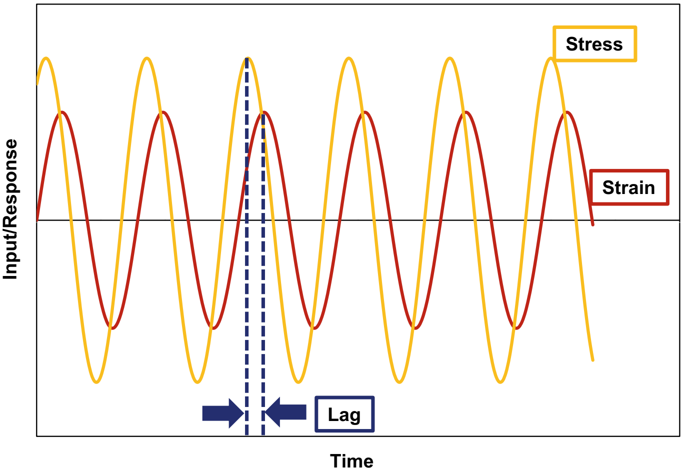

Fig. 1 Oscillatory stress input and delayed strain response

only amorphous polymeric materials can be explained by viscoelastic theory. Amorphous polymers consist of long-chain molecules where in each polymeric chain consists of thousands of molecules, held together in a chain-like fashion, which are intertwined and may or may not be chemically bonded, classified as uncross-linked, end-linked and crosslinked amorphous polymers as shown in Fig. 2.

Asphalt binders which are modified with polymers can be linearly or nonlinearly viscoelastic and there is a need to characterize this behavior of asphalt binders (Gulzar and Underwood 2019a, b, 2020; Gulzar et al. 2020a, b, c; Daryaee et al. 2020; Mansourkhaki et al. 2020a, b). In this chapter, the fundamental aspects of viscoelasticity are discussed and comparison is drawn between elastic, viscous and viscoelastic responses to different types of loading qualitatively as well as between viscoelastic solids and viscoelastic liquids, following which different forms constitutive relations and basic phenomenological models are presented. Various studies conducted over

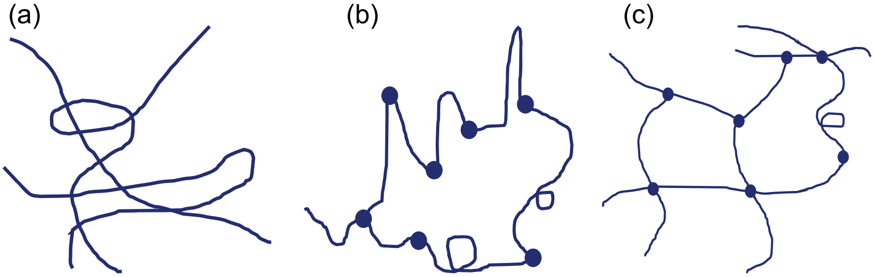

Fig. 2 Schematic representation of amorphous polymers: **a** Uncross-linked. **b** End-linked. **c** Cross-linked

past two–three decades to model the viscoelastic behavior of polymeric materials have been reviewed and insights are also provided for future scope.

2 Fundamentals of Viscoelastic Behavior of Polymeric Materials

The viscoelastic behavior is an intermediate response behavior between elastic solids and viscous liquids. The nomenclature necessary for conducting experimental studies on polymer viscoelasticity is given in Table 1 which summarizes the basic concepts and equations involved.

To qualitatively understand the mechanical response of viscoelastic materials, the following methodology is adopted. The response of elastic solid as well as of viscous fluid is qualitatively evaluated for an external input loading, then the response of the viscoelastic material is imagined to lie somewhere in between the two former responses. In this study, only one-dimensional models are considered. For elastic solids, a uniaxial bar or a spring is used while for viscous fluid, a piston or dashpot is used as shown in Fig. 3. For viscoelastic polymeric materials, a combination of springs and dashpots is considered. Based on different configurations and combinations of springs and dashpots, there are different phenomenological models which

Table 1 Linear viscoelastic polymeric material functions (Knauss et al. 2008)

Mode	Type of loading		Shear	Bulk	Uniaxial extension
Quasistatic	Relaxation		$\mu(t)$	$K(t)$	$E(t)$
	Creep		$J(t)$	$M(t)$	$D(t)$
Harmonic	Strain-based	Storage	$\mu'(\omega)$	$K'(\omega)$	$E'(\omega)$
		Loss	$\mu''(\omega)$	$K''(\omega)$	$E''(\omega)$
	Stress-based	Storage	$J'(\omega)$	$M'(\omega)$	$D'(\omega)$
		Loss	$J''(\omega)$	$M''(\omega)$	$D''(\omega)$

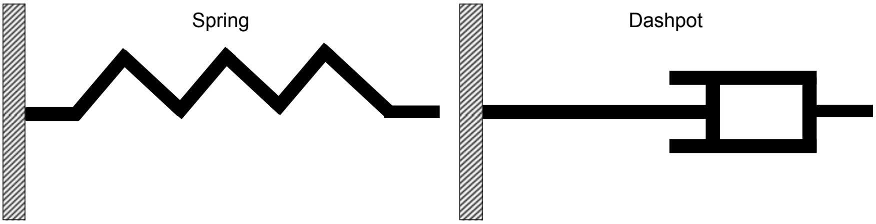

Fig. 3 Spring and dashpot mechanical idealization of elastic solids and viscous fluids respectively

define linear viscoelasticity approximately. In the subsequent sections, a comparative analysis is done between elastic response, viscous response and viscoelastic response.

2.1 Qualitative Comparative Analysis of Mechanical Responses

In doing the comparative analysis, σ denotes the normal stress while ϵ denotes the normal strain, E denotes the elastic modulus of the solid and η denotes the coefficient of viscosity of the fluid. In Fig. 4, the mechanical responses of elastic solids, viscous fluids and viscoelastic polymeric materials are compared qualitatively for different input loadings as a function of time t.

2.2 Regions of Viscoelastic Behavior of Polymeric Materials

Various experimental studies on viscoelastic polymeric materials indicate that the time scale of observations influence the values of creep compliance and relaxation modulus and temperature strongly influences the properties of viscoelastic polymeric materials. Thus, both time and temperature play a vital role in altering the measurable properties of such materials. Further, at a certain temperature closer to a critical value of temperature called as glass transition temperature, the properties change drastically. It is therefore essential to explicitly express the viscoelastic polymeric material functions such as creep compliance C and relaxation modulus M as explicit function of both time and temperature, that is $C(t,T)$ and $M(t,T)$. Figure 4 shows the temperature dependence of viscoelastic polymeric material properties in terms of relaxation modulus. The central narrow temperature range is called as transition region and its median temperature is called glass transition temperature. At temperatures quite below the glass transition temperature known as glassy region, the modulus values are high due to the hard and brittle nature of polymeric chains which are set and fixed in the polymeric matrix at low temperatures. Within the transition region, the polymeric chains consisting of large molecules show rapidly changing behavior due to the dynamics of free molecular chains, wholly or partly while at temperatures well above the glass transition temperature but less than melting point of polymeric materials known as rubbery plateau, the modulus values decrease due to higher mobility of polymeric chains, reorientation and disassociation. Creep compliance shows a similar behavior and appears as a reflective mirror image of relaxation modulus behavior as shown in Fig. 5. It should be noted that both Figs. 4 and 5 show temperature dependence of viscoelastic polymeric material properties under fixed time.

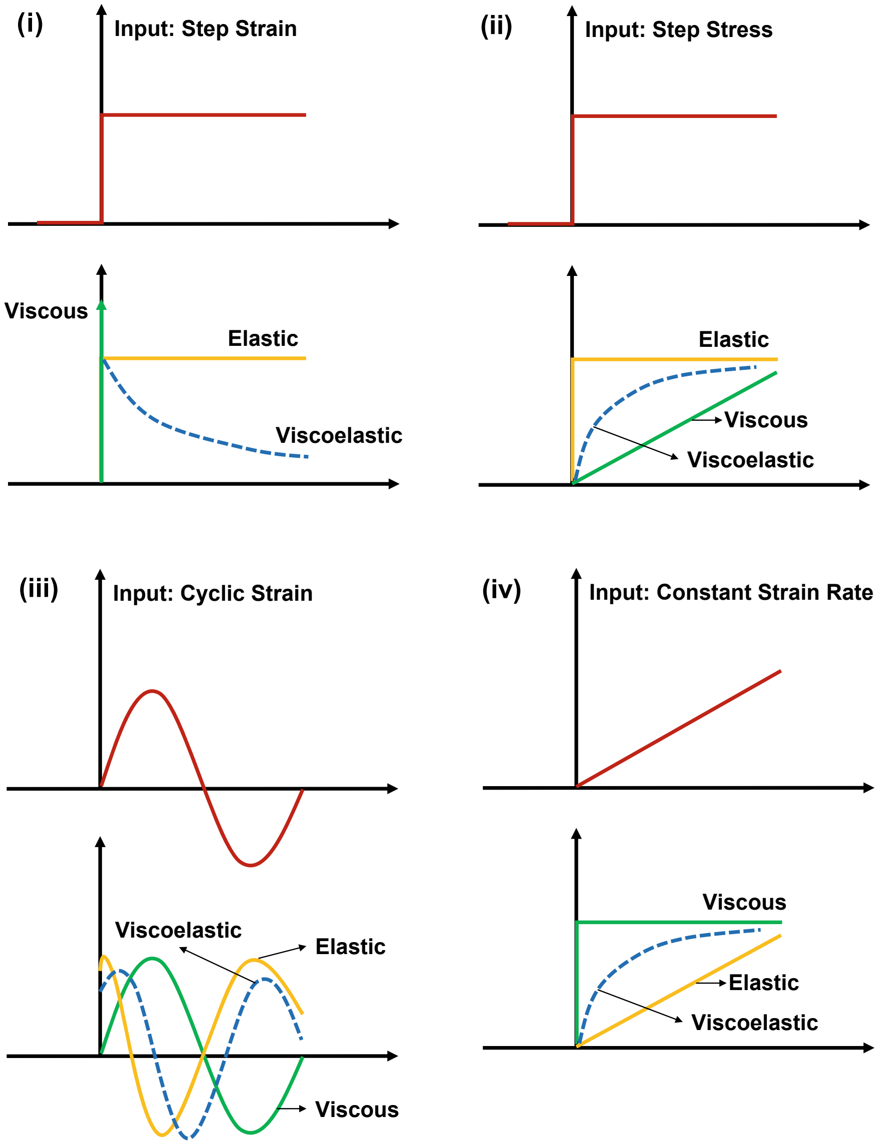

Fig. 4 Qualitative comparative analysis of mechanical responses (Gutierrez-Lemini 2014)

It is astonishing to note that the shape of variations of relaxation modulus or creep compliance with temperature resembles the shape of variation of respective material properties with logarithmic time as shown in Fig. 6. This relationship between time and temperature of polymeric viscoelastic materials as suggested by the resemblance of the shape of material functions with time and temperature is popularly called as

Fig. 5 Relation modulus as a function of temperature

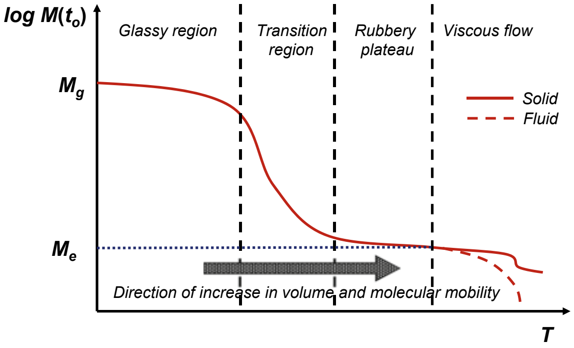

Fig. 6 Creep compliance as a function of temperature

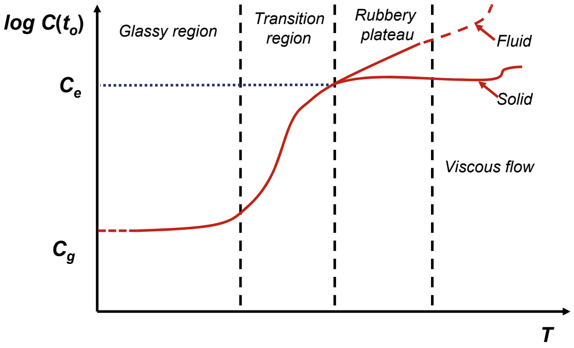

time–temperature superposition principle, which states that 'In amorphous polymeric materials, time and temperature are interchangeable'. It implies that less test temperatures correspond to short test times and high test temperatures correspond to long test times and vice versa. An implication of this principle is that reducing test temperature is equivalent to shortening test times and increasing test temperature is equivalent to lengthening or extending the test time.

3 Modeling Polymer Viscoelasticity

Modeling in polymer viscoelasticity is mainly of two types such as phenomenological modeling and molecular modeling. In phenomenological modeling, the experimental observations are expressed mathematically without considering the molecular changes involved. Thus, phenomenological modeling does not provide any information about the molecular structure of polymers. On the other hand, in molecular modeling the focus is on the individual polymeric molecular chains, their interaction and dynamics. Molecular modeling involves complex formulations and detailed analysis while phenomenological modeling is simple and provides an insight into

Table 2 Linear viscoelastic properties of some common liquids (Gutierrez-Lemini 2014)

Liquid	Viscosity at 25 °C η (cP)	Relaxation time λ (ms)	Modulus G(kPa)
Water	1	10^{-15}	10^{6}
Milk	3	10^{-9}	10^{7}
Oil	100–900	10^{-12}	10^{5}
A melt	10^{3}–10^{4}	10^{-2}	10
A glassy fluid	$>10^{14}$	10	$>10^{6}$

the overall viscoelastic behavior of polymeric materials. A brief outline of basic phenomenological elements is given in the next section followed by molecular models. The linear viscoelastic properties of some common liquids are given in Table 2.

3.1 Phenomenological Modeling of Viscoelastic Polymeric Materials.

There are five basic viscoelastic cells which enable phenomenological modeling of polymeric materials. These cells are either used independently or in combination with each other to achieve full viscoelastic modeling which is characterized by resultant material functions of creep and /or relaxation. The assemblage of these basic cells may be done in series, parallels or both, following the basic rules of equivalent stress or strain responses using Boltzmann's superposition principle as well as homogeneity or proportionality principle to define linear viscoelasticity. Generalized models can also be developed using these basic cells and the resultant functions can be derived using fundamental mathematical formulations and solution techniques. These five basic viscoelastic cells are shown in Fig. 7 and their features such as creep, relaxation and complex moduli are tabulated in Table 3 (Fig. 8).

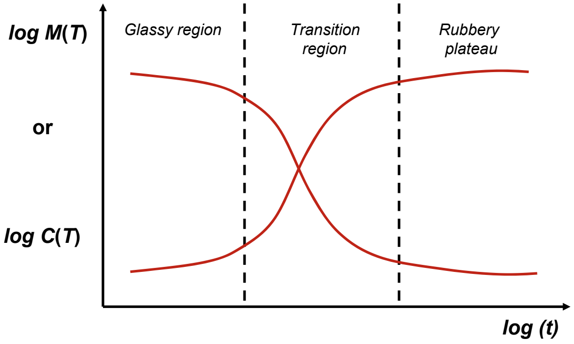

Fig. 7 Relaxation modulus and creep compliance as a function of test time under fixed temperature condition

Table 3 Features of basic viscoelastic cells used in phenomenological modeling (Chevalier and Tuong 2010)

Function	Basic cell				
	Spring	Dashpot	Maxwell cell	Voigt cell	Fractional derivative cell
$\tilde{\boldsymbol{R}}(\boldsymbol{p})$ relaxation	K	$K\tau p$	$\frac{K\tau p}{1+\tau p}$	$K(1+\tau p)$	$K(\tau p)^{\alpha}$
$\tilde{\boldsymbol{J}}(\boldsymbol{p})$ compliance	$\frac{1}{K}$	$\frac{1}{K\tau p}$	$\frac{1+\tau p}{K\tau p}$	$\frac{1}{K(1+\tau p)}$	$\frac{1}{K(\tau p)^{\alpha}}$
R(t) relaxation	$K\mathrm{H(t)}$	$K\tau\delta(\mathrm{t})$	$H(t)Ke^{\frac{-t}{\tau}}$	$K[\mathrm{H(t)}+\tau\delta(\mathrm{t})]$	$\frac{\mathrm{D}^{\alpha-1}\delta(\mathrm{t})}{\mathrm{Dt}^{\alpha-1}}$
R(t) compliance	$\frac{1}{K}\mathrm{H(t)}$	$\frac{1}{K\tau}\mathrm{H(t)}$	$\frac{\mathrm{H(t)}}{K}(1+\frac{t}{\tau})$	$\frac{\boldsymbol{H(t)}}{K}\left(1-\boldsymbol{e}^{\frac{-t}{\tau}}\right)$	$\frac{\mathrm{H(t)t}^{\alpha}}{K\tau^{\alpha}\Gamma(\alpha+1)}$
$\tilde{\boldsymbol{R}}(\omega)$ relaxation	K	$j\ K\omega\tau$	$\frac{j\ K\omega\tau}{1+j\omega\tau}$	$K(1+j\omega\tau)$	$K(j\omega\tau)^{\alpha}$
$\tilde{\boldsymbol{J}}(\omega)$ compliance	$\frac{1}{K}$	$-\dfrac{j}{K\omega\tau}$	$-j\frac{1+j\omega\tau}{K\omega\tau}$	$\frac{1}{K(1+j\omega\tau)}$	$\frac{1}{K(j\omega\tau)^{\alpha}}$

It should be noted that the use of fractional derivative cell enables to reduce the number of parameters required for characterizing the viscoelastic behavior of polymeric materials.

3.2 Molecular Modeling of Viscoelastic Polymeric Materials

The molecular modeling considers the dynamics of polymeric chains at molecular level and aims to describe the viscoelastic behavior of polymeric materials from the molecular structural changes and interaction mechanisms, both at monomeric and volumetric levels, considering the forces due to solvent molecules which may be stochastic or dissipative in nature. Such dynamics are commonly referred to as hydrodynamic interactions at molecular level. Molecular modeling, however, involves various assumptions which may not be realistically true. Three molecular models are briefly discussed in Table 4 giving details about the basic underlying principle, constitutive relation and assumptions involved. One of the first model based on molecular theory was Rouse model (Rouse 1953). This model describes the observed data from experimentation very well as long as the hydrodynamic interaction is not significant and can be ignored for all practical purposes. However, to incorporate the hydrodynamic interaction into the Rouse mode, Zimm model (Pipkin 1972) was proposed. The latter model successfully incorporated the significant hydrodynamic interaction into the constitutive model originally proposed by Rouse. Further, it is well known that the polymeric fluids comprising of linear chains of polymers undergo drastic changes in linear viscoelastic behavior under the loading due to the entanglement of the linear chains. It is also observed that in polymer melts that zero-shear viscosity increases to the 3.5rd power of molecular weight for all the molecular weights above

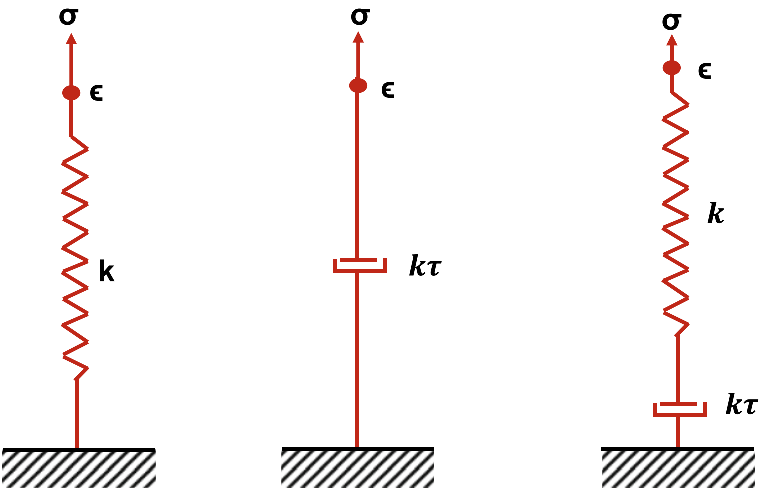

(a) Spring (b) Dashpot (c) Maxwell cell

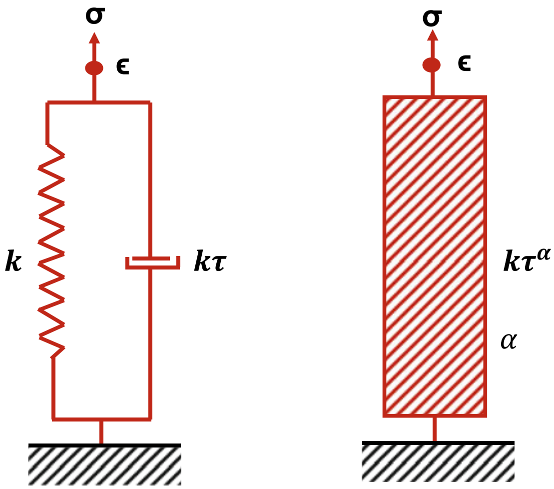

(d) Voigt cell (e) Fractional derivative cell

Fig. 8 Basic viscoelastic cells used in phenomenological modeling (Chevalier and Tuong 2010)

a certain molecular weight. This power law dependency of zero-shear viscosity on the molecular weight above a certain threshold had been an open problem in polymer fluids comprising of linear chains and the difficulty of modeling the interaction of these chains and the subsequent entanglement remained unsolved. The Doi-Edwards model (Doi and Edwards 1986) solved this problem using the mean field theory, in that, it replaced the problem of modeling numerous polymer chains by a single-chain

Table 4 Molecular models for viscoelasticity in polymeric materials (Cho 2016)

S. no.	Model	Equation	References
1	Rouse model	$G(t) = \begin{cases} G_o \exp\left(-\frac{\lambda_o}{\lambda_R}\right) & 0 < t < \lambda_o \\ G_o\sqrt{\frac{\lambda}{t}} \exp\left(-\frac{t}{\lambda_R}\right) & \lambda_o < t \end{cases}$ where $G_o = \phi \frac{k_B T}{b^3 N}$	Rouse (1953)
2	Zimm model	$G(t) \approx \phi \frac{k_B T}{b^3} \left(\frac{\lambda_0}{t}\right)^{\frac{1}{3v}} \exp\left(-\frac{t}{\lambda_z}\right)$ for $t > \lambda_o$ where $\lambda_z = \lambda_o N^{3v}$	Pipkin (1972)
3	Doi-Edwards model	$G(t) = \frac{3\rho_{\text{num}} k_B T}{5N_e} \phi(t)\Theta(t)$	Doi and Edwards (1986)

The nomenclature and formulae of the terms involved are given the respective references

problem and used an interaction parameter to model the interaction of neighbouring chains. It is important to note that the validity of Rouse model and Doi-Edwards model varies as per the frequency range considered. The later is valid for low frequency range and cannot be applied in the frequency range of Rouse model. On the other hand, the Rouse model loses its validity in the low frequency regime. Another important point to note is that these models capture the local behavior rather than the global behavior. In order to represent the complete behaviour over a vast frequency range, it is recommended to combine the modulus obtained from the two models and report them together.

4 Advances in Viscoelastic Modeling of Polymeric Materials

There have been substantial studies aiming to model viscoelasticity of polymeric materials. Various models have been developed to model the non-linear viscoelastic behavior of polymeric materials. These models are classified into four categories such as mathematical approximation based models, generalized linear viscoelastic models, simplified polymeric structure-based models and irreversible thermodynamics-based models. These models have been briefly explained and tabulated in Table 5. Of the models based on mathematical approximations, the models developed by Rivlin et al. (1956) have been of paramount importance. It is customary to develop a constitutive model using an existing functional form from an existing theoretical model. These assume an incompressible fluid for a polymeric fluid. Thus, the stress is obtained using the deformation history under viscoelasticity. The relative strain is expanded using a tensorial functional which imbibes the deformation effects of all previous histories. The Green-Rivlin model (Green and Rivlin 1959) expands the

Table 5 Models based on mathematical approximations

S. no.	Model	Equation	References
1	Rivlin-Ericksen expansion model	$\mathbf{T} + p\mathbf{I} = \underset{\tau=-\infty}{\overset{\tau=t}{T}} [\boldsymbol{C}_t(\boldsymbol{x}, \tau)]$ $\boldsymbol{C}_t(\boldsymbol{x}, \tau) = \mathbf{I} + \sum_{n=1}^{\infty} \frac{(\tau-t)^n}{n!} \mathbf{A}_n$ where A_n is the *nth order Rivlin-Ericksen tensor*	Ericksen (1956)
2	Green-Rivlin expansion model	$\mathbf{T} = -p\mathbf{I} + \int_{-\infty} \mu_1(t - t_1)[\mathbf{C}_t(t_1) - \mathbf{I}]\boldsymbol{d}t_1 + \cdots$ $+ \int_{-\infty}^{t} \int_{-\infty}^{t} \mu_2(t - t_1, t - t_2)[\mathbf{C}_t(t_1) - \mathbf{I}] \cdot [\mathbf{C}_t(t_2) - \mathbf{I}]\boldsymbol{d}t_1\boldsymbol{d}t_2 + \ldots contd$	Green and Rivlin (1959)

The nomenclature and formulae of the terms involved are given the respective references

Rivlin model using a Taylor series and as a result causes a tensorial expansion of the stress functional.

It is important to understand the temperature dependency of viscoelastic behavior of polymers and the role of thermodynamics-both reversible and irreversible. Leonov model (Leonov 1976) postulates a decomposition of deformation employing multiplicative law based on irreversible thermodynamics. Unlike metal plasticity, where an infinitesimal strain is decomposed into elastic am plastic components, Leonov argued that this approach cannot be applied to polymer case where the deformations are finite. The latter component of infinitesimal plastic theory also called as plastic strain is representative of the permanent deformation once the yield condition is exceeded.

The main success in constitutive modeling of polymer is a suite of models based on generalized linear and nonlinear viscoelasticity. The foremost model was proposed by Oldroyd (1950) based on material frame-indifference principle using a time-derivative of deformation rate tensor. It was further generalized by replacing the time derivates of strain- and stress-rate by a time derivative which is objective. This model is also called eight-constant model. However, Maxwell model Crochet and Keunings (1980) was developed by certain parameters of Oldroyd generalization model as equated to zero such as $\mu_1 = \mu_2 = \lambda_2 = a_1 = a_2 = 0$ and $\mu_1 = 2\lambda_1$. Further to this end, K-BKZ model (Kaye 1962) was developed using the formalism of hyper-elasticity and superposition principle as shown in Table 6.

> Another approach to develop constitutive model is based on simplifying the polymeric structure. A series of models used the Brownian Motion theory and Langevin formulation to characterize the polymer behavior (Tanner and Stehrenberger 1971). In order to describe the interactions between chains within a polymer, Giesekus model (Giesekus 1966,1982) was developed. It uses a non-proportionality of a tensor based on mobility due to the environment effect of the spring-dumbbell molecule as shown in Table 7.

5 Tribology and Its Role in Asphalt Binder Characterization

Tribology deals with the study of friction, lubrication, and wear of surfaces which are in contact or in relative motion. Primarily, tribology has a wide application in the field of mechanical engineering due to the kinematic nature of machines and their components. Tribology is also used in the field of lubrication, where lubricants are used to reduce wear and tear of mechanical parts as well as to reduce the friction between the parts moving relative to one another. Asphalt mixture compaction is an extremely complex process. It is governed by various factors such as material, field conditions, boundary condition properties, gradation, etc. In order to control the process of mixing and compaction, the gradation of the aggregates cannot be changed due to obvious economic and mix design considerations, however, two main factors are controlled to obtain the desired asphalt mixture compaction. Based on the literature, asphalt binders especially the modified asphalt binders have shown

Table 6 Models based on generalized linear viscoelasticity

S. no.	Model	Equation	References
1	Oldroyd generalization model	$\mathbf{T}' + \lambda_1 \overset{\Delta}{\mathbf{T}}\prime + \frac{\mu_o}{2}\boldsymbol{tr}(\mathbf{T}\prime)\mathbf{A}_1 - \frac{\mu_1}{2}(\mathbf{T}\prime \cdot \mathbf{A}_1 + \mathbf{A}_1 \cdot \mathbf{T}\prime) + \frac{a_1}{2}\boldsymbol{tr}(\mathbf{T}\prime \cdot \mathbf{A}_1)\mathbf{I}$ $= \eta_o\left[\mathbf{A}_1 + \lambda_2\mathbf{A}_2 - \mu_2\mathbf{A}_1 \cdot \mathbf{A}_1 + \frac{a_2}{2}\boldsymbol{tr}(\mathbf{A}_1 \cdot \mathbf{A}_1)\mathbf{I}\right]$	Oldroyd (1950)
2	The upper-convected Maxwell model	$\mathbf{T}\prime + \lambda_1 \overset{\nabla}{\mathbf{T}}\prime = 2\eta_0\mathbf{D}$	Crochet and Keunings (1980)
3	K-BKZ model	$\mathbf{T} = -p\mathbf{I} + 2\int_{-\infty}^{t}\left[\frac{\partial\Phi}{\partial I_{\mathbf{C}_t^{-1}(\tau)}}\mathbf{C}_t^{-1}(\tau) - \frac{\partial\Phi}{\partial I_{\mathbf{C}_t(\tau)}}\mathbf{C}_t(\tau)\right]\mathrm{d}\tau$	Kaye (1962)

The nomenclature and formulae of the terms involved are given the respective references

Table 7 Models based on simplification of polymeric structure

S. no.	Model	Equation	References
1	Spring-Dumbbell model	$\boldsymbol{T} = -p\mathbf{I} + \frac{\rho_N h_o^2 k(\langle\mathbf{h}\rangle)}{3}(\mathbf{C} - \mathbf{I})$	Tanner and Stehrenberger (1971)
2	Giesekus model	$\lambda_{\boldsymbol{G}} \overset{\nabla}{\mathbf{T}}\prime + \mathbf{T}\prime + \frac{\alpha}{G_G}\mathbf{T}\prime^2 = 2\eta_{\boldsymbol{G}}\mathbf{D}$	Giesekus (1966,1982)

The nomenclature and formulae of the terms involved are given the respective references

non-Newtonian behavior, such as shear thinning or shear thickening, as such there is a need to characterize the behavior of asphalt binders for a range of shear rates. At the same time, it causes a different film thickness of asphalt binder around the aggregates in an asphalt mixture. Tribology and its use become most evident and relevant during the compaction process of asphalt mixtures. When asphalt concrete is placed on the road, compaction happens due to particle rearrangement and reorientation under loads. Asphalt concrete consists of aggregate particles which are of different particle sizes as determined by asphalt mixture gradation. The gradation involves fixing the sizes and amounts of different aggregate particle sizes, fillers, and air voids as per the asphalt mix design. In order to study the role of tribology and linear viscoelasticity, a standard test which capture the effect of asphalt binder on the tribological behaviour only as well as shear rheology. The effect of substrate, wear, etc. should be accounted for separately. Dynamic Shear Rheometer fixtures that allow testing over wide range in a single test should be developed. Also, it is important to have a better control of sample preparation and testing setup is required to create the ideal and representative conditions of the field. Many modifications of asphalt binder have been done.

6 Conclusion

Viscoelasticity is very important in polymer technology as it plays a vital role in production, processing and characterization of polymeric materials, whether solids or fluids. Modeling viscoelastic behavior of polymeric materials requires diverse background of applied mathematics, physic, chemistry and various engineering disciplines as such the onus of researchers in this field is huge given the diversity of knowledge required and the inherent complexity of the problem makes it more challenging. In this paper, an introduction to viscoelastic behavior of polymeric materials was given followed by the detailed discussion on the fundamental aspect of viscoelastic behavior focusing on the comparative analysis of mechanical responses of elastic solid, viscous fluids and viscoelastic polymeric materials qualitatively. The regions in viscoelastic behavior have also been discussed and modeling approaches such a7 s phenomenological and molecular have been discussed. Finally, the advances in modeling viscoelastic behavior of polymeric materials are given to aid the reader in understanding the evolution of viscoelastic theory of polymers.

References

Cho KS (2016) Viscoelasticity of polymers: theory and numerical algorithms. Springer, Netherlands, Dordrecht

Chevalier Y, Tuong J (2010) Mechanical characterization of materials and wave dispersion. Wiley-ISTE, 978-1-848-21077-6

Crochet MJ, Keunings R (1980) Die swell of a Maxwell fluid: numerical prediction. J Nonnewton Fluid Mech 7(2–3):199–212

Daryaee D, Habibpour M, Gulzar S, Underwood BS (2020) Combined effect of waste polymer and rejuvenator on performance properties of reclaimed asphalt binder. Constr Build Mater 121059. https://doi.org/10.1016/j.conbuildmat.2020.121059

Doi M, Edwards SF (1986) The theory of polymer dynamics. Oxford University Press

Ericksen JL (1956) Overdetermination of the speed in rectilinear motion of non-Newtonian fluids. Q Appl Math 14:318–321

Giesekus H (1966) Die Elastizität Von Flüssigkeiten. Rheol Acta 5:29–35

Giesekus H (1982) A simple constitutive equation for polymer fluids based on the concept of deformation-dependent tensorial mobility. J Non-Newt Fluid Mech 11(1–2):69–109

Green AE, Rivlin RS (1959) The mechanics of non-linear materials with memory. Arch Ration Mech Anal 4:387–404. https://doi.org/10.1007/BF00281398

Gulzar S, Underwood S (2019a) Use of polymer nanocomposites in asphalt binder modification. In: advanced functional textiles and polymers, pp 405–432. Wiley

Gulzar S, Underwood S (2019b) Nonlinear rheological behavior of asphalt binders. In: 91st Annual meeting of the society of rheology. Raleigh, NC

Gulzar S, Underwood BS (2020a) Nonlinear viscoelastic response of crumb rubber modified asphalt binder under large strains. Transp Res Rec J Transp Res Board 2674:139–149. https://doi.org/10.1177/0361198120907097

Gulzar S, Underwood S (2020b) Stress decomposition of nonlinear response of modified asphalt binder under large strains. In: Advances in materials and pavement performance prediction (AM3P 2020). CRC Press, San Antonio, Tx, USA

Gulzar S, Underwood S (2020c) Large amplitude oscillatory shear of modified asphalt binder. In: Advances in materials and pavement performance prediction (AM3P 2020). CRC Press, San Antonio, Tx, USA

Gulzar S, Underwood S (2020d) Fourier transform rheology of asphalt binders. In: Advances in materials and pavement performance prediction (AM3P 2020). CRC Press, San Antonio, Tx, USA

Gutierrez-Lemini D (2014) Engineering viscoelasticity. Springer US, 978-1-4614-8139-3

Kaye A (1962) Non-Newtonian flow in incompressible fluids. College of Aeronautics Note 134 & 149, Cranfield

Knauss WG, Emri I, Lu H (2008) Mechanics of polymers: viscoelasticity. Springer, Boston, MA, pp 49–96

Leonov AI (1976) Nonequilibrium thermodynamics and rheology of viscoelastic polymer media. Rheol ACTA 15:85–98

Mansourkhaki A, Ameri M, Habibpour M, Shane Underwood B (2020a) Relations between colloidal indices and low-temperature properties of reclaimed binder modified with softer binder, oil-rejuvenator and polybutadiene rubber. Constr Build Mater 239. https://doi.org/10.1016/j.conbuildmat.2019.117800

Mansourkhaki A, Ameri M, Habibpour M, Shane Underwood B (2020b) Chemical composition and rheological characteristics of binders containing RAP and rejuvenator. J Mater Civ Eng 32:04020026. https://doi.org/10.1061/(asce)mt.1943-5533.0003016

Oldroyd JG (1950) On the formulation of rheological equations of state. Proc R Soc London Ser A Math Phys Sci 200:523–541. https://doi.org/10.1098/rspa.1950.0035

Pipkin A (1972) Lectures on viscoelasticity theory. Springer, Berlin

Rouse PE (1953) A theory of the linear viscoelastic properties of dilute solutions of coiling polymers. J Chem Phys 21:4628. https://doi.org/10.1063/1.1699180

Tanner RI, Stehrenberger W (1971) Stresses in dilute solutions of bead–nonlinear-spring macromolecules. I. Steady potential and plane flows. J Chem Phys 55:1958–1964. https://doi.org/10.1063/1.1676334

A Review on Tribology of Particulate Filled Polymer Composites: In the Context of Marble Dust Filled Polyester

Sandip Kumar Nayak, Alok Satapathy, and Sisir Mantry

Abstract Polymers and their composites are the rapidly growing class of materials brought revolution in the industries with their high wear resistance properties along with high specific strength, low density and high stiffness. An economical and traditional way to improve the properties of the polymers in order to make them suitable for various industrial applications is to reinforce them with short fibers and ceramic fillers. Another advantage of using these materials in the wear related industrial applications is that the properties of these composite materials can be modified at a wide range as per the requirement in order to overcome the tentative technical problems. The role of particulate fillers on the tribological behavior of polymers in dry sliding conditions have been discussed and emphasis is given on the wear response of the polymers incorporated with non-conventional particulate fillers like, industrial and construction wastes. The dry sliding wear response of micro-sized waste marble dust (a construction waste) filled polyester composites is presented and the mechanisms of wear loss are also discussed in brief.

Keywords Particulate Fillers · Polymer Composites · Wear Response · Marble Dust

1 Composites: Definition

It is very difficult to define a composite material as no proper definition of composite exits (Abdelbary 2015). Still Srinivasulu and Tejaswi (Akashi et al. 1970) define it as "the material which is made of two or more materials at the macroscopic phase can be called as a composite material". In the book *Polymer Matrix Composites and Technology* authored by Wang et al. (2011) composite materials are defined as "a multi-phase combination material of two or more component materials with

---

S. K. Nayak (✉) · A. Satapathy
Mechanical Engineering Department, National Institute of Technology, Rourkela, India

S. Mantry
Materials Chemistry Department, CSIR-Institute of Minerals and Materials Technology, Bhubaneswar, India

H. Jena et al. (eds.), *Tribology of Polymer and Polymer Composites for Industry 4.0*,
Composites Science and Technology, https://doi.org/10.1007/978-981-16-3903-6_6

different properties and different forms through compounding processes, it not only maintains the main characteristics of the original component, but also shows new character which are not possessed by any of the original components”. However, composite materials should have the following characteristics:

1. All the phases of the material are physically distinguishable and mechanically separable.
2. The physical and mechanical properties of the composite prepared are superior to the properties of its constituents.
3. The composites are heterogeneous in nature.

2 Classification

There are several ways for the classification of composite materials. However, composite materials can be commonly classified as per the use of matrices and reinforcements as shown in Fig. 1a, b respectively.

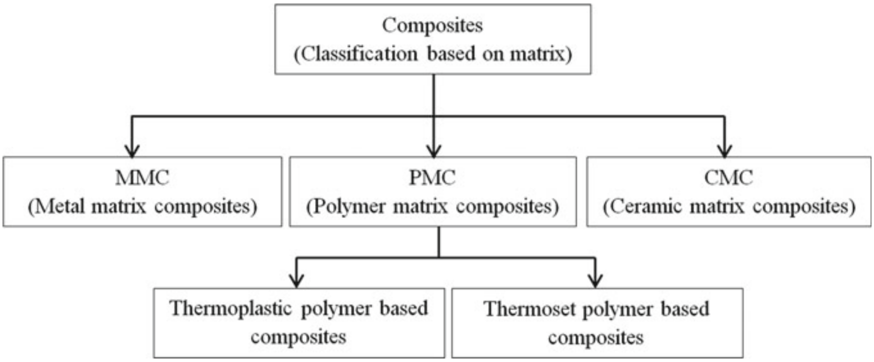

(a) Classification based on matrix material

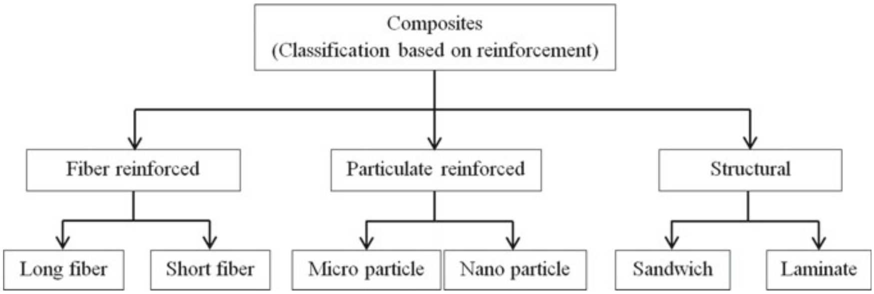

(b) Classification based on reinforcement content

Fig. 1 Classification of composite materials

3 Polymer Matrices

As shown in Fig. 1a, the polymer matrices used for the manufacturing of composite materials can be classified into two categories.

1. Thermoplastic matrices
2. Thermosetting matrices

Thermoplastic matrices: 'Polycarbonate (PC)', Polypropylene (PP)' and 'Polyamide (PA)' are the most commonly used thermoplastic matrices used for the preparation of polymer composites. The isotropic or anisotropic nature of the thermoplastic matrices depends on the curing period of this. These matrices are used normally for the composite preparation using short fiber or particulate filler as reinforcements. An important property of the composites made using thermoplastic matrices is that, the strain of the composites increases with time under constant loading condition (Abdelbary 2015).

Thermosetting matrices: 'Epoxy' and 'Polyester' are the most commonly preferred thermosetting matrices used in the polymer composite making process. Unlike, thermoplastic matrices, these are isotropic in nature. The physical and mechanical properties of the composites made up of thermosetting matrices are better than the composites made up of thermoplastic matrices. However, epoxy resins are superior in properties as compared to polyester resins (Abdelbary 2015).

4 Tribological Response of Particulate Filled Composites: Brief Research History

Tribology deals with the response of a material in wear and friction situation. Wear is the progressive loss of material from the engineering surface of a solid body owing to relative motion between the engineering surface of the body and a contacting surface/substance or substances. The effect of wear loss has been recognized to be very harmful and the loss of cost due to wear is also found to be very high. Still, wear is important for performing almost every activities in our in our day to day life. Although, researches on resolving wear related problems has been started in the industrial countries since 1960s and investigations on wear has been extensively conducted on the twentieth century, still in the twenty-first century, the problem of wear exits in industrial applications (Patnaik et al. 2010a). Unfilled polymers and their composites has been used potentially as the replacement of some conventional metallic sliding parts for the rapid progress in the development of the physical, corrosion, mechanical and tribological properties of these composites (Abdelbary 2015). In order to provide high wear resistance and improved hardness to the polymers, particulates are added as fillers into it. In the past few decades investigations have been conducted on evaluating the tribological properties of the polymers incorporated with inorganic fillers and positive output has been obtained. In this contrary on the year 1986, Friedrich (1986) published a book chapter based on the effect of filler particles on the wear behavior of polymer-fiber composite system. In this work, SiC, Al_2O_3, Glass microsphere and flint particles of different sizes have been used and the improvement in the wear resistance of the polymer-fiber composite system for each of the filler is observed. Bahadur and Gong (1992) investigated the effect of copper compounds on the sliding wear behavior of polyetheretherketone (PEEK). In the investigation, CuO, CuS and CuF_2 are used as particulate fillers in different proportions in PEEK and observed that, the resistance to wear of PEEK polymer is enhanced significantly with the incorporation of these fillers. However, the co-efficient of friction of the composites is also increased. Bahadur et al. (1993) used these copper compounds again in the Nylon 11 polymer and inspected the wear behavior of the filled composites using glass disc as the counter body. Identical results have been obtained as in the previous case but the wear rate of the composites sliding against the glass disc was much higher than sliding against the steel disc as reported by them. Sliding wear characterization of polymethylmethacrylate (PMMA) composites filled with glass particles to be used as dental application is conducted by Friedrich (1993). From the investigation, it is resulted that the wear resistance of the unfilled composite is improve significantly by the incorporation of filler. The wear rate of glass-nylon 11 composites is reduced by the use of CuO filler as an secondary reinforcement in it (Bahadur and Polineni 1996). A review conducted by Friedrich et al. (2002) on the wear of polymer composites reported that the incorporation of micro and nano inorganic fillers in the polymers improved the wear resistance of polymers significantly. The tribological behavior of polyphenylene sulfide (PPS) filled with nano-shaped alumina is studied by Schwartz and Bahadur (2000). The wear rate of the filled composite is reported to be increased irrespective of the filler amount. However, the bond strength of the polymer is increased with the incorporation of nano alumina. The wear behavior of PPS filled with the inorganic fillers like Ag_2S, CuS, ZnF_2, and SnS is investigated by Schwartz and Bahadur (2001) and observed that, the wear rate of unfilled PPS is reduced with the incorporation of fillers Ag_2S and CuS. Whereas, the wear rate of the raw PPS is increased significantly with the fillers ZnF_2 and SnS. The wear rate of PEEK composites filled with PTFE and SiC particulates is measured by Wang et al. (2000). It is concluded that the wear rate of PEEK filled with PTFE filler is reduced up to a filler volume fraction of 20% and beyond that the wear rate is increased. However, for PEEK-PTFE composites filled with SiC particulates, the wear rate of the hybrid composite is increased up to the filler volume fraction of about 7.5% and beyond that the wear rate is decreased. The role of PTFE and CuS in the wear behavior of PEEK composite is studied by Voort and Bahadur (1995). It is observed that, minimum wear is attained to the PEEK composite for the incorporation of 35 vol.% of CuS but the co-efficient of friction is increased. However, the incorporation of 5 vol.% of PTFE filler with 30 vol.% of CuS provided better co-efficient of friction to the composite. Similarly, the incorporation of micro and nano-TiO_2 fillers improved the scratch resistance of neat epoxy and the dimensional stability of epoxy is also improved with the incorporation of nano-TiO_2 particles

(Ng et al. 2001). Dry-sliding wear properties of epoxy composites filled with nano ZrO_2 particles is studied by Kurahatti et al. (2014). From the study, it is concluded that the wear rate of neat epoxy is reduced to minimum for a filler concentration of 0.5 wt.% and the value of wear rate is approximately 95% lower than the wear rate of neat epoxy. The sliding wear resistance of neat epoxy is enhanced significantly with the incorporation of graphite fillers in it as reported by Baptista et al. (2016). The self-lubricating nature of graphite helps in reducing the co-efficient of friction of the composites prepared with graphite fillers and hence the wear rate is decreased (Sudheer et al. 2014). Srinivas and Bhagyasekhar (2014) reported that the wear resistance of neat epoxy is enhanced about 85% with the incorporation of 5% of Sic particulate with 35% graphite filler. Basavarajappa et al. (2009) investigated the wear behavior of polymer composites with the variation of filler concentration. It is observed that the use of SiC particulate as a secondary filler in the polymer composite system helps in reducing the wear rate of the composites and the volume of wear loss is dependent on the test variables like sliding velocity, sliding distance and normal load. Tribological characteristics of epoxy composites filled with graphene and molybdenum disulfide (MoS_2) particles are studied by Upadhyay and Kumar (2018). It is concluded that the epoxy-graphene-MoS_2 hybrid composite performed better wear resistance than the epoxy-graphene and epoxy- MoS_2 binary composite system. Identical observations on the sliding wear behavior of polymers filled with different inorganic fillers like CuS, CuO, CaF_2, ZnF_2, SiC, NiS and PbSe is reported by the previous researchers and they observed that the wear behavior of polymers are significantly affected by the incorporation of ceramic fillers. In some cases, the wear resistance of neat polymers is improved significantly and in very few cases the wear resistance of the neat polymers is decreased. However, in each conditions the bond strength of the hardened composites is increased (Pei et al. 2016; Tanaka 1986; Xue and Wang 1997; Yu and Bahadur 1998; Zhao and Bahadur 1999; Cho 2009; Haupert and Wetzel 2005). Thus, inorganic particulate fillers are proposed as the better reinforcements in polymers, but the high cost of these conventional fillers sometimes restricts their use as the reinforcement materials. Keeping this in eye, some investigators are using industrial and construction wastes as the replacement of conventional fillers for the preparation of polymer composites without compromising the properties of the composites and proposed their use in wear related applications. In this contrary a number of investigations have been conducted on evaluating the erosion behavior of polymer composites filled with the particulates of these wastes such as red mud, copper slag, fly ash, blast furnace slag, cement kiln dust, linz-donawitz dust, granite dust, marble dust etc. (Patnaik et al. 2010b,2009; Rout et al. 2012; Biswas and Satapathy 2009,2010; Biswas et al. 2010; Padhi and Satapathy 2014,2013a; Pati and Satapathy 2015; Ray et al. 2018). Despite the fact that considerable researches have been conducted to develop waste ceramic particulate filled polymer composites for erosion application, investigations on the development of waste ceramic particulate filled composites for sliding wear applications are quite less. Earlier in 2010, Satapathy and Patnaik (2010) used red mud, an industrial waste as filler in the polyester matrix for the preparation of composites and investigated the wear behavior of the composites in dry-sliding mode. Investigation resulted that the wear resistance of hardened raw polyester is enhanced significantly with the incorporation of red mud into it. Similarly, Padhi and Satapathy (2013b) explored the effect of micro-sized blast furnace slag on the sliding wear characteristics of short glass fiber reinforced epoxy composites and concluded that, the resistance to wear of neat epoxy and short glass fiber reinforced epoxy is enhanced with the incorporation of filler. Dry-sliding wear characterization of epoxy matrix reinforced with linz-donawitz sludge is investigated by Purohit and Satapathy (2016). It is reported that the wear rate of neat epoxy is reduced with the incorporation of the filler. The resistance to sliding wear of silicon bronze alloy is enhanced significantly with the incorporation of marble dust (a construction waste) as reported by Gangwar et al. (2017). Nayak and Satapathy (2019) investigated on the dry-sliding wear response of polyester filled with waste marble dust and reported that the resistance to sliding wear of hardened raw polyester is enhanced significantly with the incorporation of marble dust. Earlier in 2020, Nayak et al. (2020) used marble dust as a secondary filler in the glass-polyester composite system to study the effect of filler on the sliding wear properties of the reinforced hybrid composites. The incorporation of marble dust as a secondary filler is reported to be significant in terms of reducing the wear rate of glass-polyester composites.

The extensive literature survey suggested that, over the past few decades, few investigators have considered industrial and construction wastes as the filler materials for the preparation of wear resistant polymer composites. This report presents the research findings of the authors on a new class of polyester composites filled with different proportions of marble dust in regard to their tribological response in dry sliding conditions.

5 Wear Response of Marble Dust Filled Polyester: A Case Study

5.1 Materials, Composite Fabrication and Dry-Sliding Wear Test

Unsaturated polyester resin, procured from A to Z Chemicals, Kolkata is used as the matrix material in the present study along with its hardener methyl ethyl ketone peroxide and accelerator cobalt napthenate. A waste marble dust collected from a nearby construction site is used as the reinforcing agent after proper treatment. The particle size and density of the marble dust used are measured to be 110 micron and 2.80 g cm^{-3} respectively. Polymer solution casting technique is an easy and conventional method of fabricating polymer composites. Using this method, five set of polyester-marble composites are prepared incorporating five different amount (0, 8, 16, 24 and 32 wt.% respectively) of marble dust in polyester matrix. The hardener and accelerator are added at a proportion of 2% by weight each with the matrix for its proper curing. The polyester-marble solution is prepared taking proper

Table 1 Test parameters and their selected levels used for the investigation (Nayak and Satapathy 2019)

Test parameters	Levels					Units
Sliding velocity (A)	25	50	75	100	125	cm/s
Sliding distance (B)	250	500	750	1000	1250	Meter
Normal load (C)	5	10	15	20	25	Newton
Filler content (D)	0	8	16	24	32	wt%

amount from both the constituents and then poured into a wax coated glass tube having diameter 10 mm. It is then kept in room temperature for 24 h so that the matrix along with the reinforcement is cured properly. The solidified composite samples are then removed from the glass tubes and cut into required size as per the ASTM dimension. A MAGNUM pin-on disc wear test apparatus is used for the dry-sliding wear characterization of the prepared composite samples. The composite samples are prepared as per ASTM G 99–05. As per the standard, the cylindrical test samples are cut with a diameter of 10 mm and length of 30 mm. Emery papers having grit size P 220 and surface roughness Ra-300 nm are used as the counter surfaces for the test trials. The emery papers are cut as per the size of the steel disc (counter surface) and attached to it with a standard adhesive so as to act as the counter surface. The test is conducted with a track diameter of 80 mm and as per the parameter combinations obtained from the Taguchi's L_{25} orthogonal array as given in Table 2. The test parameters and their individual levels selected for the test trials are provided in Table 1.

The weight loss of the composite samples after each test run is measured and the specific wear rate (SWR) corresponding to the test run is calculated using the relation givel in Eq. 1. Nayak and Satapathy (2019).

$$\text{Specific wear rate } = \Delta\text{m}\big/(\rho \times L \times N)\,\text{cm}^3\big/\text{N} - \text{m} \tag{1}$$

where ?m is the measured weight loss of the composites after a test run (g), ? is the density of composite samples (g cm^{-3}), L is the sliding distance (m) and N is the normal load (N) applied on the test sample. From Eq. 1 it can be observed that, the volume loss of the composite samples per unit load and sliding distance is the specific wear rate of the composite for that test run.

Table 2 Obtained specific wear rate and corresponding S/N ratios for different test conditions as per Taguchi L_{25} design (Nayak and Satapathy 2019)

Test run	Sliding velocity, A (cm/s)	Sliding distance, B (m)	Normal load, C (N)	Filler content, D (wt%)	Specific wear rate (mm^3/N–m)	Signal-to-Noise Ratio
1	25	250	5	0	0.0248	32.1110
2	25	500	10	8	0.0142	36.9542
3	25	750	15	16	0.0127	37.9239
4	25	1000	20	24	0.0121	38.3443
5	25	1250	25	32	0.0113	37.6546
6	50	250	10	16	0.0119	38.4891
7	50	500	15	24	0.0122	38.2728
8	50	750	20	32	0.0107	39.4123
9	50	1000	25	0	0.0634	23.9582
10	50	1250	5	8	0.0171	35.3401
11	75	250	15	32	0.0108	39.3315
12	75	500	20	0	0.0594	24.5243
13	75	750	25	8	0.0188	34.5168
14	75	1000	5	16	0.0154	36.2496
15	75	1250	10	24	0.0142	36.9542
16	100	250	20	8	0.0212	33.4733
17	100	500	25	16	0.0198	34.0667
18	100	750	5	24	0.0172	35.2894
19	100	1000	10	32	0.0139	37.1397
20	100	1250	15	0	0.0528	25.5473
21	125	250	25	24	0.0202	33.8930
22	125	500	5	32	0.0143	36.8933
23	125	750	10	0	0.0499	26.0380
24	125	1000	15	8	0.0192	34.3340
25	125	1250	20	16	0.0196	34.1549

6 Test Methodology and Results

6.1 *Taguchi's Orthogonal Array*

Taguchi's orthogonal array is an important optimized tool used for designing least number of experiments using the test parameters and their levels such that, the effect of test parameters can be investigated properly without performing the possible number of tests. In the present study, as given in Table 1, four different test parameters and five different levels from each of the parameters are considered for investigating the wear response of the composites. Considering the parameters and their levels, the possible number of test trials that should be conducted to investigate the effect of test parameters on the SWR of the composites is 4^5?=?1024. Such a number of test trial is time consuming and expensive to conduct. Thus, the number of trials should be reduced to a minimum number without hampering the purpose of study. Using the Taguchi's orthogonal array (L_{25}) the number of test runs are optimized to 25 and the combination of the levels of test parameters as per the design is given in Table 2. Considering the parameter combinations, the wear trial is conducted on the composite samples and the corresponding SWR obtained is provided in Table 2. The test is repeated three times for each of the parameter combinations and the average of these three results is only considered as the SWR for the corresponding combination. Instead of being a good optimized tool, Taguchi's array is also a strong analysis tool. The tool is used to analyze the test results obtained from the experimental investigation in order to obtain the corresponding signal-to-noise ratio (s/n ratio) and the rank of test parameters affecting the SWR. Signal-to-noise ratio can be outlined as the ratio of the variation in output response resulting from some alteration in the input responses. SWR is the desired signal in the present study that depends on the input variables as listed in Table 1. Thus, s/n ratio becomes important in the investigation to clarify the degree of significance of each control factors on the output response. Using the characteristic "smaller is better", the s/n ratio can be calculated using the logarithmic relation given in Eq. 2

$$\frac{S}{N} = -10\log_{10} \times \frac{1}{\mathrm{n}}\left(\sum Y^2\right) \tag{2}$$

where, 'S' is the variance, 'N' is the noise, 'n' is the number of experiments and 'y' is the mean.

The obtained SWR of the composite samples from the test trials as per the parameter combinations set using Taguchi's L_{25} orthogonal array are given in Table 2 along with their s/n ratios. From the results, it can be observed that the maximum SWR is obtained for the hardened raw polyester having value 0.0634 mm^3/N-m when slide with a velocity of 50 cm/s for 1000 m under 25 N load. The corresponding s/n ratio for the maximum SWR is 23.9582 as evidence from the table. Whereas, the minimum SWR is obtained for the composite sample having filler content 32% by weight having value 0.107 mm^3/N-m when tested for a distance of 750 m with a sliding velocity of 50 cm/s under 20 N load. The corresponding s/n ratio for the minimum SWR is 39.4123 which is the maximum among all the s/n ratios. Although, the effect of test parameters is somehow reflected from the observation but is not sufficient to clarify the rank of test parameters and the effect of their different levels.

In order to observe the influence of different levels of the test parameters and to find out the rank of test parameters as per their effect on the SWR, the test results are analyzed using the Taguchi's L_{25} orthogonal array and the obtained s/n ratios are given in Table 2. The analysis provided the main effects plot for s/n ratios as displayed in Fig. 2. From the figure, it can be observed that the filler content is

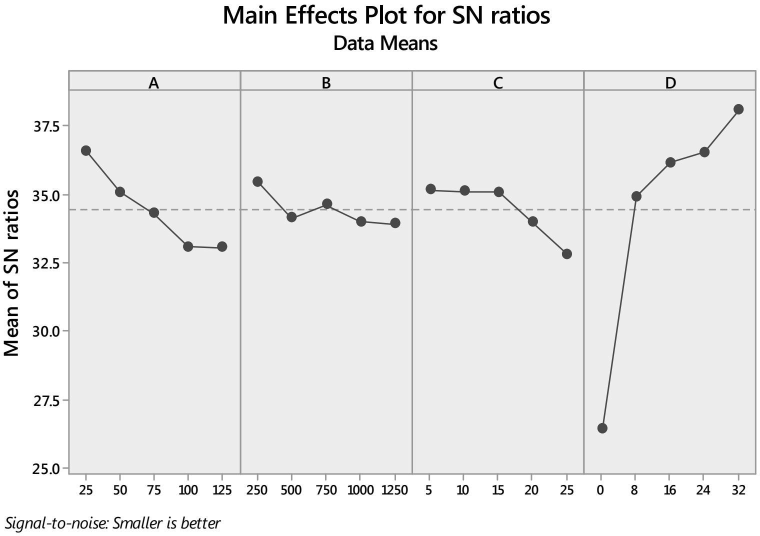

Fig. 2 Main effect plot for s/n ratios (Nayak and Satapathy 2019)

having highest influence on the SWR of the composites as the inclination of line diagram presenting filler content is highest among all. Similarly, sliding velocity, normal load and sliding distance in that sequence can be ranked as 2, 3, and 4 after filler content in terms of affecting the SWR of the composite samples. It is clear from Fig. 2 that, the combination of test parameter levels A_1, B_1, C_1 and D_5 has been observed to be the most effective combination that will experimentally influence the SWR on the basis of smaller is better characteristics. The respective interaction plots for s/n ratios obtained from the analysis are displayed in Fig. 3a–c.

7 Scanning Electron Microscopy

In order to get a clear idea on the possible wear mechanisms, the morphologies of the worn composite surfaces are studied. A JEOL JSM 6480 LV scanning electron microscope is used to take the micrographs of the worn composite surfaces. The micrographs are taken at low vacuum mode and high pressure. In order to obtain better SEM images, the samples should be conductive so as to avoid the charging and the gathering of electrons on the surface of the samples. As we know that the polymer composites are non-conductive in nature, a thin film of platinum coating is provided on the surface of the test samples in order to make these conductive before taking the micrographs.

The morphologies of the worn composite surfaces are studied in order to identify the possible wear mechanisms. In the present investigation, from the available worn surface morphologies, some are displayed in Fig. 4a–d that are showing different

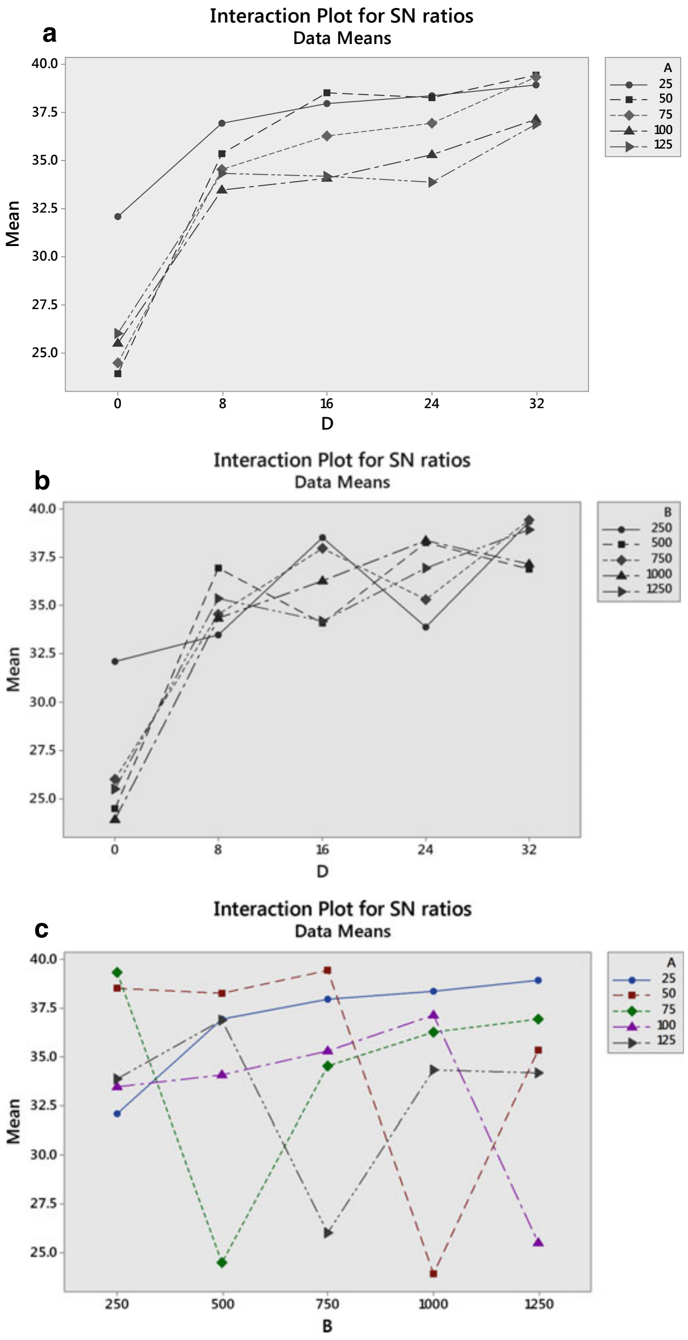

Fig. 3 **a** Interaction plot between sliding velocity and filler content for specific wear rate. **b** Interaction plot between sliding distance and filler content for specific wear rate. **c** Interaction plot between sliding distance and sliding velocity for specific wear rate

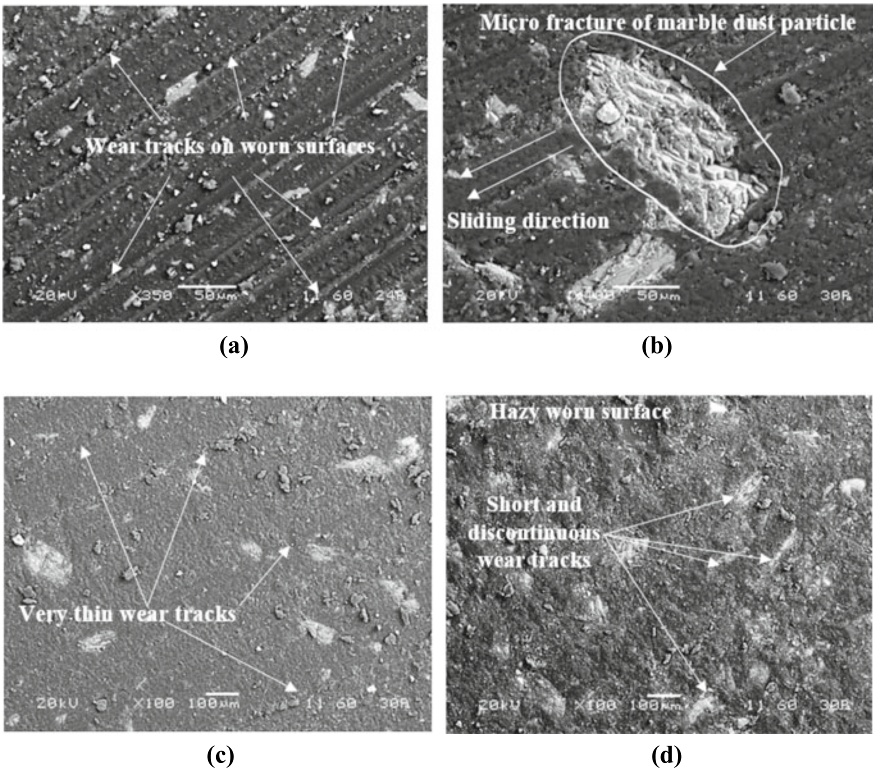

Fig. 4 SEM images of the worn composite surfaces showing the wear mechanism (Nayak and Satapathy 2019)

wear mechanisms. Figure 4a displays the micrograph of the worn composite surface consisting of 8wt% of filler after slide for 1000 m with a velocity of 125 cm/s under 15 N load. The embeded filler particles in the polyester matrix are clearly visible in the figure. The thick and continuous wear tracks on the worn composite surface explains the softness and ductileness of the composite surface. Formation small wear debris are noticed on the worn surface. Figure 4b illustrates the micrograph of the worn composite surface consisting of 16 wt% of filler when tested with the extreme parameter combinations. The figure clearly demonostrates the micro cracking of a marble dust particle, that confirms that the material removal of the composite samples in the dry sliding mode are completely dominated by micro-cracking of hard ceramic filler particles, micro-cutting of the softer matrix region by the hard and brittle particles of the counter surface and micro-ploughing of the counter surface particles on the composite surface. The plastic deformation on the worn composite surface is clearly visible. Figure 4c depict a small portion of the worn composite surface consisting of 24% of filler by weight when tested with a velocity of 125 cm/s, for 250 m, under 25 N load. The surface of the composite seems to be harder than the previous two composites as the wear tracks on the composite surface present is thinner than the previous. However, the wear tracks are continuous in nature, that clarifies that the composite is still ductile in nature. The material removal in this combination may be highly dominated by the formation of wear debris and chips. The short and discontinuous wear tracks on the worn composite surface illustrated in Fig. 4d explains the hard and brittle nature of the composite. The introduction of high amount (32 wt%) of hard and brittle filler particles may be the reason for the properties of the composite sample. The formation of small chips can be mentioned as the predominent wear mechanism for this combination of the composite.

8 Steady State Wear Analysis

The experimental investigation ensured that filler content and sliding velocity in that sequence are the significant parameters affecting the wear rate of the composites. Thus, to study their effect more clearly on the SWR of the composites, investigations are conducted considering the selected levels of filler content and sliding velocity keeping the other parameter levels constant. Each experiment is conducted three times and the average of the three results is only taken as the SWR for the particular test run.

9 Variation in Specific Wear Rate with Filler Content

From the experimental investigation, it is observed that the SWR of the composite samples are increased with the increase in sliding velocity but decreased with the increase in filler content. The role of sliding distance is almost negligible as noticed from the study. In order to study the impact of three mentioned parameters more precisely, investigation is conducted to find out the SWR of the composite samples with different filler concentrations at different sliding velocities keeping the sliding distance and normal load (25 N) constant. Figure 5a–e depict the variation in SWR of the composite samples with different filler concentration at different sliding velocities and sliding distances. From the figures, it can be observed that the SWR of the hardened raw polyester is maximum than the filled composites irrespective of the other control factors. The SWR of the composites show decreasing trend with the increase in filler content and is found minimum for the filler content of 32 wt.%. However, the difference in SWR between the unfilled composites and the composites with 8 wt.% filler is maximum and is about 40–50%. After that the reduction in SWR of the composites with the increase in filler content is almost linear. As previously observed the effect of sliding distance is very marginal but after the sliding distance of 750 m a noticeable increase in the SWR is observed. That may be due to the formation of heat which is generated between the counter surface and the test piece for which the composite sample become softer facilitating the excessive mass loss.

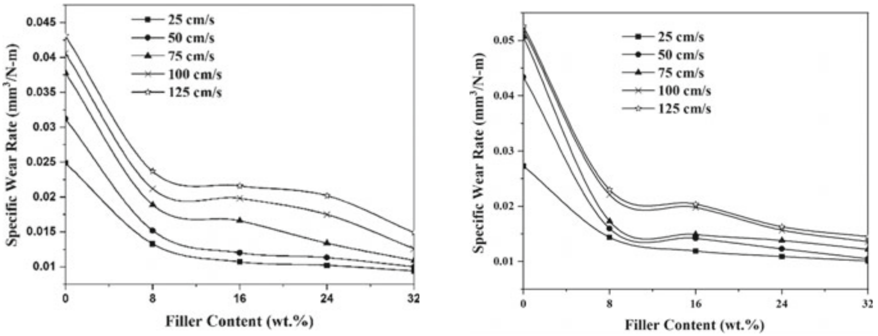

(a) Sliding distance 250m (b) Sliding distance 500m

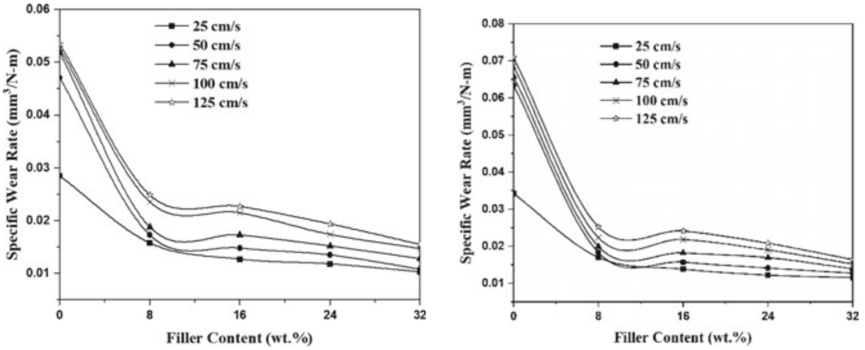

(c) Sliding distance 750m (d) Sliding distance 1000m

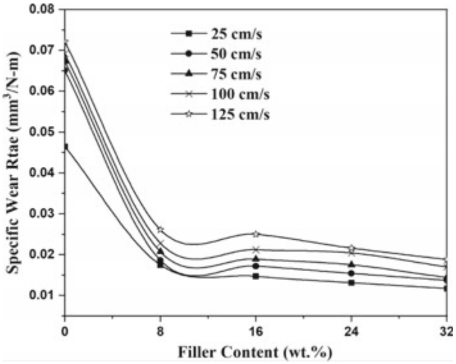

(e) Sliding distance 1250m

Fig. 5 SWR of the composite corresponding to filler content at different sliding velocities

Similar observations have been reported by Padhi and Satapathy (2013a) in their investigation conducted in 2013 using blast furnace slag as filler in epoxy matrix and by Kurahatti et al. (2011) using zirconia filler in Bismaleimidodiphenylmethane matrix.

The SEM of the worn composite surfaces consisting of different filler concentrations subject to highest damage (at velocity 125 cm/s) are taken in order to study the effect of filler content on the wear loss of the composite materials more clearly. Figure 6a–e display the micrographs of the worn composite surfaces consisting of five different filler concentrations (0, 8, 16, 24 and 32 wt.%) respectively. From the figures it can be evident that, for identical test conditions, maximum damage occurred to the hardened raw polyester consisting of no filler (6a). The thick and deep wear tracks on the worn surface and the formation of wear debris explains the damage occurred to the composite surface. Moreover, the plastic deformation and removal of matrix can be the potential mechanisms causing wear loss for the composite. As in the present research emery papers are used as the counter surface instead of the steel disc surface thus, the hard, brittle and sharp ceramic particles of the counter body tear into the composite surface causing the formation of deep wear tracks. Figure 6b illustrate such a wear track appeared on the worn composite surface consisting of 8 wt.% filler. The filler particles taken part in the wear operation can be clearly seen in the image. The removal of matrix layer in the form of wear debris and the breaking of filler particles that are evident from the figure can be the predominant wear mechanisms. To observe the condition of the micro-shaped filler particles on the worn surface, a high magnified image of the worn composite surface consisting of 16 wt.% filler is shown in Fig. 6c. From the figure it can be seen that the micro-shaped filler particles inside the wear track are cut by the sharp edges of the ceramic particles of the counter body and displayed from their own position inside the polymer. This may be the initial stage of the formation of wear debris at micro level that causes the wear loss to the composites. The mechanisms of wear loss for the composites consisting of 8 and 16 wt.% of filler are almost identical. Figure 6d presents the worn surface of the composite consisting of 24 wt.% filler. The removal of a matrix layer, formation of small wear debris and the thin wear tracks causing the wear loss are identified on the worn surface. The shape of the wear tracks and the wear debris explains that the incorporation of high amount of ceramic filler make the composite harder. However, the deformed matrix layer at the micro level confirms the existence of ductility in the composite. Incorporation of more filler (32 wt.%) in the matrix make the composite even harder as displayed in Fig. 6e. The wear tracks are almost vanished and the materials from the counter body are transformed to the worn surface due to high sliding velocity. Micro-cuttings on the matrix and filler particles are noticed on the worn surface, which can the reasons of wear loss of the composite.

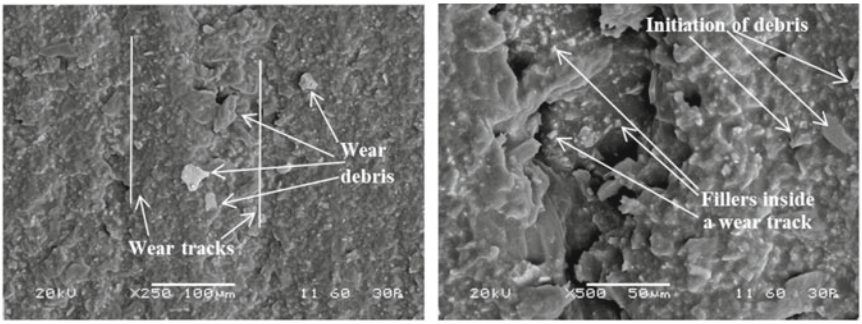

(a) Hardened raw polyester

(b) 8 wt.% filler

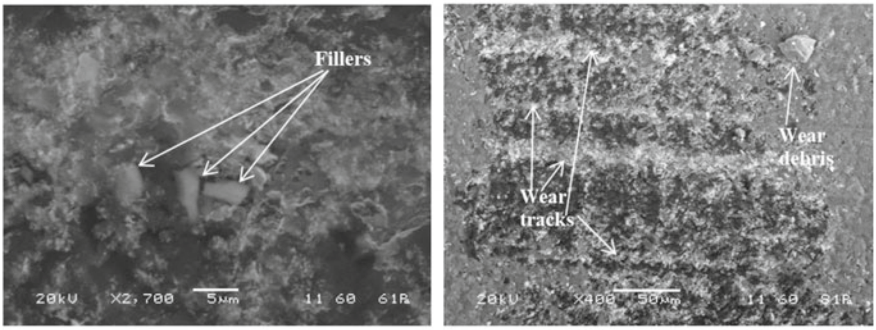

(c) 16 wt.% filler

(d) 24 wt.% filler

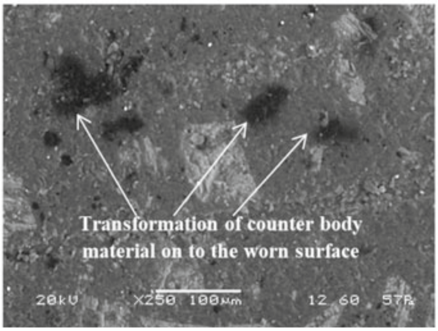

(e) 32 wt.% filler

Fig. 6 SEM micrograph of the worn composite surfaces consisting of different filler concentrations showing the wear mechanisms

10 Variation in Specific Wear Rate with Sliding Velocity

Figure 7a–e display the impact of sliding velocity on the SWR of the composites with different filler concentrations for separate sliding distances. As in the previous

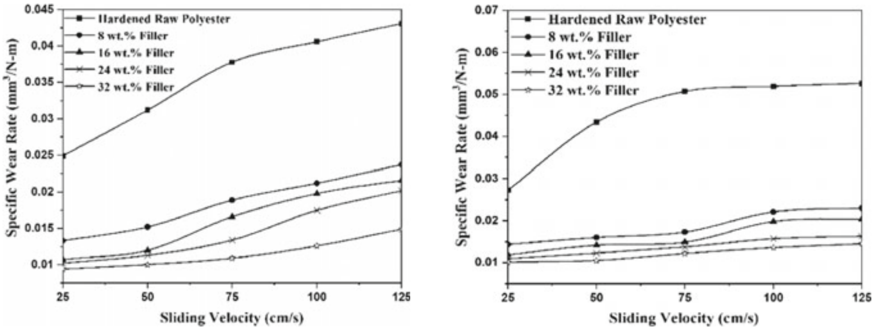

(a) Sliding distance 250m **(b) Sliding distance 500m**

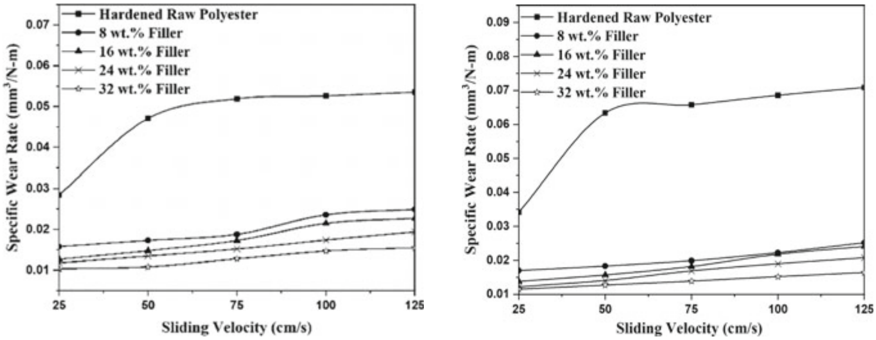

(c) Sliding distance 750m **(d) Sliding distance 1000m**

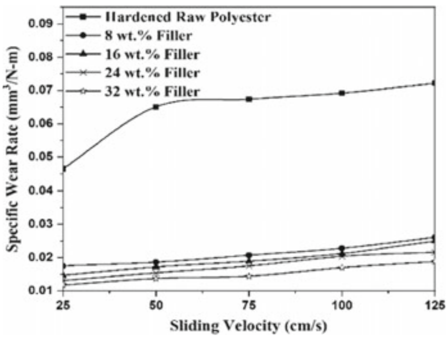

(e) Sliding distance 1250m

Fig. 7 Relationship between SWR and sliding velocities for different filler concentration case, here also the applied normal load is kept constant (25 N). From the figures it can be concluded that the SWR of the composites is affected positively with the sliding velocity, i.e. increased with the increase in sliding velocity. For the hardened raw polyester, the SWR is increased significantly for the increase in sliding velocity from 25 to 50 cm/s and beyond that the increment is linear. Whereas, for the filled composites the increment in SWR is linear up to a sliding velocity of 75 cm/s and beyond that the increment is more. However, the increment curves of the filled composites become flatter with the increase in sliding distance and almost linear for the sliding distance of 1250 m. The trend explains that, for long distance sliding, the effect of sliding velocity on SWR is reduced. Studies conducted by Nayak et al. (2020) using marble dust as filler in the glass-polyester composite system, Krishna et al. (2009) using metal and ceramic fillers in polymer matrix and Pattanaik et al. (2016) using fly ash filler in epoxy matrix also reported identical results as the outcome of their respective researches.

In order to investigate the surface condition of the composite samples at different sliding velocities, the SEM micrographs of the worn composite surfaces consisting of 32 wt.% filler tested at different sliding velocities are taken and are displayed in Fig. 8a–e. Figure 8a displays the composite slide with a velocity of 25 cm/s. It can be seen from the figure that at low sliding velocity the hard and sharp particles of the counter body could only create some scratches on the composite surface which is the only reason of the wear loss of filled composites at low sliding velocities. At sliding velocity 50 cm/s (shown in Fig. 8b), the top matrix layer of the composite surface is removed and the fillers are exposed. This confirms the proper distribution of filler particles inside the composite body. As evident from the figure at this velocity, very thin wear tracks are generated on the composite surface and small cavities are formed due to the penetration of hard and sharp ceramic particles of the counter body into the composite surface. The formation of wear tracks become clearly visible and the formation of cavities become larger at the sliding velocity of 75 cm/s (Fig. 8c). Traces of plastic deformation is marked on the worn surface which can be the predominant wear mechanism caused the wear loss to the composite. The micro shaped filler particles are noticed to experience wear and a large number of cavities are formed on the worn composite surface at a sliding velocity of 100 cm/s as evident from Fig. 8d. Micro-cuttings on the filler particles and micro-ploughing on the matrix body by the ceramic particles of the counter body is noticed on the worn surface. Including these, transformation of matrix layer and plastic flow of matrix can be considered as the mechanisms causing wear loss in this combination. At a sliding velocity of 125 cm/s, a huge amount of plastic deformation along with thick and continuous wear tracks are identified on the worn surface displayed in Fig. 8e. The high velocity sliding of the composite on the counter body facilitated the hard and sharp particles of the counter body to penetrate into the composite body and form ploughing mark on it. Formation of micro cracks is noticed on the worn surface. Overall, micro-cutting and micro-ploughing of the matrix and filler, formation of cracks and cavities, formation of wear tracks and plastic deformations on the composite body, formation of scratches and transformation of matrix layer can be the predominant wear mechanisms causing the wear loss.

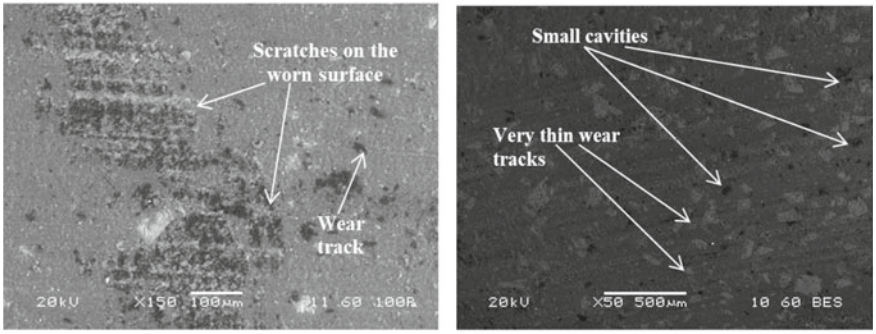

(a) Sliding velocity 25 cm/s (b) Sliding velocity 50 cm/s

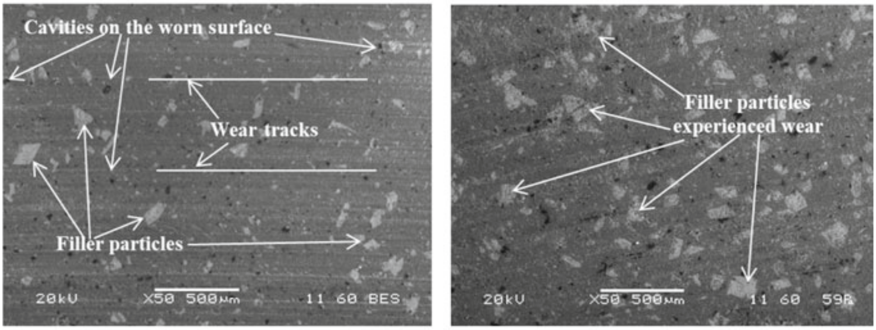

(c) Sliding velocity 75 cm/s (d) Sliding velocity 100 cm/s

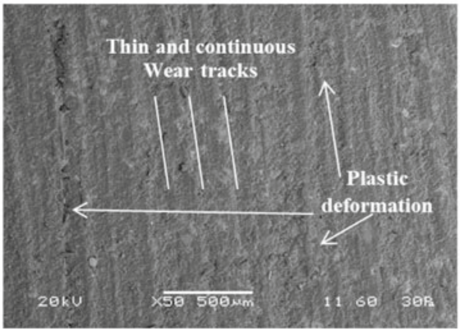

(e) Sliding velocity 125 cm/s

Fig. 8 Micrographs of the worn composite surfaces consisting of 32 wt.% filler at different sliding velocities

11 Summary of the Case Study: Marble Dust filled Polyester Composites

Marble dust, a construction waste is compatible up to 32% by weight as a filler in the polyester matrix and the preparation of the composites is possible by polymer solution casting technique. Taguchi's orthogonal array has been implemented effectively for the wear characterization and analysis of the composites. From the analysis, filler content is observed to have highest significant impact on the wear loss of the composites and after that the influence of sliding velocity is noticeable. The steady state wear analysis revealed that, for the filled composites, the wear rate is decreased almost linearly with the increase in filler concentration. However, a sudden decrease in wear rate is detected for the filled composites than the unfilled hardened polyester. The wear rate of the composites is affected positively with the sliding velocity. However, for the filled composites, the increment is linear and for the unfilled raw polyester, the wear rate rises suddenly with the increase in sliding velocity from 25 to 50 cm/s and beyond that the increment becomes linear. Figure 9 below exhibits some representative SEM micrographs of the worn composite surfaces illustrating various features emerged during the sliding wear trial.

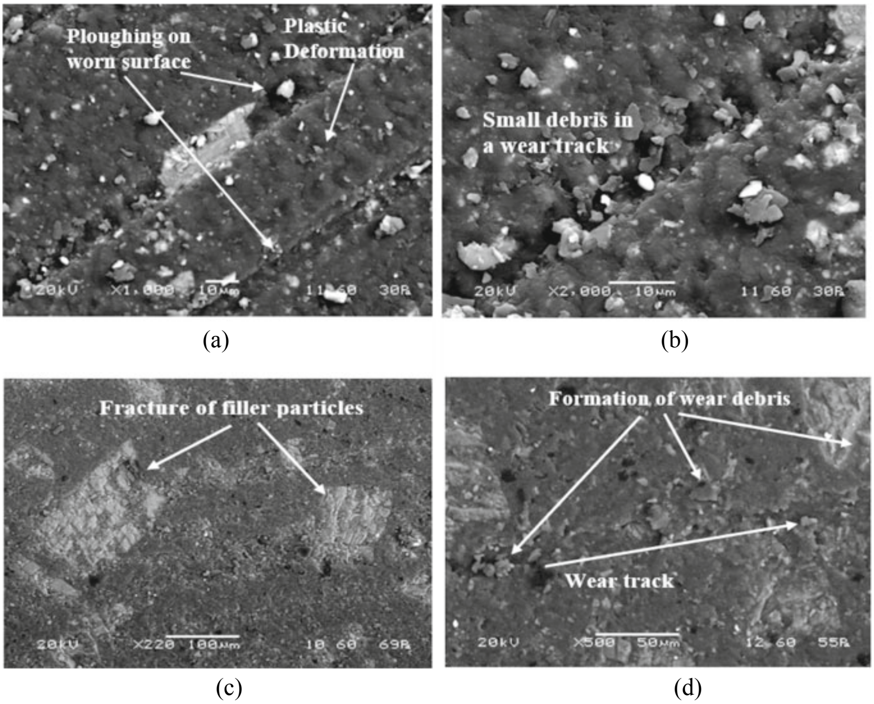

(a) (b) (c) (d)

Fig. 9 Worn surface morphologies of marble dust filled polyester

12 Sliding Wear Characteristics of Particulate Polymers: Overall Summary

Particulate filled polymer composites are nowadays used in several tribological applications. While sliding speed plays a very prominent role in determining the wear rate, it has been found in the investigations of several particulate filled composites that the fillers improve the bulk hardness of the composites and thereby their wear resistance capability gets enhanced. The influences of particle size and filler contents on the wear performance are also significant. So in order to get the best wear performance, obtaining an optimal setting of parameters is highly pertinent. In recent times, new developments are still under way to explore incorporation of additional reinforcing materials to tailor their properties for even more extreme loading and wear conditions.

13 Conclusion

A critical review of research history based on reports of past investigators on sliding wear behaviour of particulate filled polymer composites suggests that the wear resistance of polymers improve with the incorporation of micro-sized hard ceramic fillers. Use of industrial wastes such as red mud, fly ash, copper slag, blast furnace slag etc. also serves the purpose. Construction wastes like marble dust has also been gainfully utilized as a filler. The analysis of surface morphologies mostly indicates the effects of filler content and sliding velocity on the wear rate of the composites more precisely and the mechanisms of wear loss. Among the possible wear mechanisms responsible for wear loss in particulate filled composites, micro-cutting and micro-ploughing of the matrix and filler, formation of cracks and cavities, formation of wear tracks and plastic deformations on the composite body, formation of scratches and transformation of matrix layer are predominant.

14 Future Research Direction

This review indicates directions and a wide scope for future investigators to explore many other aspects of particulate filled polymer composites in regard to their tribological characteristics. Some of the suggestions for future research include consideration of all types of wear modes such as abrasion, surface fatigue and corrosion, possible use of diverse polymeric resins and hybridization of composites by additional reinforcement of synthetic/natural fibres, chemical modification of the filler, cost analysis to assess their economic viability in industrial applications and studying the effect of hygrothermal and hydrothermal aging on the wear properties.

References

Abdelbary A (2015) Wear of polymer composites. In: Wear of polymers and composites, pp 133–158

Akashi M, Yasukawa T, Murakami K (1970) Mechanical properties of wood-polymer composite materials. J. Soc. Chem. Ind. Jpn 73(7):1626–1629

Bahadur S (1995) The growth and bonding of transfer and PTFE in the tribological. Wear 183:212–221

Bahadur S, Gong D (1992) The role of copper compounds as fillers in the transfer and wear behavior of polyetheretherketone. Wear 154:151–165

Bahadur S, Gong D, Anderegg JW (1993) Tribochemical studies by XPS analysis of transfer films of Nylon 11 and its composites containing copper compounds. Wear 165:205–212

Bahadur S, Polineni V (1996) Tribological studies of glass fabric-reinforced polyamide composites filled with CuO and PTFE. Wear 200(1–2):95–104

Baptista R, Mendão A, Rodrigues F, Figueiredo-Pina CG, Guedes M, Marat-Mendes R (2016) Effect of high graphite filler contents on the mechanical and tribological failure behavior of epoxy matrix composites. Theor Appl Fract Mech 85:113–124

Basavarajappa S, Arun KV, Paulo Davim J (2009) Effect of filler materials on dry sliding wear behavior of polymer matrix composites—a taguchi approach. J Miner Mater Charact Eng 8(5):379–391

Biswas S, Satapathy A (2009) Tribo-performance analysis of red mud filled glass-epoxy composites using Taguchi experimental design. Mater Des 30(8):2841–2853

Biswas S, Satapathy A, Patnaik A (2010) A comparative study on wear behavior of copper slag filled bamboo-epoxy and glass-epoxy composites. Int Advancements Polym Mater, 1–5

Biswas S, Satapathy A (2010) A comparative study on erosion characteristics of red mud filled bamboo-epoxy and glass-epoxy composites. Mater Des 31(4):1752–1767

Cho MH (2009) The role of transfer film and back transfer behavior on the tribological performance of polyoxymethylene in sliding †. J Mech Sci Technol 23:2291–2298

Friedrich K (1986) Wear of Reinforced polymers by different abrasive. In: Friction and wear of polymer composites, vol 1. Elsevier Science B.V., pp 233–287

Friedrich K (1993) Particulate dental composites under sliding wear conditions. J Mater Sci Mater Med 4:266–272

Friedrich K, Reinicke R, Zhang Z (2002) Wear of polymer composites. Proc Inst Mech Eng Part J J Eng Tribol 216:415–426

Gangwar S, Bhat IK, Patnaik A (2017) Tribological and microstructure examination of environmental waste (Marble Dust) filled silicon bronze alloy for wear resistant applications. SILICON 9(2):249–263

Haupert F, Wetzel B (2005) Reinforcement of thermosetting polymers by the incorporation of micro- and nanoparticles. In: Polymer composites: from nano-to macroscale, pp 45–46

Krishna KG, Divakar C, Venkatesh K, Mohan CB, Lohith KSM (2009) Tribological studies of polymer based ceramic-metal composites processed at ambient temperature. Wear 266(7–8):878–883

Kurahatti RV, Surendranathan AO, Srivastava S, Singh N, Kumar AVR, Suresha B (2011) Role of zirconia filler on friction and dry sliding wear behaviour of bismaleimide nanocomposites. Mater Des 32:2644–2649

Kurahatti RV, Surendranathan AO, Kumar AVR, Wadageri CS (2014) Dry sliding wear behaviour of epoxyreinforced with nanoZrO 2 particles. Procedia Mater. Sci. 5:274–280

Nayak SK, Satapathy A (2019) Wear analysis of waste marble dust-filled polymer composites with an integrated approach based on design of experiments and neural computation. Proc Inst Mech Eng Part J J Eng Tribol 1–11

Nayak SK, Satapathy A, Mantry S (2020) Processing and wear response study of glass-polyester composites with waste marble dust as particulate filler. Polym Compos (2019):1–11

Ng CB, Ash BJ, Schadler LS, Siegel RW (2001) A study of the mechanical and permeability properties of Nano-TiO2 filled epoxy composites. Adv Compos Lett 10(3):101–111

Padhi PK, Satapathy A (2013a) Analysis of sliding wear characteristics of BFS Filled Composites Using an Experimental Design Approach Integrated with ANN Analysis of Sliding Wear Characteristics of BFS Filled Composites Using an Experimental Design Approach Integrated with ANN. Tribol Trans 2004:789–796

Padhi PK, Satapathy A (2014) Solid particle erosion behavior of bfs-filled Epoxy—SGF composites using Taguchi's experimental design and ANN solid particle erosion behavior of BFS-Filled Epoxy—SGF Composites using Taguchi's experimental design and ANN. Tribol Trans 2004:396–407

Padhi PK, Satapathy A (2013a) Analysis of sliding wear characteristics of bfs filled composites using an experimental design approach integrated with ANN. Tribol Trans 56(5):789–796

Pati PR, Satapathy A (2015) A Study on Processing, Characterization and Erosion Wear Response of Linz-Donawitz Slag Filled Epoxy Composites. Adv Polym Technol 34(4):1–8

Patnaik A, Satapathy A, Mahapatra SS (2009) Study on erosion response of hybrid composites using taguchi experimental design. Eng Mater Technol 031011–1–16

Patnaik A, Satapathy A, Chand N, Barkoula NM, Biswas S (2010a) Solid particle erosion wear characteristics of fiber and particulate filled polymer composites: a review. Wear 268(1):249–263

Patnaik A, Satapathy A, Dwivedy M, Biswas S (2010b) Wear Behavior of Plant Fiber (Pine-Bark) and Cement Kiln Dust-Reinforced Polyester Composites Using Taguchi Experimental Model. J Compos Mater 44(5):559–574

Pattanaik A, Satapathy MP, Mishra SC (2016) Dry sliding wear behavior of epoxy fly ash composite with Taguchi optimization Ashutosh. Eng Sci Technol Int J 19(1):8–14

Pei XQ, Leibniz INM, Materials N (2016) Friction and wear of polymer composites. Ref Modul Mater Sci Mater Eng 1–6

Purohit A, Satapathy A (2016) Epoxy matrix composites filled with micro-sized LD sludge: wear characterization and analysis. IOP Conf Ser Mater Sci Eng 115(1)

Ray S, Rout AK, Sahoo AK, After I (2018) Glass-Epoxy Composites Filled with Marble. UPB Sci Bull Ser B 80(4):181–196

Rout A, Satapathy A, Mantry S, Sahoo A, Mohanty T (2012) Erosion wear performance analysis of polyester-GF-Granite hybrid composites using the Taguchi method. Procedia Eng Int Conf Model Optim Comput 1863–1882

Satapathy A, Patnaik A (2010) Analysis of dry sliding wear behavior of red mud filled polyester composites using the taguchi method. J Reinf Plast Compos 29(19):2883–2897

Schwartz CJ, Bahadur S (2000) Studies on the tribological behavior and transfer film—counterface bond strength for polyphenylene sulfide filled with nanoscale alumina particles. Wear 237:261–273

Schwartz CJ, Bahadur S (2001) The role of filler deformability, filler—polymer bonding, and counterface material on the tribological behavior of polyphenylene sulfide (PPS). Wear 251:1532–1540

Srinivas K, Bhagyashekar MS (2014) Wear behaviour of epoxy hybrid particulate composites. Procedia Eng. 97:488–494

Sudheer M, Hemanth K, Raju K, Bhat T (2014) Enhanced mechanical and wear performance of epoxy/glass composites with PTW/graphite hybrid fillers. Procedia Mater. Sci. 6(Icmpc):975–987

Tanaka K (1986) Effects of various fillers on the friction and wear of PTFE-based composites. In: Friction and wear of polymer composites, vol 1, Elsevier Science B.V., pp 137–174

Upadhyay RK, Kumar A (June 2018) (2019) Epoxy-graphene-MoS 2 composites with improved tribological behavior under dry sliding contact. Tribol Int 130:106–118

Wang Q, Xue Q, Liu W, Chen J (2000) The friction and wear characteristics of nanometer SiC and polytetrafluoroethylene filled polyetheretherketone. Wear 243:140–146

Wang R-M, Zheng S-R, Zheng Y-P (2011) Introduction to polymer matrix composites. In: Polymer matrix composites and technology, pp 1–548

Xue Q, Wang Q (1997) Wear mechanisms of polyetherketone composites filled with various kinds of SiC. Wear 213:54–58

Yang Y, Boom R, Irion B, van Heerden DJ, Kuiper P, de Wit H (2012) Recycling of composite materials. Chem. Eng. Process. Process Intensif. 51:53–68

Yu L, Bahadur S (1998) An investigation of the transfer film characteristics and the tribological behaviors of polyphenylene sulfide composites in sliding against tool steel. Wear 214:245–251

Zhao Q, Bahadur S (1999) The mechanism of filler action and the criterion of filler selection for reducing wear. Wear 225–229:660–668

Introduction to Industry 4.0

T. Mohanraj and R. Jegadeeshwaran

Abstract In an automated manufacturing system, the complete production line in a manufacturing plant would be made highly independent without any human involvement. The entire automation can be feasible with the aid of the Cyber-physical system (CPS) which includes smart sensors and actuators. The smart sensors are going to be facilitating technologies to fulfill the needs of Industry 4.0. Recently, the Internet of Things (IoT) plays an essential role in renovating the "Conventional Technology" to "Next Generation Everywhere Computing". IoT is attaining a significant role in research across the globe particularly in sensor technologies, manufacturing, and automation. Industry 4.0, the process comprising the placement of machines is reformed dynamically based on the data attained through the monitoring of various activities in the factory by sensors. The sensor data comprises the state of the art machinery as well as the activities of the operators, product requirements, and customer needs. This results in a decrease in product costs.

Keywords Industrial revolution · Industry 4.0 · Tribology 4.0 · Friction · Wear · Internet of things · Connectivity · Cyber-physical system · Productivity · Automation

1 Introduction

The term "industrial revolution" is typically linked to definite ancient history in the last part of the eighteenth century. Though, recently an innovative transformation "Industry 4.0" has been described (Lasi et al. 2014) based on the earlier industrial revolutions. Essentially various subjects of industry 4.0 are existing only, yet the perspective from which they are deliberated is novel one. In industry 4.0, the physical

T. Mohanraj (✉)
Department of Mechanical Engineering, Amrita School of Engineering, Amrita Vishwa Vidyapeetham, Coimbatore, India
e-mail: t_mohanraj@cb.amrita.edu

R. Jegadeeshwaran
School of Mechanical Engineering, Vellore Institute Technology, Chennai, India

H. Jena et al. (eds.), *Tribology of Polymer and Polymer Composites for Industry 4.0*, Composites Science and Technology, https://doi.org/10.1007/978-981-16-3903-6_7

system unifies with the cybernetic world namely information technology, wireless communication, and manufacturing industries are collectively connected. Tribology addresses the concerns of friction, wear, and lubrication (Suganeswaran et al. 2020). The role of lubrication is to reduce friction and wear (Mohanraj et al. 2019; Shankar et al. 2017, 2019). It is an interdisciplinary field that embraces physics, chemistry, materials technology, and engineering.

Tribology has been supported by various industries for improving energy efficiency, and durability. The reliability of the tribological systems depends on friction, wear, as well as lubrication (Holmberg 2001). It is expected that the cost of tribological shortfalls is projected to be in an additional 1% of the gross national product (GNP) of the country (Williams 2005). Nowadays, every industry wants to become a sustainable one. This sustainability can be achieved through control in friction and wear via green tribology (Zhang 2013). Nowadays, four industrial revolutions are habitually specified. This fundamentally rose subsequently the description of industry 4.0 in order with its description. Conferring to this, someone labels at present as industry 1.0, industry 2.0, and industry 3.0 three preceding industrial revolutions concisely demarcated in the subsequent section.

2 First Industrial Revolution

The first industrial revolution, normally recognized as the “age of steam” (Xu et al. 2018), is considered through the usage of steam engines (Dalenogare et al. 2018). It is connected to automation and linked to the revolution from agriculture to the engineering domain. The first revolution commenced towards the end of the 18th era. It was described in the context of machines powered by water and steam energy in industrial applications (Lele 2019). The duration of the first revolution is frequently designated from the latter 18th to the opening of the 19th era. Occasionally particular periods can be specified as 1760–1840 (Lele 2019) and 1750–1850 (Deane and Deane 1979). In 1784, the development of the first power loom is specified as a significant time of the first industrial revolution (Kagermann et al. 2013).

3 Second Industrial Revolution

The second industrial revolution is called as “age of electricity” which is allied with mass production, linked to the thorough usage of electricity (Xu et al. 2018), ensued between the late 19th to twentieth centuries, specifically 1840–1900 (Lele 2019). It was described by bringing the electrical energy and gasoline in mass production through the workers, and the progress of railway and manufacturing of steel (Lele 2019). During 1870, the employment of the first assembly line is specified as a significant date for the second revolution (Kagermann et al. 2013).

4 Third Industrial Revolution

The third industrial revolution is called the “information age” considering the wide-range of mechanization (Xu et al. 2018). It is the first arrival of information and communication technology in the manufacturing field. Mid of the twentieth century, in the 1960s, the “Industry 3.0” is started and still ongoing easily renovating to the innovative era of industrial development, the fourth industrial revolution. It is considered through the application of electronics and information technology revolution in the industry. First Programmable Logic Controller (PLC) MODICON was introduced in 1969 is specified as a significant date for the second revolution (Kagermann et al. 2013).

5 Fourth Industrial Revolution

The fourth industrial revolution is called as “age of cyber-physical system” (Xu et al. 2018), or also called “Industry 4.0”. Industry 4.0 is considered as the interconnection of various things and people virtually with networks. The main elements of industry 4.0 are connectivity with networks and the Internet of Things (IoT), and machines named cyber-physical systems (Griffor et al. 2017; Kagermann et al. 2013). At the beginning of the twenty-first century (specifically 2011), industry 4.0 is commenced and the name was coined by the German working group (Kagermann et al. 2013). The major transformation in industry 4.0 is moving towards digitization. The schematic representation of the four industrial revolutions is shown in Fig. 1.

6 Evolution of Tribology

Tribology is a field that deals with the interaction of surfaces which involves motion, friction, wear, and lubrication. Professor Peter Jost introduced the term “Tribology’ in the year 1960 (Jost 2006). It is an interdisciplinary field that embraces physics, chemistry, materials technology, and engineering. The resisting force between the two moving surfaces is termed friction. Frictional force defends against the movement that leads to heat and augments the temperature of the surface (Chen et al. 2017b). In Tribology, friction is an undesirable one and needs to be reduced as much as possible. An increase in friction causes loss of energy and accordingly needs more energy to perform the same task (Holmberg et al. 2014).

Besides, the rotating elements quickly overheat, and its functioning elements may wear or seize due to excessive friction. Wear is associated with the contact between two surfaces and particularly the deformation and material removal due to the rubbing action of the surfaces. Mostly, the occurrence of wear is due to the

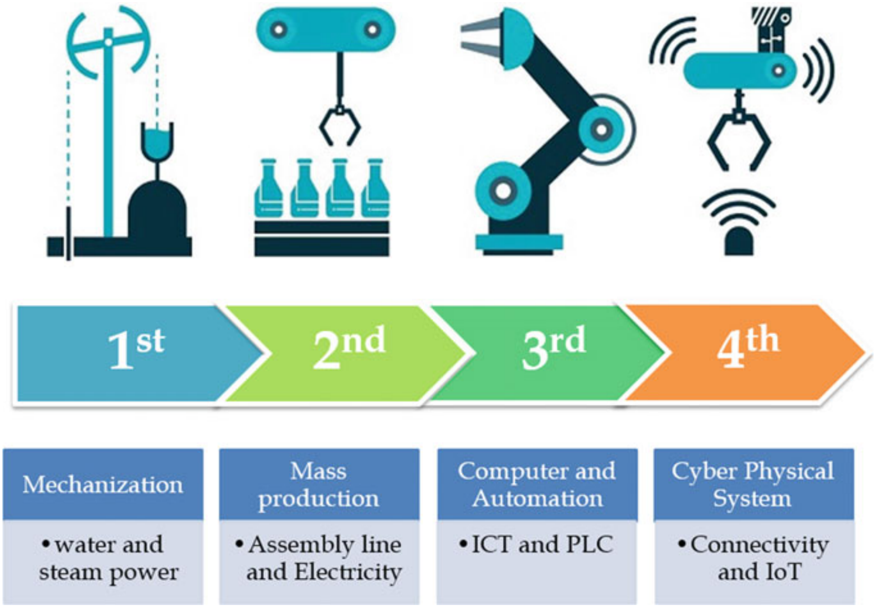

Fig. 1 Schematic representation of four industrial revolution

surface interaction at asperities (Mitchell and Osgood 1976). The effect of friction and wear can be decreased through the application of appropriate lubricants.

The development in the field of tribology was started in the stone age itself, once the fire was generated by friction between two pieces of stone can be deliberated as one of the first instances of tribology (Dowson 1978). During the Stone Age, to move heavy objects from one location to another location the lubricant (animal fat) was applied to reduce the friction. The Greek and Roman era was considered through the signs of progressions of progress in gears and bearings. The initial design of roller bearing is an eminent model of tribology. Oils produced from plants and animals were employed as lubricants and considerably decrease the wear and friction of materials in the rolling elements. From 1600 to 1750, exceptional enhancements happened in the domain of bearings and gears. The utilization of lubricants became more significant and considerable reduction in friction and wear was attained (Ciulli 2019). The various evolution of tribology is shown in Fig. 2 (Ciulli 2019).

7 Tribology and Industry

The recent developments in the field of tribology certainly inspired the technical developments associated with industrial revolutions. On the other hand, the revolutions connected with industrial revolutions presented new tribological problems for

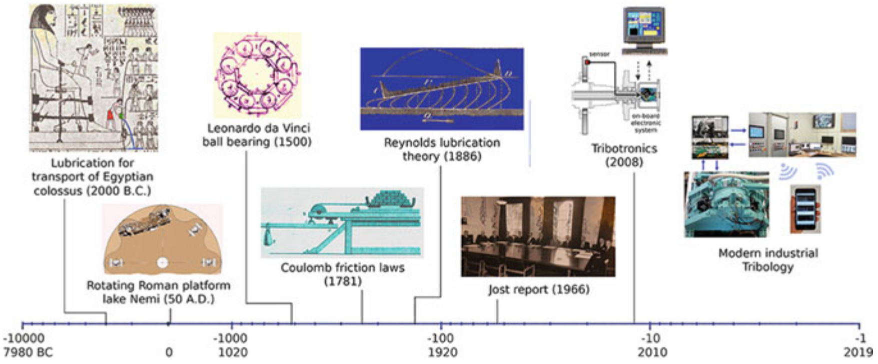

Fig. 2 The evolutions of tribology

further enhancement. As the revolutions in industry starts, revolutions in tribology also started and were described in four evolutions: from 1750 to 1850, 1850–1950, 1950–2000, and from 2000 to date. The fundamental features of industry and tribology in the course of evolutions are presented in Table 1.

The commencement of every industrial transformation can be placed in connection with significant progress in tribology which happens recently. The friction studies performed by Coulomb during 1781 in the field of tribology is considered as first industrial revolution (1784), the development of lubricant by Reynolds during 1886 is the second revolution and the official announcement of ‘Tribology” in 1966 is considered as the third revolution. The introduction of Tribotronics in 2008 (Glavatskih and Höglund 2008) is the fourth revolution.

8 Key Technologies in Industry 4.0

The conception of industry 4.0 is primarily related to mechanization and digital transformation in the engineering field. Essential characteristics of Industry 4.0 are higher computing power of computers with cheaper prices, development of networks and wireless communication, the readiness of more and more robots with artificial intelligence and machines, and ever-present usage of sensors. This industry 4.0 assurances to enhance the efficiency and productivity of industry (Dalenogare et al. 2018). The developments in technology with improved productivity and cost savings have to be employed to reduce the usage of resources and impact on the environment, as well as making new or enhanced products for every people (Chen et al. 2017a). But there may a threat of job loss for millions and very few are compensated by a very fewer number of specific jobs. This part must be carefully handled by governments and entrepreneurs (Bonekamp and Sure 2015).

A key idea of industry 4.0 is “Smart Factory” in which the operators, machinery, and resources interconnect with each other through the connected network (Wang

Table 1 Essential features of industry and tribology in the course of evolutions

Years	Industry	Tribology
1750–1850	First industrial revolution—Steam engine, mechanization. First power loom (1784)	Friction studies, Gears, and bearings, lubrication formation, mineral oils. Coulomb friction laws (1781)
1850–1950	Second Industrial revolution—Electrical energy, mass production. First assembly line (1870)	Friction, wear, lubrication relationships, Rolling element bearing, additives in lubricants. Reynolds lubrication theory (1886)
1950–2000	Third industrial revolution—Electronics, Computerization, automated production. First PLC (1969)	Elastohydrodynamic lubrication, computational and experimental tribology, micro & nanotribology, new materials for coating, rheology, bio tribology, condition monitoring. Official tribology (1966)
Since 2000	Fourth Industrial revolution—Cyber-physical system, augmented reality, Internet and cloud, IoT. Industry 4.0	Further developments in the third revolution, green tribology, superlubricity, space tribology. Tribotronics (2008)

et al. 2016). This smart factory must be harmless, flexible, and competent enough to make mass production as well as batch production with optimum utilization of resources and the continuous cooperation and communication between operators and robots. The essential features of the smart factory are customizing the products, increasing the performance, environmental sustainability, and ability to reconfigure. The enabling technology of Industry 4.0 is cyber-physical systems, sensors, connectivity (LoRa, Wi-Fi, Ethernet, RFID, Zig-Bee, Bluetooth, etc.,) big data analytics, deep learning, machine learning, cloud computing, advanced manufacturing systems, Robotics, HMI, and edge devices (Lee et al. 2018).

9 Cyber-Physical Systems

In an automated manufacturing system, there is no human involvement preferably or to a certain level, there is reduced human involvement. So, the complete production line in a manufacturing plant would be made highly independent without any human involvement. The entire automation can be feasible with the aid of the Cyber-Physical System (CPS) through the various elements like smart sensors and actuators. The smart sensors are going to be facilitating technologies to fulfill the needs of Industry 4.0. This has to be implemented with the help of IoT devices called the Cyber-Physical System (Lee et al. 2015).

The subsequent epoch of Smart Computing will be entirely dependent on CPS (Nayyar and Puri 2016). CPS is co-engineered interrelating networks of physical and computational elements. These systems will afford the foundation of essential infrastructure, form the fundamentals of budding and upcoming smart services, and advance the quality in various domains (Griffor et al. 2017). Recently, the Internet of Things (IoT), plays an essential role in renovating the “Conventional Technology” from-to “Next Generation Everywhere Computing”. IoT is attaining a significant place in research across the globe particularly in sensor technologies and automation. The most important aspect of Industry 4.0 is automation.

Cyber-physical systems are embedded systems. Conceptually, Cyber-physical systems are the integration of embedded systems along with the physical system together is the cyber-physical system. Nowadays, embedded systems are the enabling technologies for making systems smarter. They possess a certain level of computation, communication, and control capabilities. So, where there is interaction with the physical world, through different sensors and actuators is called cyber-physical systems. The significant point in CPS is the control of the real-time process from supervising of various factors and the use of computational/artificial intelligence to acquire a deep knowledge of the real-time environment, thus affording appropriate and more precise conclusions and actions (Delicato et al. 2020). CPS is a multidimensional system that integrates the cyber and dynamic physical world. Through the assimilation and combination of **C**omputing, **C**ommunication, and **C**ontrol, known as the “3C,” CPS affords real-time sensing, feedback, control, and other facilities (Liu et al. 2017). The difference between the embedded system and CPS are shown

Table 2 Difference between embedded system and CPS

Embedded system	CPS
Devices having information processing systems embedded into them	A complete system having physical components and software
Typically confined to a single device	Networked set of embedded systems
Limited resources for performing a limited number of tasks	Not resource-constrained
Main issues are real-time response and reliability	Timing and concurrency are the main issues

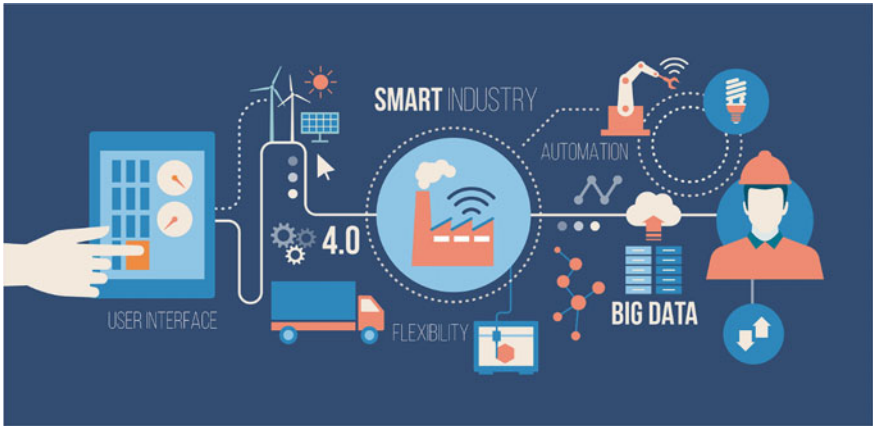

Fig. 3 Typical cyber-physical system

in Table 2. The typical example of CPS is shown in Fig. 3 (Abbaspour Asadollah et al. 2015).

10 Features of CPS

The salient features of CPS are described below (Alur 2015).

- Reactive computation:
  Reactive computation is an essential one in CPS. Reactive computation means the interaction of the system with the physical environment in a continuous manner. So, there is a sequence of observed inputs and outputs in the process and that has to be dealt with by these systems suitably.
- Concurrency:
  Concurrency is a very important one. Concurrency is the execution of multiple processes simultaneously. So, concurrent processes would exchange information

to achieve a certain expected result and these operations could be synchronous or, asynchronous in terms of their operation.

- Feedback control of the physical world
  Feedback control of these systems will have some kind of a control system with a certain form of the control element. So, the sensors sense the environment and actuators will produce the corrective action on the environment. To perform a complex task, a hybrid control system is employed.
- Real-time computation
  Real-time computation is employed in time-sensitive operations such as coordination, resource allocation.

11 Major Elements of CPS

11.1 Sensors

Sensors are the essential element in any CPS. A sensor detects or senses the variation in surroundings or system, and process the signal in a specified format (Powner and Yalcinkaya 1995). Sensors can execute several functions by detecting the physical changes of a system in reaction to a stimulus. Transducers are used to convert or transform the energy of one form to another form preferably an electrical form. The term "Transducer" is the combined term used for both sensors and actuators. The Internet of things has been fetched with different types of sensors like biosensors, smart sensors, and photonic sensors (Liu and Baiocchi 2016).

11.2 Connectivity

The connectivity is used to communicate between the machines, sensors, processors, and actuators. The following communication protocols are important for IoT. Few of them are named here. They are IEEE 802.15.4, ZigBee, 6LoWPAN, Wireless HART, Z-Wave, ISA 100, Bluetooth, NFC, RFID, LoRa, etc. (Mihovska and Sarkar 2018).

11.3 Advanced Manufacturing System

Advanced manufacturing systems include flexible manufacturing systems, supervisory control and data acquisition (SCADA), computer-aided design (CAD), computer-aided manufacturing (CAM), and additive manufacturing (3D printing) which can fabricate components from waste and fewer materials (Brown 2018).

11.4 Machine Learning and Big Data Analytics

Machine learning specifies the ability of software to investigate the large quantity of data and to study how to resolve the difficulties spontaneously. The various machine learning algorithms like Support Vector Machine, Hidden Markov Model, Convolution Neural Networks, Decision Tree, K-Nearest Neighbor, Kernel Bayes, Multilayer perceptron (Mohanraj et al. 2020), Artificial Neural Network, etc. (Mahdavinejad et al. 2018). Big data is associated with the usage of consumer data for optimizing the product design and processes.

11.5 Human–Machine Interaction

Human–machine interaction contains augmented as well as virtual reality, wearable equipment, Human–machine interface (HMI)/Man–machine interface (MMI). Robotics includes autonomous robots, swarm robots, interconnected robots, collaborative robots permitting the operator to address the more valuable process.

11.6 Architecture of CPS

- The architecture of CPS consists of the cyber and physical layers (Hahn et al. 2015). Different types of CPS components are integrated based on the effective connectivity. The architecture of CPS can be considered at various levels. In general, it has seven layers of the ISO/OSI model (Alguliyev et al. 2018; Li et al. 2012).
- **Physical layer**
  In CPS architecture, the physical layer is the first bottommost layer and it consists of sensors, actuators, which are connected through wired / wireless networks. 6LoWPAN (IPv6 over Low power Wireless Personal Area Networks) is a network layer protocol that acts as a router and can be used with any physical and data link layer. The devices interfaced with the physical layer have very little memory and managing power.
- **Datalink layer**
  The data link layer delivers the creation, transmission, and reception of data. Datalink layer process the requests received from the network layer and uses the physical layer to transfer the data. The data link layer is further split into two sublayers namely logical channel management (LLC) and media access control (MAC). LLC and MAC afford services to the network layer and shared physical environment, respectively.
- **Network layer**
  In the network layer, data frames are transmitted to the network address based on the conversion from the MAC address. It uses the IPv4/IPv6 protocols.

- **Transport layer**
  At the transport layer, data frames are fragmented into small pieces. It includes various protocols TCP, UDP, and ICMP.
- **Session layer**
  The session layer accomplishes the communication process and monitors the message transmission from the network to the network. If any failure occurs during the transmission, this layer detects the faults and transmits the data in the correct form.
- **Presentation layer**
  The presentation level synchronizes the data presented in the interface of two application processes such as the transformation of data, data encryption & decryption.
- **Application layer**
  Various domains are covered in the application layer. Application layer stores, analyses, and updates the data received from preceding layers. The protection of data is the most important issue and can be protected by data confidentiality.

12 Operation of CPS

The CPS incorporates the variables to represent the data acquired from sensors and control actions given to actuators. The setpoint is a standard value of a process parameter. The difference between the values of the actual process parameter and the corresponding setpoint is computed by the controller. After computing this deviation, the controller employs the set of equations and initiates the control action, and regulates the control variable (Kopetz 2011). In CPS, operators should be conscious of the current position of the controlled objects through the graphical user interface (GUI) / Human Machine Interface (HMI). In general, the CPS process is divided into monitoring, networking, computational processing, and actuation (Hahn et al. 2015).

13 Tribology 4.0: Tribotronics

In Industry 4.0, the contribution of tribology is a very essential one. The relationship of tribology with industry can be expressed as “Tribology 4.0”. Tribological information (friction and wear data) are transmitted to the industry through the internet and wireless communications among numerous computer devices. Today, the association of tribology with microelectronics (sensors) and information technology is enormously robust. The requirement of consistent and low-cost sensors acquiring the data from the lubricant as well as machinery decreases the manpower (Murphy et al. 2005).

The relationship between tribology and electronics is decorated by the keyword “Tribotronics” (Glavatskih and Höglund 2008). The smart factory has equipment with smart devices that are capable of monitoring and adjusting their operating conditions through the employment of sensors and actuators. Tribotronics consists of prototypes, sensors, and actuators that can enhance the tribological characteristics of the machine. They have to be updated and adjusted themselves which includes the on-line fine-tuning of tribosystems to enhance the performances.

Real-time signals connected with wear, friction, vibration, and temperature have to be acquired and analyzed to enhance the performances of the tribosystem. From which, the efficiency and consistency of the industry are improved. For illustration, sensors can be used to monitor the surface & lubricant condition and data has to be transferred by communication systems and the corresponding action can be initiated through the actuators. Probably the geometry of the tribosystem can be altered according to the actuation mechanisms. The elements of the tribotronics system are shown in Fig. 4 (Glavatskih and Höglund 2008).

A tribotronic system consists of key components as shown in Fig. 4. The performance of the tribological system is monitored by sensors which provide the temperature, pressure, coefficient of friction, frictional force, displacement, vibration, and oil properties like the total acid number, additive depletion, and other lubricant properties. The signals acquired from various sensors are processed and given to the control unit. In the control unit, decision making is performed based on the tribological algorithm, and the adequate control action is initiated to the actuators. This

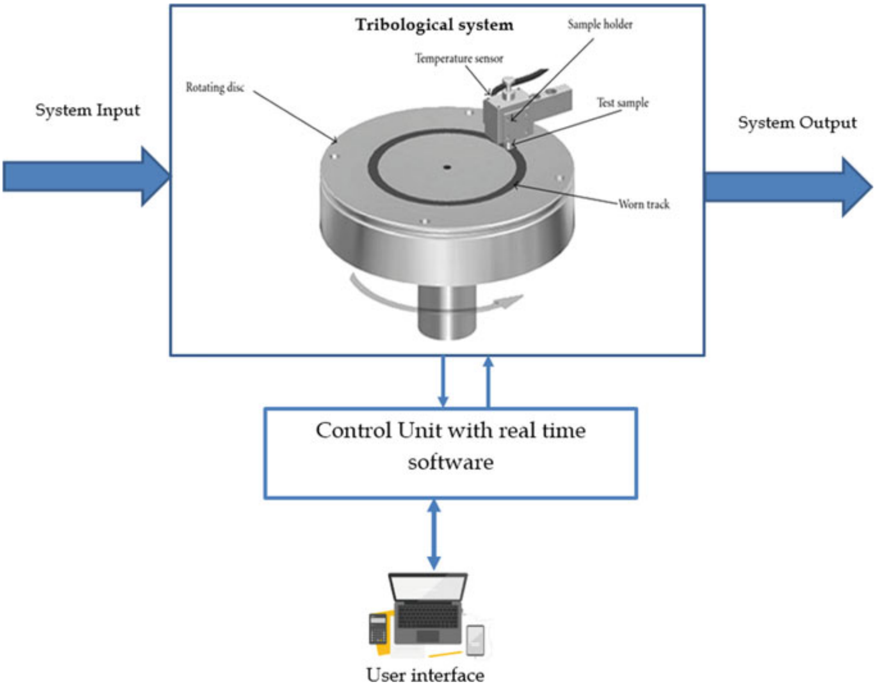

Fig. 4 Elements of tribotronic system

control action is known as a self-tuning and autonomous system. This self-tuning considerably enhances the performance of the tribological system. The knee joint of the human being is the typical example of a natural tribotronic system (Glavatskih and Höglund 2008).

14 Conclusions

Tribology plays an important role in technological and economical fields and is associated with industry from the first revolution in the industry. It is promising to identify the numerous thoughts of industry 4.0 in tribology studies. By considering the tribological features from the design stage onwards have a better influence on the tribological performance. Monitoring with sufficient sensors can provide signals acquired to enhance the performances of the tribological industry and to evade or as a minimum decrease the expensive idle time. Energy saving is certainly one of the extensive areas where tribology can have a large impact to decrease the losses and wastes, and materials also taking the benefits from smart sensors and actuators. With the incorporation of smart sensors and actuators with existing machines, that can be converted into a cyber-physical system and the system performance can be enhanced.

References

Abbaspour Asadollah S, Inam R, Hansson H (2015) A survey on testing for cyber physical system. In: Cham, 2015. Testing software and systems. Springer International Publishing, pp 194–207

Alguliyev R, Imamverdiyev Y, Sukhostat L (2018) Cyber-physical systems and their security issues Computers in Industry 100:212–223. https://doi.org/10.1016/j.compind. Accessed 17 April 2018

Alur R (2015) Principles of cyber-physical systems. MIT Press

Bonekamp L, Sure M (2015) Consequences of industry 4.0 on human labour and work organisation. J Bus Media Psychol 6:33–40

Brown AS (2018) Chain reaction. Mech Eng 140:30–35

Chen B, Wan J, Shu L, Li P, Mukherjee M, Yin B (2017a) Smart factory of industry 4.0: Key technologies, application case, and challenges. IEEE Access 6:6505–6519

Chen S, Li J, Wei L, Jin Y, Shang H, Hua M, Duan H (2017b) Tribological properties of polyimide-modified UHMWPE for bushing materials of seawater lubricated sliding bearings. Tribol Int 115:470–476

Ciulli E (2019) Tribology and industry: from the origins to 4.0. Front Mech Eng 5. https://doi.org/10.3389/fmech.2019.00055

Dalenogare LS, Benitez GB, Ayala NF, Frank AG (2018) The expected contribution of Industry 4.0 technologies for industrial performance. Int J Prod Econ 204:383–394

Deane PM, Deane PM (1979) The first industrial revolution. Cambridge University Press

Delicato FC, Al-Anbuky A, Wang KIK (2020) Editorial: smart cyber–physical systems: toward pervasive intelligence systems. Futur Gener Comput Syst 107:1134–1139. https://doi.org/10.1016/j.future.2019.06.031

Dowson D (1978) History of tribology. Addison-Wesley Longman Limited

Glavatskih S, Höglund E (2008) Tribotronics—towards active tribology. Tribol Int 41:934–939

Griffor ER, Greer C, Wollman DA, Burns MJ (2017) Framework for cyber-physical systems: volume 1, overview

Hahn A, Thomas RK, Lozano I, Cardenas A (2015) A multi-layered and kill-chain based security analysis framework for cyber-physical systems. Int J Crit Infrastruct Prot 11:39–50

Holmberg K (2001) Reliability aspects of tribology. Tribol Int 34:801–808

Holmberg K, Andersson P, Nylund N-O, Mäkelä K, Erdemir A (2014) Global energy consumption due to friction in trucks and buses. Tribol Int 78:94–114

Jost HP (2006) Tribology: How a word was coined 40 years ago. Tribol Lubr Technol 62:24

Kagermann H, Wahlster W, Helbig J (2013) Securing the future of German manufacturing industry recommendations for implementing the strategic initiative industrie 4:14

Kopetz H (2011) Real-time systems: design principles for distributed embedded applications. Springer Science & Business Media

Lasi H, Fettke P, Kemper H-G, Feld T, Hoffmann M (2014) Industry 4.0 Business & information systems engineering 6:239–242

Lee J, Bagheri B, Kao H-A (2015) A cyber-physical systems architecture for industry 4.0-based manufacturing systems. Manuf Lett 3:18–23

Lee J, Davari H, Singh J, Pandhare V (2018) Industrial artificial intelligence for industry 4.0-based manufacturing systems. Manuf Lett 18:20–23

Lele A (2019) Industry 4.0. In: Disruptive technologies for the militaries and security. Springer, pp 205–215

Li H, Lai L, Poor HV (2012) Multicast routing for decentralized control of cyber physical systems with an application in smart grid. IEEE J Sel Areas Commun 30:1097–1107

Liu X, Baiocchi O (2016) A comparison of the definitions for smart sensors, smart objects and Things in IoT. In: 2016 IEEE 7th annual information technology, electronics and mobile communication conference (IEMCON), 2016. IEEE, pp 1–4

Liu Y, Peng Y, Wang B, Yao S, Liu Z (2017) Review on cyber-physical systems. IEEE/CAA J Autom Sin 4:27–40

Mahdavinejad MS, Rezvan M, Barekatain M, Adibi P, Barnaghi P, Sheth AP (2018) Machine learning for internet of things data analysis: a survey. Digit Commun Netw 4:161–175

Mihovska A, Sarkar M (2018) Smart connectivity for internet of things (IOT) applications. In: New advances in the internet of things. Springer, pp 105–118

Mitchell L, Osgood C (1976) A theory of friction and wear based on a new characterisation of asperity interactions. Wear 40:203–222

Mohanraj T, Shankar S, Rajasekar R, Deivasigamani R, Arunkumar PM (2019) Tool condition monitoring in the milling process with vegetable based cutting fluids using vibration signatures. Mater Test 61:282–288

Mohanraj T, Yerchuru J, Krishnan H, Aravind RN, Yameni R (2020) Development of tool condition monitoring system in end milling process using wavelet features and Hoelder's exponent with machine learning algorithms. Measurement 173:108671

Murphy M, Leigh-Jones C, Kent T, Baldwin A (2005) New generation of smart sensors. In: World tribology congress, pp 861–862

Nayyar A, Puri V (2016) Smart farming: IoT based smart sensors agriculture stick for live temperature and moisture monitoring using Arduino, cloud computing & solar technology. In: Proceedings of the international conference on communication and computing systems (ICCCS-2016), pp 9781315364094–9781315364121

Powner E, Yalcinkaya F (1995) From basic sensors to intelligent sensors: definitions and examples. Sens Rev 15:19–22

Shankar S, Mohanraj T, Ponappa K (2017) Influence of vegetable based cutting fluids on cutting force and vibration signature during milling of aluminium metal matrix composites. J Tribol 12:1–17

Shankar S, Mohanraj T, Pramanik A (2019) Tool condition monitoring while using vegetable based cutting fluids during milling of inconel 625. J Adv Manuf Syst 18:563–581

Suganeswaran K, Parameshwaran R, Mohanraj T, Radhika N (2020) Influence of secondary phase particles Al2O3/SiC on the microstructure and tribological characteristics of AA7075-based surface hybrid composites tailored using friction stir processing. In: Proceedings of the institution of mechanical engineers, part c: journal of mechanical engineering science, p 0954406220932939
Wang S, Wan J, Li D, Zhang C (2016) Implementing smart factory of industrie 4.0: an outlook. Int J Distrib Sens Netw 12:3159805
Williams J (2005) Engineering tribology. Cambridge University Press
Xu LD, Xu EL, Li L (2018) Industry 4.0: state of the art and future trends. Int J Prod Res 56:2941–2962
Zhang S-w (2013) Green tribology: fundamentals and future development. Friction 1:186–194

Advances in Biopolymer Tribology

Shweta Rawat and Sarthak Saxena

Abstract In the current scenario, biopolymer and biopolymer composites are getting considerable interest in sustainable industrial development. Biopolymers produced from living organisms possess unique molecular and functional properties. The precise 3D structure of biopolymer makes them active molecules that are potentially applied in various industries like pharmaceutical, food, and nutraceutical, etc. The most commonly used biopolymers are chitosan, silk fibroin, poly tetra fluoro ethylene (PTFE), polyacetal (PA), various cross-linked polythenes, and ultra-high molecular weight polythenes (UHMWP). The most successful application of biopolymers may be considered as active materials for biomedical engineering, along with materials for food packaging, water purification, and the packaging sector. The term tribology is associated with the friction and wear properties of certain materials. Industrial advancement with the improvement of the tribological behavior of biopolymer is an emerging area in view of the wide applicability of biopolymer in modern engineering. The present paper will comprise industrially significant biopolymers, their tribological properties concern with efficiency improvement, and sustainable development. Further, it will elaborate on current challenges and future aspects of the tribological study of biopolymers for modern engineering.

Keywords Biopolymer · Biopolymer composites · Tribology · Biomedical engineering

---

S. Rawat (✉)
Department of Biochemical Engineering, Bipin Tripathi Kumaon Institute of Technology, Dwarahat, India

S. Saxena
Department of Biological Sciences and Engineering, Netaji Subhas University of Technology, Azad Hind fauz marg, Dwarka sector 3., Delhi, India

H. Jena et al. (eds.), *Tribology of Polymer and Polymer Composites for Industry 4.0*,
Composites Science and Technology, https://doi.org/10.1007/978-981-16-3903-6_8

1 Introduction

In form of macromolecules, polymers are composed of monomeric units linked to each other in different conformations (Mills and White 2012). Polymers are broadly classified into two groups, i.e. synthetic and natural (Deb et al. 2019). Natural polymers termed as biopolymers have drawn key attention to the researchers due to their cellular adhesiveness, biocompatibility, and biodegradability (K. Numata and Kaplan 2011). Biopolymers may be defined as polymers originated from living organisms, like plant cells, microbial systems, or chemically synthesized from biological systems (Rebelo et al. 2017). However, heavy dependence upon synthetic polymer may not be overlooked (Buggy 2016). A longer utilization of synthetic polymer may cause a hazardous effect on human health along with the environment (Kaushik et al. 2016). These toxic effects of synthetic polymer lead to the preferable application of biopolymer in medical devices, packaging material, cosmetics, water treatment chemicals, food additives, tissue engineering, biosensors, industrial plastics, pharmaceuticals, and the food industry, etc.(Rebelo et al. 2017). Various classes of Tribology and their key applications are given in Table 1.

In the biomedical industry, the application of different biopolymers, i.e. collagen, chitin, gelatin, starch, and xanthan gum, etc. are very significant with the aspect of biocompatibility, biodegradability, nontoxicity, mechanical durability, low immunogenicity, nonmutagenicity, nonirritant nature, and self-healing property along with economically easy availability (Jacob et al. 2018). Such “biomimetic” characteristics of biopolymers offer great applicability of these materials in the biomedical sector as wound healing products, implantable devices, drug delivery systems, and tissue engineering scaffolds (Davidenko et al. 2014; SSD Kumar et al. 2018a, b). Food industries may be considered as another largest sector, in which biopolymers are widely utilized as natural ingredients to enhance texture, stability, and physicochemical properties, etc. (McClements et al. 2009). As a natural macromolecule, biopolymers are playing a vital role as a gelling, emulsifying, thickening, and stabilizing agent for food processing (Qin et al. 2018). As an eco-friendly, renewable raw material, biopolymers are widely utilized as packaging material for the sustainable development of the food industry (Qureshi et al. 2020). Some major classes and types of biopolymers currently in use are given in Fig. 1.

The biopolymer-based functional ingredients interact with other food molecules to improve the design of novel food (Qureshi et al. 2020). In the food industry, alginate, starch, chitosan, and gelatin are considered important ingredients in replace of synthetic polymers (Qin et al. 2018). In the present scenario, the pharmaceutical industry may be considered as a very important sector with the wide application of many biopolymers, i.e. alginate (Lee and Mooney 2012), pullulan (Dailin et al. 2019) for controlled drug and gene delivery, tissue engineering, medical imaging, antimicrobial activity, and plasma expander, etc. Additionally, several industrial sectors, i.e. textile, cosmetics, and paper industries show a great dependency upon biopolymers as natural macromolecules (Anwunobi and Emeje 2011). Overall biopolymer tribology-based research areas and applications are given in Fig. 2.

Table 1 Classification of various biotribology representations and their major applications

S.N	Tribology area	Major areas for application
1	Animal Tribology	Animal locomotion; ants; beetle, butterfly's wing; earthworm; feather of birds; gecko adhesion; pangolin scale; seashell; skin shark or fish; Snails; water strider; etc.
2	Artificial articular joints	Artificial cartilage, bioscaffolds, corrosion and wear in implants, explant analysis, spinal discs, total and partial joint replaccements (hip and knee), etc.
3	Biomimetics	Bioinspired tribology, insect tribology, etc
4	Haptics	Ergonomics, surface texture, Tactile perception, etc.
5	Joint tribology	Articular cartilage; Hip joint; implant interfaces; joint fluid; knee joint; restorative joint materials; etc.
6	Medical devices	Artificial cardiovascular system, gastroscope, medical gloves, operation forceps, scalpel, urinary catheters, etc.
7	Natural Joints	Articular cartilage, biochemical and mechanically induced damage, meniscus, synovial joints, etc.
8	Ocular tribology	Contact lenses,ocular surfaces, dry eye syndrome, tear lubrication, etc.
9	Oral tribology	Dental restorative materials, mandibular joints, natural teeth, saliva, swallowing, teeth implants, tongue, toothpaste, etc.
10	Plant tribology	Diatoms; lotus leaf; etc.
11	Prosthesis tribology	Prosthetic human interfacing and coupling, tribological function, etc.
12	Skin tribology	Medical and cosmetic treatment; skin care; skin friction-induced perception and grip of objects; skin connects with the articles (tactile texture, socks, shoes, shaving devices, etc.) for daily use, skin irritation and discomfort; sport devices, synthetic skin; etc.
13	Sports tribology	Deterioration and testing of sport surfaces, equipment design and development, grip, gait analysis, players interaction, etc.
14	Tribology of the other human bodies or tissues	Bone; capillary blood flow; cells; contact lenses; hairs; ocular surfaces; etc.

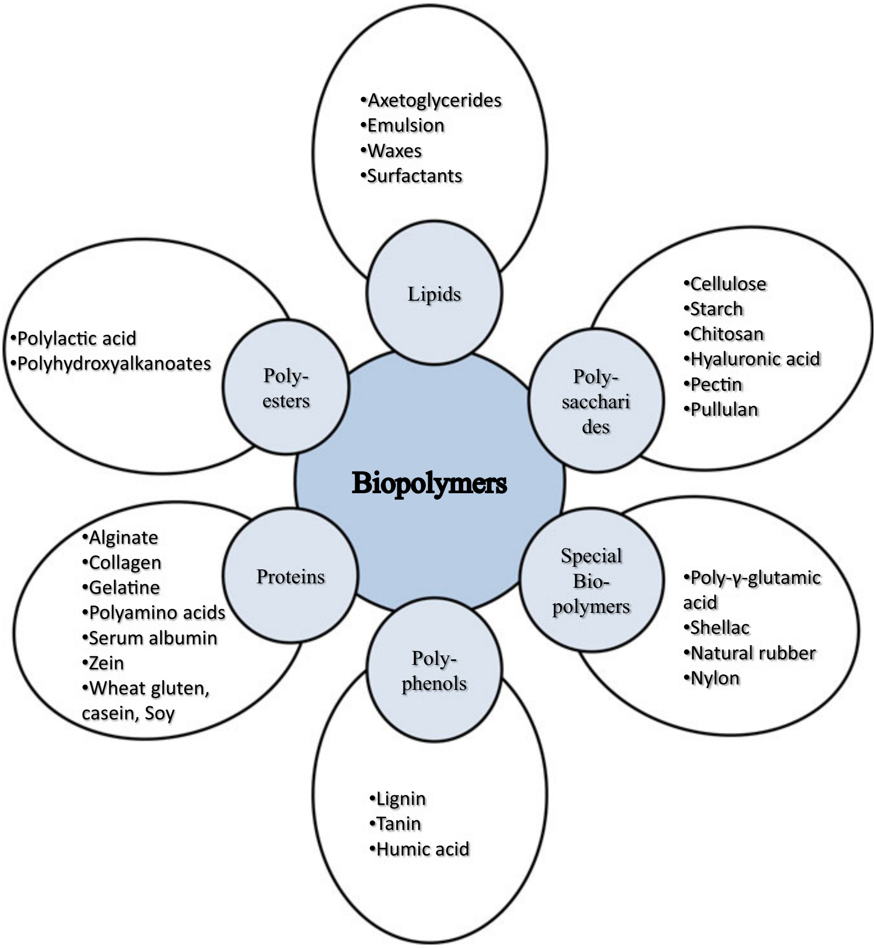

Fig. 1 Classification of different biopolymers based on their functional and structural properties

Nowadays, industries are more concerned about adopting a sustainable long-term approach without any negative effect on the environment and human health (Laine et al. 2013). This aspect put great efforts to develop materials from natural polymers rather than direct utilization of toxic, nondegradable, and mutagenic synthetic polymers (Souza et al. 2009). As per consumer demand, sustainable development of food and health industries depends upon continuous enhancement in the mechanical performance of biopolymer-based products. Tribological studies of employed biopolymers play a vital role to understand the mechanical aspect with better performance. The present chapter will help to develop the basic understanding of 'tribology' or specially termed, 'biotribology' concerned with biopolymers applied in some specific areas, i.e. biomedical, food, and packaging industry (Fig. 3). Further, it will focus on the improvement of biopolymer-based products in terms of standard design

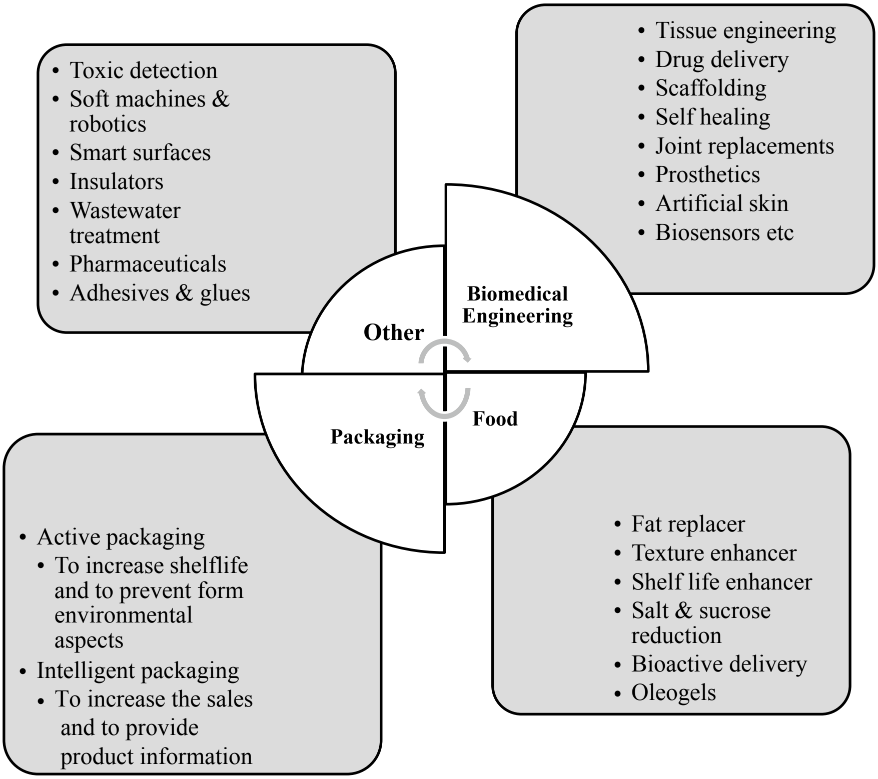

Fig. 2 Major sectors and different usage of biopolymers

as well as mechanical performance. Tribological studies will definitely show a significant impact on energy conservation issues that is one of the biggest challenges for the sustainable development of bio industries.

2 Tribological Study in Bio Industries

Tribology is the phenomena concerned with the surface of a solid or the interface between two surfaces (Sahoo et al. 2019). The most crucial components of tribological study may be considered as friction, wear, and roughness. Friction may be considered as a force resisting the relative motion between two solid surfaces or fluid layers or material elements sliding against each other. The frictional force is independent of the area of contact surfaces and is directly depends upon the applied force. The frictional force may be recognized as a non-conservative force (Cuffari 2019). Whereas, Wear is defined as surface damage, loss of material, or deformation of a

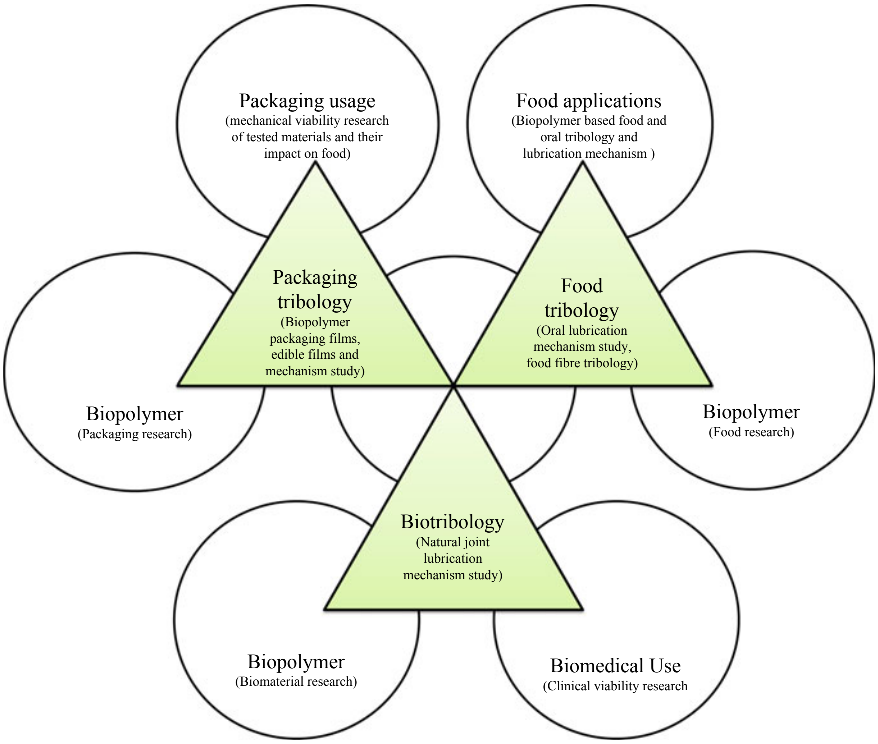

Fig. 3 Biopolymer tribology; different sectors and research baseline

body when two surfaces in contact have relative motion between them. Wear causes continuous degradation of the functional surface with the ultimate loss of functionality. The wear rate depends upon the type of loading, nature of relative motion between the contact surfaces, and temperature (Cuffari 2019). Wear may be classified into different types, as; (i) Abrasive wear (ii) Erosive wear (iii) Adhesive wear (iv) Fretting wear (vi) Corrosion and/ or oxidative wear (v) Surface fatigue. It is very clear that among these two degradation phenomena, friction is the force that occurs between two contact surfaces in relative motion, however, wear dictate material loss due to mechanical and/or chemical damage between the two surfaces in contact. Roughness in terms of surface roughness is another very important characteristic of tribology. In physics view, surface roughness plays a crucial role to determine the contact area of a surface and the contact stresses on a surface. However, the chemical perspective of surface roughness shows a major impact on shear strength, chemical compatibility, and lubrication properties of a surface (Critchley 2018). The synergistic approach to study and apply all three parameters (friction, wear, and surface roughness) jointly as a 'tribology' plays a significant role to enhance mechanical performance, efficiency, and reliability of a system. The tribological aspects are closely concerned with the techno-economic feasibility of industries. Further, tribological study and processes can positively handle the losses due to energy dissipation and material wear by improving standard design and optimizing energy efficiency (Sahoo et al. 2019).

As an interdisciplinary study concerned with biomechanics, physiology, biochemistry, clinical medicine, pathology, biology, etc., biotribology is emerging as a sister branch of tribology in the study of biological systems. Biotribological studies focus on all the aspects of tribology within the biological system (Zhou and Jin 2015). The domain of biotribology is very vast which covers the mechanical and tribological study of tissue-engineered cartilage, development of wear-resistant materials, preclinical testing to improve the implants and wear modeling of artificial joints, etc. by applying biocompatible prostheses, therapeutic medical devices, medical imaging equipment as magnetic resonance imaging (MRI), electroencephalography (EEG), etc.(Sahoo et al. 2019).

3 Tribology of Biopolymer and Biopolymer Composites Applied in Biomedical Engineering

The main perspective of biomedical engineering is to apply interdisciplinary engineering principles and design concepts for diagnostic and therapeutic purposes. In these applications, medical implants become an integral part of the living system of the patient by sustaining normal body functions (Dutta et al. 2020). The most common types, i.e. bones, hips, heart, knees, breasts, ears, eyes, and cardiovascular implants are either made of synthetic metals, ceramics, and polymers or preferably by using a biopolymer (Rowland et al. 2019). Traditional synthetic materials as Tantalum, gold, Co-Cr, NiTi, and stainless steel lead to a number of disadvantages as immunological rejection, cell and tissue necrosis, cytotoxicity, and implant loosening (Rawat and Saxena 2019). These limitations are the root cause to develop more research for biopolymer-based implants with advantages listed as biocompatibility, bioadhesion, functionality, low friction, high strength, and corrosion resistance, etc. (Rawat and Saxena 2019).

3.1 Essential Characteristics of Biopolymer-Based Implants

It is required to understand the nature of biopolymer-based implants for tribological studies. These biomaterials are supposed to fit with living tissue or any other organic matter without any adverse effect. The essential characteristics are listed below:

(i) Biocompatibility: The medical implant must be compatible with the living tissue. In this regard, biopolymer-based implants exist within the living system without any negative effect (Rawat and Saxena 2019).

(ii) Mechanical properties: The best thing with biopolymer-based implants is low modulus with high strength to elongate the life of such implants inside the body without any loosening effect (Sahoo et al. 2019).

(iii) High wear resistance: High wear resistance with a low friction coefficient is another desirable attribute for biopolymer over metallic implants.

(iv) High corrosion strength: Metal-based implants may suffer a highly corrosive atmosphere due to 37 °C, body temperature (Hansen 2008), along with the abundant presence of chlorine ions in the body fluid. At this point, biomaterial-based implants best suit with less corrosion resistance (Sahoo et al. 2019).

(v) Long fatigue life: Human joints are used to suffer additional weight and show cyclic motion. The implant material is required to sustain high loading to stop implant failure and stress shielding from fatigue fracture.

(vi) Osseointegration: Topography of the surface, chemistry, and roughness may be considered as a major parameter for good osseointegration as proper integration of the implant with the bone and other tissues is required to minimize the implant loosening risk (Rawat and Saxena 2019). In view of these essential characteristics, biopolymers may be considered more preferable over synthetic metals for proper integration of the implant with the bone and other tissues (Sahoo et al. 2019). Poly tetra fluoro ethylene (PTFE) may be considered the first biopolymer, studied by the late Sir John Charnley for total hip replacement design (Charnley et al. 1969). In recent years, ultra-high molecular weight polyethylene (UHMWPE) and new types of polythene, cross-linked polyethylenes (XLPE) showed promising clinical results with improved wear resistance (Joyce 2009). Including these biomaterials, polylactic acid (PLA), chitosan and silk are also explored as implant materials possessing characteristics of non- cytotoxicity, biocompatibility and biodegradation (Rebelo et al. 2017).

3.2 Biopolymers Employed in Biomedical Engineering

Among the most promising biopolymers, polylactic acid (PLA) is applied as an intravascular dilator in patients (Rebelo et al. 2017). PLA is a bioabsorbable and high-strength biopolymer that can be derived from natural bioresources as potatoes, rice, and corn starch (Tamai et al. 2000). In this direction, PLA-based biodegradable stents were developed by a group of researchers and applied in human models (Tamai et al. 2000). Further, the PLA composite scaffolds were studied as a carrier for the recombinant bone morphogenetic protein 2 (Chang et al. 2007). Nanocomposites of PLA with improved Young’s modulus and hardness show better performance in tissue engineering (Zhang et al. 2011).

The next commonly used biopolymer for implantable devices is silk. The β-sheet structure of silk fibroin generates a matrix of high mechanical strength with thermodynamic stability (Rebelo et al. 2017). In this direction, Altman et al. (2003) utilized the patient’s adult stem cells with silk to develop autologous tissue-engineered anterior cruciate ligaments. The highly versatile scaffolding of silk fibroin is also potentially applied to the musculoskeletal system (Meinel and Kaplan 2012).

Chitosan may be considered a widely applicable biopolymer in the medical field. Deacetylation of chitin may produce chitosan which is mostly used in medical implants as ligament, bone, liver, tendon, cartilage, neural, and skin regeneration (Rebelo et al. 2017). Chitosan-based matrices are widely studied for bone applications. To improve the mechanical strength of these scaffolds, chitosan—alginate biocomposites are developed for better performance in different medical fields (Rebelo et al. 2017). Recent studies have proved that the development of advanced materials in form of biopolymers reinforced with fillers or nanofillers have the potential to show improved performance inside the living system.

3.3 Tribological Studies in Biomedical Engineering

In the biomedical domain, tribological studies may be considered a very challenging aspect because of the continuous up-gradation of implant material (Zhou and Jin 2015). 'Biotribiology', 'Nanotribology', and 'Green tribology' may be considered as a newly established term to evaluate the tribological phenomenon of biomaterials for economical stability, ecological balance, and energy savings efficacies (Luigi 2018). Tribology may be considered an important tool to conserve energy by reducing the coefficient of friction and wear rate between the implant and adjacent surface (Zhou and Jin 2015). In this regard, eco-friendly materials as biopolymers and biodegradable lubricants may play an important role to develop an energy-efficient process with tribological concern also (Shafi et al. 2018).

3.3.1 Tribiology of Biopolymer and Biopolymer Composites

Biopolymer composites are composed of two or more constituent materials with better mechanical performance than biopolymer alone (Rebelo et al. 2017). The use of fiber-reinforced polymer (FRP) in the biomedical field especially in orthopedics offers many characteristics as low young modulus, high tensile strength, mechanical strength, and stiffness to improve their functionality as an implant to be used in bone fracture repair, dental application, and replacements of total hip, knee, ankle, and other joints (Rawat and Saxena 2019). The tribo—performance of such composites may be evaluated to test their compatibility as a biomedical implant (Yousif and Tayeb 2007). In this direction, several studies regarding the tribology of biopolymer composites are reported (Sahoo et al. 2019). Yousif and Tayeb (2007) have reported the tribological performance of oil palm fiber reinforced polyester (OPRP) composites. In continuation of that, wear and friction characteristics of these composites were tested and compared with polyester alone at different sliding distances (0–5 km), sliding velocities (1.7–3.9 m/s), and applied loads (30–70 N) under dry contact condition. The tribo—performance result concluded that

Table 2 Different materials combinations and their tribologival properties

S.N	Material combination	Friction factor	Volumetric wear (mm^3/million cycles)
1	Ceramic on ceramic	0.002–0.07	0.1
2	Eramic on metal	0.002–0.7	0.1
3	Metal on metal	0.22–0.27	1
4	UHMWP on ceramic	0.06–0.08	25
5	UHMWP on metal	0.06–0.08	40

the presence of oil palm fiber in the polyester increased the wear property by about three to four times compared to polyester alone. While the friction coefficient of these polymers was decreased by 23% than the polyester alone. The wear testing of OPRP is based on debonding, bending, tear of fibers, and deformation (Yousif and Tayeb 2007). In another study, date palm leaf reinforced polyvinyl pyrrolidone (PVP/DPL) composites were tested to determine the correlation between the fiber content of these composites and wear performance (Mohanty et al. 2014). Further, it is concluded that the addition of date palm leaf fibers (10- 40% based on the weight of fibers) leads to improve wear resistance of composites with optimum fiber content (26 wt %). With the increment of applied load specific wear rate increases at different sliding speeds for both neat PVP (0 wt %) and the friction coefficient decreases with increasing applied load. These studies conclude that the mechanical and tribological properties of biopolymer composites are correlated with each other and directly affected by fiber loading (Mohanty et al. 2014). Different materials combinations used in biomedical engineering are given in Table 2.

3.3.2 Tribology in Joint Replacement

Several studies have been evaluated to show the tribological features of articular cartilage which is defined as an aneural and avascular connective tissue that protects the end of synovial joints (Ingham and Fisher 2000). These joints minimize friction and wear during the relative motion between the joint surfaces (Lentini 2018). In this direction, Lentini (2018) investigated the tribological performance of adult bovine articular cartilage based on frictional changes due to load and static loading time. He concluded that measured friction increases as loading time elapse due to interstitial fluid exudation (Luigi 2018).

The field of tribology is surrounded by the subject knowledge of fluid mechanics, material science, lubricant chemistry, solid mechanics, and heat transfer (Jin and Fisher 1966). As a surface phenomenon, tribology includes surfaces both microscopic surface topographies as well as macroscopic bearing geometries (Zhou and Jin 2015). In biomedical, tribological studies are very significant in the functioning of artificial joints (Joyce 2009). Tribology becomes very significant in arthroplasty especially in knee and hip joint studies, dental implants, and artificial hearts where the incorporation of friction and wear between two surfaces plays a major role to

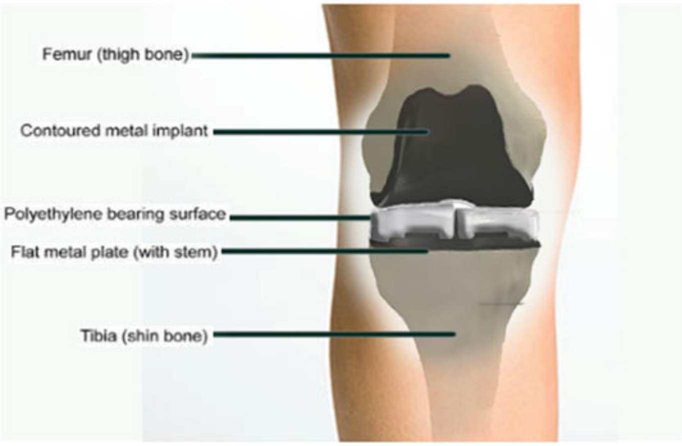

Fig. 4 Artificial knee joint (Sahoo et al. 2019)

predict the performance of medical implants within the living system (Sahoo et al. 2019). The tribology of joints depends upon biomechanical studies, i.e. structure–function relationship of joint motion and the mechanical behavior of materials that make up the joint (Mow et al.1993). In the case of synovial joint, tribology includes lubrication by synovial fluid, synovial joints friction, the mechanisms of joint lubrication, analysis of cartilage wear and damage, joint mechanics, and artificial joints development (Sahoo et al. 2019). A typical artificial knee joint is shown in Fig. 4.

3.3.3 Hip Joints

Hip joints (Fig. 5) are subjected to a large dynamic load about few times of body-weight (Jin and Fisher 1966). Friction and wear are two significant parameters as friction is involved with designing low-friction arthroplasty and wear is concerned with the integration of the prosthetic component. However, biological reactions may be adversely affected due to wear debris. Lubrication plays an important role to reduce the parameters, friction as well as wear. Low friction arthroplasty was extensively studied by Sir John Charnley with the fact that friction and the design of artificial hip joints are correlated to each other (Jin and Fisher 1966). In the early arthroplasty research, Mckee- Farrar hip replacements were clinically evaluated for long-term survival (Higuchi et al. 1997; Zahiri et al. 1999). It was observed that aseptic loosening may be the main cause of implant failure in McKee–Farrar hip replacements in both metals- on- metal and metal-on-plastic bearings (Ingham and Fisher 2000). However, general considerations as wear resistance of the bearing, implant design, and biomechanics of the reconstruction are reported to improve the surgical implantation of hip replacement (Ridzwan et al. 2007) (Fig. 6). Tribological evaluation of friction, wear and lubrication between the contact surfaces along with

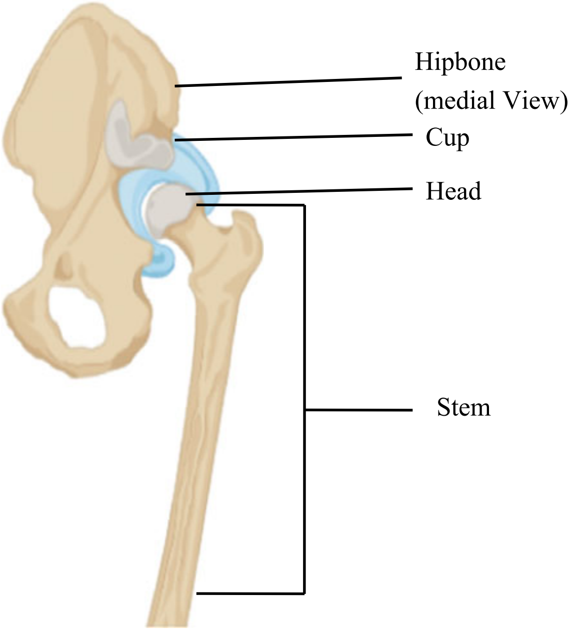

Fig. 5 Illustration of typical hip joint cup implant. (Sahoo et al. 2019)

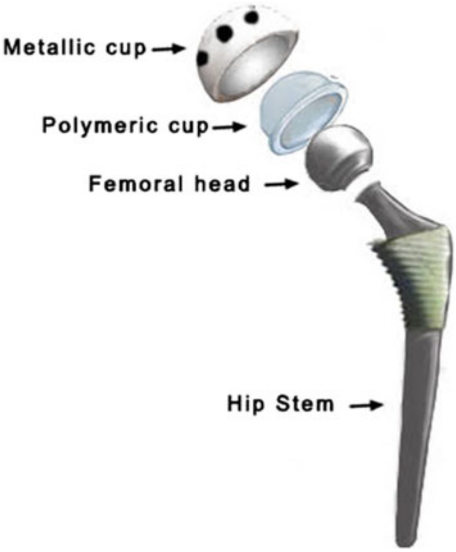

Fig. 6 Individual components required for the complete Hip implant (Sahoo et al. 2019)

contact mechanics modeling (Jin et al. 1999; Bartel et al. 2016) and study of design parameters of the femoral head radius (Plank et al. 2006) may positively impact the total hip replacements with increasing survivorship.

The theory of hip replacement is based on a ball and socket joint, in which the femoral stem and ball fit into each other and relatively move against the cup or acetabular component (Sahoo et al. 2019). Mostly used combinations of materials for hip arthroplasty are listed as metal on plastic, metal on metal, ceramic on plastic, and ceramic on ceramic. At present time, as a metal on plastic material, a very stable and reliable material, UHMWPE is usually applied as hip replacement implants due to a lower risk of wear (Sahoo et al. 2019). However, traditionally, metals on metal bearings, titanium alloy, chromium alloy, or stainless steel were applied in hip arthroplasty. Further, ceramic on ceramic may be chosen as a very good combination due to high strength and ultra low wear ceramic bearing for longer survival. The combination of two reliable materials as Ceramic on UHMWPE may be seen as a very good alternative due to scratch-resistant implant material with a very less wear rate (Sahoo et al. 2019).

4 Food Industry

Biopolymers are simple sugars, fermented products, or, amino acids. We are consuming a wide variety of food from ages to fulfill our apatite and our food includes several carbohydrates, proteins, sugars, and organic acids. Biopolymer consumption in food is escalating at a rapid pace due to a plethora of reasons as they can be used as food, gelling agent, a shelf life enhancer, or as a delivery agent of a certain compound (Fig. 7).

Besides, this class of molecular blocks also offers easy availability, biodegradability, biocompatibility, antibacterial activity, low immunogenicity, less procurement, and processing cost (Jacob et al. 2018). The most common biopolymers utilized in the food industry are listed in Table 3.

Friction is a force and wear is a process of removing material from the surface during relative motion while lubrication is the process of application of fats and oils or saliva in case of human oral tribological studies to reduce the friction and eliminate the wear (Fig. 8).

As a major component of tribology, friction, wear, and lubrication promotes the understanding of the underlying food texture and structure relationship (Axen et al. 2001; Prakash et al. 2013). During tribological studies, a friction stribeck curve is made which is generally divided into 3 sections hydrodynamic, mixed, and boundary regime (Fig. 8). In the hydrodynamic regime, friction is affected by the viscosity and sliding speed while in a mixed regime sliding speed decreases the friction. However, in the boundary regime friction remains constant and hardly affected by any change in viscosity and friction (Nguyen et al. 2017). Friction, wear, and lubrication between the machine parts was the initial concern in tribological studies till 1948 with later advancement and first study in biopolymer tribology dealing with knee

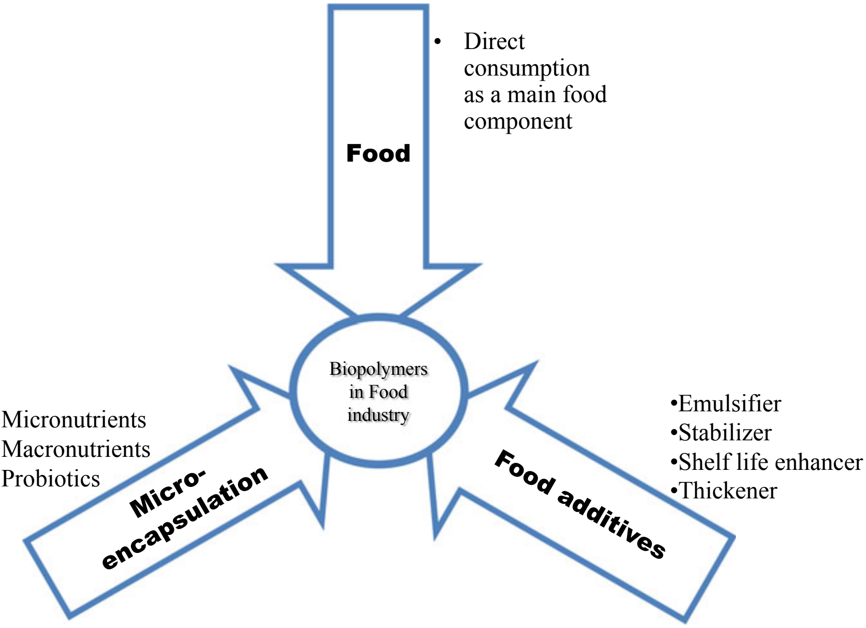

Fig. 7 Different use of biopolymers in food industry and their path of consumption

Table 3 Different Biopolymers used in food industry and their properties

S.N	Biopolymer	EC number	Molecular weight (g/mol)	Density (g/cm^3)	Melting point (°C)
1	Alginate (sodium salt)	232–680-1	216.12	1.601	263.33
2	Casein	232–555-1	2062	1.0632	280
3	Cellulose	232–674-90	342.3	1.5	260–270
4	Chitosan	618–480-0	1526.5	0.15–0.3	203
5	Collagen (type IV alpha I)	295–635-5	1587.8	0.2–0.4	160
6	Gelatine	232–554-6	20–220	1.3–1.4	35 <
7	Lignin	232–682-2	1513.6	1.39	170
8	Pectin	232–553-0	194.14	1.1–105	6.1
9	Starch	232–679-6	359.33	1.5	256–258

joint meniscectomy removal (Fairbank 1948). However, food tribology research was initiated with the first study on the effect of shear on wheat protein got published (Bernardin 1978).

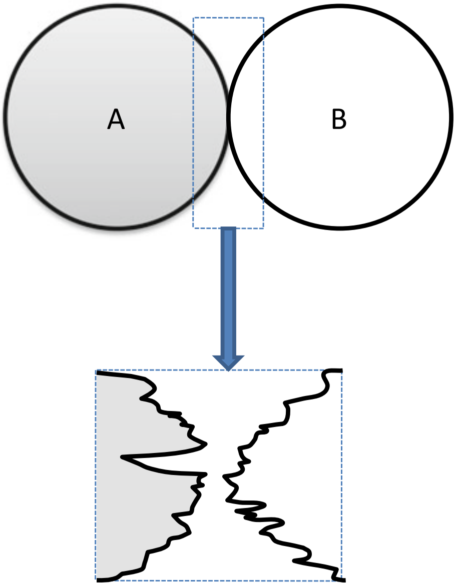

Fig. 8 Schematic view of 2 different particles interacting each other and their uneven rough surfaces causes wear

Static tribology is entirely different than the in-vivo (in-mouth) and any relation between both the situation cannot be found (Vardhanabhuti et al. 2011). The tribological study between food fibers and between food and host (sensory studies) are two major study aspects. During oral processing, we attempt mastication, salvation, aggregation, bolus formation in-mouth, and swallowing (Fig. 10).

The food tribology and rheology depend upon the firmness, hardness, melting, roughness, smoothness, and thickness of food and their impact on sensory and taste perception is in light since the 1970s (Braud and Boucher 2019). Food continuously got broken into subtly pieces to form an aggregate by blending with the saliva that forms a thin layer around the oral surfaces present in the vicinity just before, after, and during the eating. So, during oral processing, the tongue palate contact tribology dominates the rheological aspects of food for texture sensation (Anvari et al. 2018). The structure and function of food were not been assessed by the early rheometrical studies, however, recent tribological research is dealing with all these interactions along with the in-mouth sensory assessment and influence of different types of colloids on the lubrication (Farrés et al. 2014).

Frictional conditions inside the mouth suggest insights about some important food attributes such as slipperiness, mealiness, roughness, astringency, and smoothness. In the human mouth, food faces saliva which is important to prevent xerostomia (Wijk and Prinz 2005). Saliva is required in speaking, bolus formation, lubrication of mouth and in breaking of starch to facilitate food transport through the body, masticated food aggregation, and for the protection of internal bio surfaces from

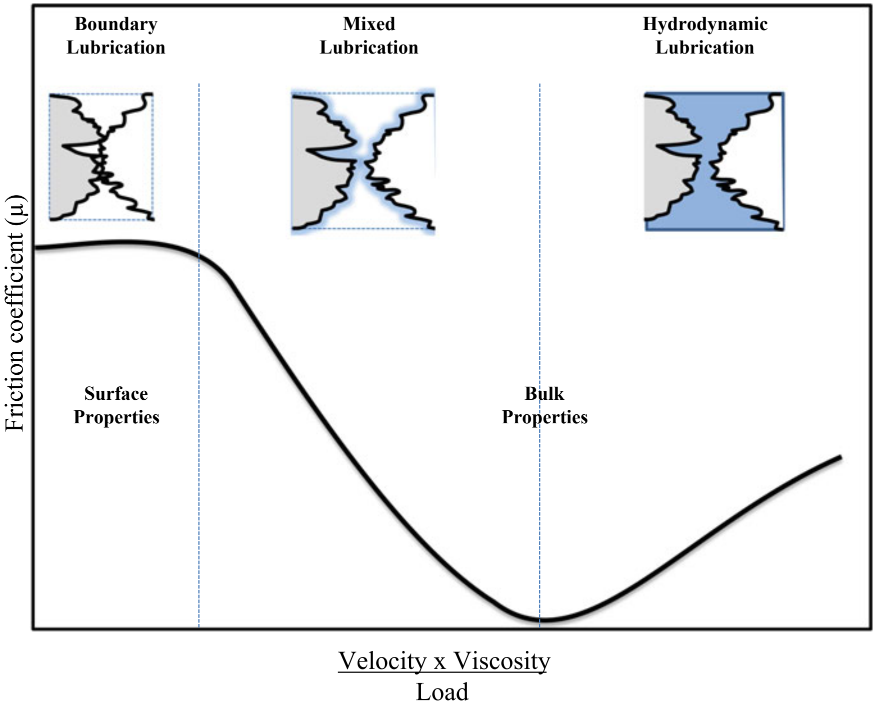

Fig. 9 Typical stribeck curve along with the lubrication conditions. (Prakash, 2017)

wear and abrasion. The human whole saliva (HWS) shows the boundary friction 2 order higher than the water (Bongaerts et al. 2007). Physicochemical properties, and mechanical processing or food mastication also affects the oral Tribology (Fig. 11).

During tribological studies, In-vivo studies against the behavior of foods in presence of oral mucosa under normal function are done on the basis of sensory evaluation through a panel while mechanical aspects of food are generally studied by different tribological testing apparatus (Prinz et al. 2007). However, Olsson and his colleagues have developed a device for measuring the sailometry and dryness based on the sliding friction principle and proved that friction values on the lips are higher as compared to the friction values in the buccal mucosa (Olsson et al. 1991). This method was required to know the status and function of the food if it wears the teeth. So that, we can avoid that food to prevent our tooth from wear (Prinz 2004). Prinz and his colleagues conducted a set of experiments and demonstrated the effect of fats on friction and lubrication. This study has concluded that fats and oils act as a lubricant but not limited to because some biopolymer gels also show good lubricating properties. The size of fat droplets significantly affects the degree of lubrication (Prinz et al. 2005). It is estimated that the fat content of food directly affects the lubricating, rheological, structural, and viscoelastic tribological properties of food but the interaction between protein and fat with the tribo-pair system requires an

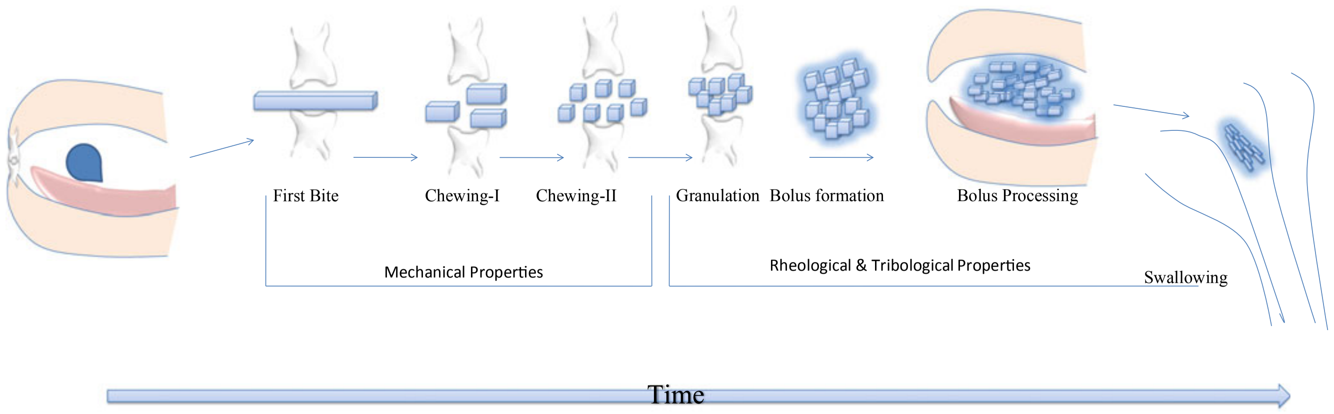

Fig. 10 Depiction of major key stages occur during oral processing of solid food. In addition figure also indicates the steps where mechanics, tribology,and rheology are important. (Stokes et al. 2013)

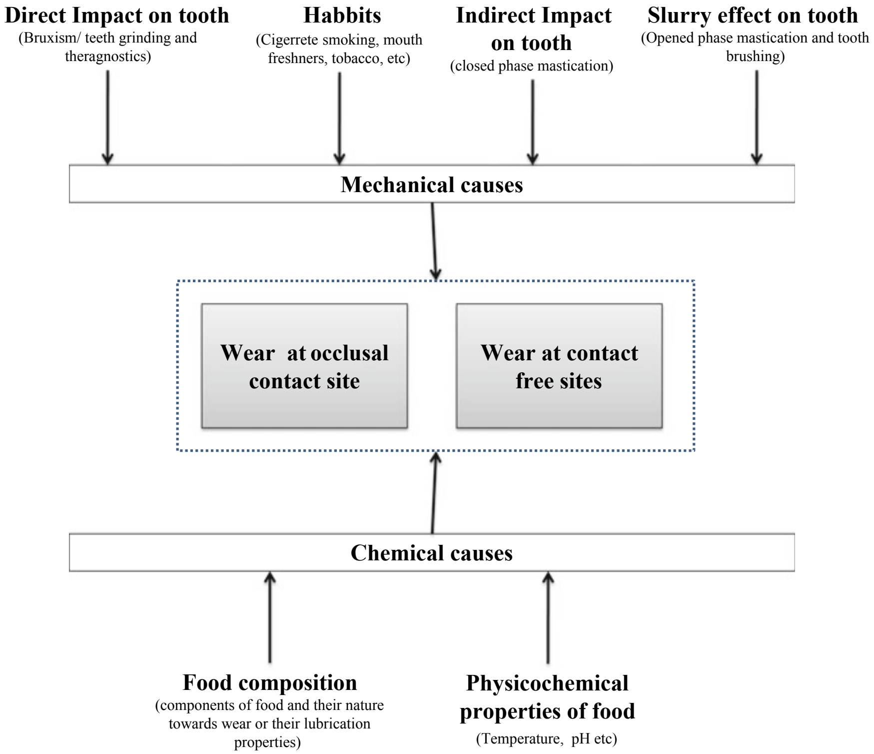

Fig. 11 Parameters influencing food tribology: the food's physico-chemical properties, route and modes of food consumption and the oral physiological properties of human mouth. (Prakash 2017; Zhou and Jin 2015)

investigation to provide some insights into the protein-fat coalescence and texture perception methods (Ningtyas et al. 2017). Among the food rheology and tribology, oral tribology is one of the least studied areas for sensory textural perception (Chen and Stokes 2012).

In earlier days, structural and textural properties of food were assessed by the typical "chew and spit" method in which food samples were given to some people for chewing for different time durations and aggregate was removed and analyzed for different rheological properties (Helkimo et al. 1978). However, the chewing strength and size of the mouth cavity could not be the same. This nonuniformity or variation in individual chewing requires more development to cover all the natural aspects that can replicate the human mouth for the tribological study (Foegeding et al. 2016).

Various attempts to study the masticating effect, salivary friction, and teeth wear were done while the study was zeroing to the soft tissues' ensalivation, function, and role in bolus formation were less. In 2007, Mazari has experimented with 2 different colored chewing gums to study the mixing inwards the bolus and inputs of teeth in the process and concluded that cheeks help in mixing, shortening the bolus, and pushing the food to swallow (Mazari et al. 2007). Tan and his colleagues have developed a numerical model to estimate the behavior of fats and also to characterize their wear interaction with different crystalline networks (Tan et al. 2019). Creep and wear recovery principle-based methods can also be utilized in new food product development and its tribological characterization (Tan and Joyner 2019). However, for different polymers or food samples, the process must be optimized because the depth of creep, loss mass, sliding speed, temperature, and fat content in the food sample varies drastically (Seighalani et al. 2021). Different traction devices have been developed for tribological studies till date and some of the instruments provide comparable conditions to the human mouth (Isschers 2008; Vardhanabhuti et al. 2011; Rodrigues et al. 2016; Stee et al. 2017; Feng et al. 2020).

A recent and more realistic study based on the polydimethylsiloxane (PDMS) disks has revealed the process of interaction and lubrication of the system with soft tribological surfaces. Besides it also stated that heavy and complex food molecules that are large for the cavities increase the friction (Taylor and Mills 2020). Another similar study has concluded that friction forces developed during oral processing are the function of food composition. The study also has stated that friction forces development depends upon the saliva quantity and size of boli (Fuhrmann et al. 2019). Biopolymer-based functional foods i.e. high internal phase emulsion (HIPE) possess ultralow friction properties and show more smoothness and creaminess as compare to commercial mayonnaise and have a potential alternative to becoming a plant-based egg (Ruan et al. 2019). An increase in protein concentration results in high heterogeneous microstructures that increase in proportion to the friction and yield stress. However, Sensory properties (creaminess and smoothness) of food decrease with an increase in protein concentration (Laiho et al. 2017). An increase in hydrocolloid concentration lowers the friction coefficient, increases the viscosity, causes phase separation, and lowers the protein stability (Zhu et al. 2019). A variety of Biopolymers is used in the food industry direct as food, as an aggregate or shelf life enhancer (Fig. 7).

4.1 Major Biopolymers and Their Tribological Properties

Biopolymers are widely used in the food industry as a gelling agent, stabilizing or thickening agent, encapsulating agent, food coating agent, fat replacer, anti-freezing, anti-aging agent, smooth texture, etc. due to their properties of viscosity increment, gelling, and film formation ability (Qin et al. 2020). Alginate ($C_{12}H_{20}O_{12}P_2$, M.W. 418.23 g/mol) has a significant impact on textural and rheological properties of food by increasing the storage modulus (G’) along with the water holding capacity of the food to enhance cohesiveness, smoothness, softness, and chewingness of the food (Kumari et al. 2017, 2018). Alginate can be used as a fat replacer it also positively affects the tribology of food, protein release, and its disintegration while negatively affects protein retention during In-vitro digestion (Kumari et al. 2019). It is perceived and proven that the oral processing and friction properties of food depend upon the fracture properties of the bolus, bolus viscosity, bolus tribology, and initial and late oral processing stages (Krop et al. 2019). That indicates the relation between rheology and oral tribology of food to its sensory properties.

Casein is a rheomorphic protein that is stable during drying, heating, and freezing which makes it valuable. However, change in ionic strength, pressure, pH, temperature, and type of solvents can modify the structure and functions of casein (Ranadheera et al. 2016). Casein cannot bear shear on low pH (2.0–4.6) and reduced in size while at normal pH (6.7–7.5) it has no effect of high shear. It shows orthokinetic aggregation and fragmentation (Ranadheera et al. 2019). Friction reduction depends upon the viscosity and the addition of hydrocolloids increases the protein solution lubrication quality and viscosity. However, frictional reduction in proteins not only dependent on the viscosity increment but also depends upon the size of molecules (Zhu et al. 2019). Wear depends upon the aging time, fat content, normal load, sliding speed, and temperature. Overall strain, depth of creep, and mass loss enhance with the addition of fat content in casein (Tan and Joyner 2019). A lower concentration of casein and casein salts for gelling effectively reduces the average gel particle's size that consequently reduces the friction while higher addition causes higher friction due to the increase in firmness (Pang et al. 2020).

Cellulose and its derivatives are used in the food industry copiously because these are very effective as rheology modifiers, thickener, moisture binders, stabilizers, and viscofiers. Different cellulose derivatives, their properties, and their application in food are given in Table 4. The addition of a small amount of cellulose gum often increases the zero shear viscosity massively and this enhanced zero shear viscosity further leads to the increment in homogeneity and dispersion stability (Jimenez et al. 2020).

Ethylcellulose (EC) or hydroxypropyl methylcellulose (HPMC) is also used as oleogels for the rheological modifications in food. An increase in EC and HPMC concentration causes an increase in flow behavior index and reduces the shear viscosity while concentration decrease causes the decrement inconsistency index. These oleogels affect the food quality and their concentration is directly proportional to the food hardness and causes loss in volume. In the bakery, a reduction in aerated volume directly hampers the texture, taste, and consumer mouthfeel. Therefore this is one of the technical challenges in their bakery use (Demirci and Lee 2020). Oils are a very important part of our food style and a combination of cellulose or its derivatives with oils shows higher lubrication, suitable thermal, mechanical and rheological properties (Sagiri and Rao 2020).

Gelatin is used as biodegradable edible films, thickening agents, emulsifiers, wetting agents, stabilizers, refined material, and microencapsulation agents. Gelatin has a unique property as compared to other biopolymer gelling agents in that it is thermal-reversible and melts in the mouth (Said 2020). Tribological behavior of food depends upon the type and dosage of fat. Gelatin is a proven best hydrocolloid due to its lubrication, gel strength, increase texture, viscosity, and synergy decrement. It is an excellent fat replacer and even increases the sensory properties in comparison to full-fat food. The addition of gelatin reduces the food viscosity and storage (G'), loss

Table 4 Different types of cellulose, their physical and tribological properties and food applications

S.N	Name	Physical properties	Rheological and tribological properties	Food applications	Listed
1	Carboxymethyl cellulose (CMC)	Tasteless, odorless, hygroscopic and white tan powder	Water Soluble	Beverages	Generally recognised as safe food food by US and listed in Food chemical codex by FAO/WHO
			Viscous	Tortillas	
			Easy dispersion and dissolution	Bread	
			Thixotropic	Cakes	
			Water holding capacity at lower solubility	Instant noodles	
			Maintains the viscosity over wide pH change	Meat analogues fomulation	
			Tolerant to salt	Syrup	
			Synergistic with other hydrocollooids	Sauces	
			Makes CMC-protein complex	Soup	
2	Methyl cellulose, Methylhydroxypropyl cellulose (MHPC) or hydroxypropylmethyl cellulose (HPMC)	Light coloured, neutral odor, neutral taste, less hygroscopic powder	Soluble in cold water	Shows thermogelation	Generally recognised as safe food food by US and listed in Food chemical Codex by FAO/WHO
			Shows thermal geling	Bakery stable sauces	
			Little thixotrophic	Bakery stable fillings	
			Pseudoplastic	Ice creams	
			Emulsifier	Whipped creams	
			High salt causes salting out	Whipped toppings	
			High sugar causes low temperature below gelling point	Formed foods	

(continued)

Table 4 (continued)

S.N	Name	Physical properties	Rheological and tribological properties	Food applications	Listed
3	Hydroxypropyl cellulose (HPC)	Neutral taste, neutral odor, water soluble, odd white compound, may be powder or in granular form	Not thixotrophic	Whipped creams	Listed in FOOD chemical Codex by FAO/WHO
			Thermoplastic	Whipped toppings	
			Insoluble in water above 45 °C	Food emulsions	
			Sugar and salt decreases the pprecipitation temperature		
			Emulsifier		
4	Ethyl cellulose (EC)	Soluble in wide range of solvants but not in water	Hydrophobic	Food encapsulation	Listed in Food chemical codex by FAO/WHO
			Ethanol soluble		
			pH change resistant		
			Stabiliser		
			Reduces moisture migration		

modulus (G”) of food significantly (Nguyen et al. 2017). Gelatin decreases the higher degree of friction coefficient of the food sample in comparison to other biopolymers and due to its unique property of melting it produces the boundary conditions (Zhu et al. 2020). The blending of gelatin with other polysaccharides e.g. chitin whiskers (CHWs) etc. develops nano-composite hydrogels. These hydrogels are more effective in terms of fracture strain, fracture stress, hardness, recovery, and increased gelling temperature (T_g). In addition to these characteristics, nanocomposite hydrogels are more stable as compare to pure gelatin gels (Ge et al. 2018).

Chitosan ($C_{56}H_{103}N_9O_{39}$, M.W. 1526.5 g/mol) is a polycationic polymer of glucosamine having some antioxidant properties and biologically adhesive with homeostatic effects that are used in clarification, encapsulation, preservation, and as an active packaging ingredient (Morin et al. 2019). Lignin is the most abundant biopolymer after cellulose. Although lignin shows high resistance to digestion as compared to other natural compounds, it is still used in food items due to its wide functions (Jha et al. 2017). Lignin is used as an egg alternate in bakery and other foods as it also gives a fluffier texture to the food (Gil-chávez 2019). Suberin is also an extracellular biopolymer mostly used as an additive in the baking industry (Mudgil 2017). Further, the Starch-lipid complex resembles the fat structure with properties such as; creaminess, glossiness, and smoothness and is used in producing low-fat mayonnaise, ice-cream, and other food items (Agyei-amponsah et al. 2019). A study has concluded that the breaking of starch molecules by the salivary α-amylase reduces friction by increasing the lubrication. After the breakdown, the small fat molecules migrate to the surface of the bolus and started acting as a lubricant (Wijk and Prinz 2005). The starch granule imbibes the water and swells to several times its initial size and releases the simple linear glucose chains. However, starch granules don’t get completely dissolved and pertains to a highly swollen state, and highly deformable starch paste further plays a vital role in the rheology, texture, and viscosity of starch (Zhang et al. 2017).

5 Packaging

Biopolymer-based food packaging has become an active packaging due to its various features like shelf life enhancement, biodegradability, eating ability, etc. (Versino et al. 2016). Several biopolymers are used in packagings such as alginate, biopolyesters, carrageenan, casein, cellulose, chitosan, collagen, curdlan, gelatin, gellan gum, lignin, pectin, polyglycolic acid (PGA), polyhydroxybutyrate (PHB), polylactic acid (PLA), pullulan, soy proteins, starch, wheat proteins, xanthan, zein, etc. not only in packaging films but these biopolymers are extensively used in producing barrels, bottles, boxes, buckets, cans, caps, closures, coatings, cups, drums, food containers, household refuse bags, jars, packaging bags, pails, vials, etc.

Polylactic acid (PLA) or polylactide is preferred in food packaging as it is a bacterial cellulosic material. PLA is brittle and can’t resist oxygen permeation up to a satisfactory level. It's blending with starch may develop materials of commercial-grade (Muller et al. 2017). PLA-Lignin films can bear high tenacity. However, PLA-starch-lignin composite films show excellent elastic modulus and tensile strength (Yang et al. 2016).

Biopolymer films are a good alternative to plastic films or cellophane. However, the addition of some compounds such as tannic acid (Luqman et al. 2018), nanoparticles (S. Kumar et al.2018a, b; Tang et al. 2018; Amjadi et al. 2019), metal–organic frameworks (Zhao et al. 2020), curcumin (Musso et al. 2017), polyvinylpyrrolidone (Gregorova et al. 2014), etc. shows an unprecedented upsurge in its mechanical, tribological, thermal, antimicrobial properties, retarded lipids extraction, shelf life, and decrease in microbial load.

Biopolymer based packaging films generate garbage after use until it's fully degradation takes place. So, researchers started focusing on zero wastage and developed edible packaging. Natural edible biopolymers are the major source of edible packaging films and also a sustainable and eco-friendly alternative to plastic packaging waste (Shit and Shah 2014). Edible films are very advantageous because they also provide indirect insights about the spoilage of food just by simply measuring the pH and also enhance the shelf life of food by its antioxidant property (Musso et al. 2017). Edible films are not only produced zero discharge but also enhance the organoleptic properties of food (Wittaya 2008).

The biodegradability of a biopolymer film can be increased drastically by increasing the starch content of up to 10% (Arvanitoyannisa et al. 1998). Carboxymethylcellulose and rice starch-based packaging films are flexible, antimicrobial, thermally stable, and antioxidant (Suriyatem et al. 2018). The biopolymer films show low oxygen permeability and good strength. However, their low elasticity and higher moisture sensitivity of some biopolymer-based films can be enhanced and desired mechanical and film properties can be achieved by adding some hydrocolloids into them (Liang and Luo 2020). Some advance biopolymer-based packaging materials such as thermoplastic starch (TPS), thermoplastic corn starch (TPCS), thermoplastic sugar palm starch (TPSPS), bacterial cellulose nano whickers (BCNW), polyhydroxy butyrate (PHB), etc. have been developed with excellent tribological properties and shown the potential of combining with the modified atmospheric packaging.

Hydroxypropyl methylcellulose (HPMC) has high formability and moisture resistance and it is used in the pharmaceutical and food industry as an outer protective layer. HPMC shows substantial wear resistance and lubrication characteristics. HPMC's shorter life span limits its use in packaging. However, its short life extends a tremendous increase in its tribological properties with the addition of Molybdenum disulfide (MoS_2) (Shi et al. 2016). Friction and wear reduction can be achieved by the addition of some nano-additives to improve the tribological properties of the polymer compound because it increases the load-bearing capacity of the composite (Shi et al. 2020). Ultra-high molecular weight polyethylene (UHMWP) is already used in packaging due to its high shear, tension, temperature, and abrasion bearing capacity, and it is proven that the addition of lignin up to 13wt. % doesn't affect its mechanical and tribological abilities. It has a proven eco-friendly packaging material production process (Gupta et al. 2016). UHWMP is a self-lubricating biopolymer having high wear, friction, and corrosion-resistant along with excellent mechanical strength and tribological properties (Guofang et al. 2004). It is estimated that nanoclay loaded UHMWP composite sheets can bear more than 100,000 cycles at 9 N load and linear sliding speed of 0.1 m/s that is advantageous because of its very low friction, wear, cost, and ease in fabrication (Azam and Samad 2018).

6 Challenges and Future Aspect of the Tribological Study of Biopolymers and Biopolymer Composites

Biopolymers and biopolymer composites have proved to be a great success in versatile fields as biomedical implants, food processing material, textile material, and packaging material. In this regard, biopolymer tribology has become very significant in order to enhance mechanical performance as well as the service life of biopolymer composed product. Tribological studies become very crucial in the biomedical field to find suitable arthroplasty materials to minimize wear. The wear minimization of biopolymers is very crucial to extend the longevity of implants. In this way, a great deal of hope for the improvement of bioimplant exists by mitigation of challenges in tribological studies. The selection of appropriate lubricant is one major area of concern for biopolymer wear testing. In this direction, a bovine serum is recognized as a suitable lubricant; however, its properties differ from synovial fluid in specific aspects (Joyce 2009). Besides UHMWPE, a relatively soft polymer polyurethane offer enhanced elastohydrodynamic lubrication as present in natural synovial joints (Dowson et al. 1991). Biopolymers employed in the biomedical application must possess a number of characteristics listed as zero or neutral inflammatory response, suitable mechanical properties according to the application, non-toxic biodegradation of end products for easy resorption or excretion, and suitable permeability and easy processability of design implant. Many parameters like material chemistry, hydrophobicity, molecular chemistry, surface charge, adsorption, degradation, erosion mechanism, etc. play a significant role to execute these characteristics. So, here, a key challenge exists to screen out suitable biomaterial from a cluster of the huge amount of biopolymers for further synthesis or composite formation to best find material as per desired application (Ulery et al. 2011). The future perspective of biopolymer tribology in the orthopedic area is concerned with the search for lubricant which is safer and economic than bovine serum for biopolymer wear testing. Further, optimum protein content determination and finding suitable additives are other challenging aspects (Joyce 2009). Extensive study is still required for better applicability of ‘High-performance polymer’ such as polyaramids (Kevlar), polyetheretherketone (PEEK), and polybenzimidazole (PBI) holding a higher level of physical properties, higher melting points, and high level of degradation resistance (Friedrich 2018). As a novel research area, ‘Green tribology’ may cover all tribological problems concerned with emerging technologies for surface characterization and better regulation of friction and wear to meet energy balance as well as environmental aspects of lubrication and surface modification techniques (Michale and Bhushan 2012). The future challenges of biopolymer application in medicine involve advanced drug loading, better encapsulation, and more controlled drug release. Better adsorption of biopolymer depends upon chemical and mechanical modification. Recent research studies explored that more flexible and durable liposome coated biopolymer may be considered as an ideal ingredient in food and therapeutic supplement. In this direction, the tribological study of biopolymer will aid new ideas to design newer materials, upgraded from the existing ones for versatile biological applications (Dutta et al. 2020).

7 Conclusion

Tribology may be considered as an umbrella to cover a close relationship between scientists, engineers, and clinicians to address the problems concerned with the interdisciplinary area of mechanical surface, materials, biology, physics, chemistry, and engineering, etc. The tribological evaluation provides a new dimension for the research and development of biopolymers in versatile industrially significant fields as biomedical, food, packaging, pharmaceutical, and textile, etc. Additionally, tribological studies show suitability to incorporate various biopolymers for controlled drug release with enhanced performance and better efficiency in drug or nutraceutical delivery. In the biomedical field, tribology is gaining significant importance by employing biopolymers such as UHMWPE, VE-UHMWPE, and polyurethane, etc., as best arthroplasty materials with minimum wear. The future research in biomedical engineering is concerned with biopolymer implant designing not only with the engineering aspect but also viewing the real biological system to obtain a desired biological response with minimization of implant failure. Further, advanced research is needed to search for novel biopolymers as the best arthroplasty materials to meet tribological aspects along with biological phenomenon for longer and qualitative patient life. Undoubtedly, the advancement in methods and techniques of tribology, as well as biotribology, will provide sustainability and reliability of biopolymer-based products for the overall wellbeing of human life with economic growth.

References

Agyei A, Joyce M, Lubica D et al (2019) Sensory, tribological, and rheological profiling of " clean label " starch – lipid complexes as fat replacers. Starch. https://doi.org/10.1002/star.201800340

Luqman AI, Halim A, Kamari A et al (2018) Chitosan, gelatin and methylcellulose films incorporated with tannic acid for food packaging. Int J Biol Macromol. https://doi.org/10.1016/j.ijbiomac.2018.08.169.

Amjadi S, Emaminia S, Nazari M et al (2019) Application of reinforced ZnO nanoparticle-incorporated gelatin bionanocomposite film with chitosan nanofiber for packaging of chicken fillet and cheese as food models. Food Bioproc Tech. https://doi.org/10.1007/s11947-019-02286-y

Anvari M, Tabars M, Melito HSJ (2018) Large amplitude oscillatory shear behavior and tribological properties of gum extracted from Alyssum homolocarpum seed. Food Hydrocoll. https://doi.org/10.1016/j.foodhyd.2017.11.008

Anwunobi AP, Emeje MO (2011) Recent applications of natural polymers in nanodrug delivery nanomedicine & nanotechnology. J Nanomed Nanotechnol. https://doi.org/10.4172/2157-7439.S4-002

Arvanitoyannisa I, Biliaderis CG, Ogawab H et al (1998) Biodegradable films made from low-density polyethylene (LDPE), rice starch and potato starch for food packaging applications : part 1. Carbohydr Polym. https://doi.org/10.1016/S0144-8617(98)00016-2.

Axen N, Hogmark S, Jacobson S (2001) Friction and wear measurement techniques. Modern tribology handbook 1. CRC Press LLC

Azam MU, Samad MA (2018) A novel organoclay reinforced UHMWPE nanocomposite coating for tribological applications. Prog Org Coat. https://doi.org/10.1016/j.porgcoat.2018.01.028

Bartel DL, Burstein AH, Toda MD et al (2016) The effect of conformity and plastic thickness on contact stresses in metal-backed plastic. J Biomed Eng

Bernardin JE (1978) Effect of shear on the nematic mesophase of the wheat storage protein A-gliadin. J Texture Stud. https://doi.org/10.1111/j.1745-4603.1978.tb01204.x

Bongaerts JHH, Rossetti D, Stokes J (2007) The lubricating properties of human whole saliva. Tribol Lett. https://doi.org/10.1007/s11249-007-9232-y

Braud A, Boucher Y (2019) Intra - oral trigeminal - mediated sensations influencing taste perception: a systematic review. J Oral Rehabil. https://doi.org/10.1111/joor.12889

Buggy M (2016) Polymeric materials. In: Reference module in materials science and materials engineering. https://doi.org/10.1016/B978-0-12-803581-8.04104-7.

Chang L, Zhang Z, Ye L et al (2007) Tribological properties of high temperature resistant polymer composites with fine particles. Tribol Int. https://doi.org/10.1016/j.triboint.2006.12.002

eld MD (1969) Med Biological Eng 7(31)

Chen J, Stokes JR (2012) Rheology and tribology: two distinctive regimes of food texture sensation. Trends Food Sci Tech. https://doi.org/10.1016/j.tifs.2011.11.006

Critchley L (2018) The fundamentals of tribology. Azom Mterials 1–4. https://www.azom.com/article.aspx?ArticleID=16441.

Cuffari B (2019) The role of tribology in sustainability 1–3. https://doi.org/10.1098/rsta.2010.0200saved.

Dailin DJ, Low LZMI, Malek RA et al (2019) Pullulan, a biopolymer with potential applications in pharmaceutical and cosmeceutical: a review. Biosci Res 16(3):2604–2616

Davidenko N, Cameron R and Best S (2014) Natural biopolymers for biomedical applications. Int J Biol Macromol. https://doi.org/10.1016/j.ijbiomac.2020.03.120.

Deb PK, Kokaz SF, Abed SN et al. (2019) Pharmaceutical and biomedical applications of polymers. In: Basic fundamentals of drug delivery. https://doi.org/10.1016/B978-0-12-817909-3.00006-6.

Demirci M, Lee C (2020) Oleogels for food applications. In: Biopolymer-based formulations. https://doi.org/10.1016/B978-0-12-816897-4.00031-X.

Dowson D, Fisher J, Jin ZM et al (1991) Design considerations for cushion form bearings in artificial hip joints. Proc Inst Mech Eng H 205(2):59–68

Dutta S, Moses JA, Anandharamakrishnan C (2020) Biomedical and food applications of biopolymer-based liposome. In: Biopolymer-based formulations: biomedical and food applications. https://doi.org/10.1016/B978-0-12-816897-4.00008-4.

Fairbank J (1948) Knee Joint changes after meniscectomy. J Bone Joint Surg Br. https://doi.org/10.1302/0301-620X.30B4.664

Farrés IF, Moakes RJA, Norton IT (2014) Food hydrocoll. In: Designing biopolymer fluid gels : a microstructural approach. Food Hydrocoll. https://doi.org/10.1016/j.foodhyd.2014.03.014

Feng C, Zhang D, Grecov D et al (2020) Effect of rheological properties of friction-enhancing greases on the friction between friction lining and wire rope. Tribol Int. https://doi.org/10.1016/j.triboint.2019.106143

Foegeding EA, Stieger M, Velde FVD (2016) Moving from molecules, to structure, to texture perception. Food Hydrocoll. https://doi.org/10.1016/j.foodhyd.2016.11.009

Friedrich K (2018) Polymer composites for tribological applications. Adv Ind Eng Polym Res. https://doi.org/10.1016/j.aiepr.2018.05.001

Fuhrmann PL, Aguayo MM, Jansen B et al (2019) Oral processing linear movement tribological set-up linear movement normal force normal force tongue / palate food / bolus food composition surface properties saliva content (in bolus) particle size food/bolus. Food Hydrocoll. https://doi.org/10.1016/j.foodhyd.2019.105441

Ge S, Liu Q, Li M et al (2018) Enhanced mechanical properties and gelling ability of gelatin hydrogels reinforced with chitin whiskers. Food Hydrocoll. https://doi.org/10.1016/j.foodhyd.2017.09.023

Gil-chávez J (2019) Application of novel and technical lignins in food and pharmaceutical industries: structure-function relationship and current challenges. Biomass Convers Biorefin. https://doi.org/10.1007/s13399-019-00458-6.

Gregorova A, Saha N, Kitano T et al (2014) Hydrothermal effect and mechanical stress properties of carboxymethylcellulose based hydrogel food packaging. Carbohydr Polym. https://doi.org/10.1016/j.carbpol.2014.10.009

Guofang G, Huayong Y, Xin F (2004) Tribological properties of kaolin filled UHMWPE composites in unlubricated sliding. Wear. https://doi.org/10.1016/S0043-1648(03)00394-6

Gupta S, Riyad MF, Ji Y (2016) Synthesis and tribological behavior of ultra high molecular weight polyethylene (UHMWPE)-lignin composites surojit. Lubricants 4(31):1–10. https://doi.org/10.3390/lubricants4030031

Hansen DC (2008) Metal corrosion in the human body: the ultimate bio-corrosion scenario. Electrochem Soc Interfac 17(2):31–34

Helkimo EVA, Carlsson GE, Helkimo M (1978) Chewing efficiency and state of dentition. Acta Odontol Scand 36(1):33–41

Higuchi F, Inoue A, Semlitsch M (1997) Metal-on-metal CoCrMo McKee-Farrar total hip arthroplasty: characteristics from a long-term follow-up study. Arch Orthop Trauma Surg. https://doi.org/10.1007/BF00426058

Ingham E, Fisher J (2000) Biological reactions to wear debris in total joint replacement. Proc Inst Mech Eng H 214(1):21–37

Isschers ROWV (2008) Lubrication properties of protein aggregate dispersions in a soft contact. J Agric Food Chem. https://doi.org/10.1021/jf0720988

Jacob J, Haponiuk T, Thomas S et al (2018) Biopolymer based nanomaterials in drug delivery systems : a review. Mater Today Chem 9:43–55. https://doi.org/10.1016/j.mtchem.2018.05.002

Jha SK, Singh HR, Prakash P (2017) Dietary fiber and human health : an introduction. Dietary fiber for the prevention of cardiovascular disease. https://doi.org/10.1016/B978-0-12-805130-6/00001-X.

Jimenez LN, Narváez CDVM, Sharma V (2020) Capillary breakup and extensional rheology response of food thickener cellulose gum (NaCMC) in salt-free and excess salt solutions Capillary breakup and extensional rheology response of food thickener cellulose gum (NaCMC) in salt-free and excess salt. Phys Fluids 10(1063/1):5128254

Jin Z, Fisher J (1966) Tribology in joint replacement. Joint replacement technology. https://doi.org/10.1533/9781845694807.1.31

Jin ZM, Heng SM, Ng HW et al (1999) An axisymmetric contact model of ultra high molecular weight polyethylene cups against metallic femoral heads for artificial hip joint replacements. Proc Inst Mech Eng Part H: J Eng Med. https://doi.org/10.1243/0954411991535158.

Joyce T (2009) Biopolymer tribology. In: Polymer tribology. https://doi.org/10.1142/9781848162044_0007

Kaushik K, Sharma RB, Agarwal S et al (2016) Natural polymers and their applications. Int J Pharm Sci Rev Res 37(2):30–36

Krop EM, Hetherington MM, Holmes M et al (2019) On relating rheology and oral tribology to sensory properties in hydrogels. Food Hydrocoll 88:101–113. https://doi.org/10.1016/j.foodhyd.2018.09.040

Kumari B, Khanal S, Bhandari B et al (2017) Effect of sodium alginate addition on physical properties of rennet milk gels. Food Biophys 12:141–150. https://doi.org/10.1007/s11483-017-9470-y

Kumari B, Khanal S, Bhandari B et al (2018) Modifying textural and microstructural properties of low fat Cheddar cheese using sodium alginate. Food Hydrocoll. https://doi.org/10.1016/j.foodhyd.2018.03.015

Kumari B, Khanal S, Bhandari B et al (2019) Simulated oral processing, in vitro digestibility and sensory perception of low fat Cheddar cheese containing sodium alginate. J Food Eng. https://doi.org/10.1016/j.jfoodeng.2019.109749

Kumar S, Shukla A, Pratim P et al (2018a) Biodegradable hybrid nanocomposites of chitosan / gelatin and silver nanoparticles for active food packaging applications. Food Packag Shelf Life. https://doi.org/10.1016/j.fpsl.2018.03.008

Kumar SSD, Rajendran NK, Houreld NN et al (2018b) Recent advances on silver nanoparticle and biopolymer based biomaterials for wound healing applications. Int J Biol Macromol https://doi.org/10.1016/j.ijbiomac.2018.04.003

Laiho S, Williams RPW, Poelman A et al (2017) Effect of whey protein phase volume on the tribology, rheology and sensory properties of fat-free stirred yoghurts. Food Hydrocoll. https://doi.org/10.1016/j.foodhyd.2017.01.017

Laine C, Harlin A, Hartman J et al (2013) Hydroxyalkylated xylans - their synthesis and application in coatings for packaging and paper. Ind Crops Prod. https://doi.org/10.1016/j.indcrop.2012.08.033

Lee KY, Mooney ZJ (2012) Alginate : Properties and biomedical applications. Prog Polym Sci 37(1):106–126. https://doi.org/10.1016/j.progpolymsci.2011.06.003

Liang L, Luo Y (2020) Technology Casein and pectin: structures, interactions, and applications. Trends Food Sci Tech. https://doi.org/10.1016/j.tifs.2020.01.027

Luigi L (2018) Frictional properties of cartilage loaded against cartilage by using a pin on disc tribometer. AIP Conf Proc. https://doi.org/10.1063/1.5045873

Mazari A, Heath MR, Prinz JF (2007) Contribution of the cheeks to the intraoral manipulation of food. Dysphagia. https://doi.org/10.1007/s00455-006-9062-3

McClements DJ, Decker EA, Park Y (2009) Controlling lipid bioavailability through physicochemical and structural approaches. Crit Rev Food Sci Nutr 49(1):48–67. https://doi.org/10.1080/10408390701764245

Meinel L, Kaplan DL (2012) Silk constructs for delivery of musculoskeletal therapeutics. Adv Drug Deliv Rev. https://doi.org/10.1016/j.addr.2012.03.016

Michale N, Bhushan B (2012) In: Nosonovsky M, Bhushan B (eds) Green tribology, its history, challenges, and perspectives, 1st edn. Springer, Berlin. https://doi.org/10.1007/978-3-642-23681-5.

Mills JS, White R (2012) The organic chemistry of museum objects. Elsevier Science. https://doi.org/10.1016/B978-0-408-11810-1.50006-4

Mohanty JR, Das SN, Das HC (2014) Effect of fiber content on abrasive wear behavior of date palm leaf reinforced polyvinyl pyrrolidone composite. ISRN Tribology. https://doi.org/10.1155/2014/453924

Morin N, Eric C, Giangiacomo L et al (2019) Applications of chitosan in food, pharmaceuticals, medicine, cosmetics, agriculture, textiles, pulp and paper, biotechnology, and environmental chemistry. Environ Chem Lett. https://doi.org/10.1007/s10311-019-00904-x.

Mow VC, Ateshian GA, Spilker RL (1993) Biomechanics of diarthrodial joints: a review of twenty years of progress. J Biomech Eng 115(4b):460–467

Mudgil D (2017) The interaction between insoluble and soluble fiber. Dietary fiber for the prevention of cardiovascular disease. https://doi.org/10.1016/B978-0-12-805130-6/00003-3.

Muller J, González-Martínez C, Chiralt A (2017) Combination of poly(lactic) acid and starch for biodegradable food packaging. Materials. https://doi.org/10.3390/ma10080952

Musso YS, Salgado PR, Mauri AN (2017) Smart edible films based on gelatin and curcumin. Food Hydrocoll. https://doi.org/10.1016/j.foodhyd.2016.11.007

Nguyen PTM, Kravchuk O, Bhandari B et al (2017) Effect of different hydrocolloids on texture, rheology, tribology and sensory perception of texture and mouthfeel of low-fat pot-set yoghurt. Food Hydrocoll. https://doi.org/10.1016/j.foodhyd.2017.05.035

Ningtyas DW, Bhandari B, Bansal N et al (2017) A tribological analysis of cream cheeses manufactured with different fat content. Int Dairy J https://doi.org/10.1016/j.idairyj.2017.06.005.

Numata K, Kaplan DL (2011) Biologically derived scaffolds. In: Advanced wound repair therapies. https://doi.org/10.1533/9780857093301.4.524.

Olsson H, Henricsson V, Axell T et al (1991) A new device for measuring oral mucosal surface friction — reference values. Eur J Oral Sci. https://doi.org/10.1111/j.1600-0722.1991.tb01036.x

Pang Z, Xu R, Zhu Y et al (2020) Tribo-rheology and kinetics of soymilk gelation with different types of milk proteins. Food Chem. https://doi.org/10.1016/j.foodchem.2019.125961

Plank GR, Ii DME, Muratoglu OK et al (2006) Contact stress assessment of conventional and highly crosslinked ultra high molecular weight polyethylene acetabular liners with finite element analysis and pressure sensitive film. J Biomed Mater Res B. https://doi.org/10.1002/jbm.b.30560

Prakash S (2017) From rheology to tribology : applications of tribology in studying food oral processing and texture perception. Adv Food Rheol Its Appl. https://doi.org/10.1016/B978-0-08-100431-9/00004-8

Prakash S, Tan DDY, Chen J (2013) Applications of tribology in studying food oral processing and texture perception. Food Res Int. https://doi.org/10.1016/j.foodres.2013.10.010

Prinz JF (2004) Abrasives in foods and their effect on intra-oral processing: a two-colour chewing gum study. J Oral Rehabil. https://doi.org/10.1111/j.1365-2842.2004.01328.x

Prinz JF, Wijk RADe, Huntjens L (2007) Load dependency of the coefficient of friction of oral mucosa. Food Hydrocoll. https://doi.org/10.1016/j.foodhyd.2006.05.005

Prinz JF, Wijk RADe, Weenen H (2005) The role of fats in friction and lubrication. In Fereidoon Shahidi HW (ed) Food lipids. ACS Publication:95–103. doi: https://doi.org/10.1021/bk-2005-0920.ch008.

Qin Y, Jiang J, Zhao L et al (2018) Applications of alginate as a functional food ingredient. Biopolymers for food design. https://doi.org/10.1016/B978-0-12-811449-0/00013-X

Qin Y, Zhang G, Chen H (2020) The applications of alginate in functional food products. J Nutri Food Sci 3(13):1–9

Qureshi D, Nayak SK, Anis A et al (2020) Introduction of biopolymers: food and biomedical applications. In: Biopolymer-based formulations. https://doi.org/10.1016/B978-0-12-816897-4.00001-1.

Ranadheera CS, Liyanaarachchi WS, Chandrapala J et al (2016) Utilizing unique properties of caseins and the casein micelle for delivery of sensitive food ingredients and bioactives. Trends Food Sci Tech. https://doi.org/10.1016/j.tifs.2016.10.005

Ranadheera CS, Liyanaarachchi WS, Dissanayake M et al (2019) Impact of shear and pH on properties of casein micelles in milk protein concentrate. Lwt- Food Sci Technol https://doi.org/10.1016/j.lwt.2019.03.090

Rawat S, Saxena J (2019) Fiber-reinforced polymer: applications in biomedical engineering. In: Grumezescu VG, Alexandru M (eds) Materials for biomedical engineering; bioactive materials, properties, and applications, pp:393–430

Rebelo R, Fernandes M, Fangueiro R (2017) Biopolymers in medical implants: a brief review. Proc Eng. https://doi.org/10.1016/j.proeng.2017.07.034

Ridzwan MIZ, Shuib S, Hassan AY et al (2007) Problem of stress shielding and improvement to the hip implant designs: a review. J Med Sci. https://doi.org/10.3923/jms.2007.460.467

Rodrigues SA, Selway N, Morgenstern MP et al (2016) Lubrication of chocolate during oral processing. Food Funct. https://doi.org/10.1039/c6fo00950f

Rowland R, Ponticorvo A, Jarrin LA et al (2019) Monitoring kidney optical properties during cold storage preservation with spatial frequency domain imaging. J Biomed Opt. https://doi.org/10.1117/1.JBO.24.11.116003

Ruan Q, Yang X, Zeng L et al (2019) Physical and tribological properties of high internal phase emulsions based on citrus fibers and corn peptides. Food Hydrocoll. https://doi.org/10.1016/j.foodhyd.2019.04.014

Sagiri SS, Rao KJ (2020) Natural and bioderived molecular gelator-based oleogels and their applications. In: Biopolymer-based formulations. https://doi.org/10.1016/B978-0-12-816897-4.00022-9

Sahoo P, Das SK, Davim JP (2019) Tribology of materials for biomedical applications. In: Mechanical behavior of biomaterials. https://doi.org/10.1016/B978-0-08-102174-3.00001-2

Said MI (2020) Role and function of gelatin in the development of the food and non-food industry: a review In: The 2nd international conference of animal science & technology, p 492. https://doi.org/10.1088/1755-1315/492/1/012086

Seighalani FZB, Joyner H, Schreyer L (2021) Identification of factors affecting wear behavior of semi-hard cheeses. J Food Eng. https://doi.org/10.1016/j.jfoodeng.2020.110348

Shafi WK, Raina A, Haq UMI (2018) Friction and wear characteristics of vegetable oils using nanoparticles for sustainable lubrication. Tribol Mater Surf Interfaces. https://doi.org/10.1080/17515831.2018.1435343

Shit SC, Shah PM (2014) Edible polymers: challenges and opportunities. J Polym. https://doi.org/10.1155/2014/427259

Shi SC, Wu JY, Huang TF et al (2016) Improving the tribological performance of biopolymer coating with MoS 2 additive. Surf Coat Tech. https://doi.org/10.1016/j.surfcoat.2016.03.055

Shi SC, Chen TH, Mandal PK (2020) Enhancing the mechanical and tribological properties of cellulose nanocomposites with aluminum nanoadditives. Polymers. https://doi.org/10.3390/polym12061246

Souza AC de, Ditchfield C, Tadini CC (2009) Biodegradable Films Based on Biopolymers for Food Industries. In: Innovation in food engineering: new techniques and products. https://doi.org/10.1201/9781420086072-c17

Stee MV, Hoog ED, Velde FVD (2017) Oral parameters affecting ex-vivo tribology. Biotribology. https://doi.org/10.1016/j.biotri.2017.05.001

Stokes JR, Boehm MW, Baier SK (2013) Oral processing , texture and mouthfeel : From rheology to tribology and beyond. Curr Opin Colloid Interface Sci. https://doi.org/10.1016/j.cocis.2013.04.010.

Suriyatem R, Auras RA, Rachtanapun C et al (2018) Biodegradable rice starch/carboxymethyl chitosan films with added propolis extract for potential use as active food packaging. Polym. https://doi.org/10.3390/polym10090954

Tamai H, Igaki K, Kyo E et al (2000) Initial and 6-month results of biodegradable poly-l-lactic acid coronary stents in humans. Circulation. https://doi.org/10.1161/01.CIR.102.4.399

Tang S, Wang Z, Li P et al (2018) Degradable and photocatalytic antibacterial Au-TiO2 / sodium alginate nanocomposite films for active food packaging. Nanomaterials. https://doi.org/10.3390/nano8110930

Tan J, Joyner HS (2019) Characterizing and modeling wear-recovery behaviors of acid-induced casein hydrogels. Wear. https://doi.org/10.1016/j.wear.2019.02.003

Tan J, Silva TLT, Martini S et al (2019) Numerical modeling of wear behavior of solid fats. J Food Eng. https://doi.org/10.1016/j.jfoodeng.2019.04.023

Taylor BL, Mills TB (2020) Surface texture modifications for oral processing applications Brogan. Biotribology. https://doi.org/10.1016/j.biotri.2020.100132

Ulery BD, Nair LS, Laurencin CT (2011) Biomedical applications of biodegradable polymers. J Polym Sci B Polym Phys. https://doi.org/10.1002/polb.22259

Vardhanabhuti B, Cox PW, Norton IT et al (2011) Lubricating properties of human whole saliva as affected by b-lactoglobulin. Food Hydrocoll. https://doi.org/10.1016/j.foodhyd.2011.02.021

Versino F, Lopez OV, Garcia MA et al (2016) Starch-based films and food coatings : an overview. Starch – Stärke. https://doi.org/10.1002/star.201600095

Wijk RA, Prinz JF (2005) The role of friction in perceived oral texture. Food Qual Prefer. https://doi.org/10.1016/j.foodqual.2004.03.002

Wittaya T (2008) Edible films and coatings: characteristics and properties. Int Food Res J 15(May):1–13

Yang W, Fortunati E, Dominici F *et al.* (2016) Synergic effect of cellulose and lignin nanostructures in PLA based systems for food antibacterial packaging. Eur Polym J https://doi.org/10.1016/j.eurpolymj.2016.04.003

Yousif BF, Tayeb NSM (2007) The effect of Oil palm fibers as reinforcement on tribological performance of polyster composite. Surf Rev Lett 14(6):1095–1102

Zahiri CA, Schmalzried TP, Ebramzadeh E et al (1999) Lessons learned from loosening of the McKee-Farrar metal-on-metal total hip replacement. J Arthroplasty. https://doi.org/10.1016/S0883-5403(99)90059-1

Zhang Q, Mochalin VN, Neitzel I et al (2011) Biomaterials fluorescent PLLA-nanodiamond composites for bone tissue engineering. Biomaterials. https://doi.org/10.1016/j.biomaterials.2010.08.090

Zhang B, Selway N, Shelat KJ et al (2017) Tribology of swollen starch granule suspensions from maize and potato. Carbohydr Polym. https://doi.org/10.1016/j.carbpol.2016.08.064

Zhao J, Wei F, Xu W et al (2020) Enhanced antibacterial performance of gelatin/chitosan film containing capsaicin loaded MOFs for food packaging. Appl Surf Sci. https://doi.org/10.1016/j.apsusc.2020.145418

Zhou ZR, Jin ZM (2015) Biotribology: recent progresses and future perspectives. Biosurf. Biotribol. https://doi.org/10.1016/j.bsbt.2015.03.001

Zhu Y, Bhandari B, Prakash S (2019) Tribo-rheology characteristics and microstructure of a protein solution with varying casein to whey protein ratios and addition of hydrocolloids. Food Hydrocoll. https://doi.org/10.1016/j.foodhyd.2018.12.005

Zhu Y, Bhandari B, Prakash S (2020) Relating the tribo-rheological properties of chocolate flavoured milk to temporal aspects of texture. Int Dairy J. https://doi.org/10.1016/j.idairyj.2020.104794

Tribological Properties of 3D Printed Polymer Composites-Based Friction Materials

Oluwatoyin Joseph Gbadeyan, T. P. Mohan, and K. Kanny

Abstract This chapter reviews the recent progress in tribological properties of 3D printed polymer nanocomposites and their applications. The printing of thermoplastic composite infused with different sizes of particles was reviewed. The processing of creating a 3D printed nanoparticle reinforced nanocomposite and their structure-property relations were discussed—valid information on several abrasion apparatus for tribological investigation was also provided. The influence of loading particles on the wear resistance and frictional behaviors of 3D printed nanoparticle reinforced nanocomposites were review. Similarly, the effect of applied load, speed (RPM), and sliding distance on the wear resistance and frictional behaviors of pure thermoplastic, including particle-filled composite, were also evaluated. The tribological properties concerning wear and friction were evaluated. The current application of 3D printed nanoparticle reinforced nanocomposites, and their revolutionary scope was also discussed.

1 Introduction

Over the decades, the field of tribology, including the investigation of friction, lubrication, and wear of materials, gained growing attention from the methodical, practical, and applied perspectives. It has become apparent that the operations of countless mechanical systems hinge on friction and wear values. Besides, the dissipation of heat energy and loss of materials resulting from high friction and wear is significant. Research in wear and friction is mostly carried out on surfaces rubbing against each other in relative motions, such as cams, gears, or rollers (Pandurangan 2018; Azam and Samad 2018). Significantly, the resistance to wear and steady friction coefficient of tribological product solely be contingent on the material selection and processing techniques used for producing the tribological product. It is well known that tribology

O. J. Gbadeyan · T. P. Mohan (✉) · K. Kanny
Composite Research Group, Department of Mechanical Engineering, Durban University of Technology, Durban 4001, South Africa
e-mail: MohanP@dut.ac.za

H. Jena et al. (eds.), *Tribology of Polymer and Polymer Composites for Industry 4.0*,
Composites Science and Technology, https://doi.org/10.1007/978-981-16-3903-6_9

deals with wear rate, friction, and lubrication of fixed contact of two surfaces interacting in a motion. The frictional output, such as energy dissipation, frictional heat, and abrasion, is inevitable in this process. Friction is related to the level of energy dissipated when contacting surfaces move over each other. The surfaces may either roll or slide or a combination of both and generate frictional heat. Furthermore, wear surely occurs on the surfaces due to the damage encouraged by the frictional work. Mechanical disruption may firstly occur, nevertheless ultimately, the entire frictional work often appears as heat (Hwang et al. 2010).

1.1 Material Selection for Friction Material

The improvement in technology relating to material development for tribological product application results in a rigorous investigation of several materials (Gbadeyan et al. 2020; Hanon et al. 2020). This investigation shows that metallic, semi-metallic, and non-metallic are classes of materials used for friction materials development. (Peng et al. 2017; Martinez and Echeberria 2016; Malachova et al. 2016; Stadler et al. 2012). The strength, stiffness, and resistance to wear and tiers of the above-mentioned material make them commonly used for friction material applications (Ajayi 2002; Thiyagarajan et al. 2016). However, studies have shown that one material cannot offer all the required properties for the tribological product. Therefore, combining two materials known as “Composite” has become a unique and growing class of materials increasingly used for such tribological applications (Gbadeyan et al. 2017). Due to complex factors such as frictional heat, thermally-induced degradation (chemical degradation) that occurs when two surfaces interacting in a motion, composite systems should have a workable structure with improved resistance to wear and good frictional heat dissipation capability. Inadequate mechanical energy dissipated in the sub-interfaces causes additional sources of weakness and has extra projections for matrix damage and wear. The composite entity does, however, provide mechanical rigidity and also attractions of means of dissipating the frictional work. In this technology advanced world where constancy is the main factor for designing and developing material for wear integrity (Hwang et al. 2010; Gbadeyan et al. 2017). Polymers and Polymer-based composites are the materials of choice for certain engineering applications (Figs. 1, 2 and 3).

1.2 Polymer or Plastic Used for the Tribological Product Application

Polymer or plastic is one of the most important additives used to sustain the structural completeness of friction material when subjected to mechanical and thermal stress. It binds pad components and also prevents from breaking apart. The selection of

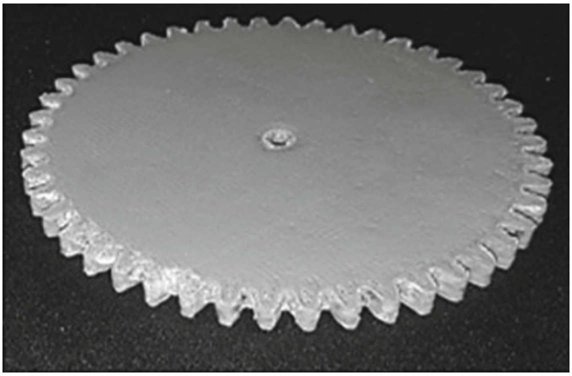

Fig. 1 3D printed gear material produced from composite materials

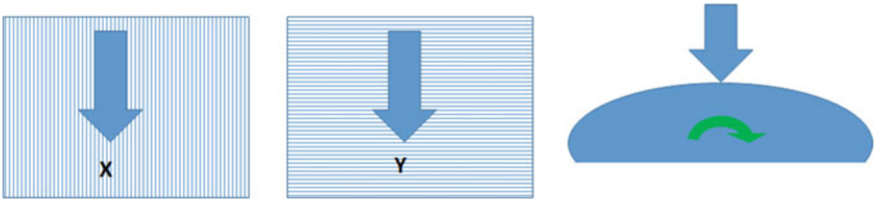

Fig. 2 Schematic diagram of the printing direction of X, Y and loading direction samples

Fig. 3 Schematic image of the Bocle test rig modified to block the ring

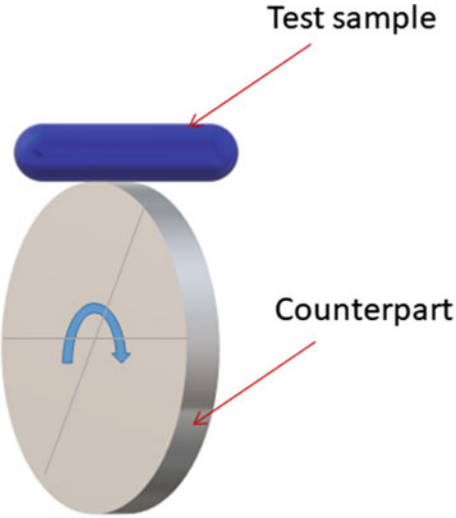

polymer or plastic referred to as binder for the tribological product application is very critical because such binder must maintain structurally intact at all times, or else pad composition disintegrates when excessive friction heat is generated (Imaekhai and Lawrence 2013). Typical binder materials such as linseed oil, phenolic resins and modified resin, cresol, boron, epoxy, PVC, and rubber can modify pad bonding characteristics and temperature resistance at an extreme temperature (Blau 2001). However, most of the abovementioned polymeric materials are not recyclable and contain toxic elements harmful to humans. Attention has been diverted to recyclable and environmentally friendly plastics such as ABS, polycarbonate, and PLA (Miron et al. 2017).

There are two phases, which are primary and secondary are in polymer composite structure, these include. The secondary phase often migrates to the primary matrix phase, which appears at the sliding contact. Generally, this subordinate phase separates at the sliding interface to provide a self-regenerating known as the "lubricant layer." The moveable additives migrate, and immovable ones are produced due to the wear of the host matrix. The composite whose matrix is nonself-lubricating generates transformed layers that make it becomes self-lubricating. Most polymer composite compositions intended for tribological applications often arrived at empirically—the major drawback of polymetric materials poor thermal stability at extreme conditions. Various attempts have been made to obtain enhanced properties of polymeric material, in which the incorporation of reinforcement materials such as fiber and nanoparticles was found to be viable ways of improvement (Nie et al. 2015; Sebastian et al. 2013; Shen et al. 2009; Kim et al. 2014). Given this, it is imperative to discuss some fillers and their function in controlling wear rate and friction coefficient.

1.3 Fillers

Fillers or friction modifies used as internal lubricate to control friction or react with oxygen to help control interfacial firms or wear debris. Similarly, lubricant often gathers the friction firm to form a layer on the counterpart. It also performs a critical role in controlling the friction coefficient of existence between the material testing samples and counterpart, which eventually reduces abrasion, vibrations, and enhancing performance (Blau 2001; Jang et al. 1477). This material in powder or flake form, natural or synthetic modify tribological properties, stopping distance, and noise propensity of friction material (Martinez and Echeberria 2016). The function of solid lubricants cannot be underemphasized as friction material performance strongly depends on the combination of several solid lubricants used to plays a complementary role that prevents malfunctioning resulting from the decomposition of solid lubricant at elevated temperature (Cho et al. 2014; Jang and Kim 2000; Kim et al. 2007; Deshmukh et al. 1295; Han et al. 2895). This unpredicted friction behavior of friction modifies decomposition affects friction film maintenance on the contact zone (Ertan and Yavuz 2011).

Similarly, the addition of more than two friction modifiers reduces reducing fade, wear, creep groans and stabilizes friction (Jang et al. 1477; Ertan and Yavuz 2011; Cho et al. 2005). A synergistic effect form by using more than two internal lubricants may perform multiple functions in the materials. For instance, a study compared the coefficient of friction and wear resistance of friction materials loaded with two divergent friction modifiers. The friction material A contains hybrid loading of Sb_2S_3 and graphite, and B was combined with Sb_2S_3 and MoS_2. The synergistic functions formed by Sb_2S_3 and graphite in friction material A offered improve fade resistance and friction stability, which was ascribed to the existence of Sb_2O_3 on the sliding interface, which plays as high-temperature solid lubricants. In this case, Sb_2O_3 performs as an internal lubricant and prevents frictional heat, resulting in fade resistance (Cho et al. 2005). It is essential to consider the effect of friction modifiers debris produced on the atmosphere when functioning as Sb_2O_3 is a potentially carcinogenic substance, which may cause airborne disease. Table 2 provides the advantages and disadvantages of the most used solid lubricants in the friction material.

Although filler infused on layer printed using a 3D printer to manufacturer material for tribological product application, the investigation on wear rate and friction of this material is mostly evaluated on layer orientations and the loading effect of reinforcement (Hanon et al. 2020). In most cases, the effect of fillers on the wear rate is more pronounced than the coefficient of friction, as polymetric material often serves as an internal lubricant. To date, very limited consideration has been given to investigating the influence of filler loading on the tribological behaviors of 3D-printed objects. The effect of materials such as bronze, graphite, and nanoclay has been investigated so far. However, the loading of these fillers reduces wear rate but has no significant effect on the coefficient of friction of 3D-printed objects.

The incorporation of fillers into the polymeric material are done using different techniques. This process could be achieved using a traditional method such as infusion, resin casting methods, and forming. These methods have been used to developed semi-metallic, metallic, and non-metallic friction material. However, these traditional techniques require costly equipment and take much time to develop complex material like brake pads and gear. Thanks to an improvement in technology that brought about 3D printing technologies, which is cheaper and less time consuming for production.

2 3D Printing or Additives Manufacturing Techniques

The huge improvements in 3D printing technologies in recent years allow this technique to compete with other old-style manufacturing methods. Several products have been created using these additives manufacturing processes (Macdonald et al. 2014; Ntie-Kang et al. 2013; Justice et al. 2009; Boetker et al. 2016). This process is used to create material such as plastic or metals by laying down successive material layers until a final product is fully made (Strikwerda and Dehue 2020; Giemza et al. 2018). 3D printing is one of the crucial developing technologies currently used to shape the approach to manufacturing and tomorrow's products and factories (Stadnicki 2017). This technique is one of the most suitable for making simple and multifaceted three-dimensional objects; however, limited plastics such as ABS or PLA are used for this purpose. Plastic was commonly used to create different products due to its availability, recyclability, and mechanical properties.

Besides, the 3D printing procedure has been largely adopted for producing engineering prototypes in past years. This technique is similar to paper printing processes, where filament made from polymeric materials is developed into filament loaded in the cartridge and print as a conventional printer does.

The improvement in 3D printer capacity in recent decades has provided opportunities for printing products from others. Materials such are polyphenyl sulfone (PPSU), Polycaprolactone (PCL), Polycarbonate (PC), Polyetherimide (PEI), and (PVA) polyvinyl acetate have been used to produced parts for different application in pastry, food, and medical industries. The 3D printer was further fortified for printing metallic, composite, and nanocomposite material (Lashgari et al. 2033). This development led to the advent of using a 3D printer to create friction materials. Searching for a combination of material and process parameters suitable for creating a final material suitable friction materials application generates enormous investigation. Several materials are obtained from neat polymetric material created using 3D printing, and the composite or nanocomposite material is created by infusing or incorporating particles of different sizes (Gbadeyan et al. 2020; Stadnicki 2017; Stadnicki 2018; Giemza et al. 2018). These materials are created using different processing parameters and characterized afterward.

3 Tribological Properties of 3D Thermoplastics

3.1 Wear Resistance of ABS Created Using the FDM Printer

The use of acrylonitrile butadiene styrene (ABS) has gained immeasurable consideration for mechanical components such as rack and pinion, mechanical links, gear, and rollers. These materials are created using Fused Deposition Modeling (FDM). The suitability of these materials for a tribological application is determined by investigating the wear and mass loss. These properties are determined as a function of printer layer orientation, sliding distance, applied forces, and time.

3.1.1 The Effect of the Sliding Period and Applied Load on Tribological Properties of ABS

The wear resistance and friction of 100% infill acrylonitrile butadiene styrene printed by Think3D printer were determined. The influence of applied force and sliding time on tribological properties of acrylonitrile butadiene styrene printed using the FDM printer was measured on a pin-on-disc abrasion testing apparatus. A white Think3D (Hyderabad) type of acrylonitrile butadiene styrene filament with 1.13 g/cm^3 Bulk Density, extruder temperature of 210–230 °C was used to create samples.

3.2 Abrasion Test

An in-house pin-on-disc fabricated using traditional procedure was used for investigating wear resistance of FDM printed ABS. The testing equipment consists of an acrylic disc that serves as a specimen holder, a DC motor connected to a disc that serves as the counterpart, and a screw jack used to apply the load, and a load cell was used to measure input load. Samples were placed in the sample holder attached to the acrylic sheet, and the sanding counterpart was positioned in direct contact with the sample at zero position cell load. The load was applied with the aid of the screw jack and cell load. Afterward, the motor was activated, and the shaft rotates with the selected RPM for 5 min. After the sample and counterpart are in fixed contact for 5 min, the motor was switched off, and the sample is removed. The weight of samples was measured before on the electronic balance machine and after the wear test to determine the mass loss. Wear rate and mass loss of five samples were investigated, and each sample was investigated by subjecting the sample to different RPM ranging from 200 to 600. The means values of the sample were reported. Equations 1 and 2 was used to determine the wear rate and mass loss.

$$\text{Percentage wear} = \frac{\text{Mass loss (g)} \times 100}{initialmass(g)} \tag{1}$$

$$\text{Specific wear rate} = \frac{\text{Mass loss (g)}}{\text{density (g/mm3)} \times \text{time (s)} \times \text{rubbing speed and load (m)}}. \tag{2}$$

3.3 Result and Discussion

The relationship of mass loss, wear-resistance, and revolution per minutes of ABS created using the FDM printer. The average value of mass loss and wear resistance at different RPMs of five samples are reported. Average mass loss of 0.0299 gms, 0.0496 gms, and 0.0712 was obtained at 200, 400, and 600 RPM. Similarly, wear percentages of 0.3045, 0.5157, and 0.7635 and wear rate values of 4.2073 X 10^{-8} g/mm, 3.4935 × 10^{-8} g/mm, and 3.3444 × 10^{-8} g/mm was obtained at 200, 400, and 600 RPM. As expected, an increase in mass loss and wear rate percentages of ABS created using an FDM printer with a corsponding increase in rotational speed was observed. This abrasion output may be attributed to the asperities' effectiveness that gradually removes layers of printed ABS, resulting in mass loss. The period at which counterpart and printer ABS samples are in fixed contact results in plastic deformation, consequently encouraging surface erosion that increases wear rate.

A decrease in specific wear rate with a corresponding rotation speed was observed. This abrasion output may be attributed to self-resistance that wear debris created on the counterpart surface, which eventually prevents the effectiveness of the counterpart asperities. The wear debris often prevents direct contact of test samples and counterpart asperities, which eventually reduces specific wear rate.

4 Measurement of Friction Resistance to the Motion of 3D Printed Components for Sliding Direction

The effect of the type of material and printed structure on the resistance fictional motion of a 3D printed component is presented in Fig. 4. A dry sliding test was conducted on available thermoplastic polymer created in FMD printing technology to evaluate sliding properties. This tribological investigation was carried out on a Bocle test rig modified to 'block on ring' shown in Fig. 3. The Bocle test rig with friction couple was calibrated for measuring friction resistance to motion samples. The dry abrasion investigation was conducted at ambient humility of 30-40% and an ambient temperature of 25 ± 1°C. A fixed sliding velocity of 0,5 m/s, 1 kg load, and 30 min was used for this investigation. The Bocle test rig consists of a counterpart made of SAE 8720 steel, and its diameter is 49.2 mm. The following filament material was 3D printed in both X and Y to create samples for testing.

D-1—Iglidur I180-PF (Igus),
D-2—Iglidur I170-PF (Igus),
D-3—PLA (3Novatica) – only Y direction,
D-4—ABS (3DXTech),
D-5—ABS CFR (3DXTech),
D-8—PA (Tarnamid T-27, Grupa Azoty S.A.)—only X direction,
D-9—PA CFR (CARBONX™),
D-10—PA C-CFR (Carbon Fibre, Mark Forged),
D-11—PA (Alloy 910, Taluman3D),
D-12—Iglidur J260-PF (Igus).

The sample used for this test was created by arranging single yarns of melted polymer printed in different directions using MakerBot Replicator 2 × printed, excluding D-10 that was created using a Makerforged Mark Two printer. The melted polymer was built parallel (in case of X printing direction) or perpendicular (in case of Y printing direction) subjected to applied load during tests. According to Giemza et al. (2018), all samples were carefully chosen from commercially available filament except for D, a PA filament prototype. The following samples were printed in both the X and Y direction, as shown in Fig. 2.

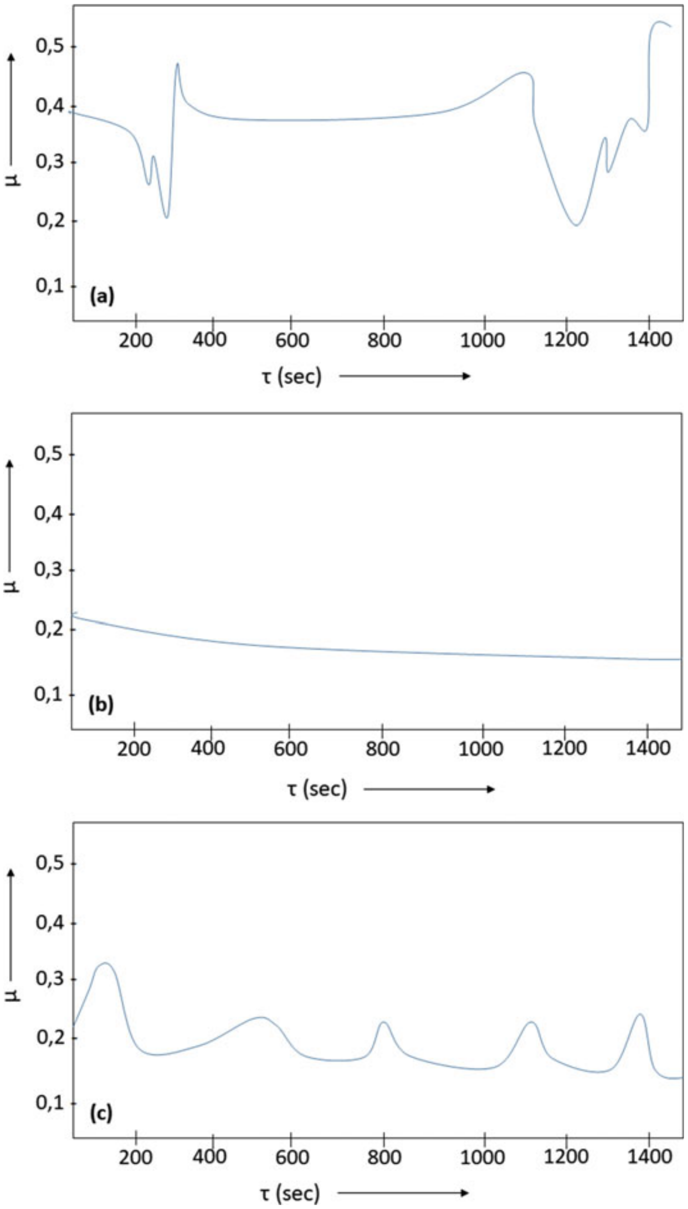

Fig. 4 The examples of the result of the coefficient of friction μ curve for 3D printed samples: **a** PLA, **b** PA C-CFR Y direction, and **c** ABS tribofilament

The friction force of printer samples measured as resistance to motion is presented in Fig. 4a–c. It was observed that the coefficient of friction values (CoF) for all samples investigated were within 0.15–0.55, a material commonly used for creating samples, and tribological products offered a high coefficient of friction values value. This frictional output may be attributed to the toughness and stiffness of these filaments. An inconsistent resistance to motion with a corresponding increase in time was observed for the PLA samples as the resistance to motion value increased from 0.4 to 0.52. However, a slight reduction in friction values with a corresponding increase in time was observed for ABS. This implies that PLA material is more tougher and stiffer than ABS, and the difference in mechanical properties of these materials may be attributed to the difference in friction behavior observed (Priya et al. 2019).

The CRF thermoplastic polymer composite PA CFR (3b) offered a more stable resistance to motion. This consistent friction coefficient curve observed for these two may be attributed to carbon fiber incorporated into the material, as it serves as an internal lubricator and also reduces the frictional heat, which eventually prevents plastic deformation and vibration during abrasion test, resulting in a stable coefficient of friction (Gbadeyan and Kanny 2018). The self-lubricating effect provided filament synergized with the internal properties of carbon fiber results in lower motion resistance observed for this set of samples. Besides, the braking of carbon fiber on counterparts during the abrasion test with a combination of layers of long polymer chain may also be attributed to a stable coefficient of friction. This output may be ascribed to the incorporation of tribofilament, commonly used for tribological application due to its stable friction coefficient and improved wear resistance (Giemza et al. 2018). It could be seen that the resistance to motion of the printed material is influenced by the type or combination of materials used. Similarly, the printing direction influenced the coefficient of friction of the printed material, as shown in Fig. 5.

The graph represented the range and average value of the friction coefficient of all the samples investigated. It was observed that the resistance to motion for printed samples was lower in the Y direction than in the X-direction in most cases. Significantly, the printing direction effect was seen for D-12, where (PA C-CFR)

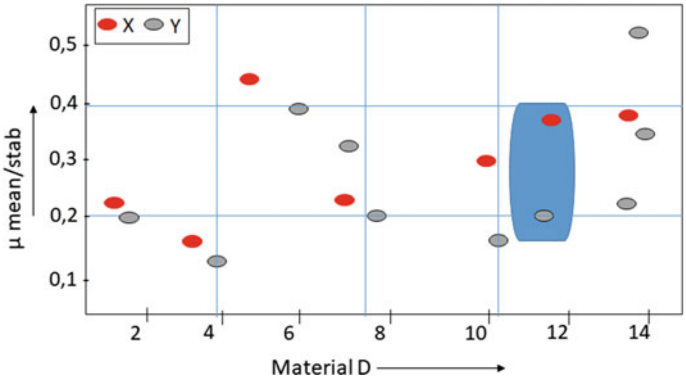

Fig. 5 Graph showing the maximum, average, and minimum values of resistance to the motion of the sample investigated in the different printing direction

– $\Delta\mu \approx 0.16$. A slight difference in the coefficient of friction of sample printed in X or Y direction was seen for samples IGUS tribofilaments D-1 ($\Delta\mu \approx 0.02$), D-2 ($\Delta\mu \approx 0.01$), D-12 ($\Delta\mu \approx 0.02$) and for samples D-4 (ABS $\Delta\mu \approx 0.03$) and D-9 (PA CFR $\Delta\mu \approx 0.03$).

On the other hand, the printing direction has no effect on friction coefficient for materials D-5 (ABS CFR) and D-11 (PA) as the range values of resistance to motion for printed samples overlap at X and Y directions. The Y and X printing directions must understand to determine the resistance of motion for printed materials. The Y-direction translates when a single yarn of the polymer is parallel to the sliding direction, while X is when printing is done perpendicular to a sliding direction. Therefore, the response of the printed material is affected by the technology of printing adopted. The adhesion between melted yarns forming layers during printed at Y direction usually offer better mechanical properties than the one printed in the X-direction. The flow of a single melted polymer during the FDM 3D printing process can also affect the structural formation of polymer yarn, which eventually affects resistance to the motion of printed material.

5 The Influence of Printing Directions on Tribological Properties of 3D Printed Component

5.1 The Effect of Three-Dimensional Printing Procedural Settings, Particularly on Printing Layers Orientations on the Tribological Properties of Polylactic Acid (PLA), High Tensile/High-Temperature Polylactic (HT-PLA), and Polyethylene Terephthalate-Glycol (PETG)

The tribological properties of the 3D printed component are investigated on a tribotester apparatus. This investigation was carried out to scrutinize the effect of three-dimensional printing procedural settings, particularly on printing layer orientations on the tribological properties of various printed polymeric materials. These materials include but not limited to polylactic acid (PLA), high tensile/high-temperature Polylactic (HT-PLA), and polyethylene terephthalate-glycol (PETG) are investigated under reciprocating sliding and dry condition. The influence of the printing layers

5.2 The Samples Printing Process

The three-dimensional 3D printing procedure settings, according to FDM technology using a Bq Witbox 2 types of 3D printed (Hanon et al. 2020). The polymer samples

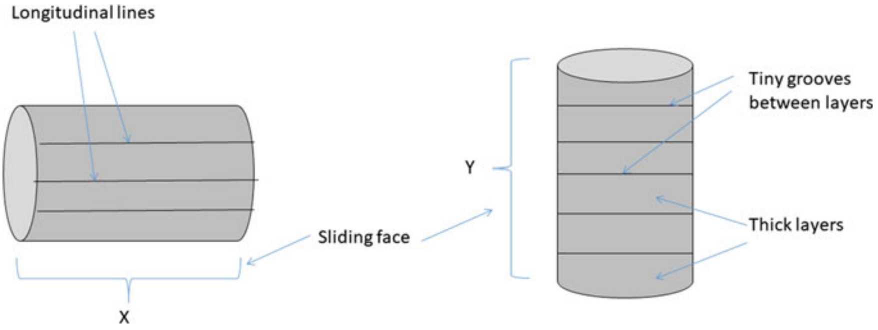

Fig. 6 Schematic diagram of the surface structure of Z and X orientation for printed samples

were printed using different printing temperature settings. Polylactic acid (PLA) and high tensile/high-temperature Polylactic (HT-PLA) were printed at 200 °C, and polyethylene terephthalate-glycol (PETG) was printed at 250 °C. These samples were printed in two different orientation, which was printed in the X and Z direction.

The sample printed in the Z orientations starts by forming shell layer parameters, thick and more uniform than normal printing lines, with a tiny groove in between layers. The samples created in the X direction are made of longitudinal lines forming the structure of each layer.

The sample printed in the Z orientations starts by forming shell layer parameters, thick and more uniform than normal printing lines, with a tiny groove in between layers. The samples created in the X direction are made of longitudinal lines forming the structure of each layer, as shown in Fig. 6. A cylindering solid sample of 8 mm diameter and 15 mm height, printed using the FDM printing process, was used to investigate tribological properties. For easier identification of testing samples, sample printed in Z printing (vertically) direction was marked with Arabic number, and sample printed in X layer orientation was distinguished in Roman number, laying down horizontal as shown in Fig. 7a.

5.3 *Tribological Investigation Procedure*

Unlubricated reciprocating linear sliding friction investigation was conducted on the printed samples. The test was carried out on a tribological measuring circuit consisting of a Spider 8 measuring converter, a computer, a tribometer, and an inverter shown in Fig. 7.

Figure 7b shows the clamping jaw, while the alternating-moving cylinder on the plate tribotester apparatus is shown in Fig. 7c. Spider 8, shown in Fig. 7d, is a device used for strain gauge measurement, which was used to transfer the measured data of the frictional force and other essential features. The applied load was measure usingC9B compact HBM sensors designed for force transducer. It was used to

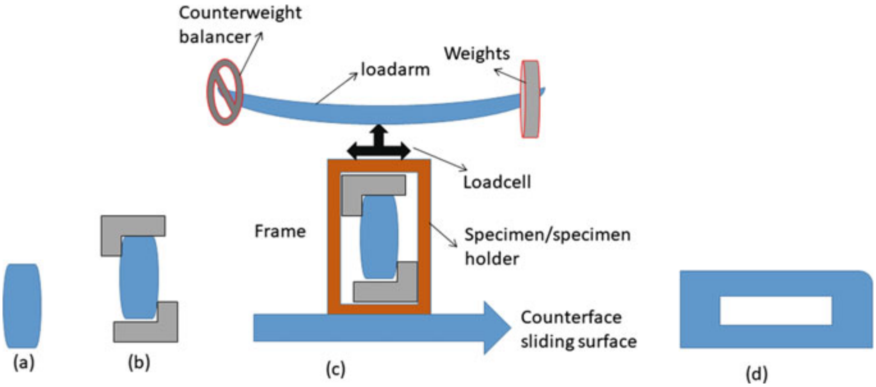

Fig. 7 Schematic illustration of **a** tribological test samples (PLA), **b** clamping mechanism of test specimen with test assembly, **c** tribometer set-up under the reciprocating sliding condition, and **d** Strain gage device

measure the dynamic static compression forces up to 5kN used for this investigation. Displacement transducer type sensor (WETA 1/10 mm) with maximum linear deviation of 0.65 was used to measure wear, and friction was examined using (PW6D) load cell. The test sample was put in the parallel clamping jaw and positioned at a fixed contact with a counterpart with a surface roughness (Ra) of 1.07 mm, and the applied load was 150 N. Three samples were investigated average the value of the three investigations was reported. The wear rate and coefficient friction were measured against sliding distance through the data provided by Spider 8. The wear sensor was in contact with the samples, positioned with the displacement probe opposite the samples at the center column of the tribometer, where the sample holder and cell load are located. This sensor was positioned to measure vertical movement of the middle column during the abrasion test when development in the wear occurs. Samples wear depth (*h*) were measure with the aid of the displacement probe. After knowing the wear depth, wear volume (*V)* was calculated by multiplying the worn area by the length (*l*) of the cylindrical specimen. The wear width (*c*) and area (*A*) were calculated using Eqs. 3 and 4 (Weistten 2016).

$$c = 2\sqrt{h(2R - h)} \tag{3}$$

$$A = R^2 cos^{-1}\left\{\frac{\boldsymbol{R - h}}{\boldsymbol{R}}\right\}\left\{\frac{\boldsymbol{c(R - h)}}{2}\right\} \tag{4}$$

Where: R = radius of the cylindrical specimen (mm), and h = wear dept (mm).

Furthermore, Archard's wear equation was used to calculate the specific wear rate (K) (Colbert and Sawyer 2010).

$$V = KF_n d. \tag{5}$$

where: V = wear volume (mm^3), (F_n) = applied load (g), and (d) is total sliding distance (m)

6 Results and Discussion

6.1 Sliding Wears Analysis of Three-Dimensional Printed Cylindrical Samples

The progress in wear depth of various samples investigated for tribological properties shown in Fig. 9. It was observed that samples wear depth continually increases with a corresponding increase in sliding distance. This tribological behavior may be attributed to poor heat dissipation, and the soft nature of the polymer materials increased yielding of samples to the shear angle of counterpart asperities, leading to a high wear depth.

On average, Fig. 8a shows that HT-PLA offered a smaller wear volume of 0.136 mm^3 on the X layer orientation. This wear volume is the smallest observed in

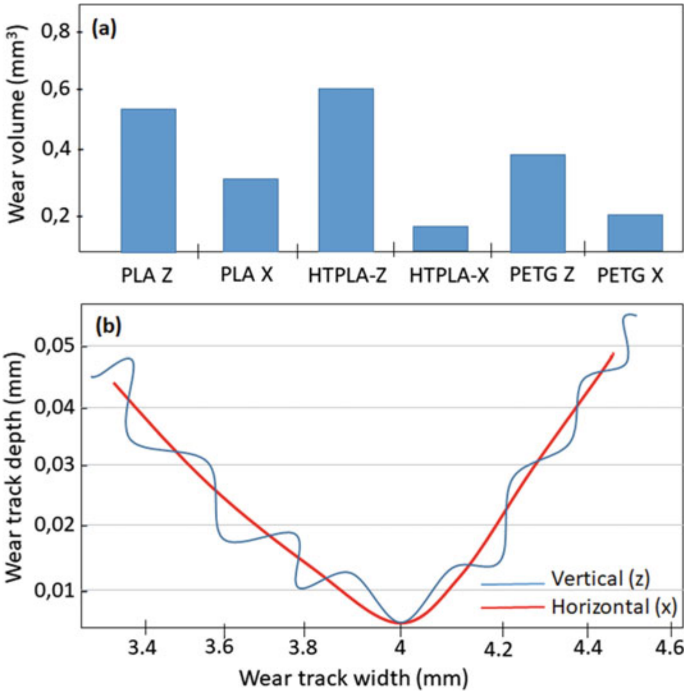

Fig. 8 Graph showing **a** the wear volume of printed samples and **b** Compassion between the wear track of printer sample in vertical (Z) and horizontal (X) orientation

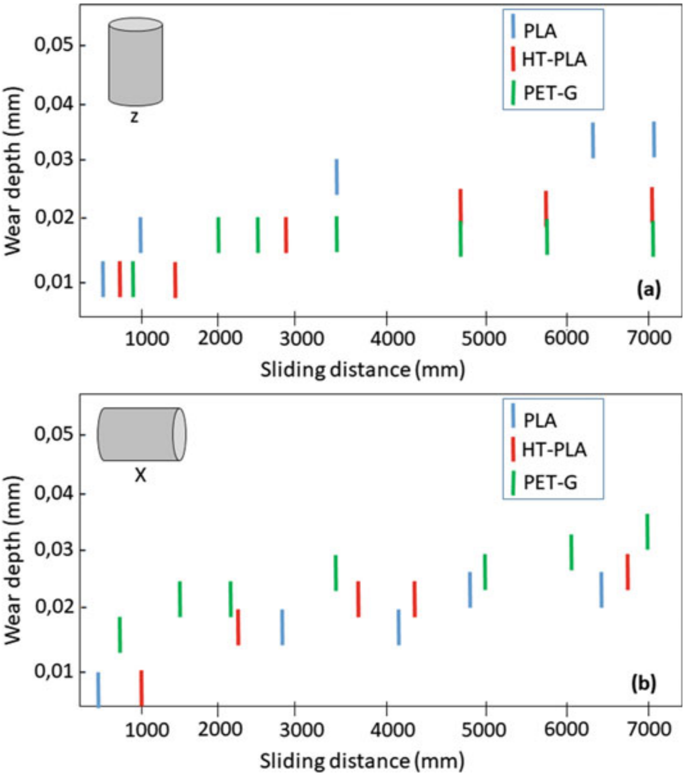

Fig. 9 Graph showing the wear depth for **a** PLA in Z; **b** PLA in X; **c** HTPLA test printed in Z; **d** HTPLA in X; **e** PETG in Z; **f** PETG in X

this investigation, irrespective of the printing orientation. However, HT-PLA offered wear volume 0.594 mm^3 on the X layer orientation higher than printer PLA and PETG. Figure 8b presents the wear track depth and width. It was observed that the samples printed in orientation X offered consistency and a smaller wear track and width than samples printed in orientation Z. This feature may be attributed to improved wear resistance for the samples printed in orientation X.

Considering the FDM 3D- printing parameter on frictional wear polymer samples created in X and Z printing layer orientation shown in Fig. 9. The results presented revealed the effect of the printing parameter on the wear resistance of the created samples from various thermoplastics. It could be seen that samples printed in X orientation offered lower wear depth than samples printed in Z orientation. This outcome may be due printing process that provides different surface quality that improves wear resistance of samples printed in X orientation.

6.1.1 Static and Dynamic Coefficient of Friction for Three-Dimensional Printed Cylindrical Samples

Figure 10 presents the relationship of frictional friction and sliding distance for each sample for thermoplastic investigated for tribological properties.

It was observed that the static coefficient of friction (CoF) is higher than the dynamic irrespective of the printing orientation. Figure 10a, b show the static and dynamic coefficient of friction. We can see that the coefficient of friction curve for both orientations starts from 0.1μ approximately. A sharp rise in CoF was seen afterward for the static and dynamic up to about 200 mm sliding distance, and later a steady increase in curve progression was observed for Z orientation samples.

Meanwhile, a consistent increase in the static and dynamic CoF values was observed for Z orientation samples. The inconsistency of static and dynamic coefficient of fiction may be attributed to the stick-slip phenomenon or the wear debris transfer on the counterpart.

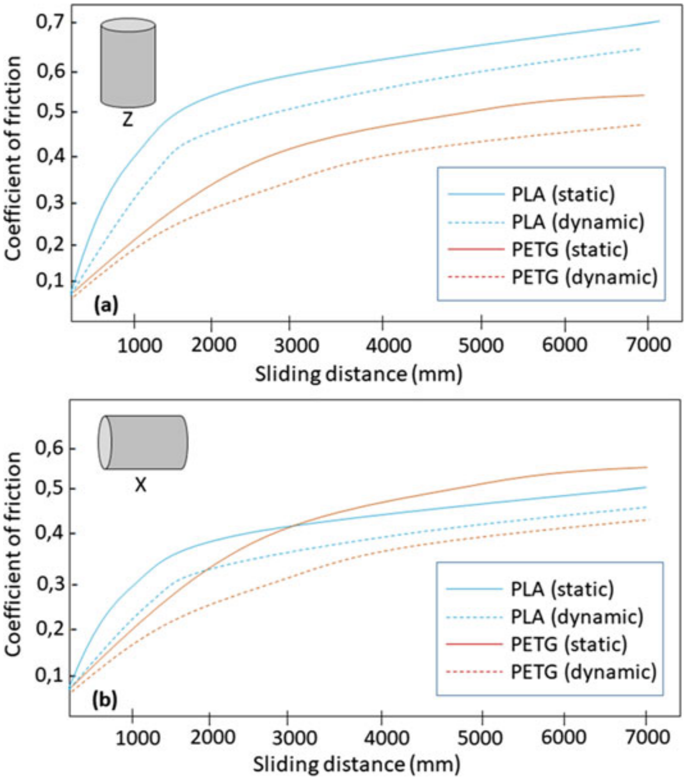

Fig. 10 Static and dynamic friction coefficient of selected 3D printed specimens in **a** X orientation and **b** X orientation

Figure 10c, d present static and dynamic coefficients of friction for HT-PLA. The friction curve for this sample was higher than that of PLA at the starting stage. However, a steady CoF value with a corresponding increase in sliding distance was observed for the HT-PLA sample printed in Z orientation. Meanwhile, CoF values obtained from the HT-PLA sample printed in Z orientation increased drastically up to 1500 mm sliding distance, and a slight increase in the coefficient of friction was observed until the end. For the static and dynamic coefficient of friction values of PETG shown in Fig. 10e, f, the curve for both orientations start for 0.1μ, and the PETG sample printed in Z orientation has a similar trend with PLA sample printer in the same orientation. A systematic increase in CoF values was observed above sliding distance for sample printed in Z orientation, and a trivial increase in the CoF curve was seen after the rapid increase at the initial stage of the sample printed in X orientation. The high-pitched rise in coefficient of friction curves observed for most of the sample investigated may be due to running state, where sample rough and inconsistent surface texture.

Figure 11 presents worn surfaces of samples in printed X orientation and Z orientation examined under an optical microscope to determine the mechanism governing tribological properties obtained for printed thermoplastic investigated. The direction of sliding wear, wear groove, and the printed layer was observed on the worn surfaces, and this may be attributed to the wear resistance and friction coefficient of the printed samples. On the micrograph of samples printed in Z orientation, a Z fragments structural formation of layers with wear grove were seen. The wear groove created more asperities, which decreases the contact sliding surface area. This structure formation often increases normal pressure effectiveness, which eventually boosts friction and wears. The worn surface of the sample printed in X orientation shows longitudinal lines, and tough wear texture was seen. Longitudinal lines are the line created by the printing layers. This structure often helps load distribution on larger sliding contact areas and reduces wear rate and friction coefficient.

This investigation confirmed that the orientation of the printing process or printing direction has a notable effect on the tribological properties of 3D printed components. The HT-PLA sample offered superior tribological properties than PLA and PETG

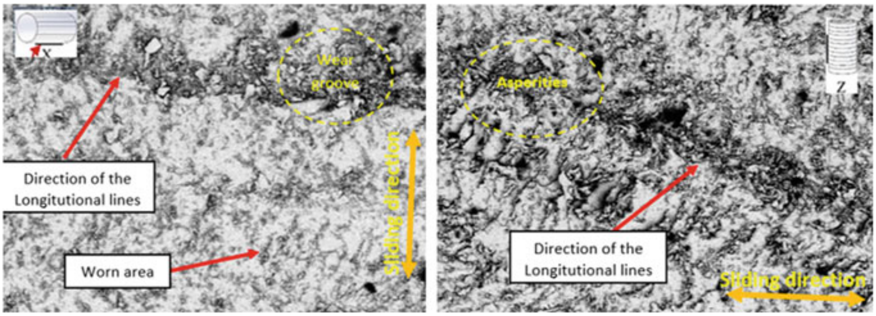

Fig. 11 Example of the worn surfaces for samples in **a** X orientation and **b** Z orientation

polymer; however, it offered an unstable coefficient of friction from beginning to the end of the CoF curve. This frictional output may be attributed to poor thermal energy resistance. Thus, it imperative to incorporate particles with improving properties on printer layers created using a 3D printed component to achieve the final material with the required properties for friction material application. The next section provides information on the development and investigation of tribological properties of filler incorporated thermoplastic 3D printed composite.

7 The Effect of Incorporating Filler on Tribological Properties of 3D Printed ABS Composite

7.1 Tribological Properties of 3D Printed Graphite-Reinforced Polylactic Acid Composite

The effect of different percentages of graphite incorporation on the tribological properties of PLA filament was investigated on a pin-on-disk. Polylactic acid infused with graphite concentration of 5%, 10%, 20%, and 30% were created using the Fused Filament fabrication process. A cylindrical sample of 8 mm created using a 3D printing procedure was paired with a pin-on-disk counterpart to examine tribological properties. Experimental results provided information on the fundamentals for selecting an optimal graphite concentration for improving the tribological properties of 3D printed PLA composite for gear, guideway block, or laminated mold application (Fig. 12).

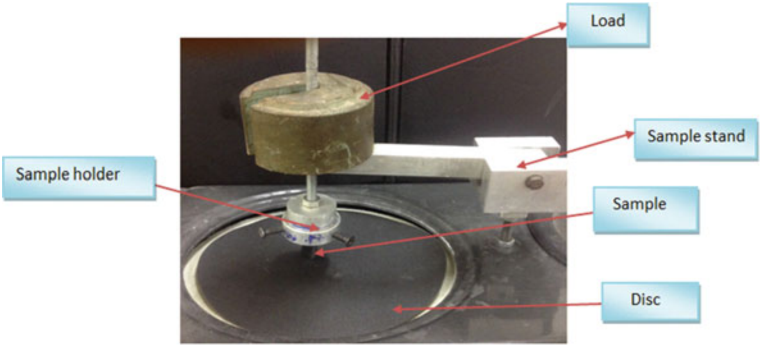

Fig. 12 Pin-on-disc apparatus (wear and friction measuring system) (Gbadeyan et al. 2017)

7.2 Materials and Methods

Pure PLA and tribo-filament Igus Iglidur 1180 were used for the investigation. Neat PLA was used to establish the improvement or weakening of tribological properties, while tribo-filament was used to establish proper test parameters and evaluate the result. A pin-on-disc tribometer was used to investigate the linear wear and the coefficient of the 3D printed samples' kinetic friction. The weight of the samples was taken before and after the test to determine the mass loss. The investigation was conducted in the stable temperature of the samples using the test apparatus replicant of pin-on-disc shown in Figs. 13 and 14. The steel counterpart used to have 0.35-0.45 surface roughness, and the sample was subjected to an applied load of 5.49 N at 2 h 27 min. The length of the pin (sample) path was 3 km, pin pressure on the disc was 0.11 MPa, and the velocity of the disc was 0.34 m/s. In the scope of the study, the tribological properties of three samples of each material were determined in separate processes, as shown in Fig. 14. Each of these samples was tested on a pin-on-disc station for 3 km.

Where: $\mathbf{F_N}$= applied force, $\mathbf{F_t}$= friction force, **n** = rotation speed, **1** = Sample and **2** = disc

7.3 Results

Figures 15 and 16 present the wear rate and friction coefficient for Iglidur 1180, pure PLA, and graphite-reinforced composite. It is observed that Iglidur 1180 exhibited a lower wear rate and coefficient of friction than neat PLA and graphite-reinforced composite.

This performance may be attributed to the improved wear resistance and relatively lesser coefficient of friction of the filament. Notably, the addition of graphite reduces the wear rate and coefficient of friction in most cases.

Fig. 13 Schematic of Pin-on-disc used for research

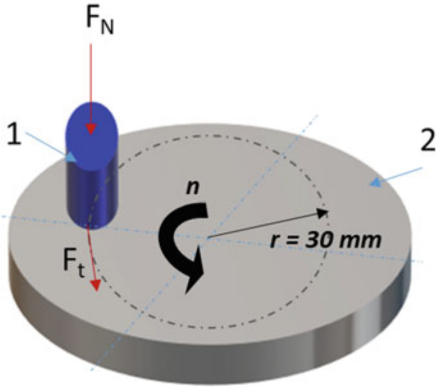

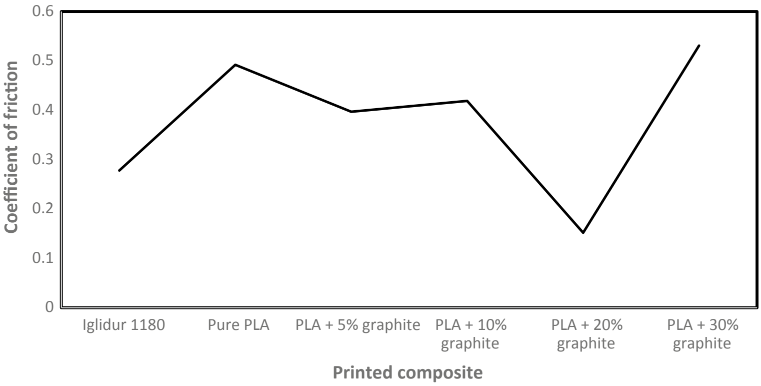

Fig. 14 Coefficient of friction for Iglidur 1180, pure PLA, and graphite-reinforced composite

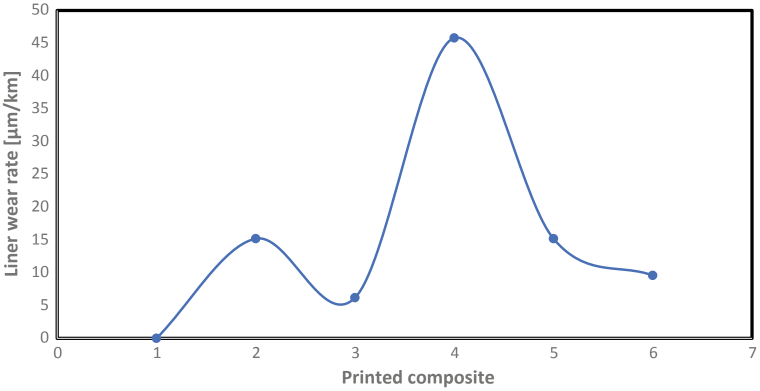

Fig. 15 Wear resistance of Iglidur 1180, pure PLA, and graphite-reinforced composite

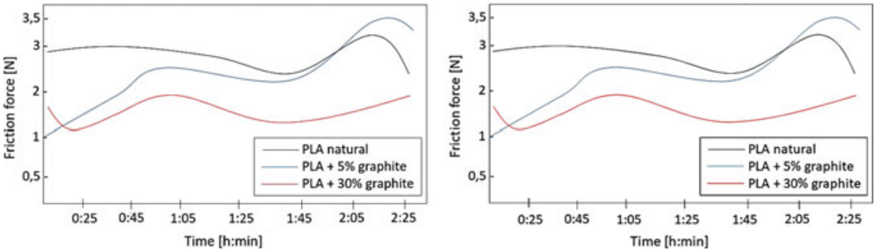

Fig. 16 Graph showing coefficient of friction for samples: Iglidur I180, PLA Natural, PLA + 5% graphite, PLA + 10% graphite, PLA + 20% graphite, PLA + 30% graphite

However, it is more significant after low graphite particle loading of 5%. This improved wear resistance and a lower coefficient of friction may be attributed to the homogeneous dispersion of grain in the matrix. This uniform dispersion enhances the bond between PLA printed layers, resulting in a tougher structure that improves wear resistance. The graphite loading at a small concentration also serves as an internal lubricator, which eventually controls friction force.

Large loading of particles in matrix often agglomerates, resulting in high wear rate and coefficient of friction. The loading of graphite above 5% exhibited a higher wear rate and coefficient. This performance may be attributed to the high loading of graphite. The worn surfaces of samples were investigated on SEM at 8000 magnification after an abrasion test to determine worn mechanisms. An irregular surface texture, the longitudinal line showing the edges of the printed layer, could be seen. The uneven surface texture reveals by Fig. 17 was due to debris generated during the wear test, which eventually prevents the direct contact of samples and counterparts. The debris transferred to the counterpart surface reduces wear rate and a lower coefficient of friction.

In summary, this investigation shows that the loading of graphite at lower concentrations positively affects the tribological properties of 3D printed components. However, this investigation was limited to micro-participle. Thus, it is imperative to investigate the loading of nanoparticle on tribological properties of 3D printed nanocomposite.

Fig. 17 Example of SEM worn surfaces of samples examine after tests

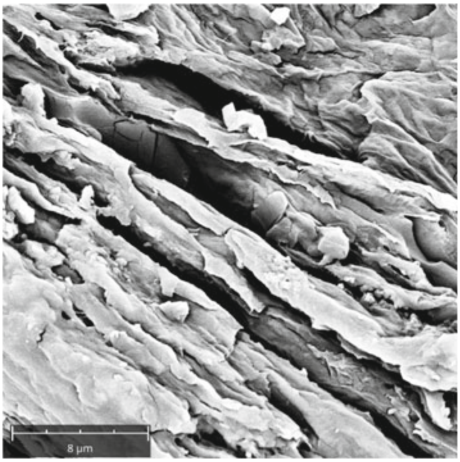

8 The Effect of Nanoclay on Tribological Properties of 3D Printed ABS Nanocomposite

Tribological properties of layered silicate-reinforced ABS and nanoclay infused ABS nanocomposite was investigated to determine the effect of nanoclay loading on nanocomposite created using additive manufacturing 3D procedure. The nanocomposite was fabricated by infusing different weight percentages of nanoclay (0–2 wt%) on each printed ABS layer using additive manufacturing. A square panel of 6 sheets with varying weight percentages of nanoclay was created with the aid of a 3D printer. The effect of nanoclay loading, different sliding distances (122.5 m, 264 m, and 424.2 m) on the tribological properties such as wear and friction at vertical and horizontal surfaces of the developed nanocomposite were investigated and compared. The tribological properties of nanocomposite vary with different loading of nanoclay and sliding distance.

8.1 Procedure for Creating Pure Acrylonitrile Butadiene Styrene Plastic and Nanoclay Reinforced Acrylonitrile Butadiene Styrene Using 3D Printing

Creating plastic of acrylonitrile butadiene styrene (ABS) was achieved in four stages. According to Gbadeyan et al. (2020), the printing of this material was done in four stages. In the first stage, the drafting of samples on the CAD program was created. This sample was designed and drawn using a Solid Edge 2019 computer-aided-program. An ISO metric file was created, and samples were drawn therein, as shown in Fig. 18.

The file was saved as Standard Tessellation (.stl) and exported in UP studio to enable finalizing the 3D print parameters. Subsequently, the 3D printer infill filament was set to 99% with no support, and the thickness of layers was pre-set to 0.2 mm. Nanoclay/acetone solution pre-calculate following different weight percentages measured with the aid of syringe was introduced and spread on each printer

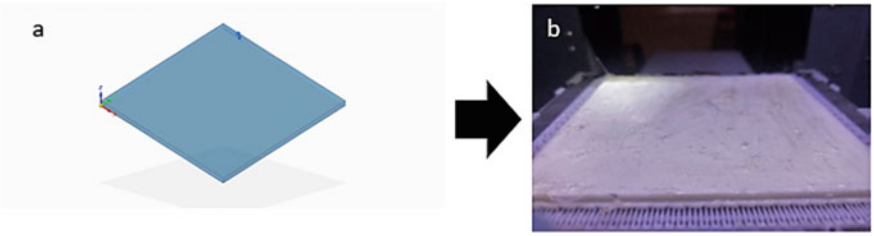

Fig. 18 Image showing (**a**) drafter gear specimen and **b** printed nanoclay infused acrylonitrile butadiene styrene nanocomposite for gear application (Gabyaden et al. 2020)

layer of acrylonitrile butadiene styrene. Six layers of acrylonitrile butadiene styrene (ABS) were 3D print, and the final material was later investigated for mechanical and tribological properties.

8.2 Tribological Investigation of Unfilled Acrylonitrile Butadiene Styrene and Nanoclay Infused Nanocomposite

In this study, tribological properties of unfilled acrylonitrile butadiene styrene and nanoclay infused nanocomposite developed with the aid of a 3D printer was investigated to measure the. This test was conducted on vertical and horizontal surfaces of the nanocomposite using a pin-on-disc apparatus of the Tribometer. The Tribometer was precisely attuned for tribological properties measurement and was also confirmed for the stability of the contact point and scrounging friction. It has a steel metal disc (diameter 350 mm and hardness 420 Hv) used as a counterpart and sliding 122.5 m, 264 m, and 424.2 m), and fixed normal load of 10 N. The resultant pressure and sliding speed were 138 N/m^2 and 0.7 m/s respectively. The wear loss was measured as a mass loss of the composite samples using a highly accurate digital weighing scale. Three samples were tested, and an average of three samples was reported. The specific wear rate and coefficient of friction were then calculated using Eqs. 6 and 7, respectively.

$$\mathbf{k} = \frac{\mathbf{V}}{\mathbf{N.x}} \tag{6}$$

$$\boldsymbol{\mu} = \frac{\boldsymbol{\tau}}{\mathbf{r.F}} \tag{7}$$

where: k = specific wear rate, V = the volume change (in m^3), x = total sliding distance (in m), μ = coefficient of friction, τ = torque induced in the specimen due to friction (in N-mm); r = radius of the disc (mm) and F = normal load acting on the specimen (in N) (Fiedrich et al. 2329; Gbadeyan et al. 2017) (Table 1).

8.3 Results and Discussion

8.3.1 The Influence of Nanoclay Loading and Sliding Distance on Tribological Behaviors of Unfilled Acrylonitrile Butadiene Styrene and Nanoclay Infused Nanocomposite at Vertical and Horizontal Surfaces

Table 2 presents wear resistance and friction coefficient for the unfilled ABS and nanoclay infused ABS nanocomposite. The wear rate of ABS was on the high side

Table 1 Advantages and disadvantages of most used fillers

Material	Advantages	Disadvantages	References
Carbon (Graphite)	• Commonly used to control tribological properties due to its ability to transfer films, which formed self-sustaining layers. • Better thermal stability. • It increases the cooling rate	• High loading of graphite reduces hardness • Increases brake pad overall heat conductivity	(Blau 2001; Friedrich 2016; Ikpambese 2014; Eriksson et al. 2002)
Molybdenum disulfide	• Good friction performance	• Poor wear resistance • Anti-fading properties	(Martinez and Echeberria 2016; Cho et al. 2005)
Antimony trisulfide	• Improves fade resistance • Reduces vibrations • Improve friction stability	• Increase wear rate • Disk thickness variation generation • Potentially carcinogenic substance	(Martinez et al. 2016; Cho et al. 2005; Varica et al. 2013; Lee et al. 2013)
Coke	• High coefficient of friction • Better abrasion resistance.	• Poor fade resistance • Unstable friction	(Ertan and Yavuz 2011)
Friction dust	• Reduces impulsive combustion • Help particle dispersion.	• Meager performance at an elevated temperature	(Blau 2001)
Metal sulphides	• Modifies and stabilizes the coefficient of friction	• Very expensive	(Ertan and Yavuz 2011)
Zirconium silicate (ZrSiO4)	• Offers a stable coefficient of friction	• Poor wear resistance	(Jang and Kim 2000)

compared to nanoclay infused ABS nanocomposite. This output may be attributed to the inadequate bond between printer layers, resulting in printed layer delamination when subjected to a fixed contact counterpart.

Similarly, the soft nature and thermal softness of acrylonitrile butadiene styrene prompted by the heat-induced by the contact may be another reason for the high wear rate. Also, as the counterpart and nanocomposite continue to rob at the same interface with the contact area, the temperature on both surfaces is amplified, allowing for easier abrasion, leading to increased wear rate (Gbadeyan et al. 2017). It was further observed that loading nanoclay decreases the wear rate of acrylonitrile butadiene styrene significantly. This notable decrease in wear rate may be attributed to better heat and wear resistance of the filler incorporated. This trend is consistent with

Table 2 The wear rate and coefficient friction for unfilled acrylonitrile butadiene styrene and nanoclay infused nanocomposite

3D printer nanocomposite	Wear rate before socking in oil	Remarks (%)	Coefficient of friction	Remarks (%)
	@ 122.5 m (sliding distance)		*@ 122.5 m (sliding distance)*	
Pure ABS	2,68 X 10^{-10}	0	0,17693	0
ABS + 0.5 wt% Nanoclay	2,06 X 10^{-10}	23	0,128462	27
ABS + 1 wt% Nanoclay	2,01 X 10^{-10}	25	0,138462	22
ABS + 1.5 wt% Nanoclay	1,36 X 10^{-10}	49	0,167923	5.1
ABS + 2 wt% Nanoclay	7.10 X 10^{-11}	74	0,084615	52
	@ 264 m (sliding distance)		*@ 264 m (sliding distance)*	
Pure ABS	$1,86 \times 10^{-10}$	0	0,22222	0
ABS + 0.5 wt% Nanoclay	1.12×10^{-10}	37	0,157143	29
ABS + 1 wt% Nanoclay	$1,13 \times 10^{-10}$	39	0,171429	23
ABS + 1.5 wt% Nanoclay	$1,07 \times 10^{-10}$	42	0,19100	14
ABS + 2 wt% Nanoclay	4.69×10^{-11}	75	0,088571	60
	@ 424.17 m (sliding distance)		*@ 424.17 m (sliding distance)*	
Pure ABS	$1,28 \times 10^{\mathbf{-10}}$	0	**0,26667**	**0**
ABS + 0.5 wt% Nanoclay	$9,16 \times 10^{\mathbf{-11}}$	28	**0,24333**	**9**
ABS + 1 wt% Nanoclay	$9,09 \times 10^{\mathbf{-11}}$	29	**0,2000**	**25**
ABS + 1.5 wt% Nanoclay	$5.61 \times 10^{\mathbf{-11}}$	56	**0,22222**	**16**
ABS + 2 wt% Nanoclay	$2,55 \times 10^{\mathbf{-11}}$	80	**0,106669**	**60**

available literature where loading nanoclay reduces the wear rate (Esteves et al. 2013; Golgoon et al. 2015).

Nevertheless, a decrease in wear rate with a corresponding increase in the weight percentage loading of nanoclay was seen. This tribological performance may be attributed to the incorporated nanoparticle's inherent properties, including but limited to improved thermal properties and heat energy dispersion capabilities (Singh et al. 2018). Homogeneous dispersion of the nanoparticle of nanoclay improves the adhesion of the printed ABS layer, forming an interlocking structure that offers better wear resistance.

Nanoclay infused provided better heat dissipation, which reduces the heat-induced by ABS and the heat generated at counterpart during the wear test, which resulted in a reduction of wear rate. The wear rate reduction trend after the addition of nanoclay consistent with other studies elsewhere (Mohan and Kanny 2019; Deepthi et al. 2014; Mimaroglu et al. 2018; Jumahat et al. 2016). Comparing the wear rate of neat ABS and nanoclay infused composite, it could be seen that the loading of different concentrations of nanoclay into ABS composite has a different effect on the wear rate. Although the loading of nanoclay reduces the wear rate of ABS composite irrespective of percentage loading, a significant wear rate reduction was observed after incorporating 2 wt%.

Table 2 shows that the loading of 2wt% reduced the ABS wear rate by 74% at 122.5 sliding distance, 75% at 264 m sliding distance, and 80% at a sliding distance 424.17. The improvement in wear resistance was observed after the addition of 2wt%. nanoclay may be due to the improved toughness and hardness of nanoparticles that prevent the nanocomposite's surface erosion, resulting in a lesser wear rate. Moreover, the debris produced during abrasion investigation often prevents direct contact of wear test samples and counterparts, reducing wear rate and samples mass loss. A significant effect of sliding distance on the wear rate of neat ABS and nanoclay filled composite was observed. A decrease in wear rate of neat ABS and nanoclay filled composite with a corresponding increase in sliding distance was seen. The lubrication effect and the heat dissipation ability of nanoclay, which reduces the temperature on the counterpart and test sample interface, may be attributed to notable wear resistance observed. The debris built on a counterpart surface reduces the nanocomposite and disc asperities direct sliding contact, and nanoparticle embedded in the nanocomposite reduces frictional heat and, in turn, reduced the wear rate.

The relationship of nanoclay loading and sliding distance on the friction (CoF) coefficient of printed unfilled acrylonitrile butadiene styrene and nanoclay infused nanocomposite at vertical and horizontal surfaces is provided in Fig. 6. A steady increase in the CoF with a corresponding increase in sliding distance was observed for ABS. The thermal softening ABS may tend to stick-slip on counterpart when in sliding condition due to heat-induced may be attributed to an increase in CoF of neat ABS. The delamination of layer due increase in time at which ABS and counterpart persist in fixed contact may be another reason for higher CoF.

Notably, different coefficient of friction values was observed with different concentration of nanoclay and sliding distances. This output shows that the drag and shear angle affect wear rate and affects the friction between the counterpart and nanocomposite. This frictional performance may also be due to the debris generated during the period counterpart, and the nanocomposite is in stationary contact. A linear decrease in the friction coefficient with a corresponding increase in sliding distances was observed for neat ABS and nanoclay infused ABS nanocomposite. The increase in CoF of ABS may be ascribed to the rapid rapture of ABS due to induced heat at the counterpart, causing stick-pick that increases vibration resulting in a higher coefficient of friction. The amount of nanoclay is incorporated in the nanocomposite may be to the random coefficient of frictions observed.

This nanoclay dispersed in the matrix formed a tougher nanocomposite with high frictional behavior. This result corresponds with literature where the loading of nanoclay increase CoF (Mohan and Kanny 2019). However, nanoclay infused ABS nanocomposite exhibited a lower coefficient of friction than neat ABS, and it is more significant after the addition of 2 wt%. The addition of 2 wt% consistently increases the coefficient of friction for ABS by 12.7% at 122.5 sliding distance, 60% at 264 m sliding distance, and 60% at a sliding distance 424.17. This frictional output may be attributed to the existence of superior adhesion at the nanofiller, and the matrix interface offers a stable structure that provides steady CoF (Pandurangan 2018; Jumahat 2016). The improved wear resistance and stable coefficient of friction observed for the nanocomposite with 2 wt% nanoclay suggest gear application material.

8.4 Summary

The tribological behavior of different materials and composite created using 3D printing or additives manufacturing techniques was reviewed in this chapter. It shows that additive manufacturing techniques compete with other traditional manufacturing procedures. The chapter further proved that Fused Deposition Modeling is one of the most suitable technology for producing a complex product such as gear in a short time. Although thermoplastic such as PLA and ABS are most used based on their mechanical strength and improved thermal properties, this chapter proved that the loading of nanoparticles and printing at different layers determines or strongly influences wear resistance and friction coefficient of 3D printed components for tribological product applications.

Comparing the investigation on tribological properties of 3D composite conducted by Giemza (2018) conducted on one layer orientation to the study conducted, on different layer orientation and different direction (X and Y direction). It was observed that the samples printed in orientation X offered consistency and smaller wear track and width than samples printed in orientation Z. It was also established that direction at which 3D component affects the tribological properties of the component or product. According to Giemza et al. (2018), the adhesion between melted yarns forming layers during printed at Y direction usually offers better mechanical properties than the one printed in the X-direction resulted in improved wear resistance and stable friction coefficient. However, the printed filament layer's dilapidation due to the inadequate bond between the layer interfaces is still occurring. To enhance this bond, new technology of nanoparticle infusion into printer layer became viable means. The effect of different percentages (5%, 10%, 20%, and 30%) of graphite incorporation on the tribological properties of PLA filament Polylactic acid and the improvement in wear resistance and coefficient of friction was observed after 20% of graphite. This loading is on the high side, and the graphite particle is costly, which eventually increases production cost. We reduced the loading percentages and the used nanoclay as reinforcement based on availability and lower cost. The experimental results showed that a small loading of 2% offered superior tribological properties. This output provided that a working tribological product could be produce at a cheaper rate.

8.5 Conclusion

This chapter reviews the tribological properties of different neat thermoplastic and particle reinforced composite and nanocomposite. It also examines different equipment converted to the Pin-on disc apparatus used to determine the wear rate and friction coefficient of 3D printed components. It also established that the tribological properties of the 3D component depend on the test parameter and the type of material used. This review confirmed that the orientation of the printing process or printing direction has a notable effect on the tribological properties of 3D printed components. The HT-PLA sample offered superior tribological properties than PLA and PETG polymer; however, it offered an unstable coefficient of friction from beginning to the end of the CoF curve. This frictional output may be attributed to poor thermal energy resistance. Incorporation of low concentration of particle at either nano or micro-size proved viable for improving the tribological properties of the 3D printer component used for gear application. With advancements in 3D technology, the printing of friction material with complex required properties such as brake pad is possible if the right materials and printing procedures are selected.

Acknowledgements Funding and infrastructure support provided by Research & Postgraduate support of Durban University of Technology & National Research Foundation (NRF) of South Africa (Grant no: 119779) is gratefully acknowledged.

References

Ajayi JA (2002) Failure analysis of railway brake blocks: mechanical properties prediction. Eng Fail Anal 9(4):451–456

Azam MU, Samad MA (2018) Tribological evaluation of a UHMWPE hybrid nanocomposite coating reinforced with nanoclay and carbon nanotubes under dry conditions. J Tribol 140(5)

Blau PJ (2001) Compositions, functions, and testing of friction brake materials and their additives. Oak Ridge National Lab, TN (US)

Boetker J, Water JJ, Aho J, Arnfast L, Bohr A, Rantanen J (2016) Modifying release characteristics from 3D printed drug-eluting products. Eur J Pharm Sci 90:47–52

Cho MHA, Ju JA, Kim SJA, Jang J (2005) Tribological properties of solid lubricants (graphite, Sb2S3, MoS2) for automotive brake friction materials. Wear, vol. 260, no. 7–8

Cho MH, Jus J, Kim, Jang Tribological properties of solid lubricants (graphite, Sb2S3, MoS2) for automotive brake friction materials," Wear, vol. 260, no. 7–8, pp. 855–860, 4/7/ 2006. http://dx.doi.org/10.1016/j.wear.2005.04.003

Colbert RS, Sawyer WG (2010) Thermal dependence of the wear of molybdenum disulphide coatings. Wear 269(11–12):719–723

Deepthi M, Sailaja R, Sampathkumaran P, Seetharamu S, Vynatheya S (2014) High density polyethylene and silane treated silicon nitride nanocomposites using high-density polyethylene functionalized with maleate ester: Mechanical, tribological and thermal properties. Mater Des 1980–2015(56):685–695

Deshmukh P, Lovell WG, Sawyer A, Mobley A (2005) On the friction and wear performance of boric acid lubricant combinations in extended duration operations. Wear, vol. 260, no. 11–12, pp. 1295–1304. http://dx.doi.org/10.1016/j.wear.2005.08.012

Eriksson M, Bergman F, Jacobson S (2002) On the nature of tribological contact in automotive brakes. Wear, vol. 252, no. 1–2, pp. 26–36. http://dx.doi.org/10.1016/S0043-1648(01)00849-3

Ertan R, Yavuz N (2011) The effects of graphite, coke and ZnS on the tribological and surface characteristics of automotive brake friction materials. Industrial Lubrication and Tribology 63(4):245–253

Ertan R, Yavuz N (2011) The effect of graphite, coke and zinc on the tribological and surface characteristic of automobile brake friction materials. Industrial Lubrication and Tribology. https://doi.org/10.1108/00368791111140468

Esteves M, Ramalho A, Ferreira J, Nobre J (2013) Tribological and mechanical behaviour of epoxy/nanoclay composites. Tribol Lett 52(1):1–10

Friedrich, Z. Zhang, and A. K. Schlarb (2005) Effects of various fillers on the sliding wear of polymer composites. Composites Science and Technology, vol. 65, no. 15–16, pp. 2329–2343. http://dx.doi.org/10.1016/j.compscitech.2005.05.028

Gbadeyan OJ, Kanny K (2018) Tribological Behaviors of Polymer-Based Hybrid Nanocomposite Brake Pad. J Tribol 140(3):

Gbadeyan JO, Kanny K, Mohan TP (2017) Influence of the multi-walled carbon nanotube and short carbon fibre composition on tribological properties of epoxy composites," Tribology - Materials, Surfaces & Interfaces, vol. 11, no. 2, pp. 59–65, 2017/04/03. https://doi.org/10.1080/17515831.2017.1293763

Gbadeyan OJ, Kanny K, Mohan T (2017) Influence of the multi-walled carbon nanotube and short carbon fibre composition on tribological properties of epoxy composites. Tribology-Materials, Surfaces & Interfaces 11(2):59–65

Gbadeyan O, Kanny K, Pandurangan MTJOOT (2018) Tribological, Mechanical, and Microstructural of Multiwalled Carbon Nanotubes/Short Carbon Fiber Epoxy Composites. vol. 140, no. 2, p. 022002, 2018

Gbadeyan OJ, Mohan TP, Kanny K (2020) Processing and characterization of 3D-printed nanoclay/acrylonitrile butadiene styrene (abs) nanocomposite gea. The International Journal of Advanced Manufacturing Technology, vol. 109, no. 3, pp. 619–627, 2020/07/01 2020, https://doi.org/10.1007/s00170-020-05648-5

Giemza B, Domański M, Deliś M, Kapica D (2018) Tribological properties of 3D printed components," (in English), of KONBiN, vol. 48, no. 1, p. 447

Giemza B, Domański M, Deliś M, Kapica D (2018) Tribological properties of 3D printed components. Journal of KONBiN 48(1):447–463

Golgoon A, Aliofkhazraei M, Toorani M, Moradi M, Rouhaghdam AS (2015) Corrosion and wear properties of nanoclay-polyester nanocomposite coatings fabricated by electrostatic method. Procedia Materials Science 11:536–541

Hanon MM, Yazan A, László Z (2020) Effect of print orientation and bronze existence on tribological and mechanical properties of 3D-printed bronze/PLA composite. The International Journal of Advanced Manufacturing Technology 108(1–2):553–570

Hanon MM, Marczis R, Zsidai L (2020) Impact of 3D-printing structure on the tribological properties of polymers. Industrial Lubrication and Tribology

Han L, Huang L, Zhang J, Lu Y (2006) Optimization of ceramic friction materials. Composites Science and Technology, vol. 66, no. 15, pp. 2895–2906. http://dx.doi.org/10.1016/j.compscitech.2006.02.027

Hwang H, Jung S, Cho K, Kim Y, Jang H (2010) Tribological performance of brake friction materials containing carbon nanotubes. Wear 268(3–4):519–525

Ikpambese KK, Gundu DT, Tuleun LT (2014) Evaluation of palm kernel fibers (PKFs) for production of asbestos-free automotive brake pads. Journal of King Saud University—Engineering Sciences. http://dx.doi.org/10.1016/j.jksues.2014.02.001

Jang H, Kim SJ (2000) The effects of antimony trisulfide (Sb2S3) and zirconium silicate (ZrSiO4) in the automotive brake friction material on friction characteristics. Wear, vol. 239, no. 2, pp. 229–236, 4. http://dx.doi.org/10.1016/S0043-1648(00)00314-8

Jang H, Lee JS, Fash JW (2001) Compositional effects of the brake friction material on creep groan phenomena," Wear, vol. 251, no. 1–12, pp. 1477–1483, 10// 2001. http://dx.doi.org/10.1016/S0043-1648(01)00786-4

Jumahat A, Talib AA, Abdullah A (2016) Wear properties of nanoclay filled epoxy polymers and fiber reinforced hybrid composites. In: Nanoclay Reinforced Polymer Composites: Springer, 2016, pp. 247–260

Justice BA, Badr NA, Felder RA (2009) 3D cell culture opens new dimensions in cell-based assays. Drug Discovery Today 14(1–2):102–107

Kim SJ, Hyung Cho M, Hyung Cho K, Jang K (2007) Complementary effects of solid lubricants in the automotive brake lining. Tribology International, vol. 40, no. 1, pp. 15–20, 1. http://dx.doi.org/10.1016/j.triboint.2006.01.022

Kim JW, Jang H, Kim JW (2014) Friction and wear of monolithic and glass-fiber reinforced PA66 in humid conditions," *Wear,* vol. 309, no. 1–2, pp. 82–88. https://doi.org/10.1016/j.wear.2013.11.007

Lashgari HR, Kong C, Adabifiroozjaei A, Li S (2020) Microstructure, post thermal treatment response, and tribological properties of 3D printed 17–4 PH stainless steel. Wear, vol. 456-457, p. 203367. https://doi.org/10.1016/j.wear.2020.203367

Lawrence I, Paul OA (2013) Critical evaluation/reassessment of (abfm) automotive brake friction materials," Standard Research J

Lee WK, Rhee TH, Kim HS, Jang H (2013) Effects of antimony trisulfide (Sb2S3) on sliding friction of automotive brake friction materials. Met Mater Int 19(5):1101–1107

Macdonald E et al (2014) 3D printing for the rapid prototyping of structural electronics. IEEE access 2:234–242

Malachova K et al (2016) Toxicity and mutagenicity of low-metallic automotive brake pad materials. Ecotoxicol Environ Saf 131:37–44

Martinez AM, Echeberria J (2016) Towards a better understanding of the reaction between metal powders and the solid lubricant Sb2S3 in a low-metallic brake pad at high temperature. Wear 348:27–42

Martinez AM, Echeberria J (2016) Towards a better understanding of the reaction between metal powders and the solid lubricant Sb2S3 in a low-metallic brake pad at high temperature. Wear, vol. 348–349, pp. 27–42. http://dx.doi.org/10.1016/j.wear.2015.11.014

Mimaroglu A, Unal A, Yetgin S (2018) Tribological Properties of Nanoclay Reinforced Polyamide-6/Polypropylene Blend," in Macromolecular Symposia, 2018, vol. 379, no. 1: Wiley Online Library, p. 1700022

Mirón S, Ferrándiz D, Juárez Mengual A (2017) Manufacturing and characterization of 3D printer filament using tailoring materials. Procedia Manufacturing, vol. 13, pp. 888–894. https://doi.org/10.1016/j.promfg.2017.09.151

Mohan, Kanny (2019) Tribological properties of nanoclay-infused banana fiber reinforced epoxy composites," Journal of Tribology, vol. 141, no. 5, 2019

Nie P, Min C, Song HJ, Chen X, Zhang Z, Zhao K (2015) Preparation and Tribological Properties of Polyimide/Carboxyl-Functionalized Multi-walled Carbon Nanotube Nanocomposite Films Under Seawater Lubrication. Tribology Lett 50(1)

Ntie-Kang F et al (2013) CamMedNP: building the Cameroonian 3D structural natural products database for virtual screening. BMC complementary and alternative medicine 13(1):1–10

Peng T, Yan Q, Li G, Zhang X, Wen Z, Jin X (2017) The braking behaviors of Cu-based metallic brake pad for high-speed train under different initial braking speed. Tribol Lett 65(4):135

Priya MS, Naresh K, Jayaganthan R, Velmurugan R (2019) A comparative study between in-house 3D printed and injection molded ABS and PLA polymers for low-frequency applications. Materials Research Express 6(8):

Sebastian R, Noll A, Zhang G, Burkhart T, Wetzel B (2013) Friction and wear of PPS/CNT nanocomposites with formation of electrically isolating transfer films. Tribol Int 64:187–195. https://doi.org/10.1016/j.triboint.2013.04.004

Shen Z, Bateman S, Wu D, McMahon P, Dellolio M, Gotama J (2009) The effects of carbon nanotubes on mechanical and thermal properties of woven glass fibre reinforced polyamide-6 nanocomposites. Composites Science and Technology 69(2):239–244. https://doi.org/10.1016/j.compscitech.2008.10.017

Singh T, Patnaik A, Chauhan R, Chauhan P, Kumar N (2018) Physico-mechanical and tribological properties of nanoclay filled friction composite materials using Taguchi design of experiment approach. Polym Compos 39(5):1575–1581

Stadler Z, Krnel K, Kovač J, Kosmač T (2012) Tribochemical reactions on sliding surface of the sintered metallic brake linings against SiC ceramic brake disk. Wear 292:232–238

Stadnicki J (2017) Czynniki lokalizacji produkcji dóbr za pomocą technologii 3D-druku. Przegląd Nauk Ekonomicznych 26:215–224

Stadnicki J (2018) Lokalizacja produkcji wykorzystującej technologię druku przestrzennego. Zeszyty Naukowe, Organizacja i Zarządzanie/Politechnika Śląska

Strikwerda, Dehue (2020) What is 3D Printing. in 3D Printing, ed, 2020

Thiyagarajan V, Kalaichelvan K, Vijay R, Singaravelu DL (2016) Influence of thermal conductivity and thermal stability on the fade and recovery characteristics of non-asbestos semi-metallic disc brake pad. Journal of the Brazilian Society of Mechanical Sciences and Engineering 38(4):1207–1219

Varrica D, Fardelli, Dongarrà G, Tamburo E (2013) Speciation of Sb in airborne particulate matter, vehicle brake linings, and brake pad wear residues. Atmospheric Environment, vol. 64, pp. 18–24. http://dx.doi.org/10.1016/j.atmosenv.2012.08.067

Weisstein EW (2016) Circular segment. From MathWorld–a wolfram web resource

Potential of 3D Printing Technologies in Developing Applications of Polymeric Nanocomposites

Mir Irfan Ul Haq, Ankush Raina, Mariyam Jameelah Ghazali, Mohd Javaid, and Abid Haleem

Abstract Additive Manufacturing (AM) technologies are taking up manufacturing challenges for engineering and medical applications by using newer and advanced materials. With the advent of nanotechnology, nanomaterials in general and nanocomposites in particular have various benefits over conventional materials. The various advantages which 3D printing offers, such as minimum material wastage, less post-processing, ease to manufacture complex geometries, etc. can be exploited in the development of nanomaterials preparation with additive manufacturing. The current chapter introduces additive manufacturing technologies and then elaborates the major 3D printing technologies commercially available. Further elaborates the advantages of additive manufacturing over conventional manufacturing processes. A section is dedicated to introduce the various methods by which nanocomposites are being fabricated and shall discuss the resulting mechanical properties. The various underlining mechanisms, potential applications of 3D printed materials in polymeric nanocomposites have been given a prominent place in the chapter. Dedicated table, summarizes the different studies related to polymer composites prepared via 3D printing technology. Applications of 3D Printed Polymeric Nanocomposites is also provided along with advantages of using 3D printing technologies. A section is dedicated to discussing challenges in using 3D printing technologies for making applications with nanotechnology. The chapter opens up new areas to be explored by scientists, engineers and doctors in using AM technologies with nanocomposites for the betterment of mankind.

Keywords 3D printing · Additive manufacturing (AM) · Nanotechnology · Polymeric nanocomposites

---

M. I. U. Haq · A. Raina (✉)
School of Mechanical Engineering, Shri Mata Vaishno Devi University, Katra, Jammu and Kashmir, India

M. J. Ghazali
Department of Mechanical & Materials Engineering, Faculty of Engineering & Built Environment, Universiti Kebangsaan Malaysia, Bangi, Malaysia

M. Javaid · A. Haleem
Department of Mechanical Engineering, Jamia Millia Islamia, New Delhi, India

H. Jena et al. (eds.), *Tribology of Polymer and Polymer Composites for Industry 4.0*, Composites Science and Technology, https://doi.org/10.1007/978-981-16-3903-6_10

1 Introduction

The ever-increasing quest for sustainability and the growing need for shorter product development cycles has led material scientists and product designers to look towards better materials and efficient manufacturing processes (Baba et al. 2019) Nanomaterials have evolved as a new class of materials and are being tried extensively for a variety of engineering (Anand et al. 2020a, b; Shafi et al. 2019; Gulzar et al. 2020) and medical applications (Haq et al. 2020). The nanomaterials encompass a wide range of materials such as Graphene, MWCNT, Nano-clay, Nano-silica, etc. However, in practical engineering applications, owing to the cost factor, toady nanomaterials are being used as a secondary constituent with micro-sized materials (Hansen 2020). This hybridization of the nanomaterials by adding one constituent of nanoscale led the development of a new class of materials, which are now known as nanocomposites (Singh et al. 2018). Based on the base material and the reinforcing nano-filler, nanocomposites are classified into different classes such as polymeric nanocomposites, ceramic nanocomposites, and metallic nanocomposites, etc. Developing a low-cost nanocomposite with improved properties that can solve future manufacturing requirements is a challenge for material scientists, researchers and engineers.

Nanocomposites include a wide variety of materials in which at least one of the constituents is having the dimensions of submicron (10–100 nm) scale, combined either by physical or chemical method (Kichloo et al. 2020). The flexibility offered by the nanotechnology to control the individual atoms, nano-composites offer properties which are otherwise impossible at the macro level. The nanofillers are of the following types a) nano-particulate, e.g., silica & metals nanoparticles, nanofiber, e.g., carbon nanotubes and cellulose nanofibers & nanoplatelets layer silicates & platelet nanoclays. The selection of nano-fillers primarily depends upon the application of nanocomposites. The composites having polymer as the base matrix, and the nanomaterial as the reinforcement are termed as Polymer Nano Composites (Fig. 1) (Wu et al. 2020). These composites offer improved properties than the matrix, i.e., polymer.

Additive Manufacturing (AM) has evolved as a disruptive technological platform wherein products are developed layer by layer in contrast to the conventional manufacturing processes that fabricate the parts by removing material from a larger workpiece. Charles Hull first developed the technology in 1986, and the technology additively manufactures parts, i.e., the part is developed layer by layer, enabling complex geometries, faster product development cycles, thus providing a vast range of engineering applications. Thus, offering better material efficiency, 3D printing leads to minimum wastage of material. AM's ability to develop and print customized complex parts has placed it as a right candidate for the development of nanomaterials in general and nanocomposites in particular. The union of nanotechnology and Additive manufacturing offers tremendous advantages, uniquely tailoring of the critical material properties in engineering products.

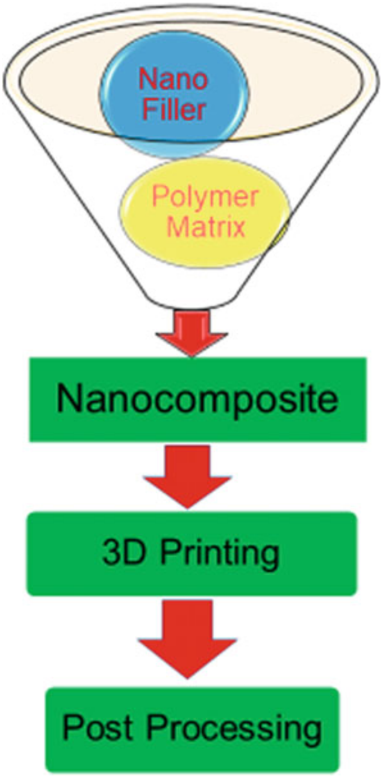

Fig. 1 Schematic Diagram of Nanocomposites Prepared via 3D printing

2 Major 3D Printing Technologies Used with Additive Manufacturing

In today's world, Additive Manufacturing plays a significant role in the manufacturing of intricate designs, undertaking customization, and improving material efficiency. As compared to the traditional manufacturing process, there are various innovative applications of additive manufacturing. The requirements of AM technologies are increasing day by day in the manufacturing industries (Horn and Harrysson 2012; Haleem and Javaid 2020). It may be noted that the AM platform is not a substitute for contemporary manufacturing processes. There are three different technological sets of AM; they are 3D printing, Scanning & imaging and software support. In this chapter, we would be discussing 3D printing technologies and their applications. The different technologies 3D printing technologies available are given below:

(a) Stereolithography (SLA)
(b) Selective Laser Sintering (SLS)
(c) Fused Deposition Modelling (FDM)
(d) Laminated Object Manufacturing (LOM)

(e) Inkjet 3D Printing (IJP)
(f) Digital Light Processing (DLP)
(g) Electron Beam Melting (EBM)
(h) Direct Metal Laser Sintering (DMLS)
(i) PolyJet 3D Printing
(j) Colour-Jet-Printing
(k) Drop on Demand Printing
(l) Sand Binder Jetting (SBJ).

3 Advantages of Additive Manufacturing Over Conventional Manufacturing Processes

Additive manufacturing can manufacture 3D objects from CAD inputs as per the requirement of customers. This technology has created major advancements and fulfils major challenges previously faced by designers and manufacturers (Gao et al. 2015; Haleem and Javaid 2019) (Aziz et al. 2020). The major advantages associated with additive manufacturing technologies as compared to the contemporary manufacturing systems are as under:

(a) Developing & creating complicated shape
(b) Lesser requirement of human resources
(c) Lesser wastage of materials
(d) Use of new type/non-conventional of material
(e) Technological flexibility
(f) Rapid built-up of parts.

4 Fabrication Methods for Polymeric Nanocomposites

Various parameters are taken into consideration for using AM technologies for the development of polymeric nanocomposites, such as cost, material compatibility, printing speed, and accuracy (Edgar and Tint 2015). As the material properties change upon adding the nanomaterials into the polymer matrix, hence every AM process which otherwise is suitable to print the base matrix may not be compatible with nanocomposite development. Table 1 provides an overview of the technologies which are compatible with nanocomposite fabrication. Many nanofillers are available, depending on the target application and the required compatibility between the matrix and filler. Figure 2 provides an overview of the various nano-fillers available.

Table1 Methods of nanocomposite development through 3D printing

Additive manufacturing method	Working principle	Compatible materials	References
Fused deposition modeling (FDM)	Material is extruded through a nozzle in semi-molten state layer by layer	Thermoplastics like PLA, ABS, PETG, Nylon, PEEK, etc.,	Chadha et al. (2019)
Selective laser sintering (SLS)	The laser selectively binds the powder		Salmoria et al. (2011)
Stereolithography (SLA)	Solidification by UV light of a photosensitive polymers	Photopolymers (UV-curable)	Manapat et al. (2017)
Optical projection SLA	The process similar to SLA, but dynamic photomasks developed by means of a digital mirror set up used here		Naffakh et al. (2010)
PolyJet	UV assisted solidification of an inkjet deposited layer using different materials		Elliott et al. (2013)
UV-3D printing	Extrusion followed by solidification of resin just after leaving the nozzle		Lebel et al. (2010)
Binder jetting	Liquid binder selectively printed of an over powder layer followed by solidification	Solutions/suspensions	Azhari et al. (2015)

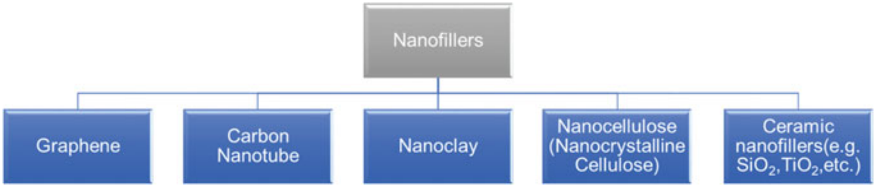

Fig. 2 Nanofillers for polymeric nanocomposites

4.1 Physical and Mechanical Properties of 3D Printed Polymeric Nanocomposites

The study of mechanical properties of the nanocomposites developed via 3D printing, such as tensile strength, flexural strength, etc. is very crucial in determining the possible applications of these nanocomposites. This section includes a discussion of the different studies related to the mechanical characterization of polymer-based nanocomposites. In this regard, the testing carried out by Yang et al. (2017) using carbon fibre as reinforcement in ABS showed the improved results for tensile and flexural strength with 10 wt. %. In another study, the comparison of Graphite flakes and carbon fibre as a reinforcement in ABS was reported by Ning et al. (2017). It was observed that carbon fibre reinforced ABS resulted in better tensile strength in comparison to the graphite flakes reinforced ABS. The results were obtained for the concentration of 5 wt. %.

Further, the use of short carbon fibre as reinforcement in PLA shows an improvement of different mechanical properties (Ferreira et al. 2017). The addition of 5 wt. % carbon fibre leads to an increase of 11.82%, 16.82%, 21.86%, and 22.5% in flexural stress, flexural modulus, flexural toughness, and tensile strength, respectively. A further increase in the concentration to 10 wt. % led to a decrease in ductility and yield strength. The addition of graphene platelets in PLA by Prashantha and Roger (2017) also improved mechanical properties. An improvement of 27 and 30% in tensile strength and elastic modulus, respectively, was observed with 10 wt 0% graphene.

In a similar investigation using graphene platelets in ABS, Dul et al. (2016) performed an investigation by varying the concentration of the graphene and preparation method of the samples. It was observed that the preparation of samples with horizontal and vertical orientation resulted in improved mechanical properties. In another study by the same author group using carbon nanotubes as reinforcement in different concentrations in ABS, it was revealed that the 6 wt. % led to an improvement in tensile strength and elastic modulus (Dul et al. 2018).

The study carried out by Ferreira et al. (2019) show an increase in flexural modulus by 191.38% and Young's modulus by 70.10% by using 20 wt. % carbon-reinforced PETG. Berretta et al. (2017) performed an investigation using carbon nanotube reinforced PEEK. It was observed that with the addition of 1 wt. % CNT, there is a slight increase in the tensile strength with a negligible effect on shear strength. However, a further increase in concentration (5 wt. %) led to a decrease in both the tensile strength and shear strength.

Tekinalp et al. (2014) performed an investigation using carbon fibre as a reinforcement in ABS. The samples were prepared by using compression moulding and FDM techniques. It was observed that the addition of carbon fibres having a length of 0.2–0.4 mm resulted in the improvement in elastic modulus and tensile strength by 700 and 115%. Tian et al. (2016) performed investigations with carbon fibre as a reinforcement material in PLA printing. They obtained improved mechanical properties with a variable layer thickness of the samples. Authors reported an increase in the flexural strength and modulus of elasticity, with the increase in carbon fibre content up to 27%.

Another study performed by Nakagawa et al. (2017) reported the use of carbon fibres in ABS. The results were obtained for the varied composition of carbon fibres, wherein it was observed that there is an increase in the strength with the increase in the composition of carbon fibres. Plymill et al. (2016) performed an investigation by using the carbon nanotubes and graphene as reinforcement in PLA. It was observed that with the addition of 0.1 wt. % of carbon nanotubes resulted in an increase of 41% and 16% in the tensile strength and modulus of elasticity, respectively. Further, with the addition of 0.2 graphenes by wt. %, authors observe an improvement of 47% and 17% in these properties.

Thus, the studies performed reveals that the addition of various reinforcements in polymers leads to the improvement in the different mechanical properties of the prepared nanocomposites. Table 2 summarises the different findings related to the different polymer-based nanocomposites produced by 3D printing technology.

4.2 Applications of 3D Printed Polymeric Nanocomposites

The 3D printed polymeric nanocomposites can provide a variety of applications in areas, such as automobiles, aerospace, tooling, moulding, medical equipment, etc., They are critical, especially where, intricate product designs are involved (Valino et al. 2019). The technology being in its primitive stages, particularly from a cost point of view, it has not been able to replace the traditional subtractive or conventional methods of fabrication. The 3D printed polymeric composites can extensively be used in aviation, aerospace, and military applications (Tian et al. 2016). The intrinsic advantages of the process of AM such faster production rate, flexibility to carry out design iterations, ease to manufacture customized parts further widens its scope in the critical areas of aerospace and aviation (Coykendall et al. 2014).

Some recent studies focused on the biocompatibility aspects of these 3D manufactured parts have further widened their scope in the medical field. 3D printing and nanotechnology can be augmented to develop parts for orthopaedic and dental applications, as AM can develop composites that are functionally graded (Haleem and Javaid 2019; Javaid and Haleem 2018). In addition to the applications mentioned above, 3D printed parts can be used extensively in the area of tooling and moulding as good mechanical strength, dimensional accuracy and surface finish can be better achieved through this process (Yan et al. 2009).

5 Economic Aspects of 3D Printing

3D printing is economical and has led to a disruptive change in the manufacturing sector. In the upcoming days, this technology could provide additional development and innovations in manufacturing industries. This technology is economical due to the following reasons:

a. Quick and easy manufacture of physical parts from a 3D model
b. Eliminates the need for customized manufacturing facilities
c. Customers can now print objects in their homes/offices

Table 2 Summary of the different studies related to polymer composites prepared via 3D printing technology

Base matrix	Nano filler	Methodology	3D printing technology	Key findings	References
Acrylonitrile butadiene styrene (ABS)	Organic Montmorillonite (OMMT)	Twin melt extrusion	FDM	Mechanical strength improved by adding OMMT into ABS Linear shrinkage ratio and thermal stability also improved by adding OMMT	Weng et al. (2016)
Polybutylene terephthalate(PBT)	CNT- and graphene	melt extrusion	FDM	3D printed PBT/CNT objects exhibit better conductive and mechanical performance than 3D printed PBT/graphene structures	Gnanasekaran et al. (2017)
Acrylonitrile butadiene styrene (ABS)	Graphene nanoplatelets	Melt compounding and extrusion	FDM	Graphene nanoplatelets addition improved the tensile modulus of ABS The coefficient of thermal dilation reduced considerably in the of 3D printed parts Creep compliance reduced by Graphene addition	Dul et al. (2016)
Acrylonitrile butadiene styrene (ABS)	TiO_2	Extrusion	FDM	A slight degradation of ABS observed due to TiO_2addition during the different steps 10% TiO_2 nanocomposites exhibit a higher breaking point stress in comparison to the pure polymer	Skorski et al. (2016)
Resin	Graphene oxide	Ultrasonication	Stereolithography	Increased tensile strength at an annealing temperature of 100 °C Increased thermal stability with increasing annealing temperature	Manapat et al. (2017)
Polylactic acid (PLA)	10 wt.% graphene	As received	FDM	The electrical resistivity perpendicular to layers observed as less than the volume resistivity Improvement in mechanical and thermomechanical properties of PLA	Prashantha and Roger (2017)

(continued)

Table 2 (continued)

Base matrix	Nano filler	Methodology	3D printing technology	Key findings	References
Polyvinylidene fluoride	$BaTiO_3$ nanoparticles	Ultrasonication	FDM	Improvement in the piezoelectric property	Kim et al. (2018)
Polylactic acid (PLA)	MWCNT	Magnetic stirring followed by Ultrasonication	Liquid Deposition Modeling (LDM)	Improvement in the electrical conductivity of the developed nanocomposite as compared to the pristine PLA matrix	Postiglione et al. (2015)
Polylactic acid (PLA)	Nanosize carbon black and multi-wall carbon nanotube	Peeling standard method	FDM	The process parameters such as extruder temperature, bed temperature, and print speed significantly affect the adhesion force of polymers to fabrics for 3D printing	Sanatgar et al. (2017)
Polylactic acid (PLA)	Hydroxyapatite (HA) powder	Screw extruder	Fused filament fabrication	The porosity of 30 vol. % for bone implants achieved Improved Young's modulus of the scaffolds of the order of the trabecular human bone tissue	Niaza et al. (2016)
Acrylonitrile butadiene styrene (ABS)	Lignin-coated cellulose nanocrystal (L-CNC)	Twin-screw extrusion	FDM	The dispersion and interfacial adhesion of L-CNC with ABS was excellent Mechanical and thermal properties improved	Feng et al. (2017)
Linear low-density polyethylene (LLDPE) + Rubber	MWCNT		FDM	Effect of the process of compression moulding vs fused deposition modelling on the mechanical behaviour studied Radom alignment of carbon nanotubes in the 3D printed composites resulted in decreased electrical conductivity	Daver et al. (2016)
Polylactic acid (PLA)	Nanoclay	Twin-screw extruder	FDM	Nanocomposites exhibited higher elastic modulus (15%) compared to PLA	Coppola et al. (2017)

(continued)

Table 2 (continued)

Base matrix	Nano filler	Methodology	3D printing technology	Key findings	References
Poly (ethylene glycol) diacrylate (PEGDA)	Silica (SiO_2)		Stereolithography	The addition of SiO_2 led to an improvement in the tensile and compressive strength Best strength observed in the case with 1 wt.% SiO_2	Dizon et al. (2019)
Polylactic acid (PLA	Graphene		FDM	– Improved creep resistance in PLA/graphene composites observed – Wear resistance improved by 14% in the case of PLA-graphene as compared to PLA – A 65% reduction in COF as compared to PLA	Bustillos et al. (2018)
Polylactic acid (PLA)	Nano-clay		FDM	– Increase in the storage modulus as compared to neat PLA – Improvement in thermal stability by addition of nanoclay – Improvement in elastic modulus than neat PLA specimens	Coppola et al. (2018)
Resin	Quantum dots(QDs)	hot-injection synthesis followed by Ultrasonication	PolyJet process	– Increase in surface tension with an increase in the concentration of QDs – Increase in viscosity – The rheological results suggest that adding QDs do not shift the polymer out of the printing region	Elliott et al. (2013)
Epoxy	MWCNT		Stereolithography (SLA)	– A 0.05% (w/v) concentration of MWCNT improved the ultimate tensile stress and fracture stress by 17% and 37%, respectively	Sandoval et al. (2007)
Geo-polymer	Graphene oxide	Stirring	Melted extrusion modeling	Improved compressive strength higher and electrical conductivity Graphene Oxide a useful rheological modifier	Zhong et al. (2017)

(continued)

Table 2 (continued)

Base matrix	Nano filler	Methodology	3D printing technology	Key findings	References
Acrylonitrile butadiene styrene (ABS)	Nanoclay	Melt intercalation	FDM	Improvement in mechanical properties such as tensile strength, compression strength, and hardness initially when the batch loading is increased from 5 wt.% to 10 wt.%; however, a decreasing trend is observed afterwards A reduction in the porosity for the developed nanocomposites	Francis and Jain (2016)
Photoreactive resin	Graphene oxide	Ultrasonication	Stereolithography	Mechanical strength, as well as stiffness (Young's Modulus) and elongation, decreased with the addition of GO Degradation in the thermal properties upon an increase in the GO content Agglomeration of the GO main reason for the change in properties	Zhakeyev et al. (2019)
Acrylonitrile butadiene styrene (ABS)	Carbon nanotubes and graphene		FDM	Addition of GnP into the ABS matrix reduces the mechanical strength Weak covalent bonds between graphene and ABS The addition of CNT into the ABS improves the flexural and the tensile strength of the composite	Vidakis et al. (2020)
Poly(vinyl alcohol) (PVA)	Graphene	Ultrasonication and stirring	FDM	GNP (8 wt.%) exhibited best mechanical properties with Young's modulus of around 49.1 MPa, ultimate tensile the stress of 10.6 MPa, and an elongation at break of 128.4%	Yang et al. (2010)

(continued)

Table 2 (continued)

Base matrix	Nano filler	Methodology	3D printing technology	Key findings	References
Acrylonitrile butadiene styrene (ABS)	Carbon nanotube and short carbon fibre		FDM	Improvement in tensile strength, tensile shear strength for both the composites Matrix fracture and fibre pull out the primary failure mechanism	Zhang et al. (2018)
Polyether ether ketone(PEEK)	Carbon nanotube		FDM	With 1% CNT no significant change in properties 5% of CNT led to the degradation of mechanical properties Void formation observed in the printed part	Berretta et al. (2017)
Polylactic acid (PLA)	CNT and graphene		FDM	A 47% improvement in the tensile strength with 0.2% graphene Around 41% improvement in the tensile strength with 0.1% CNT	Plymill et al. (2016)

d. Capability to print customized food, meals and snacks in restaurants and home
e. Economical for various medical treatments
f. Capability to create an accurate replica of human body parts
g. Applicable to print human cells
h. Improve the economy due to its potential for lower production costs
i. Minimizes the requirement of tools, jigs, fixtures, etc.
j. One go manufacturing of the part
k. Lesser wastage of raw materials.

These technologies are now available to test any ideas and design rapidly in lesser time and cost. There is a freedom of creative design and customization of products, and a wide range of materials like metal, glass, paper, ceramics, silver, biomaterials, etc. can be used in these technologies. Research is ongoing on 3D printing and its development in different fields. It has great potential for product design and development to produce customized parts with a higher level of flexibility. The technology helps address various ongoing issues.

6 Challenges in Using 3D Printing Technologies for Developing Nanocomposites

The merging of 3D printing and nanotechnology poses many challenges to the scientific community (Ivanova et al. 2013). Figure 3 provides an overview of the various challenges posed. The issue of cost efficiency of the nanomaterials and after that the relatively complex procedure involved in the development of nanocomposites that are compatible with 3D printing restricts the widespread applications of the 3D printing for nanocomposite development for various engineering applications. Also, the commercially available 3D printers are not designed to handle composites; and they have to be modified. Therefore, the use of these printers for composite fabrication may not result in the printed part's desired properties.

The issue of agglomeration of the nanoparticles in the base matrix also is an issue that leads to the degradation of the properties as the nanoparticle agglomerates behave like bulk. The agglomeration can, however, be addressed by adding organic linkers or prior chemical treatment. The settling down of the nanoparticles in the powder-based methods also leads to inhomogeneity in the developed parts. The addition of nanoparticles in the polymeric materials also leads to alteration of the optimized 3D printing parameters for the development of these composites as the flow behaviour and the viscosity of the nanocomposites is entirely different from the base matrix (Kim and Creasy 2004). This behaviour may lead to nozzle clogging and formation of aggregates in the developed parts. The poor adhesion at the interface of the matrix and the nanoparticle also leads to higher porosity in comparison to the base matrix.

Environmental concerns of the nanoparticle additives also pose a challenge as some of the particles tend to oxidize in air. The disposal, use, and recycling need to be addressed by incorporating Life Cycle Analysis of the parts manufactured by

Fig. 3 Challenges faced to merge 3D printing and nanotechnology

AM technologies (Campbell 2009). Apart from the challenges mentioned above, a big challenge is the poor thermo-mechanical behaviour, which may lead to loss of design integrity throughout use and time. These properties need to be improved.

7 Conclusions

The augmentation of additive manufacturing with nanotechnology has helped to develop customized nanomaterials applications with improved properties at an overall lower cost and with shorter product cycle times. The tremendous advantages associated with the additive manufacturing technologies have made them a feasible option to produce intricate engineering components, needing different properties at different locations, particularly with lower mass. The introduction of nanofillers into polymer matrices and subsequent use of various 3D printing technologies has substantially improved the mechanical, physical, and thermal properties of the resulting nanocomposites. Many nanofillers have been tried with various polymer matrices, and literature has reported that the addition of these nanofillers via additive manufacturing leads to the improvement of overall physical and mechanical properties. The medical sector requires a different type of material to produce implants, body parts, tools, smart devices and connecting devices. The literature suggests that advanced nanocomposites can be of good use in various engineering applications and medical applications. However, some economic and technical challenges hinder the scale exploitation of these technologies. Researchers need to consider a holistic approach to improve the economic and technological benefits, which can be achieved by synergizing the two technologies of additive manufacturing and nanotechnology.

8 Future Outlook

Future studies can be directed towards developing low cost and effective methodologies to develop nanocomposites compatible for a wide range of base matrices and nanofillers. Also studies aimed at mitigating the drawbacks associated with existing methods so as to develop nanocomposites with better properties. Moreover, a better understanding of the underlying mechanisms, optimizing the process parameters and studying the effect of various parameters on various mechanical, thermal and physical properties of these nanocomposites is needed for widening the applications of these materials. Application focused studies can also be undertaken to develop nanomaterials for critical applications such as automotive, dentistry, orthopedics, etc.

References

Anand R, Haq MIU, Raina A (2020a) Bio-based nano-lubricants for sustainable manufacturing. In: Nanomaterials and environmental biotechnology. Springer, Cham, pp 333–380. https://doi.org/10.1007/978-3-030-34544-0_18

Anand R, Raina A, Ul Haq MI, Mir MJ, Gulzar O, Wani MF (2020b) Synergism of TiO_2 and graphene as nano-additives in bio-based cutting fluid-an experimenta investigation. Tribol Trans 1–21. https://doi.org/10.1080/10402004.2020.1842953

Azhari A, Toyserkani E, Villain C (2015) Additive manufacturing of graphene–hydroxyapatite nanocomposite structures. Int J Appl Ceram Technol 12(1):8–17

Aziz R, Haq MIU, Raina A (2020) Effect of surface texturing on friction behaviour of 3D printed polylactic acid (PLA). Polym Test 85:106434

Baba ZU, Shafi WK, Haq MIU, Raina A (2019) Towards sustainable automobiles-advancements and challenges. Prog Ind Ecol Int J 13(4):315–331

Berretta S, Davies R, Shyng YT, Wang Y, Ghita O (2017) Fused deposition modelling of high temperature polymers: exploring CNT PEEK composites. Polym Test 63:251–262

Bustillos J, Montero D, Nautiyal P, Loganathan A, Boesl B, Agarwal A (2018) Integration of graphene in poly (lactic) acid by 3D printing to develop creep and wear-resistant hierarchical nanocomposites. Polym Compos 39(11):3877–3888

Campbell TA (2009) Measuring the nano-world. Nano Today 4(5):380–381

Chadha A, Haq MIU, Raina A, Singh RR, Penumarti NB, Bishnoi MS (2019) Effect of fused deposition modelling process parameters on mechanical properties of 3D printed parts. World J Eng 16(4):550–559. https://doi.org/10.1108/WJE-09-2018-0329

Coppola B, Cappetti N, Di Maio L, Scarfato P, Incarnato L (2017) Layered silicate reinforced polylactic acid filaments for 3D printing of polymer nanocomposites. In: 2017 IEEE 3rd international forum on research and technologies for society and industry (RTSI). IEEE, pp 1–4

Coppola B, Cappetti N, Di Maio L, Scarfato P, Incarnato L (2018) 3D printing of PLA/clay nanocomposites: Influence of printing temperature on printed samples properties. Materials 11(10):1947

Coykendall J, Cotteleer M, Holdowsky J, Mahto M (2014) 3D opportunity in aerospace and defense: additive manufacturing takes flight. A Deloitte Ser Addit Manuf 1

Daver F, Baez E, Shanks RA, Brandt M (2016) Conductive polyolefin–rubber nanocomposites with carbon nanotubes. Compos A Appl Sci Manuf 80:13–20

Dizon JRC, Chen Q, Valino AD, Advincula RC (2019) Thermo-mechanical and swelling properties of three-dimensional-printed poly (ethylene glycol) diacrylate/silica nanocomposites. MRS Communications 9(1):209–217

Dul S, Fambri L, Pegoretti A (2018) Filaments production and fused deposition modelling of ABS/carbon nanotubes composites. Nanomaterials 8(1):49

Dul S, Fambri L, Pegoretti A (2016) Fused deposition modelling with ABS–graphene nanocomposites. Compos A Appl Sci Manuf 85:181–191

Edgar J, Tint S (2015) Additive manufacturing technologies: 3D printing, rapid prototyping, and direct digital manufacturing. Johns Matthey Technol Rev 59(3):193–198

Elliott AM, Ivanova OS, Williams CB, Campbell TA (2013) Inkjet printing of quantum dots in photopolymer for use in additive manufacturing of nanocomposites. Adv Eng Mater 15(10):903–907

Feng X, Yang Z, Rostom SS, Dadmun M, Xie Y, Wang S (2017) Structural, mechanical, and thermal properties of 3D printed L-CNC/acrylonitrile butadiene styrene nanocomposites. J Appl Polym Sci 134(31):45082

Ferreira I, Vale D, Machado M, Lino J (2019) Additive manufacturing of polyethylene terephthalate glycol/carbon fiber composites: An experimental study from filament to printed parts. Proc Inst Mech Eng Part L J Mater Des Appl 233(9):1866–1878

Ferreira RTL, Amatte IC, Dutra TA, Bürger D (2017) Experimental characterization and micrography of 3D printed PLA and PLA reinforced with short carbon fibers. Compos B Eng 124:88–100

Francis V, Jain PK (2016) Experimental investigations on fused deposition modelling of polymer-layered silicate nanocomposite. Virtual Phys Prototyp 11(2):109–121

Gao W, Zhang Y, Ramanujan D, Ramani K, Chen Y, Williams CB, Zavattieri PD (2015) The status, challenges, and future of additive manufacturing in engineering. Comput Aided Des 69:65–89

Gnanasekaran K, Heijmans T, Van Bennekom S, Woldhuis H, Wijnia S, de With G, Friedrich H (2017) 3D printing of CNT-and graphene-based conductive polymer nanocomposites by fused deposition modeling. Appl Mater Today 9:21–28

Gulzar O, Qayoum A, Gupta R (2020) Experimental study on thermal conductivity of mono and hybrid Al2O3–TiO2 nanofluids for concentrating solar collectors. Int J Energy Res. https://doi.org/10.1002/er.6105

Haleem A, Javaid M (2019) Polyether ether ketone (PEEK) and its manufacturing of customized 3D printed dentistry parts using additive manufacturing. Clin Epidemiol Glob Health 7(4):654–660

Haleem A, Javaid M (2020) 3D printed medical parts with different materials using additive manufacturing. Clin Epidemiol Glob Health 8(1):215–223

Hansen CJ (2020) 3D and 4D printing of nanomaterials: processing considerations for reliable printed nanocomposites. In: 3D and 4D printing of polymer nanocomposite materials. Elsevier, pp 25–44

Haq MIU, Khuroo S, Raina A, Khajuria S, Javaid M, Haq MFU, Haleem A (2020) 3D printing for development of medical equipment amidst coronavirus (COVID-19) pandemic—review and advancements. Res Biomed Eng 1–11

Horn TJ, Harrysson OL (2012) Overview of current additive manufacturing technologies and selected applications. Sci Prog 95(3):255–282

Ivanova O, Williams C, Campbell T (2013) Additive manufacturing (AM) and nanotechnology: promises and challenges. Rapid Prototyp J

Javaid M, Haleem A (2018) Additive manufacturing applications in orthopaedics: a review. J Clin Orthop Trauma 9(3):202–206

Kichloo AF, Aziz R, Haq MIU, Raina A (2020) Mechanical & physical behaviour of 3D printed polymer nanocomposites-A review. Int J Ind Syst Eng. https://doi.org/10.1504/IJISE.2020.10028678. (Article in Press)

Kim H, Fernando T, Li M, Lin Y, Tseng TLB (2018) Fabrication and characterization of 3D printed BaTiO3/PVDF nanocomposites. J Compos Mater 52(2):197–206

Kim J, Creasy TS (2004) Selective laser sintering characteristics of nylon 6/clay-reinforced nanocomposite. Polym Testing 23(6):629–636

Lebel LL, Aissa B, Khakani MAE, Therriault D (2010) Ultraviolet-assisted direct-write fabrication of carbon nanotube/polymer nanocomposite microcoils. Adv Mater 22(5):592–596

Manapat JZ, Mangadlao JD, Tiu BDB, Tritchler GC, Advincula RC (2017) High-strength stereolithographic 3D printed nanocomposites: graphene oxide metastability. ACS Appl Mater Interfaces 9(11):10085–10093

Naffakh M, Díez-Pascual AM, Marco C, Gómez MA, Jiménez I (2010) Novel melt-processable poly (ether etherketone)(PEEK)/inorganic fullerene-like WS2 nanoparticles for critical applications. J Phys Chem B 114(35):11444–11453

Nakagawa Y, Mori K, Maeno T (2017) 3D printing of carbon fibre-reinforced plastic parts. Int J Adv Manuf Technol 91(5–8):2811–2817

Niaza KV, Senatov FS, Kaloshkin SD, Maksimkin AV, Chukov DI (2016) 3D-printed scaffolds based on PLA/HA nanocomposites for trabecular bone reconstruction. In: journal of physics: conference series, vol 741, No. 1, p. 012068. IOP Publishing

Ning F, Cong W, Hu Z, Huang K (2017) Additive manufacturing of thermoplastic matrix composites using fused deposition modeling: A comparison of two reinforcements. J Compos Mater 51(27):3733–3742

Plymill A, Minneci R, Greeley DA, Gritton J (2016) Graphene and carbon nanotube PLA composite feedstock development for fused deposition modeling

Postiglione G, Natale G, Griffini G, Levi M, Turri S (2015) Conductive 3D microstructures by direct 3D printing of polymer/carbon nanotube nanocomposites via liquid deposition modeling. Compos A Appl Sci Manuf 76:110–114

Prashantha K, Roger F (2017) Multifunctional properties of 3D printed poly (lactic acid)/graphene nanocomposites by fused deposition modeling. J Macromol Sci Part A 54(1):24–29

Salmoria GV, Paggi RA, Lago A, Beal VE (2011) Microstructural and mechanical characterization of PA12/MWCNTs nanocomposite manufactured by selective laser sintering. Polym Testing 30(6):611–615

Sanatgar RH, Campagne C, Nierstrasz V (2017) Investigation of the adhesion properties of direct 3D printing of polymers and nanocomposites on textiles: effect of FDM printing process parameters. Appl Surf Sci 403:551–563

Sandoval JH, Soto KF, Murr LE, Wicker RB (2007) Nanotailoringphotocrosslinkable epoxy resins with multi-walled carbon nanotubes for stereolithography layered manufacturing. J Mater Sci 42(1):156–165

Shafi WK, Raina A, Haq MIU (2019) Performance evaluation of hazelnut oil with copper nanoparticles-a new entrant for sustainable lubrication. Ind Lubr Tribol 71(6):749–757. https://doi.org/10.1108/ILT-07-2018-0257

Singh N, Mir IUH, Raina A, Anand A, Kumar V, Sharma SM (2018) Synthesis and tribological investigation of Al-SiC based nano hybrid composite. Alex Eng J 57(3):1323–1330

Skorski MR, Esenther JM, Ahmed Z, Miller AE, Hartings MR (2016) The chemical, mechanical, and physical properties of 3D printed materials composed of TiO_2-ABS nanocomposites. Sci Technol Adv Mater 17(1):89–97

Tekinalp HL, Kunc V, Velez-Garcia GM, Duty CE, Love LJ, Naskar AK, Ozcan S (2014) Highly oriented carbon fiber–polymer composites via additive manufacturing. Compos Sci Technol 105:144–150

Tian X, Liu T, Yang C, Wang Q, Li D (2016) Interface and performance of 3D printed continuous carbon fiber reinforced PLA composites. Compos A Appl Sci Manuf 88:198–205

Valino AD, Dizon JRC, Espera Jr, AH, Chen Q, Messman J, Advincula RC (2019) Advances in 3D printing of thermoplastic polymer composites and nanocomposites. Prog Polym Sci 98:101162

Vidakis N, Maniadi A, Petousis M, Vamvakaki M, Kenanakis G, Koudoumas E (2020) Mechanical and electrical properties investigation of 3D-printed Acrylonitrile–Butadiene–Styrene graphene and carbon nanocomposites. J Mater Eng Perform 1–10

Weng Z, Wang J, Senthil T, Wu L (2016) Mechanical and thermal properties of ABS/montmorillonite nanocomposites for fused deposition modeling 3D printing. Mater Des 102:276–283

Wu H, Fahy WP, Kim S, Kim H, Zhao N, Pilato L, Kafi A, Bateman S, Koo JH (2020) Recent developments in polymers/polymer nanocomposites for additive manufacturing. Prog Mater Sci 111:100638

Yan Y, Li S, Zhang R, Lin F, Wu R, Lu Q, Wang X (2009) Rapid prototyping and manufacturing technology: principle, representative technics, applications, and development trends. Tsinghua Sci Technol 14(S1):1–12

Yang C, Tian X, Liu T, Cao Y, Li D (2017) 3D printing for continuous fiber reinforced thermoplastic composites: mechanism and performance. Rapid Prototyp J 23(1):209–215

Yang L, Chen Y, Wang M, Shi S, Jing J (2020) Fused deposition modeling 3D printing of novel poly (vinyl alcohol)/graphene nanocomposite with enhanced mechanical and electromagnetic interference shielding properties. Ind Eng Chem Res 59(16):8066–8077

Zhakeyev A, Leung DY, Xuan J (2019) GO-modified flexible polymer nanocomposites fabricated via 3D stereolithography. Front Chem Sci Eng 13(4):736–743

Zhang W, Cotton C, Sun J, Heider D, Gu B, Sun B, Chou TW (2018) Interfacial bonding strength of short carbon fiber/acrylonitrile-butadiene-styrene composites fabricated by fused deposition modeling. Compos B Eng 137:51–59

Zhong J, Zhou GX, He PG, Yang ZH, Jia DC (2017) 3D printing strong and conductive geo-polymer nanocomposite structures modified by graphene oxide. Carbon 117:421–426